MECHANICS OF THE LINEA ALBA AND SUTURE-BASED WOUND CLOSURE

GERARD M. COONEY, BENG., MSC.

A thesis submitted to the University of Dublin, Trinity College in partial fulfillment of the requirements for the degree

Doctor of Philosophy

January 2016

Supervisor

Dr. Ciaran K. Simms

Co-Supervisor

Dr. Des Winter

Examiners

Dr. Conor Buckley & Dr. Stéphane Avril

Education is not

the filling of a pail,

but the lighting of a fire.

W. B. YEATS

Declaration

I, Gerard Cooney, declare that this thesis has not been submitted as an exercise for a degree at this or any other university and it is entirely my own work.

I agree to deposit this thesis in the University's open access institutional repository or allow the library to do so on my behalf, subject to Irish Copyright Legislation and Trinity College Library conditions of use and acknowledgement.

Gerard M. Cooney, January 4^{th} 2016

Abstract

Over the past thirty years there has been a dramatic change in the methodology of abdominal surgery. The introduction of digitalisation, miniaturisation, improved optics, novel imaging techniques and computerised information systems in the operating theatre in the form of minimally invasive laparoscopic surgery have greatly reduced risk to the patient and the length of time required to complete the surgery. However, there are still medical situations that require the more invasive laparotomy surgery and it is estimated that the same number of people (two million for each laparoscopic and laparotomy surgeries) undergo the procedure in the USA each year. Unfortunately, despite the medical advances in recent years, incisional hernia can form post-operatively, having a prevalence of approximately 1-5% for laparoscopic surgery and as high as 20% for open laparotomies. There are claims that the risk of incisional hernia is related to the quality of wound closure. This thesis therefore aims to develop a novel wound closure method that will reduce the risk of incisional hernia occurring.

The design of a novel wound closure method requires a fundamental understanding of the mechanical properties of the tissue involved. To achieve this, the tensile mechanical characterisation of the porcine and human linea alba, as determined by uniaxial and equi-load biaxial testing using image-based strain measurement methods is presented due to the limited data available in the literature and which use less accurate methods of stretch measurement. Significant anisotropy was observed in the tissue of both species with deformation heavily biased in the longitudinal direction under equal application of load. It was found that the response of porcine linea alba to uniaxial and biaxial loading is similar to that of human linea alba, permitting the use of a porcine model for investigations into wound closure methodology. Additionally, a finite element model of the uniaxial experiments quantified the effect of clamping and tissue dimensions (which are suboptimal for tensile testing) on the

porcine uniaxial results. A correction factor was produced that was used to scale the porcine uniaxial data to account for the effects of clamping. These results provide an improved assessment of the mechanical properties of the porcine and human linea alba to help further an understanding of wound closure.

The suture pullout characteristics of both porcine and human linea alba are investigated to ascertain an optimal placement of sutures for surgical wound closure. This is performed again in response to the very limited data available in the literature. It was found that the relationship between pullout force of the suture, bite separation and bite depth is quadratic and characterises low separation and high depth as optimal parameters. Of the parameters used in the study, it was found that resistance to pullout could be improved by as much as 290%. Both human and porcine tissue were observed to exhibit the same behaviour, again corroborating the use of a porcine model for investigations into wound closure methodology. Orientation of suture application was also found to significantly affect the magnitude of suture pullout. Suture styles applied longitudinally across a transverse defect were observed to be more beneficial and it was concluded that it could especially reduce the risk of laparoscopic incisional hernia.

Since the abdomen is itself a pressurised vessel, it is generally described as being subjected to multi-axial loading; not solely in the direction of the abdominal muscles aponeurotic processes. To more adequately describe the effect that suture-based wound closure has on the apposition of the linea alba laparotomy defect, it is necessary to create an environment that adequately reflects an in-vivo standpoint. To this end, deformation tests on porcine linea alba (intact abdominal wall) with a suture-closed laparotomy incision were performed on a surrogate abdominal rig. This was done in order to more accurately ascertain the optimum bite depth and bite separation of a continuous suture to be used to close a laparotomy defect through quantitative measurement of wound apposition. The conclusions proved to be the same as that of uniaxial suture pullout, validating uniaxial pullout as a reliable source. Theoretical and experimental evaluation of suture pullout was also investigated in order to predict the pressure of suture pullout beyond what is capable of the surrogate rig. However, the theoretical model tended to under-predict the experimental results due to the types of assumptions used.

In conclusion, a detailed understanding of the mechanics of the linea alba and suture-based

wound closure has been developed and used to improve upon clinical methodologies and could potentially reduce the risk of post-operative complications. Two clinical recommendations were developed and accepted by a surgical consultant. A suture bite depth of 16mm and a bite separation of 5mm is advised for laparotomy closure and transverse incisions closed using longitudinal applications of suture are advised for laparoscopic closure to help minimise the risk of incisional hernia.

Acknowledgements

It is hard to believe that three years have passed since I took up a permanent residence in the Parsons building in Trinity College Dublin.

First and foremost, I would like to express my sincerest gratitude to my supervisor Dr. Ciaran K. Simms for his expert guidance, encouragement and continued support. Of all people I have met in academia, Ciaran's passion in his work and that of his students has been nothing short of a phenomenal inspiration to me. Similarly, Prof. Des Winter has been a source of boundless interest and enthusiasm. His suggestions and advice on the technical aspects of this PhD, as from the point of view of a surgeon, have been an invaluable resource. It has been an absolute joy and privilege to have been able to work with both Ciaran and Des and I hope we can work together again in the future.

I would also like to thank everyone in the musculoskeletal lab at Washington University in St. Louis. I can't fully express how wonderful it was to have the opportunity to work with Ass. Prof. Spencer Lake and his group. Without their help and kindness, I would certainly not be where I am today. I would like to express my particular thanks to Spencer who went out of his way, beyond what would be expected of anyone, to allow me to further my studies in WashU and make me feel at home. Go Bears!

My special thanks to Dr. Michael Takaza, good friend and former colleague, whose advice and late evening chats helped make all this possible. I would also like to praise Dr. Kevin Moerman for his help with modelling, making the impossible look like childsplay. I would like to additionally thank all the technical and workshop staff in the department who helped make my ideas a reality.

I have to pay a special tribute to everyone who I shared an office with over the course of my study: Michael Takaza, Michael Gibbons, Steven Whelan, Steven Yates, Feng, Rudi,

Diarmuid, Richard, Greg, Guibing, Mathew and Melika. The endless coffee runs, constant banter and side-splitting laughter made the dullest days that much brighter.

Lastly, I would like to thank my parents, brothers and close friends for their support through it all. You've all had to put up with me at my worst during times of stress. I'm sure I can hear a collective sigh of relief as a write this!

Contents

List of Figures

List of Tables

Publications

First Author Journal Papers

- G. M. Cooney, K. M. Moerman, M. Takaza, D. C. Winter, C. K. Simms, Uniaxial and biaxial mechanical properties of porcine linea alba (2015), *Journal of the Mechanical Behaviour of Biomedical Materials*, 41, 68–82.

  http://www.sciencedirect.com/science/article/pii/S1751616114003105

Co-Authored Journal Papers

- M. Takaza, G. M. Cooney, G. McManus, P. Stafford, C. K. Simms, Assessing the microstructural response to applied deformation in porcine passive skeletal muscle (2014), *Journal of the Mechanical Behaviour of Biomedical Materials*, 40, 115–126.

  http://www.sciencedirect.com/science/article/pii/S1751616114002628

Conference Abstracts

- G. M. Cooney, D. C. Winter, C. K. Simms, Towards a wound closure device for laparoscopic surgery, *Bioengineering in Ireland*, Dublin (2013).

- G. M. Cooney, D. C. Winter, C. K. Simms, Mechanical characterisation of the porcine linea alba, *Bioengineering in Ireland*, Limerick (2014).

- G. M. Cooney, D. C. Winter, C. K. Simms, Mechanical characterisation of the porcine linea alba, *World Congress of Biomechanics*, Boston (2014).

- G. M. Cooney, D. C. Winter, C. K. Simms, The suture pullout characteristics of porcine linea alba, *Bioengineering in Ireland*, Maynooth (2015).

- G. M. Cooney, D. C. Winter, C. K. Simms, The suture pullout characteristics of porcine linea alba, *European Society of Biomechanics*, Prague (2015).

- G. M. Cooney, D. C. Winter, C. K. Simms, Optimising suture-based wound closure using a surrogate abdominal rig, *Bioengineering in Ireland*, Galway (2016).

Glossary

Term	Definition
Anterior	Relating to or situated towards the front of the body
Aponeurosis	Flat, broad tendinous structure towards the front of the body
Arcuate Line	An imaginary line that marks the lower limit of the posterior rectus sheath. It occurs approximately 5cm inferior to the umbilicus
BMI	Body mass index is a measurement of a person's mass, normalised by their height. It is calculated by dividing the mass by the square of the height.
Caudal	See inferior
Contra-	Opposite
Cranial	Related to the skull or in the direction of the skull
Dorsal	Pertaining to the back
Fascia	A sheet of fibrous connective tissue enveloping or separating any soft structures of the body
Hernia	Protrusion of an organ, or part of an organ, through the wall of a cavity that normally contains it
Inferior	Located closer to the bottom of the feet than another
Infra-	Below. See inferior
Ipsi-	Same
Laparoscopy	A minimally invasive surgical procedure using small, keyhole sized ports, a fibre optic camera and long thin instruments
Laparotomy	Surgical procedure usually involving a large cranio-caudal incision in the abdominal wall along the linea alba
Lateral	Relating to or situated towards the side
Linea Semicircularis	See Arcuate Line
Medial	Relating to or situated towards the midline
Obese	Being grossly overweight, typically with a BMI greater than $30 kg/m^2$
Port	See trocar
Posterior	Relating to or situated towards the back of the body
Pubic Symphysis	The midline cartilaginous joint connecting the left and right rami of the pelvis
Superior	Located closer to the top of the head than another
Supra-	Above. See superior
Trocar	A surgical instrument with a cutting point encased in a tube used for gaining access in laparoscopic surgery, also referred to as a port
Umbilicus	Scar on the abdomen at the site of attachment of the umbilical cord
Ventral	Pertaining to the front
Viscera	Soft internal organs of the body
Xyphoid Process	Small, cartilaginous extension of the lower part of the sternum

Chapter 1

Introduction

Over the past thirty years there has been a dramatic change in the methodology of abdominal surgery. The introduction of digitalisation, miniaturisation, improved optics, novel imaging techniques and computerised information systems in the operating theatre have greatly reduced risk to the patient and the length of time required to complete the surgery. Laparoscopic surgery is a relatively new surgical procedure that has significantly changed the way abdominal surgery has been performed since the late 1980s [Wexner & Cohen (1995)]. The first reported laparoscopic surgery was performed by a surgeon called Phillipe Mouret in Lyon in France who conducted a cholecystectomy[1] using a gynaecologists instruments. This minimally invasive technique is performed through keyhole-sized ports in the abdominal wall which considerably reduces trauma, lowering the risk of infection, shortening hospital stays and improving cosmetic results, it has rapidly increased in popularity with over two million patients undergoing laparoscopic procedures in the USA each year [Fuller et al. (2003)]. However, there are still medical situations that require the more invasive laparotomy surgery and it is estimated that the same number of people (two million) undergo the procedure in the USA each year [Nezhat et al. (2013)]

Unfortunately, despite the medical advances in recent years, incisional hernia can form post-operatively, a situation whereby contents of the abdominal cavity protrude through a weakness in the abdominal wall as a result of improper trocar site wound closure (commonly at the linea alba near the umbilicus [Hegarty (2007), Katkhouda (2010), Moran (2005)]).

[1] Cholecystectomy: The surgical removal of the gall bladder

Such cases have a prevalence of approximately 1-5% for laparoscopic surgery [Boldo et al. (2007), Bowrey et al. (2001), Helgstrand et al. (2011), Heniford et al. (2000), Kadar et al. (1993), PLAUS (1993)] and can even be as high as 20% for open laparotomies [Bucknall et al. (1982), Mudge & Hughes (1985), Park et al. (2006), Sanz-Lopez et al. (1999)], meaning that, in the U.S alone, up to 200,000 cases of both port site incisional hernia and post-laparotomy incisional hernia occur each year. Patients who suffer from obesity are at considerably more risk of developing a hernia [Uslu et al. (2007)] post-operatively due to greater intra-abdominal pressure and a large fatty layer that inhibits the surgeons access, view and dexterity. Unfortunately the incidence of incisional hernia looks set to steadily rise due to increasing levels of obesity apparent in nearly all developed countries [Flegal et al. (2002)].This outlines a clear need for a more robust solution to the current methodology of wound closure in laparoscopic/laparotomy surgery.

In response to such issues, Trinity College Dublin was approached by St. Vincents Hospital Dublin to attempt to find a suitable solution. One significantly limiting factor is the lack of any formalised technique. Surgeons typically use a suture length to wound length ratio of 4:1 [Bhat (2014)] despite there being little evidence in the literature to justify its use. Efforts have been made to quantify the optimum characteristics for suture-based wound closure [Campbell et al. (1989), Descoux et al. (1993)]. However, these studies focus on singular characteristic parameters of wound closure. As such, an adequate portrayal of the effect of a combination of parameters on the incidence of incisional hernia falls short. This knowledge gap implies that there may be more suitable aspects of a methodology to wound closure that could potentially save lives if implemented. Therefore, this project endeavors to repair that oversight.

However, it is first important to understand the mechanical properties of the abdominal tissue most associated with laparoscopic and laparotomy surgeries; the linea alba, which is the load-bearing tissue commonly involved in midline hernia formation. Unfortunately, there is limited data on the mechanical properties of the linea alba with current studies presenting conflicting results and varying experimental protocols [Campbell et al. (1989), Descoux et al. (1993), Förstemann et al. (2011), Gräβel et al. (2005), Hollinsky & Sandberg (2007)]. A particular challenge is the aspect ratio of the linea alba (approximately 2:1), complicating tensile testing significantly. Förstemann et al. (2011) presented the uniaxial

tensile response of cadaveric human tissue, yielding a stress variation of between 2-5 MPa at 10% strain in the transverse direction (parallel to fibres) and 0.2-0.85 MPa in the longitudinal direction (cross-fibre). Gräβel et al. (2005) also performed uniaxial mechanical tests on fresh human linea alba, reporting considerably less stiff mechanical profiles, but with greater scatter. Both studies use machine cross-head displacement to approximate the strain occurring in the material. However, this approach does not account for slippage of the tissue from the grips or transducer deformation. The use of image-based strain measurement methods [Ben Abdelounis et al. (2012), Lyons et al. (2013)] may have a significant improvement on the accuracy of observed mechanical properties. Furthermore, uniaxial tensile tests may not adequately represent in-vivo deformations of the tissue. The tissue is most likely loaded biaxially in-vivo during increased intra-abdominal pressure (IAP).

It is also necessary to develop an understanding of the function and physiology of the abdominal environment before any true/solid conclusions can be made. Also crucial in the design and development of a surgical device and/or medical device is an environment that ensures accurate and repeatable testing. An early stage surrogate abdomen is currently in development in Trinity College Dublin by the musculoskeletal research group under the direct supervision of Dr. Ciaran Simms and Dr. Des Winter. The rig (seen below in Figure 1.1) is currently capable of simulating the extrusion properties of porcine intestines using reconstituted powdered potato (RPP) as a suitable substitute, the culmination of a study performed recently by the Musculoskeletal research group [Lyons et al. (2015, 2013)]. Using this device, it may be possible to evaluate and further our understanding of the mechanical properties of the linea alba as well as test possible wound closure methodologies, both suture-based and mesh-based [Lyons et al. (2015)]. Evaluation of the rig itself may also determine its possible role as an apparatus for the development of surgical devices.

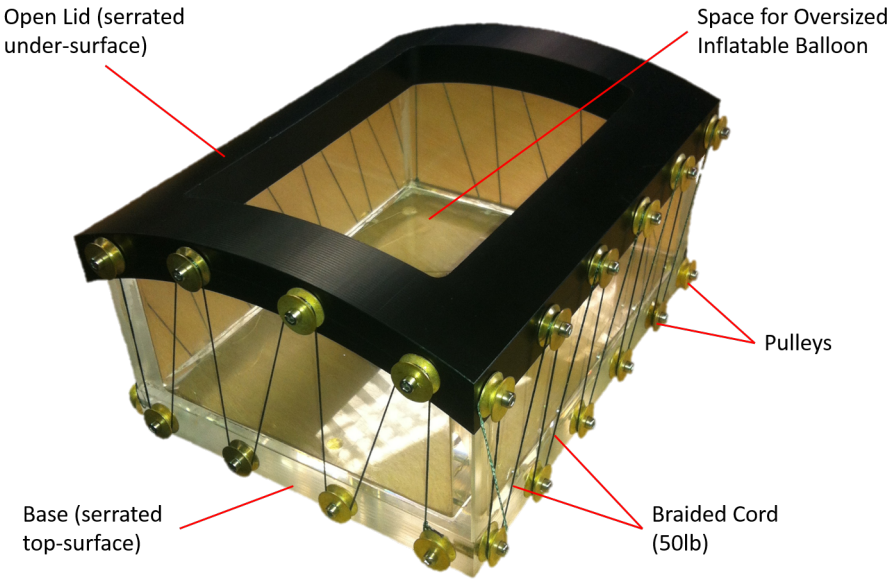

Figure 1.1: The surrogate abdominal rig currently in development in Trinity College Dublin Lyons et al. (2015).

Another issue that is of interest is the comparison of human and porcine linea alba. Obtaining human tissue of any sort in large quantities can be quite problematic within Ireland. Therefore it is necessary to use porcine as a suitable substitute for testing. However, though pigs and humans share similarities, the differences of human and porcine linea alba have not been quantified. To this end, a collaborative study into the mechanical properties of human linea alba has been organised with the muskuloskeletal research group in Washington University in St.louis, Missouri headed by Dr. Spencer Lake. The USA based group are responsible for the supply of human cadavers during a three-month study to be performed at the college.

In conclusion, the preliminary aims of this project have been established as the following:

1. Identify the mechanical properties of the linea alba using more robust techniques.

   (a) Perform Uniaxial and biaxial mechanical experiments on porcine tissue.

   (b) Determine the extent of error accumulated by using non image-based strain measurement methods.

   (c) Quantify the effect that the compression of the tissue grips have on the recorded mechanical properties of the tissue.

2. Quantify the ideal suture based wound closure parameter combinations (bite depth and separation).

    (a) Design a protocol and perform uniaxial suture-pullout experiments to determine ideal bite depth and separation.

3. Quantify the difference between human and porcine tissue and evaluate the potential use of porcine tissue as a surrogate for device evaluation.

    (a) Perform identical mechanical characterisation and suture pullout tests on human tissue from a reliable source.

4. Use the surrogate rig to evaluate the mechanical characteristics and wound closure methodologies already outlined.

    (a) Perform this evaluation using both human and porcine abdominal walls depending on availability.

Chapter 2

Background

2.1 Introduction

This chapter provides a background essential to understanding the content of this thesis. It begins with an initial outline of how laparoscopic and laparotomy surgeries are performed. Next, the anatomy and physiology of the abdominal wall are discussed, the load-bearing tissues regarded in specific detail. The different wound closure methodologies are then discussed, beginning with those for the more invasive laparotomy and ending with an alternative for laparoscopic surgery. The generation of intra-abdominal pressure is then reviewed before a final discussion about the different types and forms of hernia.

2.2 Laparoscopic/Laparotomy Surgery

Traditionally, surgery has required large incisions allowing the surgeon to access the patients body with his/her hands while maintaining sufficient light to monitor their performance. In the case of the abdomen, it is called a laparotomy; a severely invasive and risky procedure that is still performed today depending on the circumstance. It requires weeks, and in some cases months, of recovery time. Until recently (late 1980's), laparotomies were the only available solution for surgeons faced with a patient's internal bodily problem. Over the past twenty years, however, there has been a dramatic change in the methodology of surgery. The introduction of digitalisation, miniaturisation, improved optics, novel imaging techniques

and computerised information systems in the operating theatre have greatly reduced risk to the patient and the length of time required to complete the surgery.

Many surgeries have become image-guided; the use of miniature cameras to help guide the path of tools from outside the body with the aid of separate external displays. An advantage of this is that only small keyhole incisions are required (only as large as the tools requiring passage); eliminating the necessity for the surgeon to have direct contact and reducing the amount of tissue damage when compared with laparotomy. This minimally invasive technique is called laparoscopic surgery (See Figure 2.1 below). With the aid of novel articulating surgical tools and devices, it is possible for the surgeon to maintain precise movements and actions comparable with direct contact [Townsend et al. (2004)].

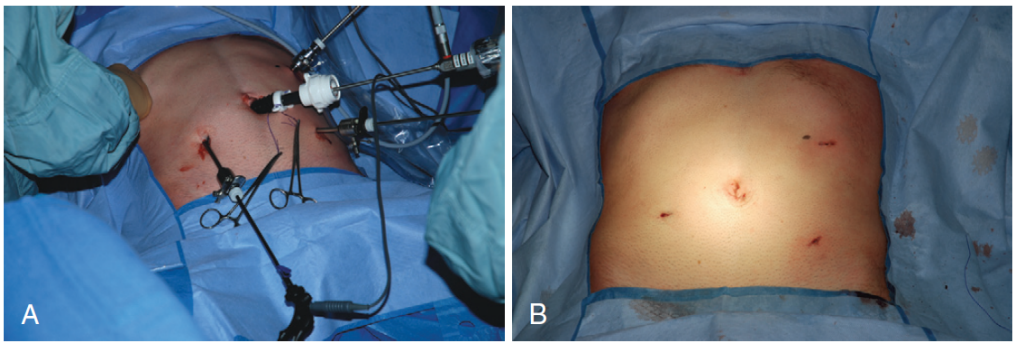

Figure 2.1: Minimally invasive laparoscopic surgery. A) The instruments are passed through trocars in the abdominal wall. B) The small incisions at the completion of the surgery. The largest incision at the umbilicus is to allow the passage of bigger tools, or the retraction of tissue [Townsend et al. (2004)].

For some procedures, even laparoscopic surgery is not possible where the procedure requires steady and precise movements that are impossible through even the most practiced human reflex. The use of robotic surgical devices and machines help act as an interface between the operating surgeon and patient. These commercially available systems employ instruments that have a greater degree of freedom than conventional laparoscopic instruments as the robotic device is not limited by the relative simplicity of the human hand. Using this system it is even possible for surgeons to perform over great distances. One drawback by this interface is that the surgeon has no tactile sense of the tissues but must adapt by using visual feedback information [Bitterman (2006)]. An example of a robotic laparoscopic surgery in progress can be seen below in Figure 2.2. It should be noted that these systems are also used in laparotomies, where a deft touch is required.

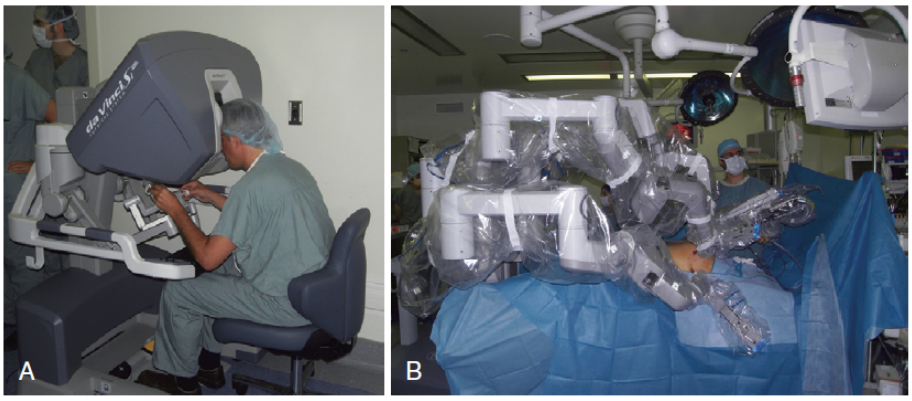

Figure 2.2: An example of robotic Surgery. A) Surgeon at console using hands and feet to control robot arms. B) Robotic setup at patient [Townsend et al. (2004)].

2.2.1 Laparoscopic Access Techniques

Laparoscopic surgery involves the insertion of ports through the layers of the abdominal wall to get access to the abdomino-pelvic cavity. Typically, laparoscopic surgery involves the use of three or more ports; one main trocar port to facilitate passage of the laparoscope and other large tools (an opening with a diameter ranging from 10-15mm) and two or more secondary ports allowing the introduction of smaller manipulation tools (openings often varying from 3mm to just above 5mm diameter). To facilitate port access, a small incision is made in the skin, subcutaneous fat and locally relevant structural tissues.

For most laparoscopic procedures the patient is supine[1]. The first and largest port is usually established centrally at the umbilicus; using the natural passage to the abdominal cavity, sealed at birth, by applying a steady force, twisting the port until it punctures through. However, this method can be prone to infection [Tinelli (2012)] and in some cases the surgeon will opt for a more bacteria free environment; through a curvilinear incision around the umbilicus, a small incision just below it through the linea alba, above the arcuate line on the border of the umbilical and hypogastric regions (see Figure 2.3 below), or through a small incision three fingerbreadths above the umbilicus verging on the epigastric region (depending on the surgical target) [Hegarty (2007), Katkhouda (2010), Moran (2005)].

[1] The supine position is an orientation of the body where the subject is lying down with the face up.

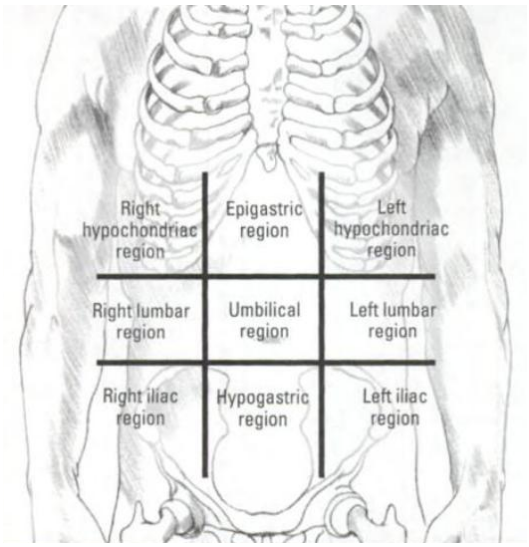

Figure 2.3: Regions of the abdomino-pelvic cavity [Wilkins & King (2002)].

A pneumoperitoneum[2] is then created through this initial opening by gas insufflation (up to a pressure of approximately 15±1 mmHg; 1.99±0.13 kPa) and, once established, a camera is inserted through the trocar cannula. Subsequent secondary ports are then introduced. Their insertion carries less risk than the main port as the abdominal wall is lifted away from the bowel by the pneumoperitoneum and the point of the trocar can additionally be monitored, by laparoscopic camera from the main port, as it pierces the parietal peritoneum. Their positioning is dependent on the surgical target and on the preference of the surgeon. Instruments introduced through the ports should ideally converge on the surgical target at an angle of between 60-90 degrees to ensure adequate manoeuvrability. Ports are usually located 15cm apart to prevent trocars interfering with one another during surgery [Moran (2005)].

If piercing through the right and left lumbar regions, the anterior and posterior rectus sheath as well as the transversalis fascia and peritoneum must be incised while passage through the rectus muscle is accomplished by reflecting the muscle fibres. Through the right and left iliac regions below the arcuate line, there is no posterior rectus sheath. Therefore only the anterior rectus sheath, transversalis fascia (thicker below the arcuate line) and the parietal peritoneum need to be incised at this point before the trocar can be pushed into the

[2] The pneumoperitoneum in laparoscopic surgery is the creation of an artificial space in the abdominal cavity through gas insufflation.

abdominal cavity.

Traditionally, the pneumoperitoneum is created using a device called a Veress needle. It involves the blind insertion of a spring loaded disposable or re-useable Veress needle through the linea alba, made visible by a small skin incision, to the peritoneal cavity to facilitate gas insufflation. This is then followed by the blind insertion of the first trocar. However, this has been increasingly abandoned as a practiced technique as it carries a risk to the bowel, and in slim patients major injuries to the aorta and iliac vessels have been reported [Gould & Philip (2011), Moran (2005)]. New single-port techniques have also been developed whereby a large port (20mm diameter) at the umbilicus is used which allows for the passage of a laparoscope and two surgical instruments. It helps minimise the scarring and incisional pain associated with the multiple points of entry used during traditional laparoscopic surgery [Kehoe (2011)]. However, this technique is not applicable in all situations.

2.2.2 Laparotomy Technique

Laparotomy is much more invasive than its laparoscopic counterpart. Requiring significantly larger incisions, severe tissue damage can accrue. There are many different types of incision that can be used for laparotomy; the choice of such incisions being influenced by the operation planned, the location of the probable pathology, the body habitus [3] of the patient, and the presence or absence of previous scars [Scott-Conner (2009)]. These factors also influence the size of the incision. However, should the incision pass through muscle, the surgeon may choose to minimise the incision length as muscle cells cannot regenerate once destroyed [Damjanov (2013), Mulholland & Doherty (2006)].

The surgeon begins by making a straight incision through the skin and fatty outer layer of the patient's abdomen (see Figure 2.4 A below). The fat and skin are then pulled slightly to the side to give the surgeon a better view of the deeper tissues underneath (Figure 2.4 B). With the aid of both a scalpel and scissors, a second incision is made through these interior layers (Figure 2.4 C). These layers are also pulled to the sides by retractor clips allowing the surgeon to perform with ease (Figure 2.4 D).When muscle layers are encountered, they are

[3] Body habitus is the medical term for physique and is defined as endomorphic (overweight), ectomorphic (underweight) or mesomorphic (normal weight)

split in the direction of their fibers rather than divided; preventing denervation of the muscle [Scott-Conner (2009)]. The operation is concluded by suturing closed first the internal tissue layers and then the skin [Demetriades et al. (2015)].

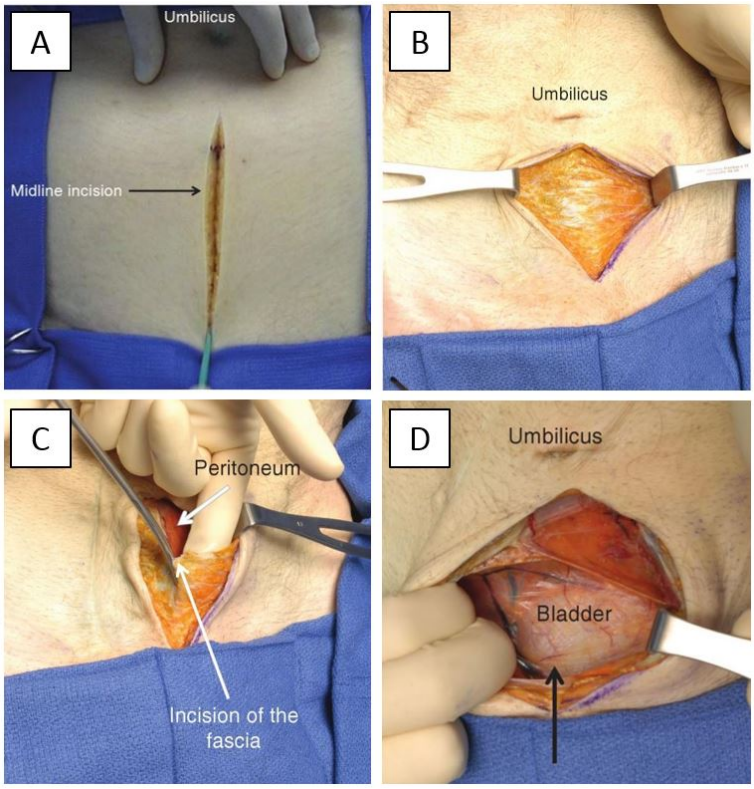

Figure 2.4: Laparotomy access technique for a typical infra-umbilical midline incision showing A) the initial cut through the superficial fatty layer, B) the metal retractors used to help present the sub-cutaneous tissues, C) the cut through the internal tissues and D) the retraction of the external and internal tissues of the abdominal wall [Demetriades et al. (2015)].

The three most common types of laparotomy incision are vertical midline incisions, horizontal (transverse) incisions and oblique incisions. Vertical midline incisions (see Figure 2.5 A below) provide the best form of access to the abdomino-pelvic cavity. Being centralised, the surgeon can reach any part of the cavity with ease. This makes it an ideal choice for exploratory laparotomy [Scott-Conner (2009)]. The incision follows the path of the linea alba, an acellular internal tissue whose fibers run transversely. This method can be problematic in that severing the fibers of this load-bearing tissue can make it more difficult to heal than other options; the forces applied laterally due to muscle contraction exacerbating wound apposition. However, the tissue is sparsely vascularised and therefore relatively bloodless making bleeding during surgery less of an issue.

Horizontal/transverse incisions (see Figure 2.5 B below) are sometimes made slightly oblique so that the skin approximates in such a way during healing that it affords positive cosmetic results. The surgeon will usually try to follow the path of underlying oblique muscle fibres and fibres of the fascial tissues. The rectus muscle is usually retracted away as its fibres run counter to the direction of the incision. This is less problematic than the vertical incision as the internal forces act in the direction of the incision and not against closure [Mulholland & Doherty (2006), Scott-Conner (2009)].

Similarly, oblique incisions follow the path of the underlying fascial tissue and muscle. Using the body's natural architecture as a guideline increases the healing capability of the patient and helps reduce the occurence of post-operative problems.

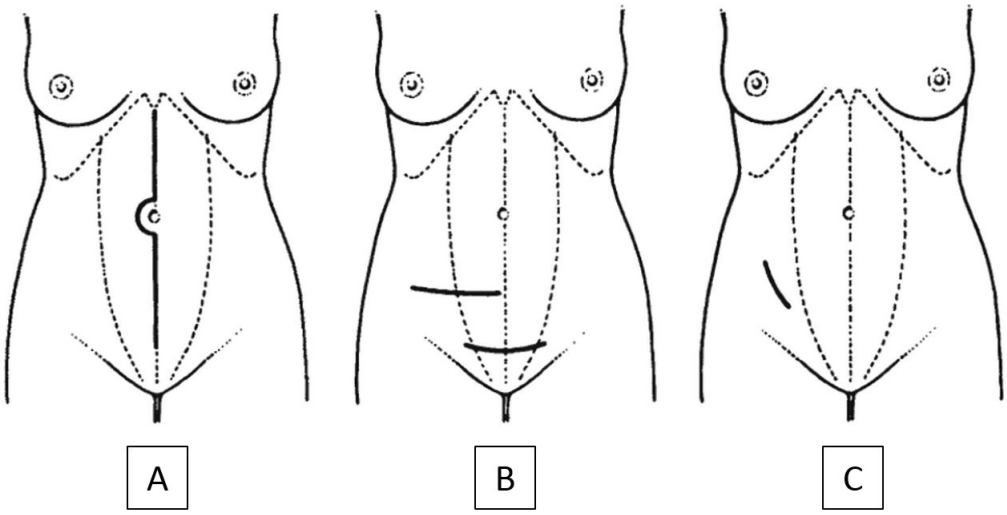

Figure 2.5: Three examples of types of laparotomy incisions typically used; A) a vertical midline incision, B) horizontal/transverse incisions and C) an oblique incision [Skandalakis & Skandalakis (2013)].

2.3 Physiology of the Abdominal Wall

The abdominal wall acts as the boundary of the abdominal cavity; encasing the visceral organs within, protecting them from the outside environment and anchoring muscles to permit functional movement. It is split into a posterior region (back), lateral region (sides) and anterior region (front). Laparoscopic surgery of the abdomen is generally performed through the anterior region which is depicted below in Figure 2.6. The lower abdomen is divided into

two separate zones by the arcuate line (linea semicircularis) which is defined by the position of the oblique aponeuroses relative to the rectus muscle. It is generally located midway between the umbilicus and pubis and represents the transition zone in which the aponeurosis of the external oblique, the internal oblique, and the transversus abdominis muscles all pass anterior to the rectus muscle [Bourgeois et al. (2005)].

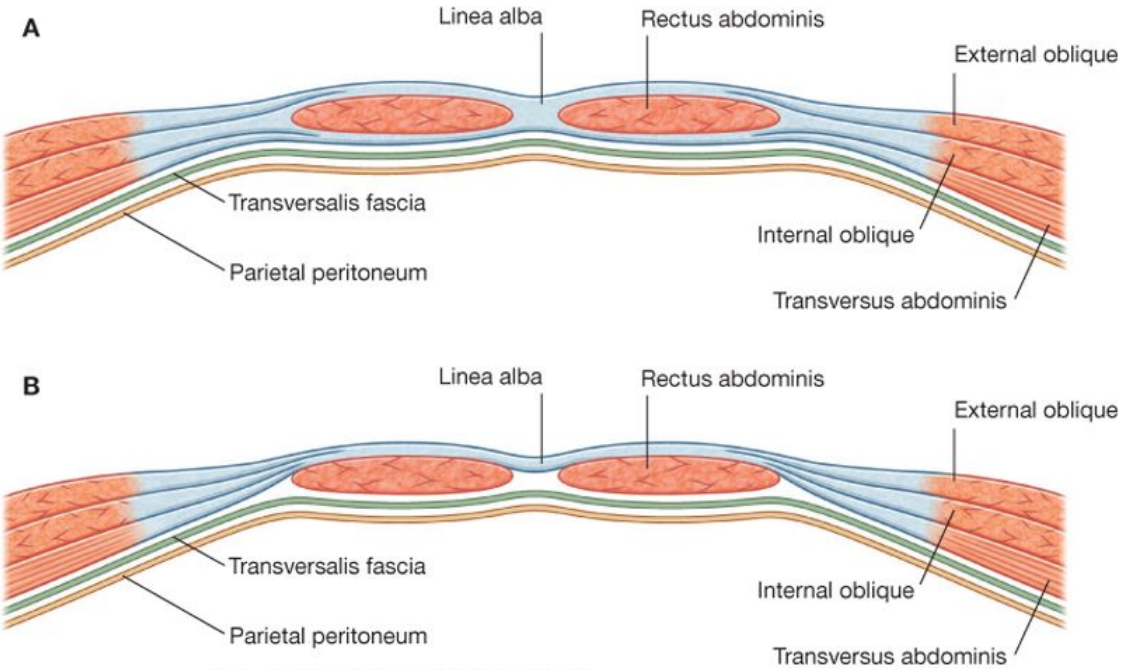

Figure 2.6: Organisation of the rectus sheath. A) Transverse section through the upper three-quarters of the rectus sheath. B) Transverse section through the lower one-quarter of the rectus sheath [Drake et al. (2009)].

The anterior abdominal wall contains several tissue-types (see Figure 2.6); the most notable of which are linea alba, transversalis fascia and parietal peritoneum tissues and the rectus abdominis, external oblique, internal oblique and transversus abdominis muscles.

2.3.1 Inactive Tissues

The linea alba is a vertical fibrous band of tissue that divides the anterior abdominal wall along the midline in the lower abdomen. It is formed by the fusion of the decussating aponeurotic fibres of the rectus sheath (originating from the lateral abdominal muscles) and is represented by a slight median groove in the abdominal wall [Bendavid (2001), Fritsch & Kühnel (2008), Snell (2011)], as can be seen above in Figure 2.6. It is identified by its

boundary to the rectus muscles on either side ; see Figure 2.7 below.

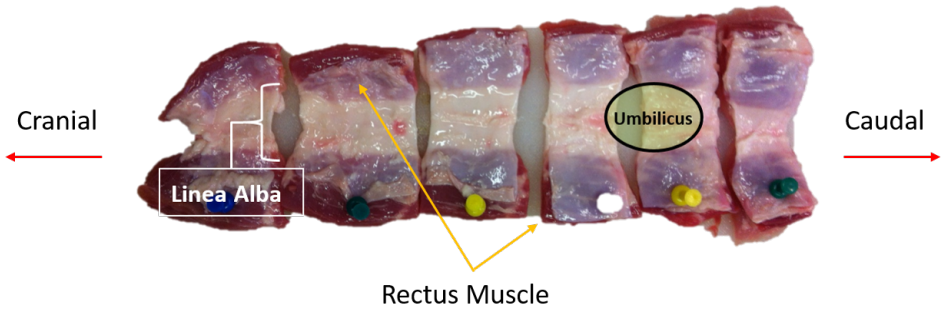

Figure 2.7: Identifying the linea alba [Cooney et al. (2015)].

These aponeurotic fibres that make up the linea alba are essentially like tendons or ligaments, with the major difference being that they originate from large flat muscles and thus take on the form of large, flat sheets. The orientation of the collagen fibres in the tissue differs from ventral to dorsal, dividing into three separate zones of oblique, transverse and irregular fibres respectively as can be seen in a cross-sectional sketch of the linea alba below in Figure 2.8 (i) and the confocal image of human linea alba in Figure 2.8 (ii). It is a continuing pattern seen in the ventrolateral abdominal muscles [Axer et al. (2001*b*), Gräβel et al. (2005)].

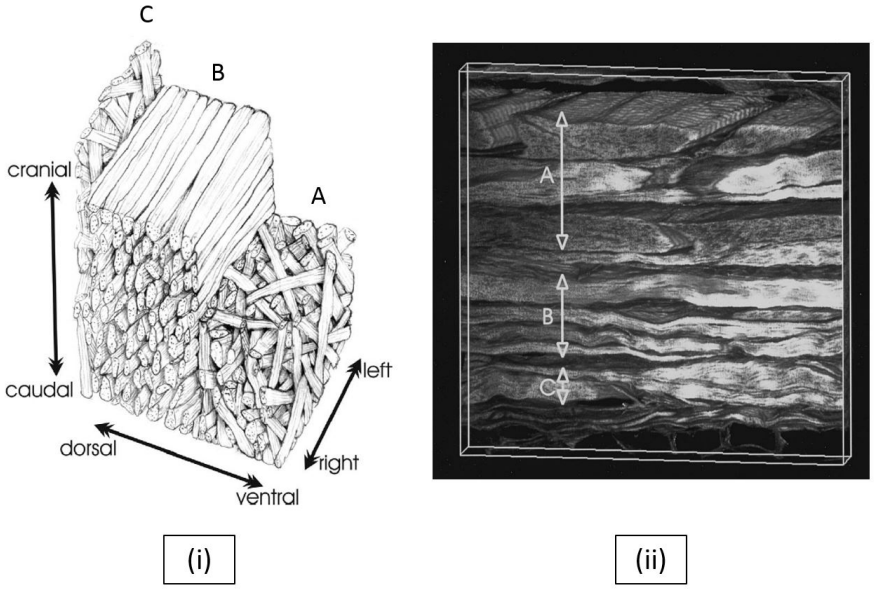

Figure 2.8: Structural representation of the linea alba showing i) an anatomical model of collagen fiber architecture in the linea alba [Gräβel et al. (2005)]. ii) depicts the structure derived from confocal microscopy of histological samples. The ventral side of the linea alba is at the top of the picture, the dorsal at the bottom [Axer et al. (2001*a*)]. The architectural zones of both images are described from ventral to dorsal as: (A) oblique fibre layer, (B) transverse fibre layer, and (C) irregular fibre layer

The function of the linea alba is to help maintain the IAP and prevent un-necessary loading of directionally biased muscles (rectus abdominis; functions principally in the cranio-caudal direction). It is a junction of the lateral muscle aponeuroses of both sides of the abdomen which pass around the rectus muscle (see Figure 2.9 below) and prevent it from being loaded laterally. The muscle fibres of the rectus muscle are principally orientated in the cranio-caudal direction. Any lateral load/deformation applied to this muscle would most likely impair its functionality. Effectively separating the right and left rectus abdominis muscles, it also allows for a greater degree of precise movement than what would be observed with a single, undivided band of continuous muscle. It is considered important surgically as longitudinal incisions in it are relatively bloodless [Weber et al. (2011)]. While the linea alba is relatively narrow but thick below the umbilicus (navel), it can be as much as 2.5cm wide and flat above it. This may account for the rarity of midline hernias below the umbilicus [Morales-Conde (2002)].

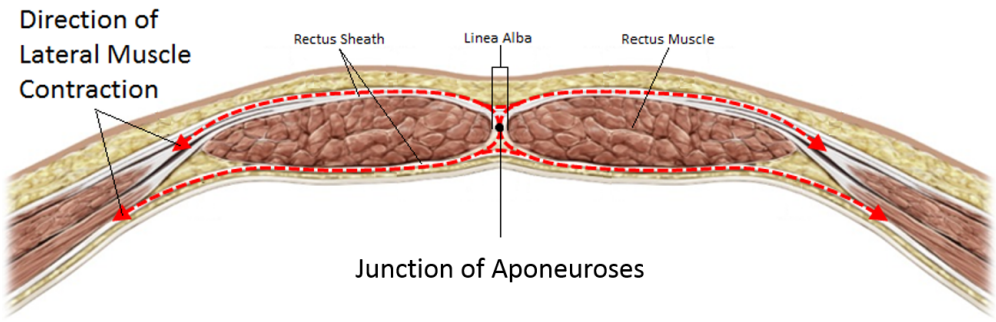

Figure 2.9: Cross-section of the abdominal wall showing the direction of applied force by the lateral muscles on the lateral load-bearing tissues of the abdominal wall [Knisley (2013)].

The aponeuroses of the abdominal muscles combine to form an intra-muscular fibrous layer known as the rectus sheath.The sheath consists of an anterior and posterior layer on either side of the rectus abdominis. The anterior layer is reinforced by the aponeuroses of the external oblique muscle and the posterior layer is reinforced by the aponeuroses of the transversus abdominis muscle (section 2.6). This layered arrangement is evident from the costal margin (medial margin formed by the false ribs) above to a variable point below, usually midway between the umbilicus and the symphysis pubis [Strauch et al. (2009)]. At this point, the posterior rectus sheath ends in a curved margin called the arcuate line of Douglas, as alluded to above. This can be seen in the series of images shown below in Figure

2.10, depicting a histological view of the abdominal wall localised at the linea alba. Note the morphological differences going from supra-umbilical to infra-umbilical (cranial to caudal). In the supra-umbilical zone, the posterior and anterior rectus sheath join to become the linea alba with it being composed primarily of irregular fibres at this point. In the transition zone the linea alba appears smaller as both rectus muscles are positioned closer together. Approaching the infra-arcuate zone the space between the rectus muscles virtually closes up with no posterior rectus sheath present. Fibre orientation becomes mostly oblique at this point [Axer et al. (2001*a*)]. The posterior side of the rectus muscle is sheathed solely by the transversalis fascia and peritoneum in this zone.

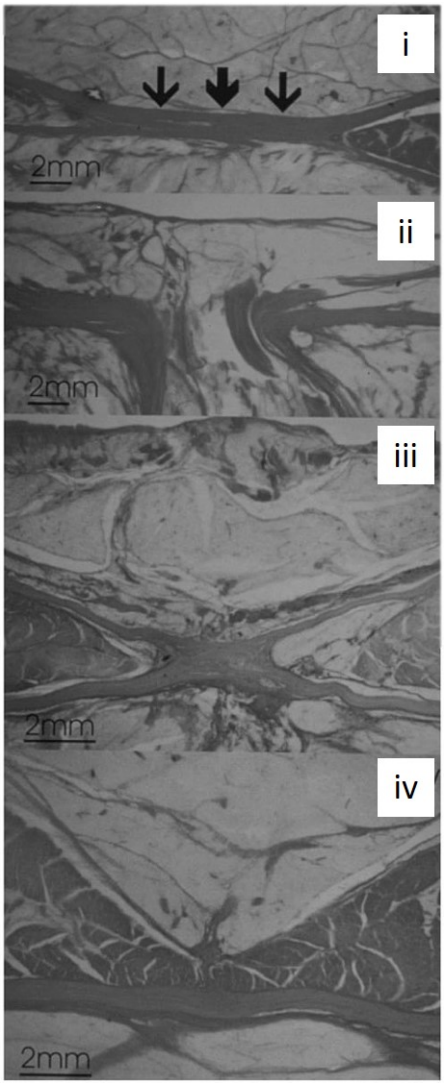

Figure 2.10: Light microscopic images of the linea alba (black arrows). Examples of the larger-scale architectural pattern of the linea alba in four cranio-caudal zones are shown from top to bottom: (i) supraumbilical part, (ii) umbilical part, (iii) transition zone, (iv) infraarcuate part. Posterior side is top and anterior side is bottom [Axer et al. (2001*a*)].

Because of its link to the aponeuroses of three muscles of varying directions of contraction, the rectus sheath has a layered collagen structure with collagen fibres running in several directions. However, the anterior and posterior rectus sheaths can have very different structures above the arcuate line. The anterior sheath retains a predominantly oblique fibre structure (see Figure 2.11 A) as it is progenerated by the aponeuroses of the oblique muscles while the posterior sheath remains mostly transverse, being an extension of the transverse fibre aponeuroses of the transverse abdominus muscle [Axer et al. (2001*a*,*b*)].

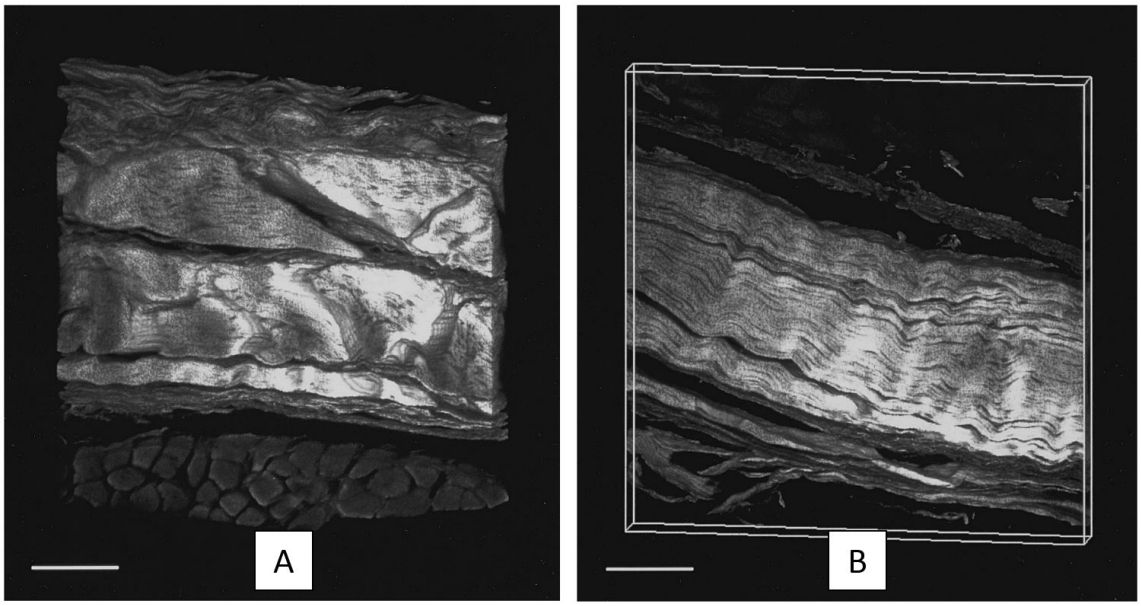

Figure 2.11: Confocal microscopy examples of fibres in the anterior (A) and posterior (B) rectus sheath. Layers of oblique fibres can be seen in (A) while (B) retains a mostly transverse structure. Bar = 100 μm [Axer et al. (2001*a*)].

The transversalis fascia (TF), sometimes referred to as the endoabdominal fascia, forms a complete, uninterrupted sheet around the interior of the anterior abdominal wall and lies deep to the transversus muscles and the linea alba. Its primary function is to separate the layers of tissue and muscle of the abdominal wall from the internal organs of the abdominal cavity rather than provide a load-bearing structural support; having little intrinsic strength. Loose areolar fibrous fatty tissue called extraperitoneal fat separates the TF from the underlying parietal peritoneum [Bell et al. (2012), Netter (2010)].

The TF is thicker in the lower half of the abdomen, below the arcuate line, due to the absence of the posterior rectus sheath (part of the lining around the rectus muscles that combine to form the linea alba). Above the arcuate line, the TF is so closely attached to the

overlying posterior rectus sheath that the rectus sheath, peritoneum and TF appear to form a single layer that can be difficult to distinguish [Wood et al. (2010)].

From a standpoint of physiology and anatomy, little is known about the transversalis fascia [Bendavid (2001)]. It was originally stated by Sir Astley Cooper (first described and named the tissue more than two centuries ago) that the transversalis fascia contains two layers; a deep/posterior layer and an anterior layer [Cooper (1807)]. It was believed by Cooper that this structure varied from bi-layer to single layer depending on the anatomical position of the particular transversalis fascia under scrutiny; as can be seen below in Figure 2.12. However, the number of layers is still, as of yet, a topic of considerable debate. Most academics do agree that, at the very least, a thickened layer of transversalis fascia is encountered in certain regions of most individuals [Bendavid (2001), MacFadyen (2004)].

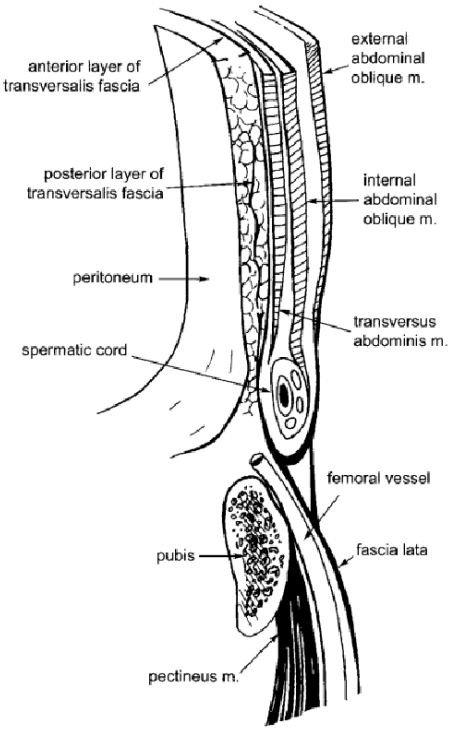

Figure 2.12: Longitudinal section of the anterior abdominal wall and inguinal region showing both the posterior layer and anterior layer of the Transversalis Fascia [MacFadyen (2004)]

The peritoneum is a thin serous membrane (smooth stratum containing a thin layer of cells that excrete a serous fluid) that lines the wall of the abdomino-pelvic cavity and covers most of the intra-abdominal organs; limiting and confining their movement. It is the most extensive membrane in the body and even covers more surface area than the skin.

It curves to surround the hollow viscera, the liver and the spleen and to form ligaments (produced by certain folds of the peritoneum) and mesenteries (peritoneal fold attaching to small intestine; the space between which is technically outside the peritoneal cavity) [Rossi & Rossi (2001)]. It consists of two layers: a superficial mesothelial stratum and a deep connective stratum. The mesothelium is a single-layer epithelium made up of mesothelial cells. The deep connective stratum is made up of elastic collagen-reticular fibres arranged into loose bundles that interlace in a plane parallel to the surface. One of the principle functions of the peritoneum is to minimise friction of muscle movement and allow free movement of the visceral organs. It is also serves to resist or localise infection, and store fat [Di Zerega & DeCherney (2000), Rossi & Rossi (2001)].

Although they are ultimately one continuous sheet, there are two types of layer of peritoneum: the parietal peritoneum and the visceral peritoneum. The parietal peritoneum is attached to the abdominal wall and the visceral peritoneum is wrapped around the internal organs themselves that are located inside the intra-peritoneal cavity. The potential space between these two layers is called the peritoneal cavity and is filled with a serous fluid that experiences extremely low friction/drag that allows the two layers to slide freely over one another [Di Zerega & DeCherney (2000), Rossi & Rossi (2001)]. The peritoneum in general plays a relatively minor role in solute and fluid exchange. It is a trait exploited in peritoneal dialysis in the event of kidney failure, whereby dialysis solution is injected into the peritoneal cavity which interacts with the capillary membranes present in the peritoneum [Nolph (1989)].

2.3.2 Muscles

The rectus abdominis is a long strap muscle that extends from the costal cartilages and xyphoid process to the front of the symphysis pubis and pubic crest along the abdominal wall [Snell (2011)]. It is divided into distinct segments by three transverse tendinous intersections that allow the muscle to curve as it contracts while exerting a bending force on the spine. The muscle is broader above the arcuate line and is closer to the midline; the linea alba separating the right and left rectus muscle [Snell (2011), Tank & Grant (2012)]. The rectus abdominis is important as a postural muscle and is responsible for flexion of the lumbar spine; bringing the

rib-cage and the pelvis together simultaneously (if neither is fixed). It also assists in breathing and plays an important role in respiration when forcefully exhaling, such as when performing the act of coughing. It also functions as a corset, in combination with transversus abdominis, trussing the abdominal organs in place and pushing them upward to make a fulcrum over which the thoracoabdominal diaphragm is draped [Ward (2003)]. It also helps in creating intra-abdominal pressure when active in order to allow a person to vomit or defecate.

The external oblique muscle forms the surface muscle layer of the lateral abdominal wall. It is the largest of the three muscles of the lateral abdominal wall and functions to pull the chest downwards, bringing the thorax closer to the pelvic rim; aiding the functional capability of the rectus abdominis. As such, it can aid in expiration due to the increasing pressure in the abdominal cavity. It also has limited actions in both lateral flexion and rotation of the vertebral column [Morales-Conde (2002)].

The internal oblique muscle is located under the external oblique muscle in the antero-lateral division of the abdominal wall. Its fibres run perpendicular to the external oblique muscle [Bendavid (2001)] and, as such, its contraction creates an opposite pull to that of the external resulting in rotation; lowering the thorax on the ipsilateral side of the contraction. It acts with the external oblique of the opposite side to achieve this torsional movement of the trunk. It also acts to oppose the forces created upon contraction of the diaphragm, helping to reduce the volume of the thoracic cavity during exhalation [Morales-Conde (2002)].

The transversus abdominis muscle (so named for its fibre orientation) forms the deepest layer of muscles of the anterolateral abdominal wall. It is the main muscle in the retention of the abdominal viscera. This makes it very important in terms of respiration as it displaces or blocks the visceral mass under the diaphragm at the end of the initial stage of inhalation. The powerful traction of this muscle on the linea alba tends to separate the margins of a laparoscopic incision, which accounts for the high frequency of wound dehiscence subsequent to vertical midline incision of the abdominal wall [Bendavid (2001), Morales-Conde (2002)].

2.3.3 Use of Pigs in Research

Much academic research currently is based on using animal tissue (mostly porcine) in liu of human tissue which can be difficult to obtain, especially in large quantities. Anatomically,

humans and pigs can be somewhat different however. Humans have 12 pairs of ribs whereas pigs are known to have as many as 15. This means that muscle placement may differ which would result in aponeuroses that intersect with the linea alba at slightly different angles. Accordingly, the microstructure of the linea alba which defines its anisotropy may be slightly different in pigs than in humans. Furthermore, both external oblique muscles in pigs seen in Figure 2.13A below can be seen to almost join at the linea alba below the umbilicus; something not seen in human tissue (see Figure 2.13B). In both cases however, the linea alba is wider and thinner above the umbilicus (see Figure 2.13A & C) [Antranik (2016), Cochran (2010), Rath et al. (1996)].

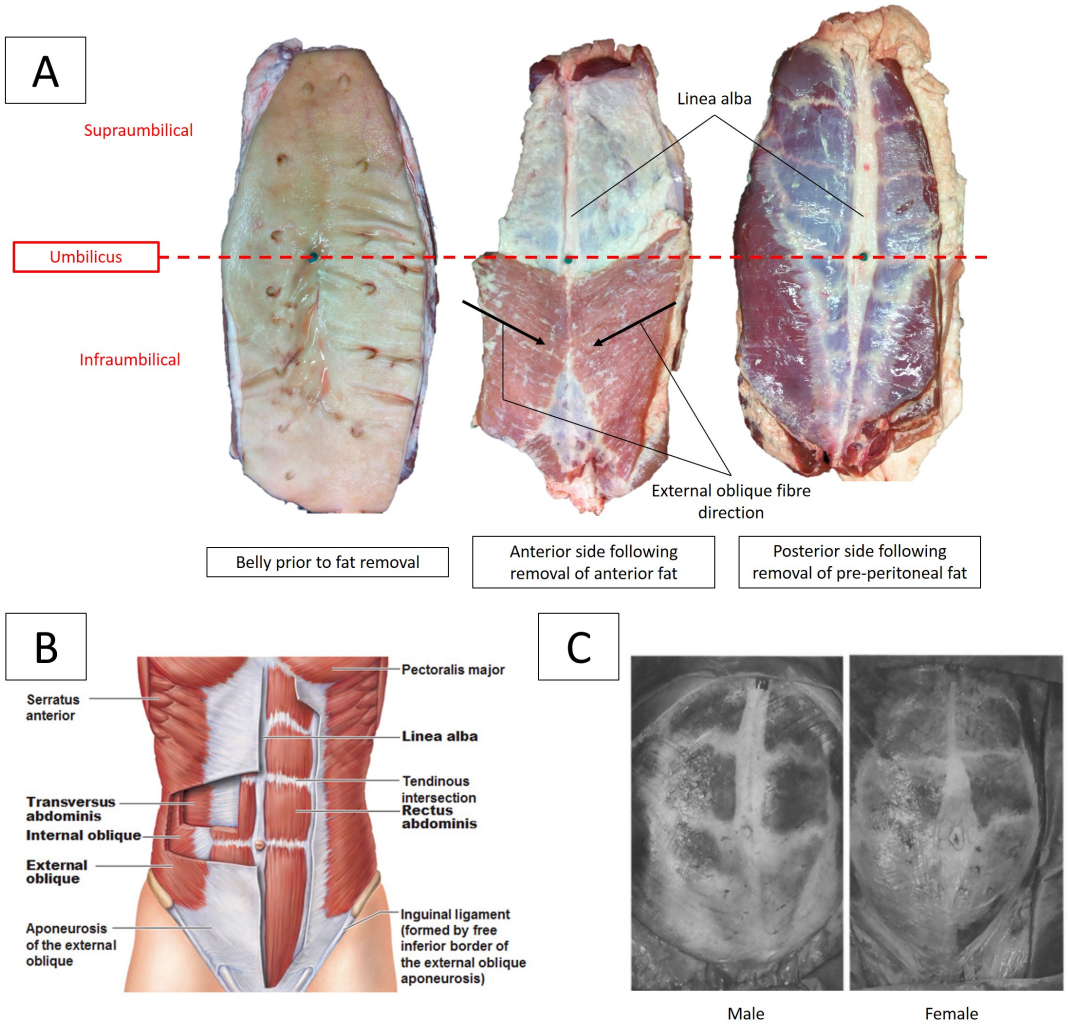

Figure 2.13: A comparison of porcine and human abdominal anatomy showing (A) a dissection of the porcine abdominal wall highlighting the linea alba and fibre orientation of the abdominal muscles, (B) a Graphical depiction of the human abdominal wall [Antranik (2016)] and (C) the human abdominal wall of cadaveric specimens (male and female) with surface fat and external abdominal muscle removed [Rath et al. (1996)].

2.4 Post-Operative Wound Closure Methodology

At the end of the surgery, the apertures created during the procedure require closing. In general, secondary port sites 5mm can be allowed to heal naturally and only require suturing of the skin. In primary port sites ≈10mm and greater, the body's immune system is insufficient to repair the incised fascial tissue alone and can result in incisional hernia (see Section 2.6.2). In such cases artificial closure of the skin and tissue is encouraged in order to help aid the body's own response [Cinel et al. (1997), Ghavamian (2010)]. Presently there are two devices used in laparoscopic wound closure; surgical sutures and meshes.

2.4.1 Surgical Sutures

Surgical sutures are medical devices that are used to hold tissues of the body together following an injury or surgery. This involves using a needle with an attached length of suture thread. Its physical application is similar to that of conventional sewing. The use of sutures as a surgical technique dates back to 3000 BC in ancient Egypt, where sutures were used to complete the act of mummification. Early sutures used by Romans to treat the wounds of live patients were manufactured using animal gut or intestines [Nutton (2004)]. The first synthetic suture threads (absorbable and non-absorbable based on poly-vinyl alcohol) were produced in the 1930s; the relative ease of mass production of this type of suture, coupled with emerging sterilisation techniques at the time, helped reduce the amount of deaths as a result of sepsis following surgery during World War Two. Absorbable sutures do not need to be removed, but are theoretically more inflammatory and may be more likely to result in a severe reaction. It must also be noted that absorbable sutures lose tensile strength over time as they break down. However, they are advantageous for use with internal tissues where suture removal would require another invasive surgery [Chung (2015)]. Both absorbable and non-absorbable sutures can come in two different forms, braided and monofilament. Monofilament sutures are advantageous in that they provide less drag, have no interstices to support bacteria growth and have a smooth surface that allows easy passage through tissue. However, braided sutures are more pliable and flexible, have considerably better knot-holding security and can support increased tension. A further sub-category of some common suture types can be seen below in Table 2.1 [Boess-Lott & Stecik (1999), Chung (2015), Defense (n.d.)].

Table 2.1: The different suture types

Suture Types								
Absorbable					**Non-Absorbable**			
Braided		**Mono-filament**			**Braided**		**Mono-filament**	**Metal**
Vicryl	Vicryl Rapide	Monocryl /PDS II	Fast Absorbing Catgut	Chromic Catgut	Ethibond	Silk	Ethilon	Staples

Vicryl sutures are braided, synthetic and absorbable and can offer greater strength than other absorbable suture types. There is generally less tissue reaction and it can come in another variant called Vicryl Rapide that is designed to break down more quickly for use with faster healing tissues such as mucous membrane.

Monocryl is a mono-filament synthetic suture that is more pliable than Vicryl sutures, making it easier to handle and knot. PDS II sutures are similar but have a much longer duration of absorption than monocryl sutures and are stiff and difficult to handle.

Fast absorbing Catgut sutures (made from raw material of sheep and beef intestines) are advantageous in that they are ideal for tissues where rapid healing is expected to occur (sub-cutaneous tissue and tying superficial blood vessels). However, they are known to increase the formation of pus and have high tissue reactivity. The Chromic Catgut suture has been treated with chromic oxide so that it will resist digestion or absorption for longer periods of time.

Ethibond is a braided, polyester synthetic, non-absorbable suture that has a highly adherent coating that is relatively non-reactive and acts as a lubricant to mechanically improve the physical properties of the uncoated suture.

Silk is advantageous in that it is highly compliant, making it easier to handle. However, it causes a host reaction since silk itself is a foreign protein. Therefore it is generally used only in uncontaminated wounds that are in well-perfused areas of the body (ex. the face).

Ethilon monofilament sutures afford good knot security and low tissue reactivity. However, even though they are non-absorbable, the knot security decreases over time in-vivo. Therefore they are typically not used in cases where permanent retention is required.

Metal suture staples have commonly been used for surgical wound closure. They are advantageous in that they can be easier and quicker to apply than any other suture type and

the wound healing results are equivalent. However, metal sutures can be highly irritating for the patient and are generally reserved for emergency situations [Boess-Lott & Stecik (1999), Chung (2015), Defense (n.d.)].

Most current-day sutures are made from polymer fibers and modern absorbable suture materials can be tailored to have a specific degradation rate, allowing for both a short and long-term life span. In laparoscopic surgery, manual surgical suturing and knot-tying remain important as there is not yet a simple mechanical substitute that is able to function coherently for specific manoeuvres in the tight spaces of the body [Zucker (2001)].

2.4.2 Suture Techniques

Usually, for laparoscopic incisions, the surgeon may only use one loop of suture to close the wound by tying it off with a knot. However, the longer incisions used in laparotomy require a more complicated suturing technique. There are many different techniques and patterns of surgical suturing of laparotomy incisions designed to be used for different tissues and/or situations. Overall, the multitude of patterns each fall into one or more of four categories: (1) Simple or mattress, (2) Interrupted or continuous, (3) Appositional (inverting or everting) and (4) Tension-relieving. Examples of some of the different suture patterns can be seen below in Figure 2.14 along with their corresponding suture bite cross-section [Hendrickson (2013)].

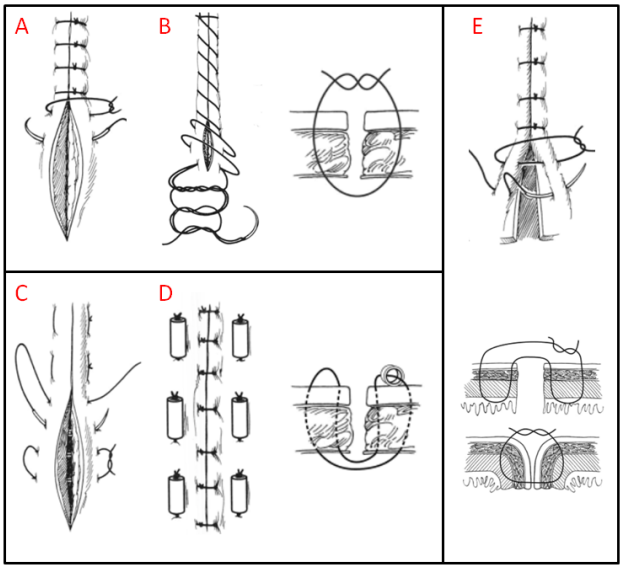

Figure 2.14: Types of suture pattern: (A) Simple interrupted suture, (B) Simple continuous suture, (C) Interrupted horizontal mattress suture, (D) Tension-relieving interrupted horizontal mattress suture, (E) Inverted interrupted Lembert suture [Hendrickson (2013)]

Simple or matress patterns involve one (simple; Figure 2.14a,b,e) or two (mattress; Figure 2.14c,d) passages of the suture on each side of the wound. These are often combined with interrupted (Figure 2.14a,c,d,e) or continuous (Figure 2.14b) patterns whereby knots are tied following each suture passage or one suture thread is used to create a series of connected passages with a knot tied on each end of the suture line respectively. Appositional patterns close the the wound so that the like faces of the incision remain in contact. Inverting (Figure 2.14e) and everting appositional patterns force the edges of the incision to roll inwards and outwards respectively (outer or inner layers apposed). Tension relieving patterns (Figure 2.14d) are designed for tissues under greater tension. They are usually employed to create a slight eversion so that when the suture is removed, the resultant scar has a tendency to flatten rather than widen. Rubber pieces placed along the length of the suture are often used in this pattern in order to help relieve the tension on the wound itself, preventing excessive aggravation [Hendrickson (2004, 2013), Slatter (2003)].

The suture pattern most commonly associated with peritoneum and fascia closure in the abdominal wall is the simple continuous suture pattern. It is quicker and simpler to apply than the interrupted pattern; due to limited space available to the surgeon, each application of a new suture may cause aggravation to the one applied prior to it as the surgeon will have to push tissue/fat to the side in order to gain access. However, the interrupted is beneficial in that it allows the surgeon to precisely adjust tension at each point along the wound [Slatter (2003)].

2.4.3 Meshes

Prosthetic meshes are an alternate method of wound closure that are more commonly used to repair fascia at trocar entry sites following laparoscopic surgery that have excessive scar tissue (possibly due to previous surgeries having been performed in the same region). Scar tissue has different inherent mechanical properties than its native tissue and can be considerably weak by comparison [Hollinsky & Sandberg (2007)]. Therefore using sutures can be problematic as they rely chiefly on the mechanical properties of the tissue at the wound site and, in the case of scar tissue, can often result in incisional hernia [Cassar & Munro (2002), Luijendijk et al. (2000)]. The advantage that meshes have over sutures in this regard is their ability

to be anchored further down the length of the tissue, away from any scarred tissue. This also allows the full extent of the damaged region to be tension-free, permitting more natural, uninhibited repair. They also create a barrier between the incision site and the abdominal viscera, preventing any interaction. Meshes are typically fixed to the patients abdominal wall by sutures, tacks or glue [Beldi et al. (2011), Hollinsky & Göbl (1999), Lyons et al. (2015), Schmidt & Langrehr (2006)].

However, using meshes to treat conventional first-time laparoscopic surgical incisions may be inadvisable as they do not act to fully close the opening that was created as is true with the act of suturing (forcing the two sides of the incision to become co-linear). It merely acts as a tension-release plug. This means that more tissue needs to be repaired which in turn can potentially increase the chance that a greater amount of scar tissue will form. Other complications associated with the use of meshes include mesh adhesion to the abdominal viscera, mesh migration and/or shrinkage, complications relating to the fixation method and mesh erosion into an organ [Chand et al. (2012), Ferrone et al. (2003), Jenkins et al. (2010), Lyons et al. (2015)].

2.5 Intra-Abdominal Pressure

The intra-abdominal pressure (IAP) is the natural pressure within the abdominal cavity arising due to its compartmentalised nature and being bordered by muscles (the most active of which is the diaphragm). At rest the abdomen experiences a positive pressure of 0.5-1.5kPa and in ill patients this can rise to 2-2.5kPa [Addington et al. (2008), Campbell & Green (1953), Cobb et al. (2005), Malbrain et al. (2004), Ravishankar & Hunter (2005)]. During exercise the abdomen can experience pressures greater than 20kPa for short intervals of time. However, if the abdomen is subjected to sustained high pressures, organ dysfunction and/or failure can occur; organs become compressed which causes constituent fluids (incompressible due to their water content) to be expelled via a network of vessels. Simple automatic responses like coughing or sneezing can also temporarily raise the IAP significantly.

2.5.1 Physiology of Coughing

In obese patients, herniations of laparoscopic wounds (incisional hernia) are a common occurrence at the incision site before the tissue can fully heal. Therefore, in order to successfully prevent herniation, the closed wound needs to be able to withstand the common pressures generated by the body such as the act of coughing and simple bowel movements (abdominal straining) or equilibration of pressure in the middle ear and sinuses (valsalva manoeuvre; involving abdominal muscle contraction). It has been found in some studies that cough impulses especially can be problematic and can lead to eventual herniation [Nassar et al. (1997)], which cause a brief but significant increase in intra-abdominal pressure. This increases tension in the abdominal wall and focuses the forces involved around weaker parts of the wall (i.e. site of incision closure).

A cough is induced as a result of the stimulation of receptors within the airway depending upon interactions with branches of the vagus nerve, nucleus retro-ambiguous, and nucleus ambiguous of the medulla oblongata at the base of the brain. Vagal afferent nerves are responsible for regulating involuntary coughing. However, higher cortical influences can control cough behaviour, either inhibiting or voluntarily producing a cough [Middleton et al. (1978)].

There are three stages to coughing: inspiration, compression and expiration [Leith et al. (1986)]. Inspiration is the inhalation of a variable volume of air which can be supressed to some extent in some cases in order to minimise the penetration of foreign bodies into the airway.

Compression describes the physical contraction of the costal and abdominal muscles at the onset of expiration. The glottis is closed as the muscles activate, preventing any air from escaping. The diaphragm remains contracted as the volume of air in the lungs decreases, causing an increase in the intra-abdominal pressure.

During expiration the glottis opens and the diaphragm relaxes. The diaphragm is forced upwards by the pressure in the abdomen, causing the air in the lungs to be forcefully exhaled. The high pleural pressure also aids in expiration.

2.5.1.1 The Muscular Influence

Essentially, all the muscles that attach to the rib-cage have the potential to generate a breathing/coughing action as a result of their physical contraction. However, those specifically linked with the abdominal wall are principally involved with the expiratory stage of breathing/coughing. These muscles, seen below in Figure 2.15, are sometimes referred to as the muscular corset [McConnell (2011)].

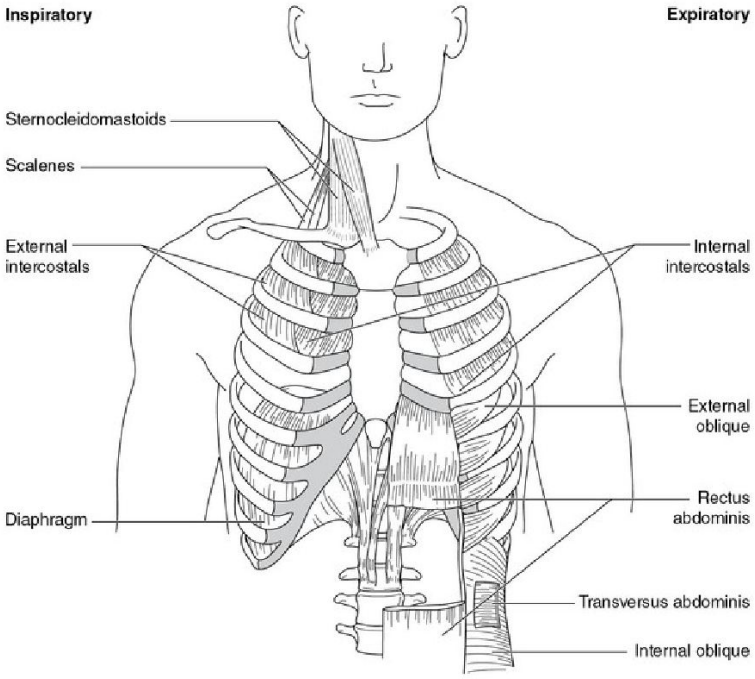

Figure 2.15: The breathing pump muscles [McConnell (2011)]

During coughing the abdominal muscles contract, pulling the abdominal wall inward and increasing abdominal pressure. It has been stated that this pressure rises to approximately 102.6-121.2mmHg (13.64-16.13kPa) [Addington et al. (2008)]. At rest, the abdomen experiences a positive pressure of 0.5-2.15kPa (see Section 2.5). This increase in intra-abdominal pressure during coughing causes greater stress to be applied to the abdominal wall and organs and, as such, can be detrimental to the healing of closed laparoscopic wounds. In severe cases where sutures have been improperly applied (more common in obese patients where the surgeon experiences decreased visibility) herniation can result.

2.6 Hernia

A hernia is defined as the displacement and protrusion of an organ, or part of an organ, through the cavity wall that normally contains it [Dorland (1980)]. The abdominal cavity is bound on its lateral and ventral side by a combination of muscle, fat and non-cellular tissue called the abdominal wall. The cavity is also bounded superiorly and inferiorly by the diaphragm and pelvis respectively. All these components act to enclose and pressurise the abdomino-pelvic space. This is what then allows hernias to form. When the pressure inside the abdominal cavity is greater then the pressure beyond its boundaries, a weakness/opening in those boundaries could result in the viscera exuding through (i.e. a hernia). This can be mortal as the exuding viscera can then become strangulated (incarcerated hernia) and eventually cease to function entirely [Bendavid (2001, 2004)]. There are many different types of hernia though the most common types that affect the abdominal wall are umbilical and incisional hernias.

2.6.1 Umbilical Hernia

An umbilical hernia involves the protrusion of the intra-abdominal contents through a weakness or defect at the site of the umbilical cord usually as a result of abnormal decussating fibres in the linea alba. As a result of this deficiency, the visceral organs can sometimes form outside the abdominal cavity during foetal development. Umbilical hernia is therefore a common incidence among newborns but, although the defect can sometimes be quite large, it tends to resolve itself without any treatment by 2-3 years [Lissauer & Clayden (2007)]. Obstruction or strangulation of the hernia is quite rare because the underlying defect is usually too large to be of any issue. In adults it is largely acquired and is more frequent in pregnant or obese women. An acquired umbilical hernia directly results from increased intra-abdominal pressure caused by obesity, heavy lifting, a long history of coughing, or multiple pregnancies [Brandt (2008)].

2.6.2 Incisional Hernia

Incisional herniae arise due to a defect in the abdominal wall as a result of an incompletely healed surgical incision. This is usually directly caused by haematoma, seroma or infection at the site of the surgical wound. The incidence of incisional herniation following a laparotomy or other large open surgery is reported to be as high as 20% [Bucknall et al. (1982), Mudge & Hughes (1985), Park et al. (2006), Sanz-Lopez et al. (1999)]. Fink et. al. reported that risk of hernia increases significantly from 12.6% at year one to 22.4% three years after surgery; a relative increase of 60% [Fink et al. (2014)]. For minimally invasive techniques such as laparoscopic surgery, an incidence rate of approximately 1-3% was reported [Boldo et al. (2007), Bowrey et al. (2001), Heniford et al. (2000), Kadar et al. (1993), PLAUS (1993)] A commonly cited potential cause of these incisional herniae is the inadequate closure of one or more layers of the abdominal wall. In obese patients there is a greater associated risk that herniation will occur following laparoscopic surgery due to the increased difficulty accessing the tissues required to be sutured (as can be seen in Figure 2.16) making surgical error more likely. Increased IAP in obese patients due to their weight also presents a further factor of risk of herniation [Imme & Cardi (2005), Lambert et al. (2005), Sugerman et al. (1996)].

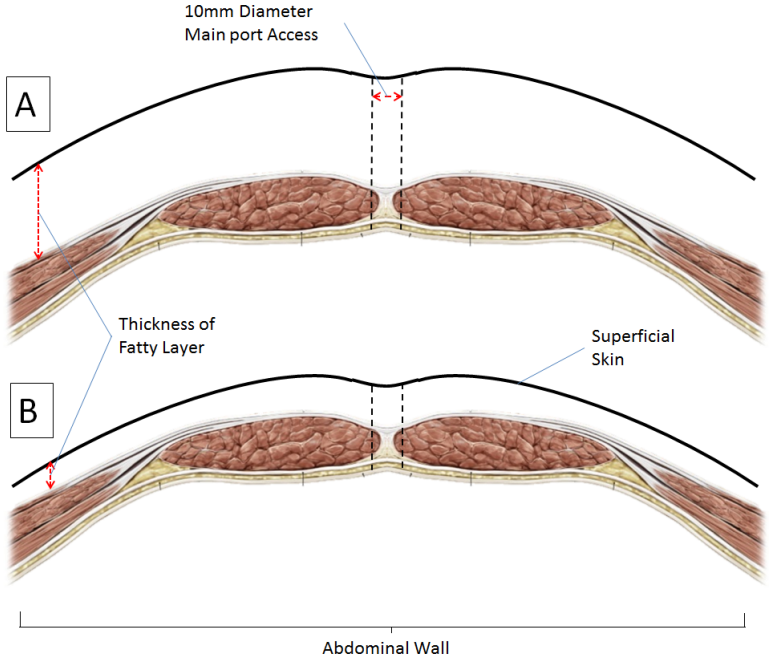

Figure 2.16: Cross-section of the abdominal wall showing that for the same access port diameter, an increase in the size of the fatty layer due to obesity (A) can hinder access to objective tissues (Linea alba) when compared with someone of normal weight (B) [Knisley (2013).

Smoking, the use of steroids, age and diabetes can also diminishes the bodies ability to self-repair. Therefore this population is also at greater risk of developing an incisional hernia after open or laparoscopic surgery than the general population [Imme & Cardi (2005), Sørensen et al. (2005), Sugerman et al. (1996)]. Due to this significant risk to the large proportion of people that may need to undergo laparoscopic surgery, there is a need for research into procedural methodology and equipment design to help secure the patients safety.

Chapter 3

Literature Review

3.1 Introduction

This chapter begins with a short account of some models of the abdoment and intra-abdominal pressure. How constituent tissues are stressed and how they respond to that stress in order to maintain the IAP will be a matter of interest. In order to develop an optimal wound closure technique, it is important to first understand the inherent mechanical properties of the separate tissues that define it. To this end, this chapter concludes with a review of studies on the tensile (uni-axial and equi-axial) mechanical properties of these tissues that have been carried out to-date.

3.2 Physical Models of IAP

One example of a surrogate rig being used as a novel method for repeatable testing was in a study performed by Schwab et al. [Schwab et al. (2008)]. A bio-mechanical model for the simulation of three-dimensional pressure and shear forces in the inguinal region was developed; seen below in Figure 3.1. This allowed for a simulated IAP of approximately 20-25kPa (the approximate pressure experienced by the body in an agitated state; see section 2.5) with a rough wall elasticity in the range of 20-30%.

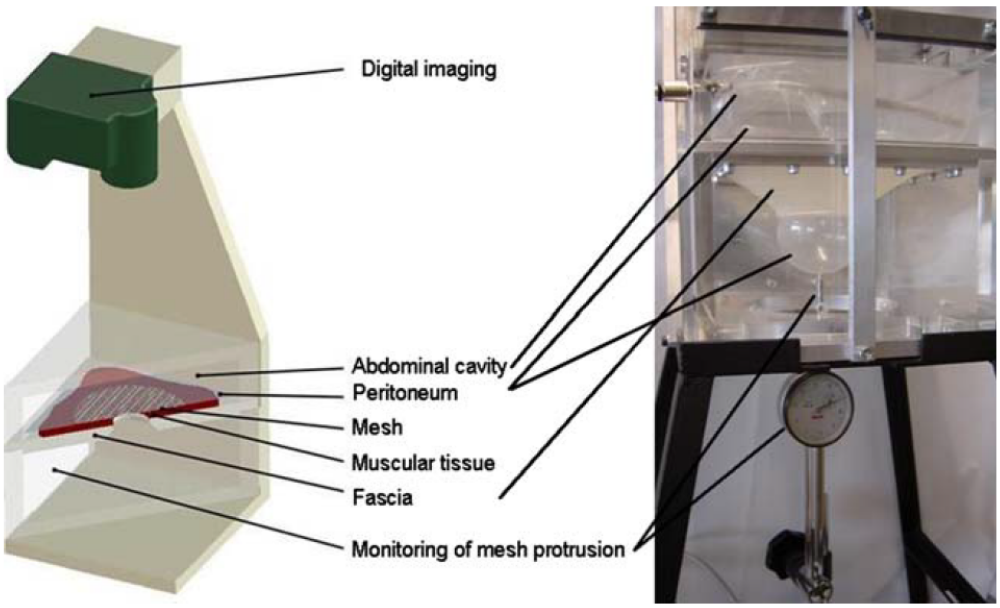

Figure 3.1: An example of a physical surrogate model of the abdomen using synthetic materials [Schwab et al. (2008)].

By using two surrogate layers as substitutions for the fascia and peritoneum. It was possible to replicate the occurrence of a hernia in an in-vivo scenario and assess the performance of different types of meshes; investigating the impact of varying overlap, defect size, mesh type or fixation technique in a model of otherwise static bio-mechanical parameters. The so-called hernia test stand (Figure 3.1) is characterized by two main components. The first component is a pressure chamber that simulates the abdominal cavity. This includes a highly elastic and ultra-thin silicone sac to mimic the peritoneum, which can be expanded by air pressure. By replacing the genuine abdominal wall by a standardized silicone membrane with comparable bio-mechanical properties, it is possible to eliminate a primary source of error due to variations in the anatomical specimen. This works quite well as a geometrical approach. However, there has been no detailed comparison of the surrogate materials used and their biological counterparts, meaning the hydrostatic nature of biological tissue could mean it would present a different mechanical response.

In another study by Lyons et al. [Lyons et al. (2015)], a biomechanical abdominal wall model of hernia repair was developed using intact porcine abdominal walls, a pressurised surrogate rig and reconstituted powdered potato (RPP) used to mimic the extrusion properties of viscera (see Figure 3.2 below). The rig, shaped to dimensions similar to that of the

human abdominal cavity, allowed the ex-vivo pressurisation (≈1-20kPa) of an abdominal wall theoretically similar to that experienced in-vivo.

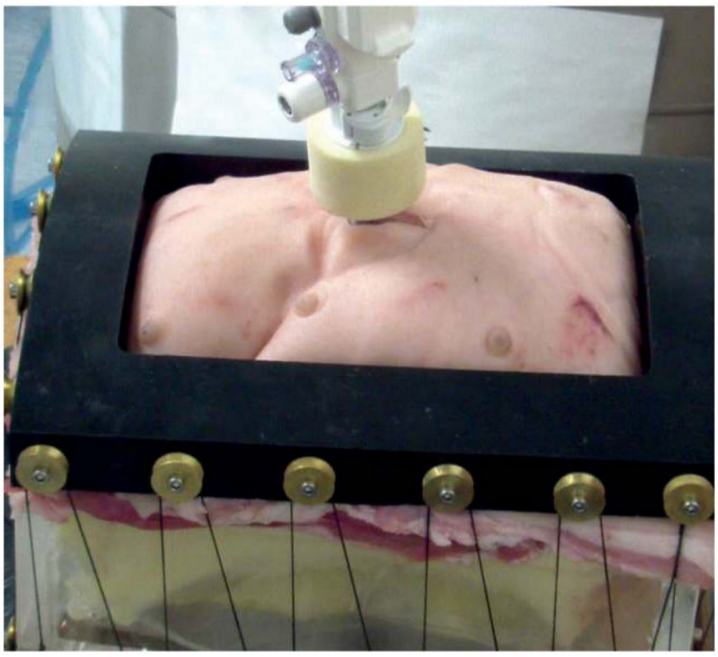

Figure 3.2: An example of a physical surrogate model of the abdomen using a combination of biological tissues and synthetic materials [Lyons et al. (2015)].

RPP was found to exhibit extrusion properties similar to that of abdominal viscera for different defect sizes and, using it as a model, a three-dimensional relationship between defect diameter, mesh diameter and pressure at onset of hernia was obtained. Herniation was defined as the pressure at which RPP/mesh began to extrude from the defect. By using biological tissue, this physical model becomes quite relevant to an in-vivo standpoint. Though inter-specimen variation is an issue, the significance of the error has theoretically been reduced with the use of RPP as surrogate viscera; being a uniform material that can be produced to a specific and repeatable constancy. Two drawbacks from this model are that porcine tissue is used in lieu of human tissue and that frozen tissue is used instead of tissue freshly harvested. This may offer some scope to future investigations but, as it stands, this model appears the most representative of in-vivo biomechanics.

3.3 Mathematical Models of the Abdomen

Some studies, such as the volume/pressure study performed by Mulier et al. [Mulier et al. (2009)], simplify the abdominal space by relating it to uniform geometrical shapes. By making the assumption that the abdominal cavity can be represented as an infinite pressurised cylindrical vessel, the approximate stress experienced by the abdominal wall can be derived by using the formula for hoop stress:

$$\sigma_\theta = \frac{Pr}{t} \tag{3.1}$$

Where σ_θ = Hoop stress, P = Pressure/force acting radially, r = Radius of the curved inner surface of the wall, t = Wall thickness.

Lyons et al. [Lyons et al. (2014)] used this method to approximate the circumferential wall stress of the abdomen which they found to be 10kPa with regards to a 1kPa IAP. Similarly, they were able to estimate the change in volume the abdomen experiences during breathing by approximating the abdominal cavity as an elliptical hemi-cylinder; quantifying a drop in volume from 15.7 Litres to 12.7 Litres.

3.3.1 Mathematical Model of Anisotropic Tissues

The architecture of the tissues of the abdominal wall (and also essentially true of most tissues of the body) makes them anisotropic[1] in nature (see section 2.3.1). As a result of this directional dependency, it is possible to roughly model this response for bi-axial loading cases (knowing the uni-axial material properties) by applying Hooke's Law for transversely isotropic materials.

This can be used to predict strains under equibiaxial tensile loading for a range of fibre and cross-fibre direction stiffnesses (E_T and E_L respectively) and Poisson's ratio (ϑ_{TT}, ϑ_{TL} and ϑ_{LT}), as was performed by Lyons et al. [Lyons et al. (2014)] who derived the stiffness for rectus sheath from uni-axial experimental data obtained in the study. High fibre direction stiffness was paired with low cross-fibre direction stiffness and vice-versa to

[1] Anisotropy is the property of being directionally dependent, as opposed to isotropy, which implies identical properties in all directions

represent extreme experimental cases. As such, it was possible to model the behaviour of the tissue under equibiaxial loading scenarios. There are limitations to this analytical approach, particularly that anisotropic tissues are generally non-linear and closer to a fibre reinforced composite than a transversely isotropic material. However, it is useful as an approximation for understanding the behaviour of the material.

3.4 The Abdominal Wall Under IAP

As mentioned in section 2.5, the IAP at rest is typically 1kPa and can rise to as much as 20kPa in extraneous situations that involve muscle contraction. Due to how the internal fascia of the abdominal wall encompass part of the abdomen and have a direct aponeurotic connection to the abdominal muscles, they bear the majority of the load applied by the muscle contraction. As the fascial tissues are quite stiff in the direction of their fibres, the IAP proportionately increases; intra-abdominal fluids not being able to escape with sufficient speed to other parts of the body [Förstemann et al. (2011), Lyons et al. (2014)]. An example of this contraction can be seen below in the MRI and ultrasound images of the abdominal wall in Figure 3.3 [Hides et al. (2006)].

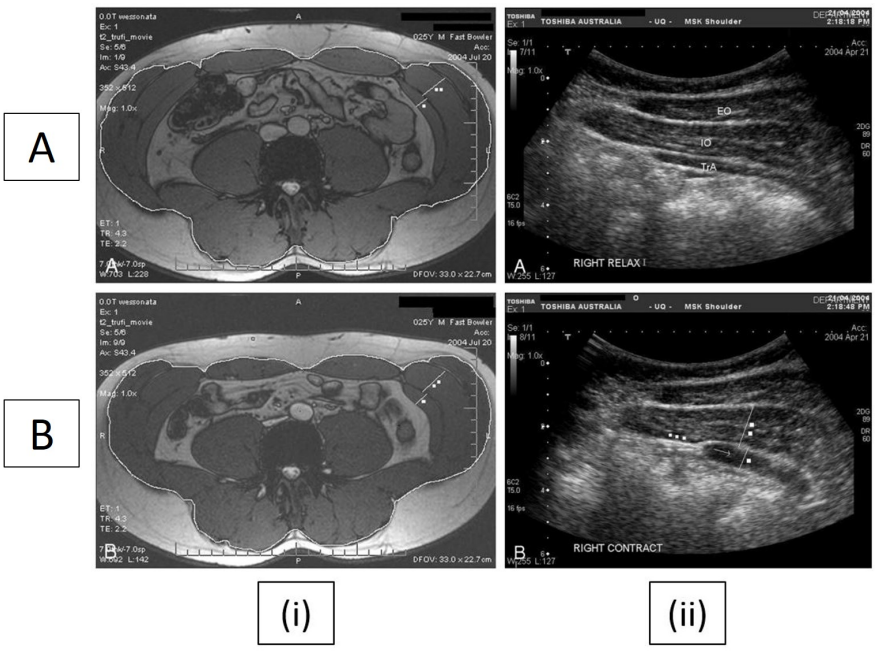

Figure 3.3: (i) MRI of the deep musculofascial corset and (ii) Ultrasound images of the right anterolateral abdominal wall at rest (A) and after abdominal muscle activation (B). A comparative difference in muscle thickness is observed [Hides et al. (2006)].

As the muscles contract (internal oblique, external oblique and transversus abdominis) they increase in girth and effectively reduce in length, pulling on the rectus sheaths and linea alba respectively. The organs and viscera compress slightly as the anterior wall contracts. The rectus abdominis muscles experience very little change, morphologically speaking, as the load applied by the lateral muscles is not directly applied to them, and is instead applied to the rectus sheath which encircles the rectus muscles and has no aponeurotiic connection with them. As such, the rectus sheath and linea alba act as the principal load-bearing tissues of the abdominal wall [Hides et al. (2006)].

3.4.1 Mechanical Loading of Principal Structures

The fascia and peritoneum are in a constant state of tension due to the intra-abdominal pressure where the abdomen is at rest (between 1-1.5kPa [Malbrain et al. (2004)]). However, as the abdominal muscles contract and decrease the volume of the cavity space, the tensile forces relax and both tissues experience contraction. Contrary to this, the linea alba and rectus sheathes experience increased tensile forces due to its direct link to the anterolateral abdominal muscles via the aponeurosis of the rectus sheath (principally the transversus abdominus; see Figure 2.6 & 3.14) [Bendavid (2001)]. The scarpa fascia is another thin layer of the abdominal wall that separates the rectus sheath and linea alba from the subcutaneous fat (see Figure 3.4 below). It has little mechanical significance, having no interaction with abdominal muscle (which plays a significant role in creating IAP), though some anatomists suggest it is responsible for attaching the skin to the deeper structures so that the skin does not sag with gravity but still stretches as the body flexes or changes shape with exercise [Ullah et al. (2013)].

The transversalis fascia exhibits anisotropic mechanical properties, being stiffer in the transverse (lateral) direction than in the longitudinal (cranio-caudal) direction [Kureshi et al. (2008)]. It is theoretically under constant transverse tension when the abdomen is at rest, due to resting IAP. Around the level of the umbilicus the transversalis fascia has a thin structure made up of an arrangement of collagen fibres (see Figure 3.4). Because it harbours no direct aponeurotic connection with the lateral abdominal muscles and is shown to fail at stresses inferior to that of other tissues (which are not observed to fail in all cases) [Förstemann

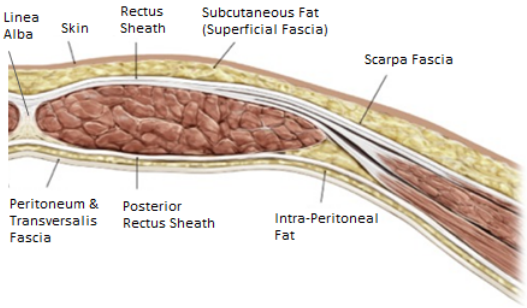

Figure 3.4: Cross-section of the abdominal wall showing the anatomical position of the constituent tissues and their relative thickness [Knisley (2013)]

et al. (2011), Kirilova et al. (2011), Lyons et al. (2014)], it is not considered a significant load-bearing structure of the abdominal wall.

Likewise, the linea alba exhibits anisotropic mechanical properties. It displays great stiffness in the transverse direction when compared with longitudinal [Förstemann et al. (2011)]. However, due to its connection with the three different anterolateral muscles which contract in opposing directions to the rectus abdominis, the linea alba has a layered structure of different collagen fibre orientations (oblique, randomly orientated and transverse). It has been stated by Viidik (1978) that the mesh-work character of the collagen architecture has some dynamic properties and, as such, can be deformed less or more before the fibres themselves come under substantial strain. This may be the role of the oblique fibres in movement, torque and stabilisation where longitudinal deformation of the linea alba occurs; a deformation which is limited by the stiffness of the rectus abdominis muscle's cranio-caudal array of muscle fibres and their mechanical contribution during contraction. Its structure defined by the aponeuroses of the lateral abdominal muscles which apply a load upon contraction, the transverse layer of the linea alba plays a significant role in resisting intra-abdominal pressure laterally, confining any significant expansion/deformation to the cranio-caudal axis of the tissue; whose mechanical properties are chiefly defined by the oblique layer of collagen fibres [Axer et al. (2001*b*), Viidik (1978)].

The rectus sheath is responsible for transmitting any load applied by the lateral muscles to the linea alba. Like the linea alba, it exhibits significant anisotropy [Lyons et al. (2014), Martins et al. (2012)]. As such its collagen fibre structure is arranged parallel to the direction of load and, bifurcating around the rectus abdominis, it helps to deflect any laterally applied

load from the muscle and any lateral load generated by the IAP; it having no direct aponeurotic connection with the muscle itself. It also serves to check the bowing of the rectus abdominus during contraction, thereby increasing its mechanical efficiency. Overall it acts to help maintain the integrity of the abdominal cavity [Singh (2011)].

To conclude, due to their direct link with the abdominal muscles, complex fibre structure and encapsulation of a large proportion of the abdominal cavity, the rectus sheath and linea alba are considered the principal load-bearing structures of the abdominal wall.

3.4.2 Tissue Properties of the Principal Structures

During laparoscopic port insertion, depending on the port site location, one or more of the mentioned tissue structures of the abdominal wall are punctured by the trocar. Consequently, these structures must be closed post-operatively. Therefore, understanding the mechanical properties of these structures needing closure is important to ensure that the stiffness between the tissue and the synthetic material used in its closure be matched. The non-linear anisotropy and viscoelastic nature of soft tissues make their structural properties particularly difficult to quantify and, as such, producing surrogate materials to replace them is no easy task. The mechanical properties of the soft tissues of the abdominal wall have, in general, been poorly reported in the literature. Quite often it is the case that publications contradict each other or exhibit a large variability in their results possibly due to species differences of specific tissues or varying experimental protocols between publications or the physical differences between donors. This highlights the difficulty in analysing a complicated structure using simplified techniques that have long been considered infallible in conjunction with conventional materials with more simplified structures.

3.4.2.1 The Abdominal Wall

Song et al. [Song et al. (2006*a*,*b*)] used an innovative technique to measure the elasticity of the abdominal wall of human patients during laparoscopic surgery. During surgery the peritoneal cavity is inflated with carbon dioxide. By applying Laplace's law for a thin-walled pressure vessel, Song et al. were able to determine the stress in the abdominal wall from the applied insufflation pressure. The strain was then determined by using image processing

techniques to track a series of markers placed on the surface of the abdomen (see Figure 3.5 below). However, in order for the thin-walled assumption to be valid the cylindrical vessel must have a wall thickness of no more than one-tenth (sometimes cited as one-twentieth) its radius [Goswami (2012)]. Song et al. reported a mean thickness of approximately 30mm (including superficial fatty layer and skin) and an average transverse radius of approximately 200mm (with sagittal radius of curvature changing dramatically with increased pressure from 600-300mm). In principle, this implies that their use of Laplace's thin-walled assumption is not strictly valid. It also must be understood that the markers used in this instance are placed on the surface of the skin, which is separated from the load-bearing tissues by a thick layer of fat. Fat is more compliant than the tissue underneath and so will not accurately mimic the same strain profiles. It is therefore not possible to accept the results stated as the general combined mechanical properties of the constituent tissues. However, this study does provide a more simplified understanding of the mechanical properties of the abdominal wall and is beneficial as a comparison with other literature (see Figure 3.7 at the end of this section).

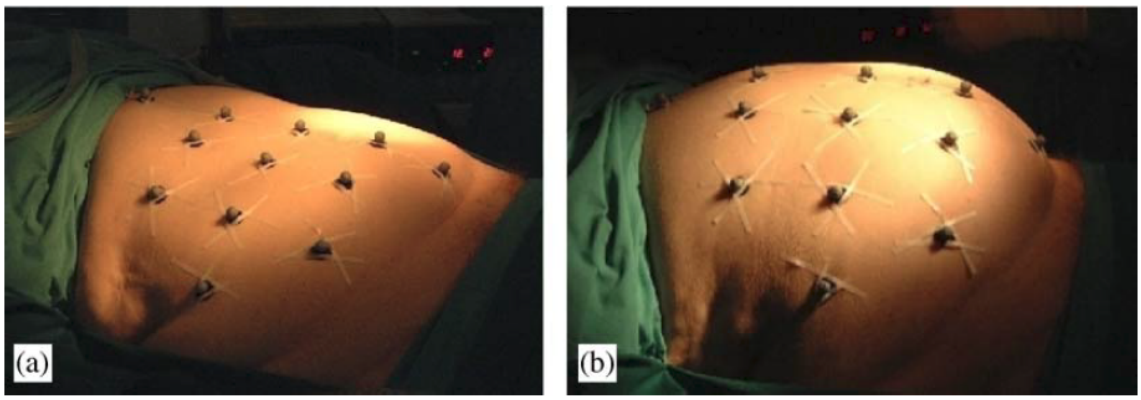

Figure 3.5: Twelve infrared markers were placed in a squared mesh format using sterilised tape, covering the surface and anatomical boundaries of half of the abdominal wall (a) flat abdomen before inflation (b) dome-like inflated abdomen. [Song et al. (2006*a*,*b*)]

Similarly, Podwojewski et al.[Podwojewski et al. (2012)] performed an experiment to quantify the mechanical characteristics of the abdominal wall of porcine specimens. These specimens had an overall mean wall thickness of ≈30mm; similar anatomical dimensions to that of human subjects, as described by Song et al.(2006). The experiment was performed by first securing the abdomen in grips and then applying a displacement load (maximum of 35mm; within the range of physiological displacement of the abdominal wall [Klinge

et al. (1998)]) along the relative sagittal axis using a rigid sphere of 12cm diameter (below in Figure 3.6 b). The load was applied at 80mm/min which was judged as slow enough to characterise the quasi-static response. Prior to loading the specimen was preconditioned using air pressure (Figure 3.6 a) for five cycles of 20mm amplitude. The applied force and sphere displacement were reported.

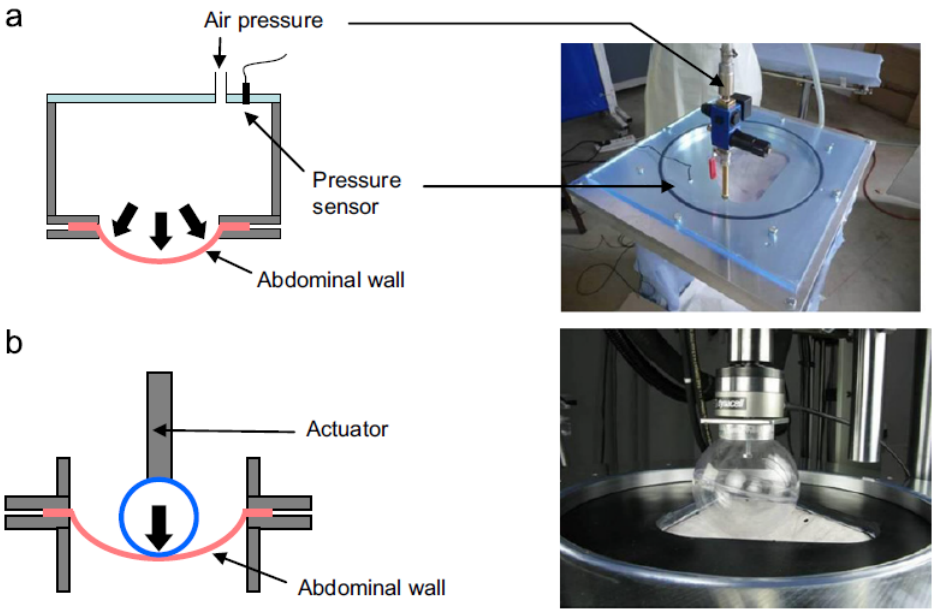

Figure 3.6: Loading mechanisms: (a) Pressure loading and (b) contact loading. [Podwojewski et al. (2012)]

While not reporting the specific circumferential stress and strain of the abdominal wall itself, these variables can be determined theoretically using Laplace's law for thin walled cylinders (see Equation 3.3 below), the data presented by Podwojewski et al. and the mean approximate thickness of the skin which can be found within the literature ($t_{Abdomen}$=1.3316mm [Lee & Hwang (2002)]). Using the data provided by Podwojewski et al. it is possible to work out the relative transverse perimeter of the abdominal wall as it is being axially deformed by applying Ramanujan's formula for the perimeter of an ellipse (an elliptical formula rather that cylindrical formula is used as the ends of the wall are bound while it is being deformed by the rigid sphere, producing an elliptical shape; see Figure 3.6), displayed below in Equation 3.2 [Berggren et al. (2004)]. This perimeter can then be used to find the relative surface strain as the load is increased.

$$p \approx \pi \left[3(a+b) - \sqrt{(3a+b)(a+3b)} \right] \tag{3.2}$$

Where p = Elliptical circumference/perimeter, a = Greater eliptical radius (half the transverse width of the abdominal wall), b = Lesser elliptical radius (axial displacement)

$$\sigma_\theta = \frac{\left(\frac{F}{pl}\right) r}{t} = \frac{\left(\frac{F}{A}\right) r}{t} = \frac{Pr}{t} \tag{3.3}$$

Where σ_θ = Hoop stress, F Applied axial force, p = Elliptical perimeter, l = Length of specimen, A = Area, P = Pressure/force acting radially, t = Wall thickness (skin in this case; for comparison with Song et al. where markers are placed on skin surface)

One setback of using this particular derivation is that it will not accurately define the strain in a directionally dependant (anisotropic) material as it assumes there is uniform strain in all directions. It also must be noted that it is assumed the application of force using a rigid sphere produces a mechanical response akin to pressure acting within a cylinder. Another point of note is that Podwojewski et al. work under the assumption that the act of freezing porcine abdominal walls before testing will have no significant impact on the mechanical properties. However, since muscle contains an abundance of cells it is natural to assume that a freeze-thaw cycle may alter the mechanical properties of the abdominal wall as a whole (as it was found to do so in arteries [Venkatasubramanian et al. (2006)]). Nevertheless, when comparing the mechanical profile to that of Song et al.(see Figure 3.7 below), yields a similar elastic modulus (slope of the linear region of the profile, excluding toe regions) if one accounts for the fact that Podwojewski's data doesn't include the 1kPa pre-load as is experienced by Song's abdominal wall in the form of resting IAP [Malbrain et al. (2004)]; concluding that the effect of freezing may be negligible. The greater toe region evident in Podwojewski et al. can be attributed to this absent pre-load.

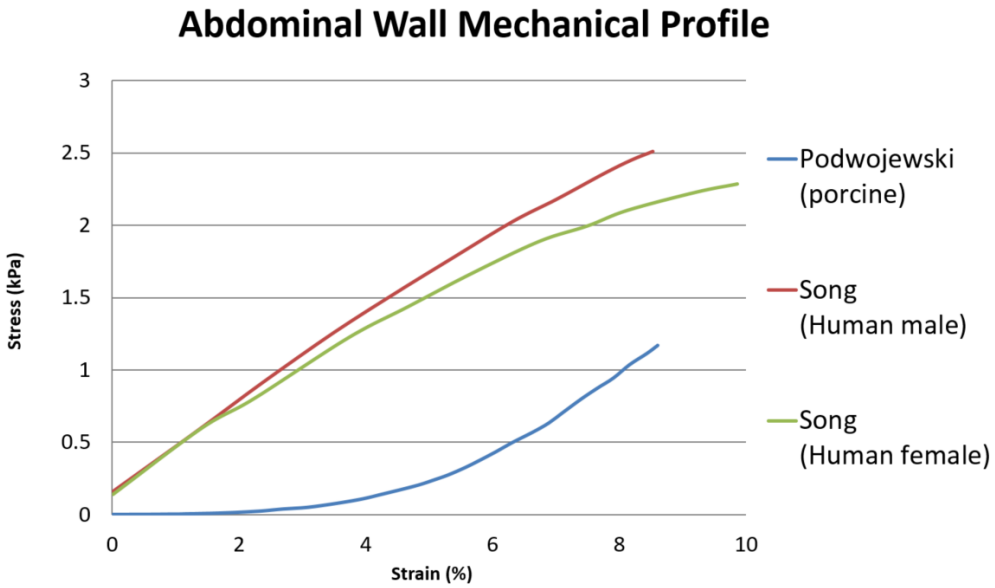

Figure 3.7: Mechanical profiles of the abdominal wall as derived from the literature[Podwojewski et al. (2012), Song et al. (2006*a*,*b*)].

Nilsson et al. [Nilsson (1982)] also investigated the mechanical properties of the abdominal wall. However, the breaking strength and elastic stiffness are reported in Newtons. Having provided no information on cross-sectional area, comparison with other literature is therefore impossible.

3.4.2.2 The Linea Alba

There are few apparent mechanical studies on the linea alba evident in the literature. This is possibly as a result of the shape of the tissue itself. Being as little as 2.5cm wide, it can be a difficult tissue to accurately test within the standard length to with ratio of 4:1 [ASTM (Standard E8/E8M)]. Furthermore, the tissue is not found within the body in any great abundance and, as such, it would not yield a large test sample size per specimen.

Förstemann et al. [Förstemann et al. (2011)] were one of the few groups who managed to perform an in-depth mechanical study on the human linea alba following harvesting and cryo-preservation of the samples over several months. Using punched samples of consistent size (see Figure 3.8 below) obtained from 50 donors (male and female), 91 uniaxial tensile tests in the transverse direction and 93 uniaxial tensile tests in the longitudinal direction were carried out using a Instron tensile testing machine. By applying a constant rate of deformation (28.5%/min strain rate), the force, length and time were recorded and an output

mean stress/strain profile determined. Results were presented as a related force (force/width). However, since the thickness was reported as 1mm in all cases the results can be taken as stress (force/[width x area]). A maximum of 10% strain was applied for all samples; yielding a stress variation of between 2-5 MPa in the transverse direction and 0.2-0.85MPa in the longitudinal direction. The graphed output of the averages can be seen in Figure 3.10at the end of this section. One minor drawback from this study is that it uses strain derived from the constant change in grip-grip distance. This will only provide a very general understanding of the mechanical properties of the tissue. The strain occurring within the material, unlike the machine cross-head derived strain, may not increase linearly with time due to slippage of the tissue from the grips and may cause an appreciable difference in both types of strain measurement (cross-head strain versus tissue strain). However, this study performed by Förstemann et al. is currently one of the only such investigations on the linea alba which provides a definitive mechanical profile of the tissue and strictly adheres to conventional standard operating procedures for tensile experiments.

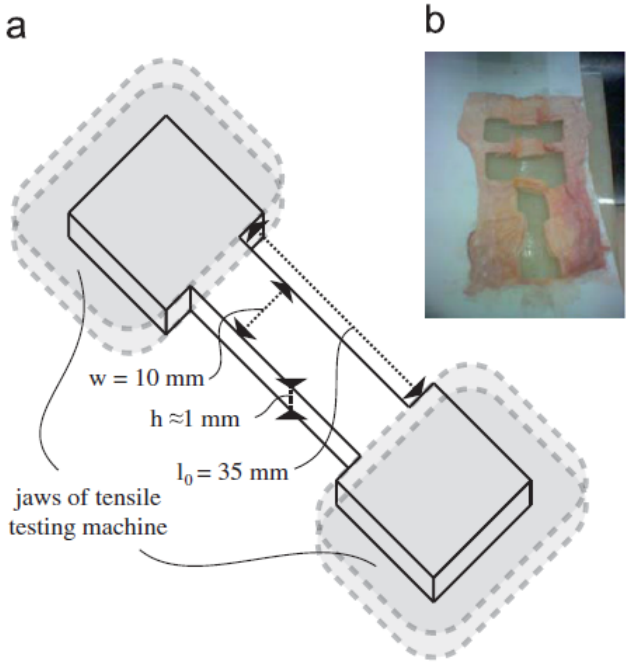

Figure 3.8: (a) Specimen dimensions. (b) Linea alba after specimens' preparation by punching. The upper two specimens were taken in transversal direction of the linea alba, the lower one in its longitudinal direction [Förstemann et al. (2011)].

A study by Gräβel et al.[Gräβel et al. (2005)] investigated the biomechanical anisotropy

of the human linea alba. A total of 165 (186 samples minus 21 which were excluded from the reported results) samples, from different regions of 31 abdominal walls (16 male and 15 female) underwent mechanical testing. Sample dimensions had a common width of 1cm and were dissected from each linea alba transversely, obliquely and longitudinally according to what is described as the "main" fibre directions (a confusing term used to describe a layered fibre structure of differing architecture). All dissected samples included a small amount of rectus sheath; use in fixing each sample to the mechanical testing device (see Figure 3.9a below). This device consisted of an octagonal frame with eight concentric arms, each equipped with a crank carrying a spring scale with an emery paper clamp fixed on one end. Before the experiment the test samples were uniaxially attached to the rig via the clamps and two pins inserted at either end of the sample at the junction of rectus sheath and linea alba (Figure 3.9b). A loading force was then applied to the sample from 2 to 24N in steps of 2N. At each step increase in force the change in length of the sample was recorded by measuring the distance between the two pins by hand. A force/strain curve was then output for each test.

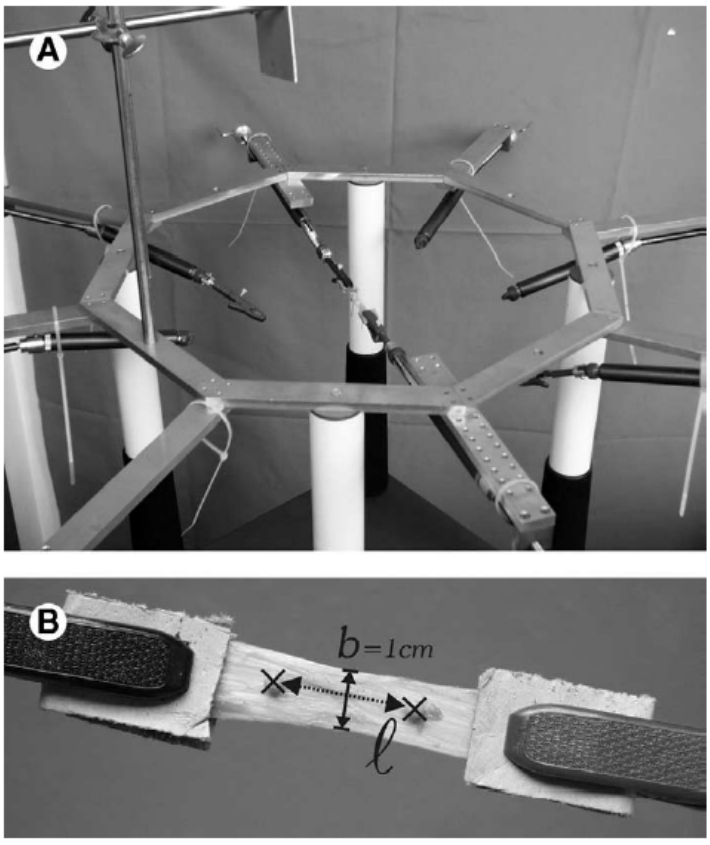

Figure 3.9: (A) Test device. (B) Specimen fixed to the clamps [Gräβel et al. (2005)].

Using the assumption stated by Förstemann et al. (2011) that the relative thickness of the linea alba is approximately 1mm, it was possible to convert the results reported by Gräβel et al. (2005) from force (N) to stress (N/mm^2). Unfortunately there are several drawbacks from this type of experiment. Use of a crank spring to measure force makes the system more prone to tactile and human error that could result in over/under loading the sample. In addition, the methodology of step application of force gives the tissue opportunity to relax which may cause differences in any recorded strain measurements. Measuring the sample length manually also includes a further factor of human error. Furthermore, using the RS/LA interface[2] as a site for marker placement could also cause differences in strain measurements due to the different local collagen fibre architecture at that point. The results also exhibit negative initial strain in some cases which could be as a result of the tissue relaxing in-between measurements, though more information is needed to clarify this. Due to the significant difference in experimental methodology, it is therefore not possible to compare the results of this investigation and that of Förstemann et al.; both papers exhibiting radically different results (Förstemann et al. tending towards a considerably stiffer response as seen below in Figure 3.10). Furthermore, the initial loading recorded at zero strain (see Figure 3.10) may be as a result of a pre-load that is applied without normalising the curves back to the origin. However, it was not made clear in the methods reported. This study was principally intended to highlight the differences in mechanical properties depending on the direction of the applied load rather than focusing on quantifying those properties and, as is evident from the results, the simplified experiment methodology succeeds in explaining that there is a difference. However, the deviation in results is too significant to take as the definitive mechanical characteristics of the linea alba.

[2] The RS/LA interface is an abbreviation of the interface of the linea alba and rectus sheath; the physical junction where they meet before the rectus sheath splits around the rectus abdominis muscle.

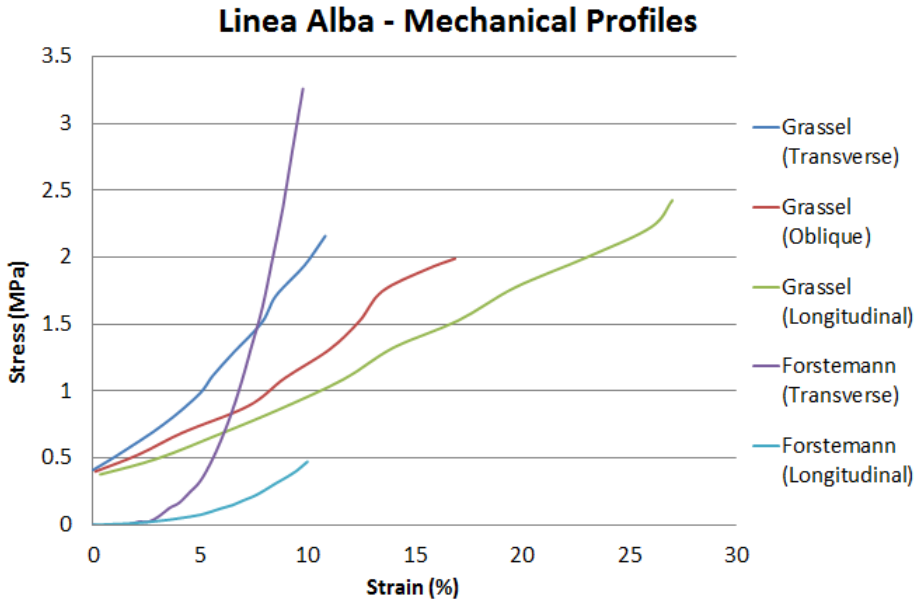

Figure 3.10: Mechanical profiles of the linea alba as derived from the literature [Förstemann et al. (2011), Gräβel et al. (2005)].

Laparoscopic surgery involving the incision of linea alba tissue will often result in scar tissue to form at the site of incision following patient recovery [Sanders & Winter (2007)]. Hollinski et al. [Hollinsky & Sandberg (2007)] analysed the difference in strength between scar tissue and normal tissue at the linea alba based on reports that the incidence rate of incisional hernia is approximately 11-15% in the first postoperative year [Wissing et al. (1987)]. It was found that the load-bearing capacity of scar tissue is approximately 30% less than that of the linea alba in nearly all directions; the higher fibrin content in scar tissue having a significant impact on the biomechanical properties. This concludes that if a follow-up laparoscopic surgery is required, there is significantly more risk attributable to the patient if the same port site is chosen.

Several studies have been performed that focus on the biomechanics of suture pullout (using steels sutures with similar dimensions to conventional polymer sutures) in the linea alba. Using cadaveric human female linea alba, Campbell et al. [Campbell et al. (1989)] attempted to assess several issues associated with surgical suturing that are commonly taken for granted by surgeons worldwide. Employing uni-axial tensile testing techniques, they concentrated on the effect the diameter of the suture, the bite size[3] and the thickness of the

[3] The bite size describes the length of tissue separating the insertion point of the needle and the edge of the

linea alba (above and below the linea semicircularis) had on the maximum force required to instigate failure. The tests were a simplified representation of in-vivo suturing using one loop of suture of defined diameter, pulled through a specific point in a transverse linea alba sample which was gripped on one end using clamps. The ends of the suture were then tied off to the base of the machine. The tissue was stretched and the force at failure recorded. It was found that increased tissue thickness (diminished in old age women and below the linea semicircularis) improved maximum pullout force. A similar pattern was observed with increased suture bite size, but above 1.2mm this trend levelled off and little difference was noted. However, edge effects were not taken into account in this study which could account for the eventual plateau of the trend. This occurs right at the point at which the bite depth is greater than the distance from the bite to the horizontal edge of the tissue.

Alternatively, it was found that increased suture diameter did little to improve the maximum pullout force concluding that, as long as the strength of the suture can be assured, the use of small diameter sutures will not exacerbate wound closure. While this study does make some informative conclusions, it must be noted that cadaveric tissue was used. As the process of embalming tissue uses chemicals that significantly change the mechanical properties of the tissue itself, and as there is little prospect that this effectual change is uniform throughout (there is no way to ensure that the cross-links that do form between collagen fibres will not distort the scale of anisotropy of the tissue) it may be that the use of cadaveric tissue does not accurately represent the response of fresh tissue. There have been some studies on bone that attempt to quantify this effect [Cömert et al. (2009), Zech et al. (2006)]. However, to the authors knowledge, there have been no such studies performed on soft tissues.

A similar study involving suture pullout was performed by Descoux et al. [Descoux et al. (1993)] who focused on determining the ideal distance between suture bites. Again cadaveric tissue was used to assess the point of failure of the tissue attached by two sutures spaced a defined distance apart. It was found that the pullout force dropped linearly as they were brought closer than 12mm apart. It was also observed that using multiple sutures closer together provided no increase in pullout force when compared with fewer sutures 15mm apart. Therefore it was concluded that a space of 10-15mm between sutures is optimal. However, in

incision

another study by Lyons et al. [Lyons et al. (2015)] it was shown that herniation can occur at relatively low pressures (∼5kPa) for a defect diameter as small as 10mm. Therefore, it may be possible that a bite separation of 10mm will not be able to prevent a hernia from occurring post-surgery. Overall, suture pullout of the linea alba is a subject of little focus in the literature and could benefit from further investigation.

3.4.2.3 The Rectus Sheath

Although the linea alba around the umbilicus is most commonly the region of choice for main trocar access in laparoscopic surgery, patient complications, or scar tissue accrued by previous laparoscopic surgeries, can necessitate the use of an alternate access point. The optimal access technique in these patients is the direct visualisation entry method, of which the port entry location is usually at the rectus muscle off mid-line [Patel (2012)]. This technique therefore requires the incision of the rectus sheath (access through the rectus muscle is accomplished by parting the muscle fibres without damaging them). As it is also a load-bearing tissue of the abdomen it is important to quantify the mechanical properties of the tissue to fully understand the implications of port access in this region. However, like the linea alba, very little conclusive data on the mechanical properties of the rectus sheath currently exist in the literature.

A study performed by Martins et al. [Martins et al. (2012)] is one of the few that provides quantitative stress-stretch data curves on the tissue (anterior rectus sheath only). Samples dissected from human female cadavers (12 in total) were tested in tension in the cross-fibre and fibre directions. A considerable range of stress-strain curves were generated. However, only the samples listed below in Table 3.1 (corresponding profiles can be seen in Figure 3.13 at the end of this section) are of interest as they are the only examples of female cadavers that may not have had children within their lifetime (only one specimen is a certainty). This is due to the fact that pregnancy may have a permanent effect on the mechanical properties of the tissue. While there is no evidence to support this in the literature, it is postulated that specimens who've previously had children would have stronger anterior rectus sheaths as an increase in the intra-abdominal pressure affecting the abdominal wall can be expected [Frezza et al. (2007)]. Therefore, isolating these samples was deemed a worthy precaution

in order to develop a better understanding of the mechanical properties of the tissue in its natural state (having not been subjected to excessive trauma). Care was taken to ensure that the samples were not subjected to biased loading (where the sample is more slack on one side) with the aid of an alignment device as can be seen below in Figure 3.11.

Table 3.1: Isolated specimen information from Martins et al. [Martins et al. (2012)]

Sample #	Age (*Years*)	Height (*m*)	Weight (*Kg*)	BMI (kg/m^2)	Parity (*#ofchil.*)	Samples (*Trans.*)	Samples (*Long.*)
6	18	1.79	104.2	32.52	0	1	1
8	59	1.65	67.5	24.8	Unknown	1	1
12	65	1.79	65	25.71	Unknown	2	1

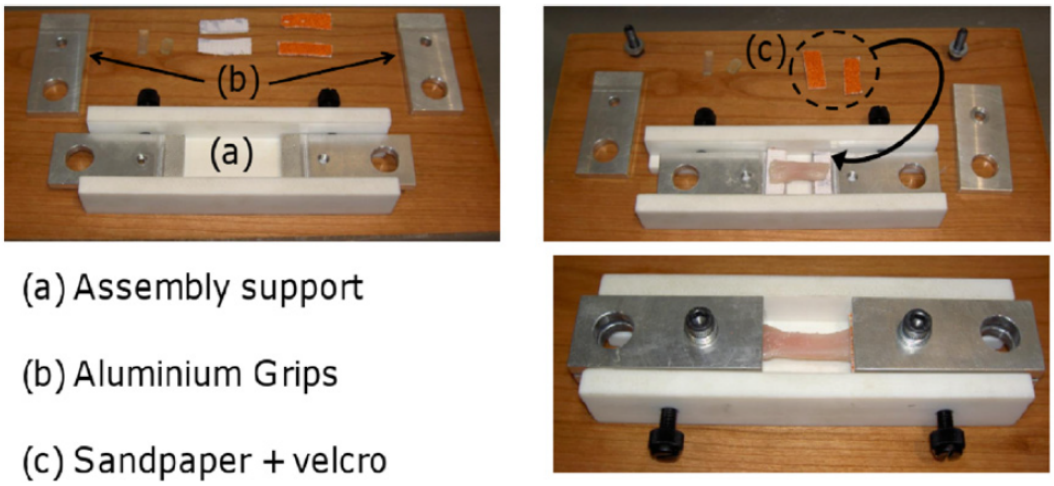

Figure 3.11: Tissue-clamp fixation [Martins et al. (2012)].

Maximum average stress in the fibre direction (transverse direction) was reported to be 12MPa with a corresponding mean stretch of 1.71 (mean of total sample specimens). Such a large stretch seems inconsistent with the approximate strength reported (E=30MPa) which raises the concern of possible slippage occurring during the experiment (a consequence that cannot be avoided when using grip-to-grip distance as a measure of the stretch/strain occurring within the material). One point of note is that there was found to be a statistically significant difference between the ultimate tensile strength of the rectus sheath in specimens with a BMI $> 25kg/m^2$ (overweight to obese) compared with those with a BMI $< 25kg/m^2$ (normal healthy weight). However, caution must be exercised due to the relatively small sample size. Since there is no apparent pattern or correlation between transverse and longitudinal samples,

it would stand to reason that any slippage occurring during the experiment may corrupt any statistical analysis (as it is impossible to quantify the amount of slippage per sample, or even ascertain if it is relatively constant between samples, with the experimental method described) [Martins et al. (2012)].

A method of measuring the surface strain of the tissue as it is being loaded was employed in a short communication by Abdelounis et al. [Ben Abdelounis et al. (2012)] where the effect of loading rates on the elasticity of the human anterior rectus sheath (cross-fibre) was studied. Instead of deriving strain calculated from the recorded cross-head displacement of the Instron tensile testing machine they were using, the relative displacement between two dots imprinted on the surface of the rectus sheath sample, tracked using image processing software, was used (see below in Figure 3.12). This ensures that only the strain occurring within the sample is being recorded and, as such, any subsequent slippage from the grips will not impinge on the recorded strain values (the measured force changing proportionally with any change in strain). With a strain rate of approximately 50%/min (quasi-static loading) and 83.33%/min (high loading rate) and a pre-load of 0.2N, seventeen samples from three fresh post-mortem subjects were mechanically tested using a 1kN load-cell and resultant stress/strain curves were ascertained. The elasticity for both quasi-static and high loading rates were found to be 5.6MPa and 14MPa respectively. This is significantly different to the 10MPa (cross-fibre) reported by Martins et al.. At a test speed of 5mm/min it is very unlikely that the strain-rate was high as the corresponding width and thickness would have to be very small; for a length of 2mm the strain rate would be approx. 25%/min. Abdelounis records a maximum failure strain of approximately 25.1% whereas Martins reports a 3-fold difference of approximately 75% for the equvalent cross-fibre result. This shows that slippage, if strain is measured using machine cross-head displacement, can corrupt results (as is noted by the 2-fold difference observed between the two methodologies). Rath et al. [Rath et al. (1997)] reported a maximum strain of 36% in a similar study using machine cross-head displacement to determine strain. However, the sample orientation was determined by the orientation of the linea alba and not the collagen fibre direction of the rectus sheath. Therefore, depending on the area of the rectus sheath from where the samples were obtained, an oblique fibre direction may result.

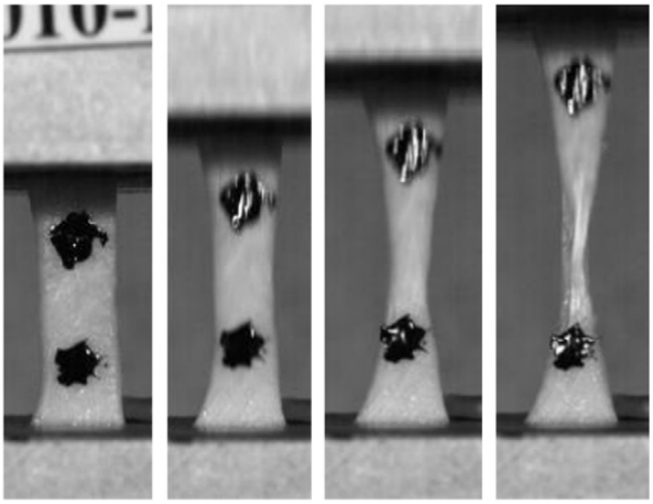

Figure 3.12: Rectus sheath specimen under tension, with a pre-load of 0.2 N on the left and before failure on the right. [Ben Abdelounis et al. (2012)].

One drawback to note in the work by Abdelounis et al. is that a 1kN load cell is used which may not be sensitive enough for the relatively small loads applied in each experiment (about 3.5N for a thickness of 1mm in quasi-static conditions). The sample size (three cadavers) is not very large for a comprehensive analysis and mean could be a deviation of its true value as a result. In addition, samples were only tested in the cross-fibre direction and so there is not enough information to provide an outlook of the overall mechanical characteristics of the rectus sheath. Furthermore, the standard deviation of the stiffness was approximately 50% of the mean value in both cases; a large deviation which could be caused by difference in sex or genetic variation between specimens or possibly the insensitivity of the load-cell. In addition, while image analysis does account for any slippage from the grips, the use of just two reference dots may not adequately describe the more local strains in the material (as can be seen in Figure 3.12 where necking occurs between the dots).

A recent paper published by Lyons et al. [Lyons et al. (2014)] describes both the uni-axial and bi-axial mechanical response of the rectus sheath. Using novel imaging methods, stretch was measured directly from the surface of the tissue rather than relying on machine-derived stretch which does not account for any slippage of the tissue from the grips. Rather than measuring the displacement between two dots (the method employed by Abdelounis et al.), the averaged z-axis displacement was measured from four separate regions of the tissue. This engenders a more universal assessment of the stretch occurring within the tissue and makes assessing localised irregular stretching that may imply failure or improper loading

of the sample a simple matter. An eleven-fold difference in uni-axial stiffness between the fibre and cross-fibre directions was reported. Bi-axial loading yielded an approximate seven-fold increase. Due to the more accurate method of measuring stretch, coupled with a strict adherence to performing tests in a consistent environment, inter-sample deviation was less pronounced than what is envisaged elsewhere in the literature.

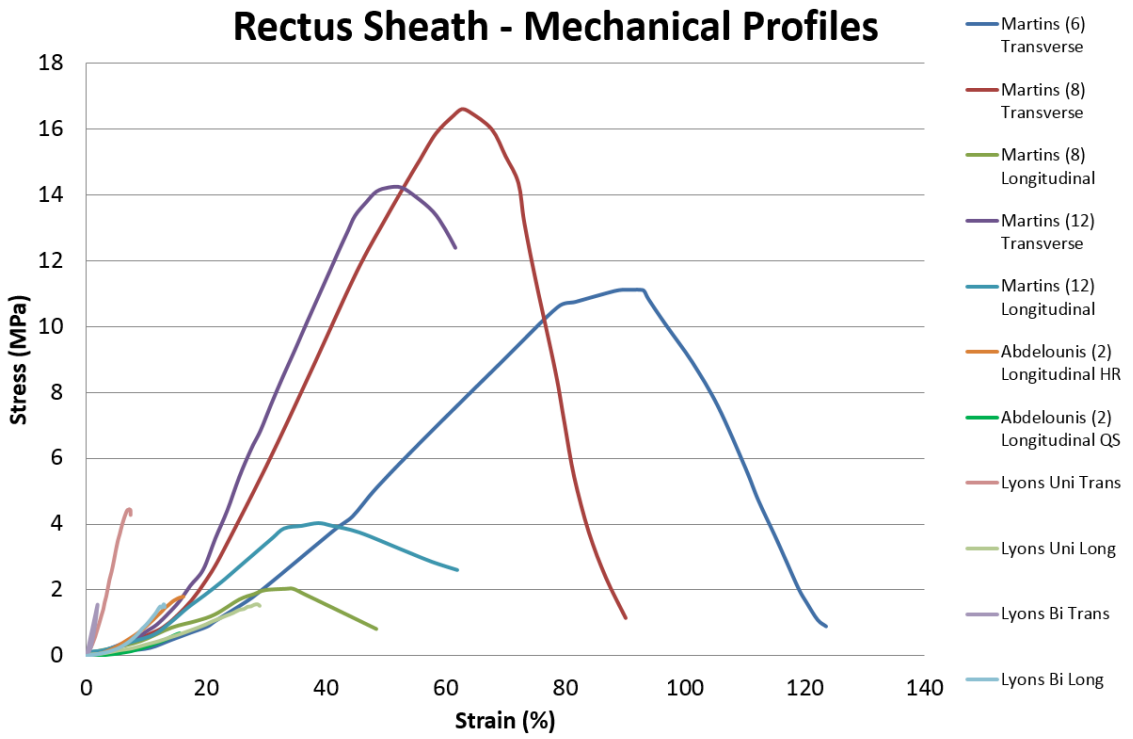

Figure 3.13: Mechanical profiles of the rectus sheath as derived from the literature [Ben Abdelounis et al. (2012), Lyons et al. (2014), Martins et al. (2012)].

3.4.2.4 The Transversalis Fascia

Although the transversalis fascia and the peritoneum are technically separate layers, above the arcuate line the tissue is so closely attached to the overlying posterior rectus sheath that the posterior rectus sheath, peritoneum and TF appear to form a single layer that can be difficult to distinguish (Section 2.3.1). Below the arcuate line the TF is thicker due to the lack of rectus sheath and, as such, it is reasonable to assume that it would exhibit greater strength as a result. There have been several published studies on the TF mechanical properties, but only below the arcuate line and around the inguinal region where it is easily identified. There is also significantly more interest in the TF of the inguinal region or below the arcuate line due

to the high prevalence of inguinal hernia occurring in the populace (3.2% of young healthy males [Akin et al. (1997)]).

A study performed by Kirilova et al. [Kirilova et al. (2011)] investigated the mechanical properties of both the umbilical fascia and transversalis fascia (inguinal region) in humans. Umbilical fascia does not originate solely at the umbilical site, nor does it harbour a direct connection with the midline fascia. It is principally defined as a thin fascial layer that extends between the medial umbilical ligaments from the umbilicus inferiorly to the urinary bladder [Townsend et al. (2004)]. As such it is separated from the fascia transversalis by extraperitoneal (subserous) tissue. This all occurs below the arcuate line as can be seen below in Figure 3.14.

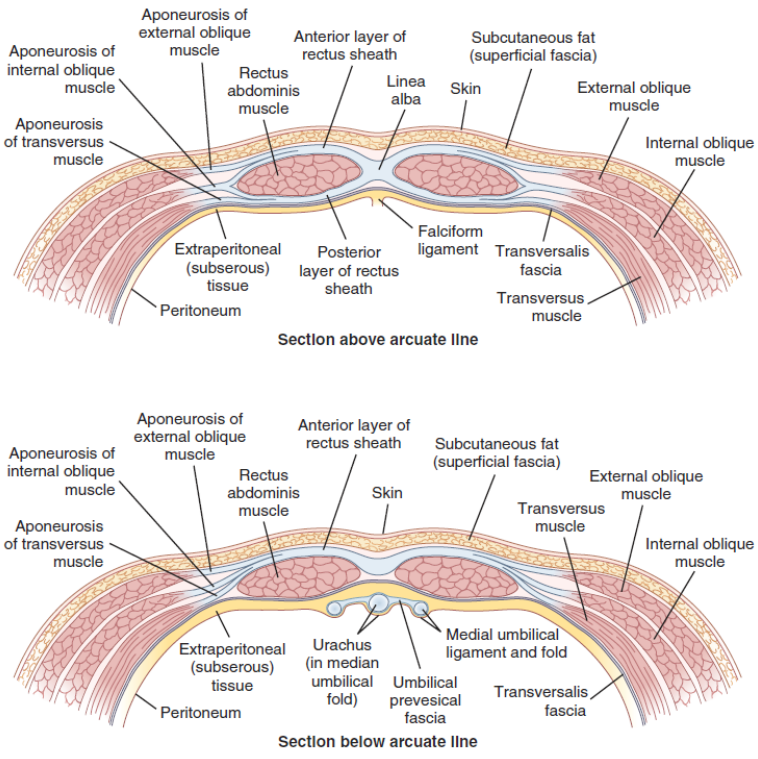

Figure 3.14: The abdominal wall and constituent fascial architecture above and below the arcuate line [Townsend et al. (2004)]

Kirilova et al. uniaxially tested 90 samples (10mm x 70mm) from both regions in the fibre and cross-fibre directions and a detailed summary was compiled of their mechanical properties. An example of a transverse sample being tested can be seen below in Figure 3.15; note the clearly defined fibre direction. However, the bulk of their results were published in

terms of median absolute deviation (MAD)[4]. A consequence of this is that a standard mean of the data cannot be obtained and, as such, this data cannot be used as a comparison to other literature that report the mean and deviation of the data. However, it was confirmed that no statistical difference exists between the mechanical properties of transversalis fascia and umbilical fascia below the arcuate line. Kirilova et al. did produce several example stress/strain curves from longitudinal samples dissected from the inguinal region of one donor which could be useful as a minor comparison to other literature. Of this data a peak stress of approximately 1.5MPa stress at a stretch ratio of 1.2 was observed (seen in Figure 3.16 at the end of this section), though it was noted that there was a large deviation between the samples.

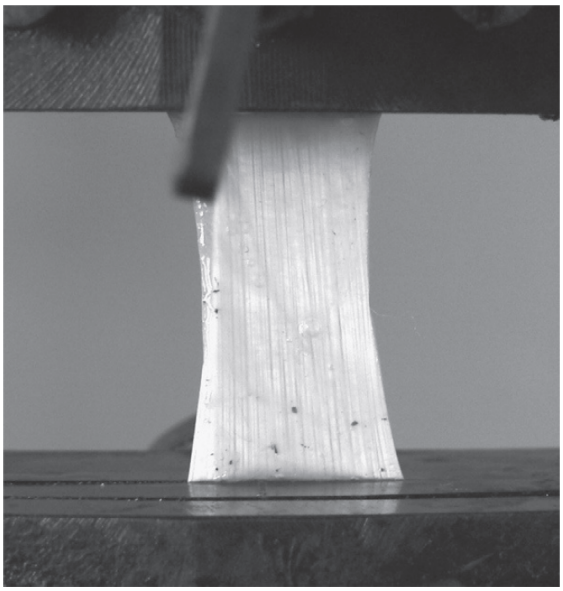

Figure 3.15: A transverse human fascia sample during testing [Kirilova et al. (2011)].

Minns et al. [Minns & Tinckler (1976)] reported an ultimate tensile strength (UTS) of 2.56MPa for TF samples of patients that had previously underwent prosthetic herniorrhaphy[5] (samples obtained from both femoral and inguinal regions) and a value of 3.15MPa for patients of normal health (samples obtained from the inguinal region only). The strain at rupture was ascertained to be 58.5% and 57% respectively showing no change in elongation of

[4] Median absolute deviation is a robust method of measuring variability and is largely unaffected by the presence of outliers in the data.

[5] Prosthetic herniorrhaphy is an operation to treat a hernia that first involves opening the hernial sac and returning the contents to their normal place before obliterating the hernial sac and closing the opening with the aid of a prosthetic mesh.

the tissue despite the change in UTS. All samples were cut in the fibre direction (transverse). One point of note in this study is that the dimensions of the samples were cut to lengths of 20mm with a 2mm width. Such a small width could be problematic as any misaligned cut due to human error could have a greater impact on the perceived results. Since the width is extremely small, any slight miscalculation of the width will have a greater effect on the variability of the results than would be the case for samples of greater width. No standard deviations were provided so it is impossible to be certain how accurate the methodology was. Results from this test are incomparable with those reported in Kirilova et al.; each testing different sample orientations. Furthermore, Kirilova et al. tested at an approximate speed of 7.8mm/min, over three times as fast as Minns et al. with a speed of 2mm/min; further calling into question any possible comparison. It must also be noted that the fascia was obtained from the femoral region rather than the inguinal or abdominal midline regions, further increasing the possibility that there may be different mechanical characteristics associated with the tissue in comparison with Kirilova et al. (see Figure 3.16).

A similar study bu Kureshi et al. [Kureshi et al. (2008)] examined the differences between herniated and non-herniated TF in both the transverse and longitudinal directions. Herniated samples were obtained from 19 males and 1 female undergoing inguinal hernia repair surgery while four non-herniated controls were harvested from an equivalent anatomical site in transplant organ donors who had no history of herniation. Tissue samples were uniaxially tested and the stress strain response was derived from load-cell and machine cross-head designations. A statistically significant increase in failure stress and stiffness was observed in the transverse anatomical plane when compared to the longitudinal plane (mean anisotropy ratio of 2:1). However, there was no significant difference found between the key mechanical properties (break stress, strain or modulus) for herniated TF and non-herniated TF (Figure 3.10 shows the representative stress-strain curves of herniated transversalis fascia). Additionally, no significant differences were found in mean collagen fibril diameter, density or fibre bundle spacing leading to the conclusion that located tissue at the site of hernia do not exhibit any different properties to healthy tissue from alternate donors with no history of hernia. One point of concern with this study is that a sample length of 5mm was used which makes it impossible to keep the standardised length to width ratio of 4:1.

It must be noted that this study on the differences of herniated and non-herniated inguinal

TF was influenced, in part, by theories proposing that inguinal hernia is a form of connective tissue disorder [Bendavid (2004)]. If such is the case, the mechanical properties of herniated tissue caused by improper healing after surgery and natural phenomenon cannot be satisfactorily compared. Further research would be needed to clarify if there is no significant difference. However, a natural assumption would be that a connective tissue disorder would infer weaker mechanical properties than healthy tissue (whether that tissue be subjected to herniation or not). However, Kureshi et al. did state that there were no significant differences observed in the properties of both normal and herniated TF; leading to the conclusion that inguinal hernias are not caused by connective tissue disorders (or rather, not in the case of the TF).

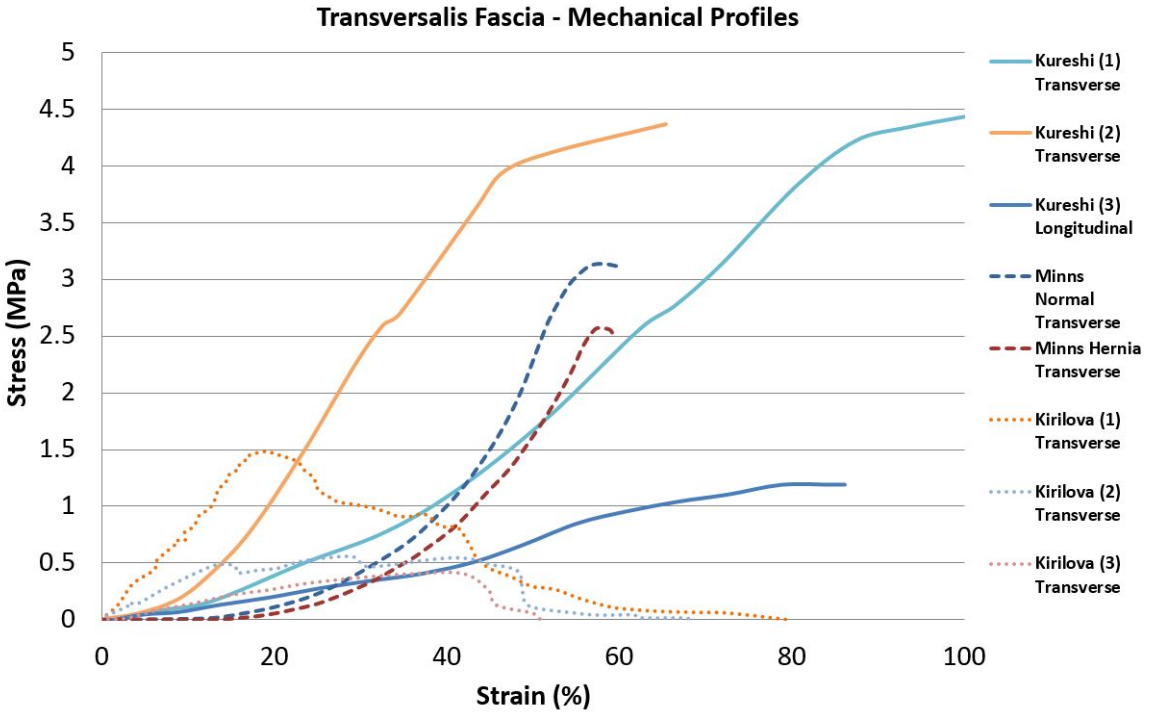

Figure 3.16: Mechanical profiles of the transversalis fascia as derived from the literature [Kirilova et al. (2011), Kureshi et al. (2008), Minns & Tinckler (1976)].

3.4.2.5 The Variable Nature of Abdominal Tissue

Overall there is significant deviance in the mechanical properties of abdominal soft tissues as seen in the literature. Figure 3.17 below highlights the difficulty in attempting to observe any pattern in their profiles; the majority affirming unique stiffness's and behaviour. This is most

likely as a result of different experimental protocol. For cases involving the use of human tissue, irregular mechanical responses afforded by intrusive chemical embalming may be an issue. There is no strict universal standard for embalming and, as such, it is impossible to be certain that the same extent of chemical cross-linking of collagen is maintained between studies; and possibly even between samples obtained from alternate regions in the same study.

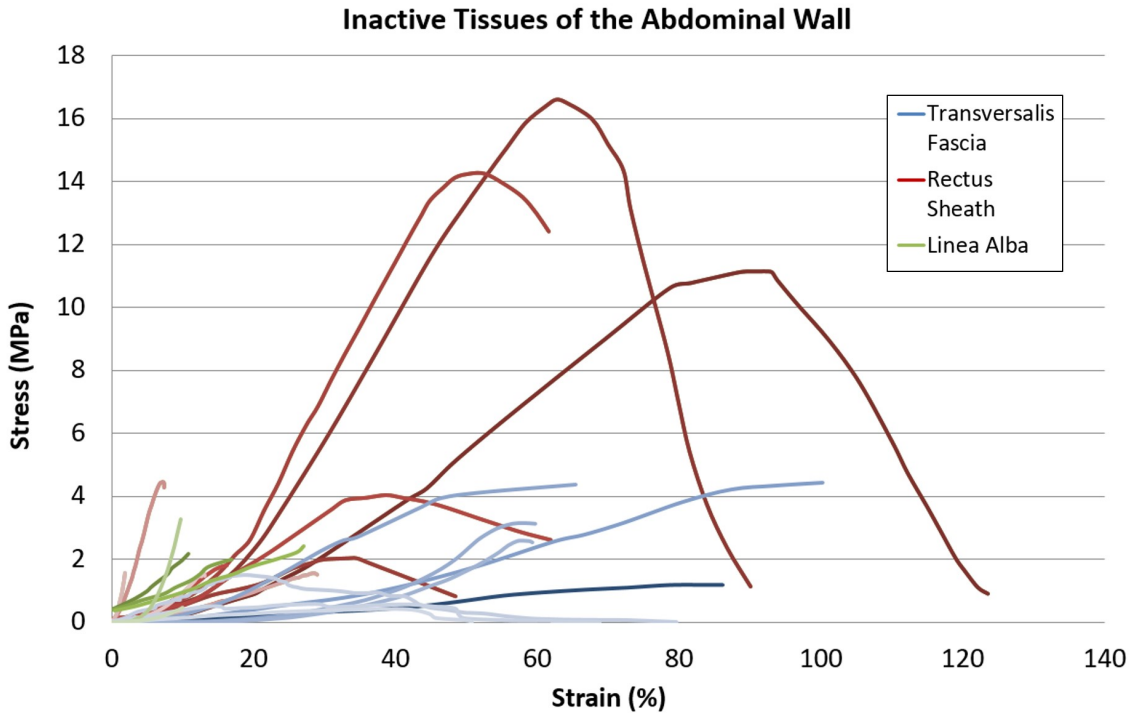

Figure 3.17: Mechanical profiles of all inactive tissues of the abdomen as derived from the literature. Profiles of the transversalis fascia are shown in shades of blue, rectus sheath in shades of red and linea alba in shades of green.

3.4.3 Human-Porcine Differences

Pigs have long been used for scientific experimentation in lieu of human specimens. They have a similarly sized heart and body length to humans, meaning their internal physiology is of a comparative scale. Decellularised porcine tissue is often used as a scaffold for human cells [Methe et al. (2013)]; both species utilising the same basic components. However, this does not mean that the mechanical properties should necessarily be similar.

Humans have a more active lifestyle. Exercising the abdominal muscles more regularly might suggest a requirement for stiffer fascial tissues. However, pigs have a greater proportion

of the weight of the internal organs acting directly on the abdominal wall, rather than the pelvic floor in humans. Furthermore, pigs have a significantly greater BMI than humans (18.5-25kg/m^2 for healthy humans compared to 127kg/m^2 in some breeds of pigs [Johnson & Nugent (2003)]) and obesity in humans is associated with increased IAP [Lambert et al. (2005)]. This means that the typical IAP at rest for pigs should be considerably greater than the approximate 1kPa average seen in humans, though data is not available. In addition to this, pigs have a greater number of ribs than humans do. This could mean that muscle attachment, and therefore the angle/direction of aponeurotic fibres, could be different [Pond (2003)].

There is difficulty in quantifying the difference between human and porcine fascial tissue from the literature. There is no example of a mechanical study being performed on both and comparing adequately between isolated studies is problematic mainly due to differences in experimental protocol. It is likely that there is a difference in the mechanical properties. However, it is possible that the difference may not be extreme. Ultimately, these tissues serve the same purpose in both species. It may yet be possible to use porcine tissue as a model for the human abdomen. It's potential as a surrogate would be highly advantageous for surgical device testing and evaluation.

3.5 Current Devices on the Market

Currently there are few devices on the market that allow for safer and more accurate closure of surgical incisions to the abdominal wall. SuturTec [Meade & Brecher (1995)] devised an instrument (see Figure 3.18 below) that automatically places the needle of a suture a set distance in from the edge of the incision. It then rotates the needle so that it pierces the tissue on the other side of the incision. The surgeon can then advance the device down the length of the incision a chosen distance and repeat the process until he/she is ready to tie off the suture.

Figure 3.18: SuturTek 360^o fascia closure device [Meade & Brecher (1995)].

The device eliminates the need to touch the needle directly, thereby providing a measure of safety. Its described as providing fast, high quality clinical results. However, its expense means that few surgeons consider it an option [Winter (2013)]. Each unit is disposable and needs to be replaced following surgery. Unfortunately it doesn't allow for a controlled separation of suture bites which would guarantee repeatability. Therefore there is still the possibility that it may not reduce the incidence of incisional hernia as it relies heavily on the surgeon's choice of placement of each suture; little different from how manual wound closure is performed.

Several devices have been developed that focus on aiding or maintaining wound closure through tension relief. TopClosure tension relief system (see Figure 3.19A below) attaches multiple tabs across the wound site using adhesive or staples depending on the natural loading applied to the tissue around the wound. Ratchet clips are then tightened to relieve tension on the tissue around the immediate vicinity of the wound itself, actively reducing the severity of scarring as the wound heals. It can be used on its own for minor superficial wounds or in tandem with sutures to improve the quality of healing of more severe wounds [*TopClosure - 3S System* (n.d.)].

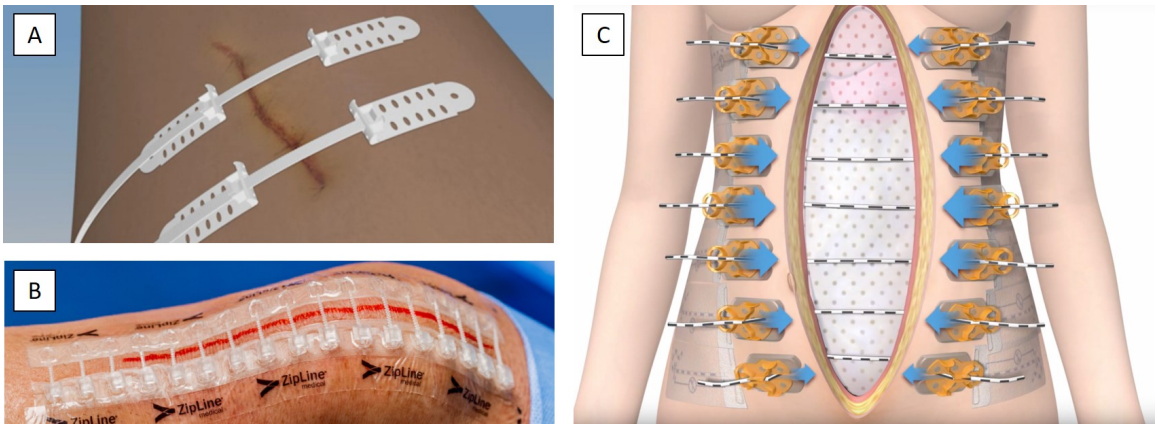

Figure 3.19: Tension relief closure devices; A) TopClosure tension relief system, B) Zip 16 surgical skin closure device and C) ABRA abdominal closure system [*ABRA - Abdominal | Dynamic Tissue Systems* (n.d.), *TopClosure - 3S System* (n.d.), *Zip 16 - Surgical Skin Closure* (n.d.)].

ZipLine medical also produced a therapeutic device to help minimize scarring in superficial skin tissue (see Figure 3.19B. A patch is placed over the incision site and adhered using adhesive. Plastic screws span the incision that, when tightened, reduce tension on the incision site and maintain apposition. However, this device is not suitable for supporting closure of wounds on its own in highly loaded areas of the body. It provides a faster and more effective method of skin closure than that of sutures [*Zip 16 - Surgical Skin Closure* (n.d.)].

The ABRA abdominal closure system (see Figure 3.19C) was designed to help restore the primary closure option for full-thickness, retracted mid-line abdominal defects. This is where the full length of the abdominal wall is incised, making it difficult to retract for closure without damaging the tissue at the edge margin of the incision. The ABRA system pulls muscle planes and skin together from their lateral retracted state with relentless dynamic appositional traction, leaving the leading edge of the fascial margins undisturbed when performing definitive primary closure. It dramatically reduces the length of stay of patients, their short-term morbidity risks and future healthcare costs [*ABRA - Abdominal | Dynamic Tissue Systems* (n.d.)].

3.6 Conclusion and Project Objectives

It is clear that there is significant interest in the incidence of incisional hernia post-laparotomy and trocar site hernia (TSH) following laparoscopic surgery. Data from the literature demon-

strates an incidence of approximately 20% and 1-5% for laparotomy and laparoscopic surgeries respectively (see section 2.6.2). Since wound closure is most cited as the key risk factor in developing incisional hernia, there is a need for the development of a more robust method of wound closure. This focus in mind, this project aims refining the methodology of suture-based wound closure. However, in order to progress, the mechanical characteristics of the tissues of the abdominal wall must be ascertained to interpret the mechanical characteristics of the load-bearing fascial tissue involved in order to understand the tissues behaviour under loading (i.e. is the tissue anisotropic and if so, to what extent?). Characterising the stress-strain relationship is fundamental starting point to understanding the nature of the tissue itself. In both cases the linea alba is the most frequently chosen incision site for laparoscopic and laparotomy surgeries.

Very little data on the mechanical properties of the constituent tissues of the abdominal wall currently exists in the published literature. Different publications on similar studies also tend to be contradictory and can sometimes disagree on testing protocol. As such, it is necessary to perform further mechanical tests on the constituent tissues and characterise their response in order to be certain. Throughout the literature there is only one example where image processing is used to directly measure the strain of the tissue itself, rather than using machine cross-head displacement to derive an indirect measurement. Using new and innovative methods such as this coupled with a more refined testing protocol (sample extraction, size, alignment and experimental variables such as strain rate) it may be possible to more accurately characterise the tissue.

Furthermore, there is little evidence in the literature on biaxial tests being performed on the individual tissues which (Lyons et al. being an exception [Lyons et al. (2014)]), in theory, would be more indicitive of in-vivo loading. Inflation and deformation of the abdominal wall as a whole (as described in Section 3.4.2.1) essentially describes multi-axial, uniformly applied stress. However, the response is the cumulative effect of all the supportive layers working in tandem and, as such, cannot be applied to the individual tissue layers which may have different mechanical properties. Therefore it is necessary to perform further bi-axial testing on the tissues in question.

It must also be noted that the differences in the porcine and human mechanical properties of the different tissues have not been quantified. Theoretically, it is not clear if there is

a significant difference or not (see Section 3.4.3). The literature has shown to contain limited information on the mechanical properties of each tissue, a problem which is further compounded by the fact that the collection studies mentioned in this review use different species of tissue, but never compare both in the same study. It is therefore necessary to quantify the inter-species difference, or lack thereof, in order to further understand the mechanical properties of each tissue and confirm the relevance of using porcine tissue as a surrogate.

There is also very little conclusive evidence to describe and ideal suturing methodology. Though a few suture pullout papers exist attempting to define optimal parameters for suture bite and separation [Campbell et al. (1989), Descoux et al. (1993)], problems with experimental procedure and differences in protocol mean it is difficult to obtain concrete conclusions. It is still an area of little understanding that must be addressed.

3.6.1 Towards Device Development and Clinical Practice

Currently there is a surrogate abdominal rig that has previously been developed in-house in Trinity College Dublin. Further evaluation of this rig could help demonstrate its potential for surgical device testing, development and evaluation. This would be highly beneficial as it could eliminate the need for live animal or human testing early on in a devices development. Furthermore, if a porcine abdominal wall can be shown to behave appreciably similar to that of human in the rig, it would impart that porcine tissue may be a suitable surrogate for human tissue for surgical device development; advantageous in that fresh human tissue is notoriously difficult to obtain.

In section 3.4.2.2 it was shown that there is insufficient quantifiable data to describe an adequate suturing methodology for wound closure. This betrays a sizable knowledge gap with regards to clinical practice. There is no universal method for wound closure. Surgeons tend to use their own personal preference which can differ widely. This alone could be responsible for the high incidence of incisional hernia. It is therefore imperative that this also be addressed.

3.6.2 Objectives

The aim of this study is focused solely on the knowledge gap identified within the literature. To that end, the following project objectives have been established:

1. Identify the mechanical properties of the linea alba using more robust techniques.
    (a) Perform Uniaxial and biaxial mechanical experiments on porcine tissue.
    (b) Determine the extent of error accumulated by using non image-based strain measurement methods.
    (c) Quantify the effect that successive freeze-thaw cycles have on the mechanical properties of the tissue.
    (d) Quantify the effect that the compression of the tissue grips have on the recorded mechanical properties of the tissue.
2. Quantify the ideal suture based wound closure parameters (bite depth and separation).
    (a) Design a protocol and perform uniaxial suture-pullout experiments to determine ideal bite depth and separation.
    (b) Compare the effect that different size sutures have on the resultant pullout force.
    (c) Design a protocol and perform apposition experiments on the surrogate rig using an array of different suturing parameters. Use conclusions to evalusate uniaxial results.
3. Quantify the difference between human and porcine tissue and evaluate the potential use of porcine tissue as a surrogate for device evaluation.
    (a) Perform identical mechanical characterisation and suture pullout tests on human tissue from a reliable source.

Chapter 4

Research Approach

It has been noted that the incidence of incisional hernia following either laparoscopic or laparotomy surgery is quite high. However, before progressing, it was necessary to research the physical mechanical properties of the tissue in question, the linea alba. Porcine tissue was sourced from Rosderra Meats in Edenderry and ethical approval was attained to be able to handle and experiment on animal tissue.

In order to make comparisons to humans it was necessary that human tissue be sourced for comparative testing. To this end, a collaborative effort was conducted with a research group in Washington University in St.Louis, Missouri headed by Dr. Spencer Lake. It required attending the university for a period of three months to perform mechanical tests on human linea alba which was easily sourced by the medical school within the college.

Adequately comparing different variables of bite depth and separations of a continuous suture style required the design of a uniaxial jig that could be used in conjunction with a tensile testing machine to record the force required to pull a defined suture parameter setup cleanly from the tissue. For suture pullout experiments on both human and porcine tissue, bio-absorbable sutures traditionally used for internal fascia were obtained from a contact at St.Vincents Hospital Dublin.

These uniaxial suture pullout experiments worked under the assumption that the physical environment is not too different from that which can be seen in-vivo. However, the linea alba is subject to multi-axial loading in-vivo. It was therefore necessary to perform laparotomy suture-based wound-closure experiments on a surrogate abdominal rig previously developed

by Lyons et al. [Lyons et al. (2015)]. Using these results it was then possible to evaluate the uniaxial suture pullout experiments.

Chapter 5

Uniaxial and Biaxial Mechanical Properties of Human and Porcine Linea Alba

5.1 Introduction

In order to develop optimal wound closure methodologies for the linea alba it was first necessary to identify the mechanical properties of the tissue; an area of limited focus in the literature. This chapter describes all of the experimental and computational methods used in this thesis to determine the mechanical properties of both human and porcine linea alba. To this end, both uni-axial and bi-axial tensile tests were performed on sections of the linea alba of both species to obtain stress-stretch characteristics of the tissue. This allowed for the identification of whether the tissue was anisotropic or isotropic with biaxial tests being theoretically relevant to an in-vivo standpoint. The porcine experimental data was used to define a 1st order isotropic hyper-elastic Ogden and uncoupled fibre constitutive model. This model was implemented in finite element code (using FeBio simulation package) and used to quantify the effect of the small physical sample size on the results.

5.2 Materials and Methods

5.2.1 Sample Preparation

Fresh human tissue that has not been embalmed is difficult to obtain, and accordingly porcine tissue was used in this study. Pigs have a similarly sized heart and body length to humans but it is unknown if they share histological similarities. Nevertheless, pigs were chosen as a suitable substitute to humans. Twenty porcine abdominal walls were obtained from a swine abattoir (Rosderra Meats, Edenderry, Co.Offaly, Rep. of Ireland). Specimens were chosen at random from both male and female populations; all females being nulligravida. All were adults, approximately 26-28 weeks in age and were frozen within 24 hours of death.

Due to the difficulty in obtaining human tissue in the Republic of Ireland, it was necessary to source and test human tissue internationally for an appropriate comparison. To this end, in a collaborative effort with Washington University in St.Louis, 13 freshly frozen human cadaveric abdominal walls were obtained from the medical school located within the college. Specimens varied in age (>60 years) and sex and were of a caucasian background.

Prior to sample extraction porcine and human specimens were allowed to defrost for 36 hours at 4^{o}C. A rectangular section was then cut from the abdominal wall following the midline (see Figure 5.1 below depicting porcine tissue).

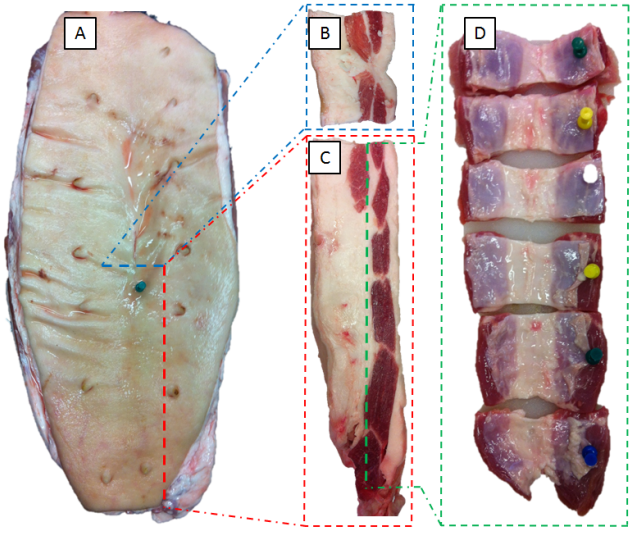

Figure 5.1: The porcine abdominal wall (A) with corresponding cross-sectional cuts of the approximate area of interest (B and C) and the tissues (posterior side) having been cut along the tendinous insertions of the rectus abdominis following anterior and posterior fat removal (D).

Typical porcine and human linea alba were both observed to have an average width of 25±5 mm, as shown in Table 5.1 & 5.2 below (Transverse grip-to-grip distance corresponding to tested tissue width; sample widths being approximately normally distributed). Anterior and preperitoneal fat, as well as rectus abdominis muscle, were removed and the isolated linea alba tissue was stored in phosphate-buffered saline solution at 4^oC prior to testing. This study refers to tissue orientation in terms of the body axis rather than the constituent collagen fibres, so the terms "Transverse" and "Longitudinal" mean both the fibre and cross-fibre directions of the tissue respectively.

Table 5.1: Sample dimensions of porcine uni-axial tensile test specimens (G-G = grip-to-grip).

Transverse					**Longitudinal**				
Pig #	**Sample #**	**Thickness (mm)**	**Width (mm)**	**G-G Distance (mm)**	**Pig #**	**Sample #**	**Thickness (mm)**	**Width (mm)**	**G-G Distance (mm)**
1	1	1.70	9.56	10.38	**6**	1	2.78	5.97	15.66
	3	2.17	11.87	12.83		2	3.46	4.34	17.58
2	2	1.76	11.54	21.33	**7**	1	1.26	13.49	17.22
	3	2.10	11.73	24.52		2	1.20	13.44	17.70
	5	1.59	11.84	16.91	**8**	1	1.16	13.59	23.62
3	1	2.00	8.83	18.83		2	1.08	12.08	21.40
4	1	1.72	9.02	16.16		3	1.66	11.76	24.67
	3	1.40	10.23	21.74		4	1.15	12.01	18.92
5	1	1.18	11.10	27.06	**9**	1	2.80	12.86	23.01
	2	1.67	9.18	23.41		2	1.91	16.22	30.60
	3	1.74	9.09	25.29		3	1.76	12.88	25.93
	4	1.71	10.14	22.36		4	1.38	9.55	24.04
	5	1.59	10.39	18.80	**10**	1	1.24	12.28	29.07
6	1	1.14	9.99	27.64		2	0.97	11.78	23.46
7	5	1.02	9.28	20.31		3	2.12	12.26	31.05
8	3	1.12	10.27	18.90		4	1.24	10.01	34.20
Average:		1.60	10.25	20.41	**Average:**		1.70	11.53	23.63
Std (σ):		0.35	1.07	4.82	**Std (σ):**		0.74	2.92	5.51
Aspect Ratio:		1.99:1			**Aspect Ratio:**		2.05:1		

Table 5.2: Sample dimensions of human uni-axial tensile test specimens (G-G = grip-to-grip).

Transverse					Longitudinal				
Spec. #	**Sample #**	**Thickness (mm)**	**Width (mm)**	**G-G Distance (mm)**	**Spec. #**	**Sample #**	**Thickness (mm)**	**Width (mm)**	**G-G Distance (mm)**
1	1	1.27	11.79	20.00	**1**	1	1.39	11.40	24.00
2	1	1.71	11.62	20.00	**2**	1	1.53	13.40	38.00
	2	1.56	11.63	20.00	**3**	1	1.34	11.72	24.00
3	1	1.18	11.69	23.50	**5**	1	0.86	11.91	22.00
4	1	1.55	9.09	21.00	**6**	1	1.59	12.86	21.00
5	1	1.07	8.75	19.50		2	1.14	10.92	23.00
	2	1.22	10.60	20.00	**7**	1	1.07	11.35	26.00
Average:		1.37	10.74	20.57	**Average:**		1.27	11.94	25.43
Std (σ):		0.24	1.31	1.37	**Std (σ):**		0.26	0.89	5.77
Aspect Ratio:		1.92:1			**Aspect Ratio:**		2.13:1		

Below in Figure 5.2 is a depiction of the different tissue layers around the linea alba. Figure 5.2(i) shows an example of the anterior layers in a porcine specimen, while Figure 5.2(ii) shows posterior layers in a human specimen. The tissue is typically buried deep in both anterior and posterior fat and connects centrally with the delicate/insubstantial scarpa fascia tissue on the anterior side.

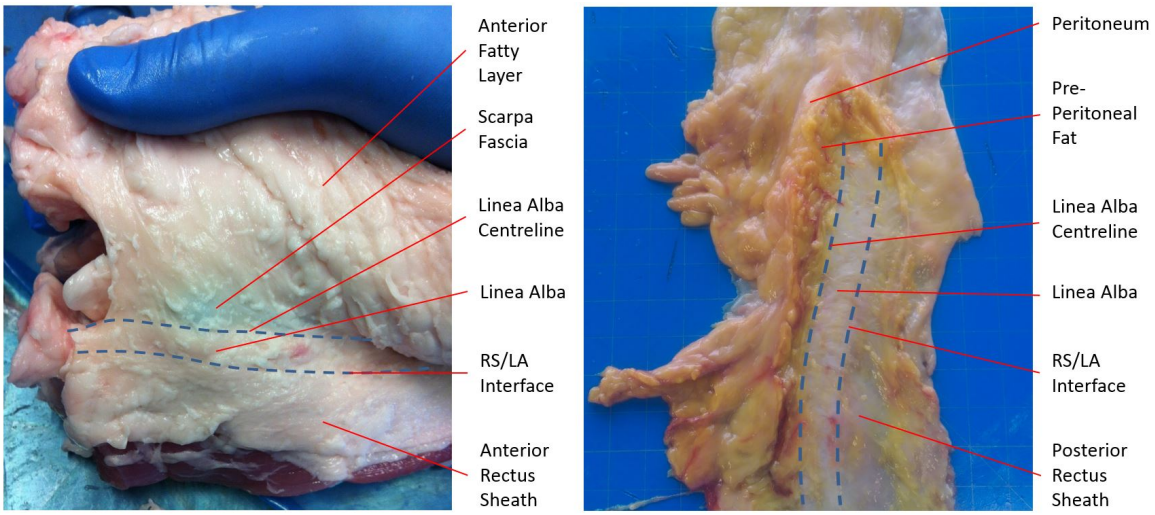

(i) (ii)

Figure 5.2: The anterior view of a porcine tissue sample (i) and posterior side of a human tissue sample (ii) showing the different tissue layers that surround the linea alba.

5.2.2 Uniaxial Testing

For uniaxial tensile tests, 32 samples, both longitudinal (cross-fibre direction; 16 samples) and transverse (fibre direction; 16 samples), were obtained from 10 different pigs. Likewise, 14 samples were obtained from 7 human abdominal walls; 7 samples being tested in each orientation. Rectangular shaped samples with a length-to-width ratio as close to 4:1 (as required by the ASTM standard [ASTM (Standard E8/E8M)]) as was possible were dissected. However, the relatively small width of the linea alba tends to limit sample grip-to-grip length (G-G Distance; see Table 5.1 & 5.2), thereby reducing this ideal ratio in the transverse direction; blood vessels being a limiting factor in the longitudinal direction. The typical aspect ratio obtained in this study was approximately 2:1 for both transverse and longitudinal test specimens (Table 5.1 & 5.2). Dog-bone shaped samples were avoided as the tissue tended to warp under the blade as pressure was applied, making it difficult to cut precise curves with the aid of a punch.

Custom made stainless steel grips lined with emery paper to reduce slippage during loading were used to grip each specimen. The tissue was first aligned with the grips using a custom made alignment apparatus (see Figure 5.3B below). A 0.2 Nm torque wrench was used to tighten the grips to ensure the sample was not damaged due to over-tightening [Lyons et al. (2014)]. An array of six dots was drawn on the posterior surface of the sample prior to its attachment to the 100 N load cell via the grips (see Figure 5.3A & C). The human tests were performed with the same clamping setup secured in a mechanical testing system that was previously custom-made for the Musculoskeletal research group in Washington University [Fang et al. (2014)].

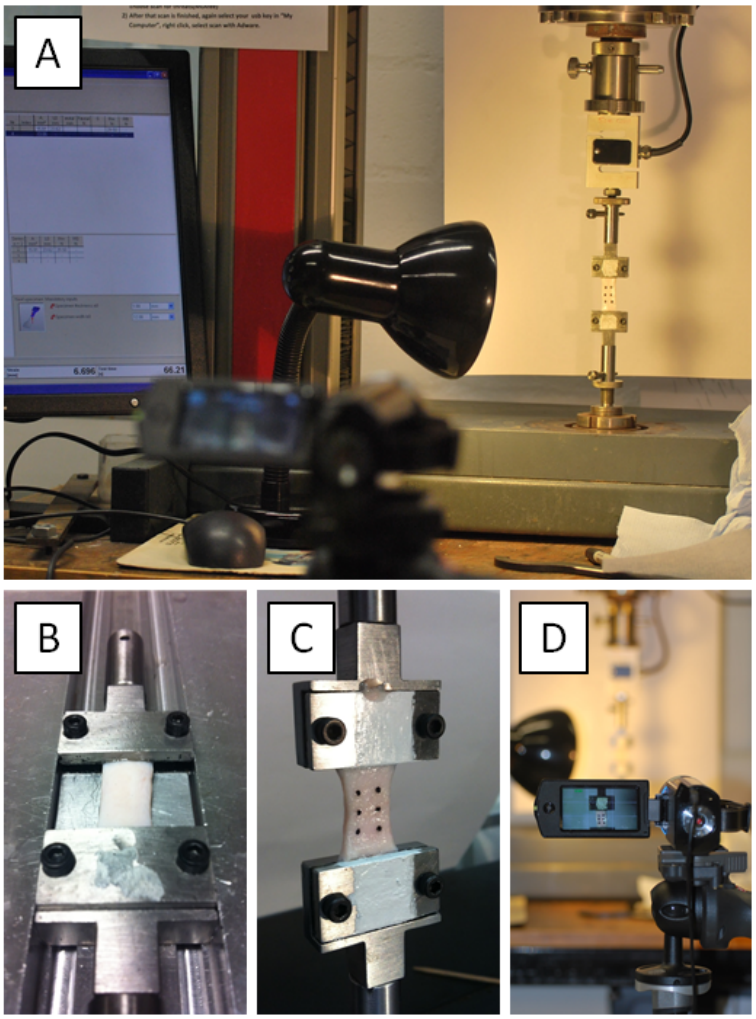

Figure 5.3: The set-up for uniaxial tensile testing (A). (B) Shows the sample alignment jig, (C) shows the sample and grips following attachment to the Zwick tensile testing machine and (D) shows camera placement while recording the duration of the experiment.

Specimens were stretched at a quasi-static strain rate of 28.5%/min [Förstemann et al. (2011)] using a displacement-controlled Zwick Roell Z005 materials testing machine fitted with a 100 N load cell. A high definition Samsung HMX-QF20 camera (Samsung Electronics Co., Gyeonggi-Do, Korea) was used to record the deformation of the sample (see Figure 5.3D) at 2 Hz. A pre-stress of 0.1 MPa (Engineering stress) was applied to remove slack within the sample which represented 2-5% of the maximum stress applied. The experiment was terminated when tearing began at the grips or along its length (characterised by a 20% drop in force experienced by the load cell if not visually perceived) or when the load experienced by the load cell rose above 90 N.

Custom MATLAB (R2013b, The Mathworks, Natick Massachusetts, USA) image and

post-processing tools were used for uniaxial tensile test analysis to calculate the strains occurring on the surface of the sample, as this eliminated the effects of slippage from the grips and transducer deformation [Moerman, Kerskens, Lally, Flamini & Simms (2009), Moerman, Holt, Evans & Simms (2009), Takaza, Moerman, Gindre, Lyons & Simms (2013)]. Image analysis allowed for six dots (three rows of two) applied to the sample (see Figure 5.3C) to be tracked, see Figure 5.4 below. The labelled regions (vertical separation of the dots A, B, C & D) and the layered first and last images with the traces and path of the dots clearly marked are shown.

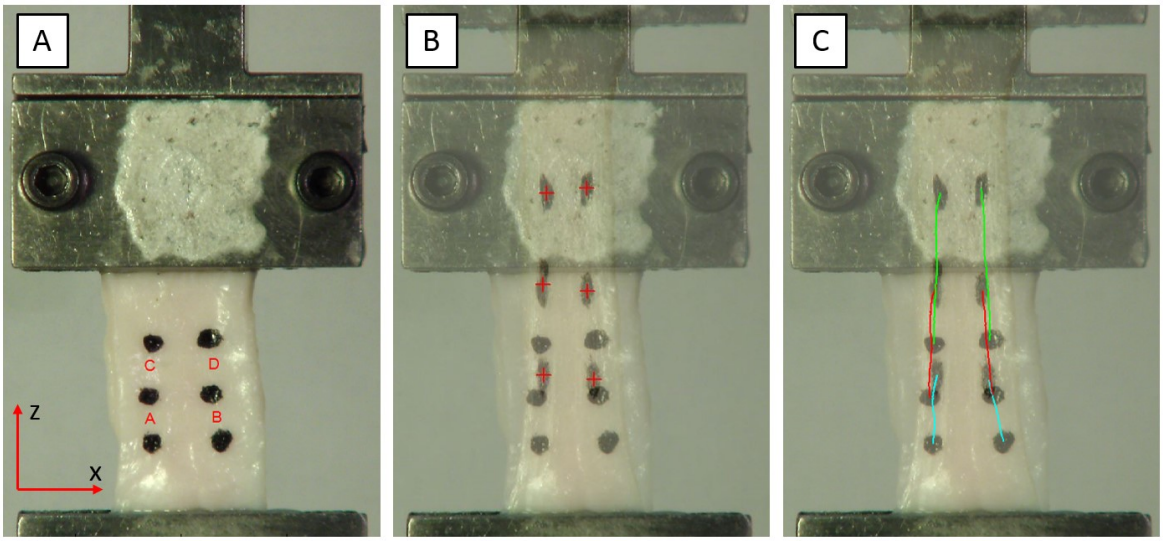

Figure 5.4: An example transverse (fibre-direction) test specimen showing the labelled regions between dots (A), the centre of each dot being tracked during analysis (overlaid first and last images) (B) and the plotted path that each dot takes (C).

The local stretch ratios (λ) were calculated as shown in Eq. (5.1):

$$\lambda_{iz} = \frac{l_{iz}}{L_z} \tag{5.1}$$

where λ_{iz} represents the local vertical z-axis (axis of displacement) stretch of the respective region (A, B, C or D; see Figure 5.4), l_{iz} is the local length of the deformed region following "i" deformation steps and L_z is the local initial length of that region. These four local stretch ratios were averaged to give an overall approximation of the stretch occurring within the sample.

For numerical analysis, stress metrics are of interest. In the case of uniaxial loading and

incompressibility ($\lambda_x\lambda_y\lambda_z = 1$) a uniaxial Cauchy stress (σ) can be derived using Eq. (6.2):

$$\sigma_{Cauchy} = \frac{F}{A_O}(\lambda_z) \tag{5.2}$$

where F is the recorded force, A_O is the initial sample cross-sectional area and λ_z is the average sample stretch ratio. Cauchy stress/stretch curves were then generated for all samples. It is noted here that if the sample dimensions and/or the clamping affect the experiment the loading deviates from being purely uniaxial. However, using finite element analysis, such effects can also be simulated and since all components of Eq. (6.2) are known, an equivalent measure of "uniaxial Cauchy stress" can be derived despite the non-uniaxial conditions. As such, model fitting is independent of the uniaxial loading assumption.

The accuracy of the automatic marker tracking method was assessed by comparison with manual marker tracking, see Table 11.1 in the Appendix, showing average differences of less than 1%.

5.2.3 Biaxial Testing

For biaxial tensile tests, a total of 20 square samples were obtained from 10 different pigs. For biaxial tests on human tissue, a total of 13 square samples were obtained from 6 different abdominal walls. Typical sample length and thickness for both species were approximately 21 mm and 1.3 mm respectively, yielding a cross-sectional area (CSA) of about 27 mm^2, see Table 5.3 & 5.4 below.

Table 5.3: Porcine biaxial sample dimensions.

Pig #	Sample #	Thickness (mm)	Length of One Side (mm)	CSA Inside Hooks (mm)
11	1	1.27	16.00	20.32
12	1	1.94	22.80	44.18
	2	1.99	19.00	37.72
	3	2.02	16.00	32.24
13	1	1.65	18.00	29.66
14	1	1.23	19.10	23.40
	2	1.29	21.00	27.14
15	1	1.41	21.00	29.66
	2	1.37	20.00	27.30
	3	1.04	21.00	21.89
16	1	1.57	18.00	28.31
	2	1.30	17.00	22.10
17	1	1.17	25.00	29.13
	2	1.32	21.00	27.62
18	1	1.07	26.00	27.82
	2	1.10	21.00	23.10
19	1	1.11	23.00	25.53
	2	0.91	21.00	19.16
20	1	1.37	24.00	32.94
	2	1.08	21.00	22.73
Average:		1.36	20.55	27.60
Std (σ):		0.32	2.77	6.03

Table 5.4: Human biaxial sample dimensions.

Spec. #	Sample #	Thickness (mm)	Length of One Side (mm)	CSA Inside Hooks (mm)
1	1	1.36	22.34	30.36
	2	1.27	21.24	26.97
2	1	1.24	21.18	26.36
	2	1.03	21.13	21.83
	3	0.76	20.00	15.24
3	1	1.68	21.09	35.52
	2	1.44	22.30	32.00
4	1	1.64	22.29	36.52
5	1	1.75	20.94	36.70
	2	1.17	21.31	24.90
	3	1.04	20.80	21.65
6	1	0.81	20.80	16.91
	2	0.64	19.00	12.07
Average:		1.22	21.11	25.92
Std:		0.36	0.93	8.17

A biaxial rig [Lally et al. (2004), Prendergast et al. (2003)] developed for integration

with a standard uniaxial tensile testing machine to apply equibiaxial load was adapted so that it could effectively eliminate friction and accommodate larger sample dimensions and hence apply equibiaxial load to the square samples prepared. This rig comprised a number of working assemblies as shown in detail in Figure 5.5 below. The adaption includes a new equilibration system (model brass pulleys, see Figure 5.5A & B) to convert the uniaxial displacement-controlled load to biaxial force-controlled load with minimal friction. The biaxial loading device consists of a balanced set of rotating beams of equal length which are free to pivot on polished steel shoulder screws (see point 3 in Figure 5.5). Braided fishing line (50 lb breaking strain) joins the arm of one beam to another arm of the beam adjacent to it. A double-pulley (8 mm diameter each) situated along the length of this line allows any movement of either of the arms to which it is attached to be converted to a single movement. The resultant combination of the four inter-connected double-pulleys results in equal load in each set of pulleys. More braided line connects each double-pulley set to two smaller (6 mm diameter) pulleys through a pulley bracket attached to the base plate, further balancing the system. These, in turn, are connected to a linea alba sample via two fishing hooks each, with a total of 16 hooks per sample (four on each edge). An aluminium block with a 2 mm wide and 5 mm deep ridge offset 2 mm from the edge was used to guide each hook into place. This jig was used to test both porcine and human specimens.

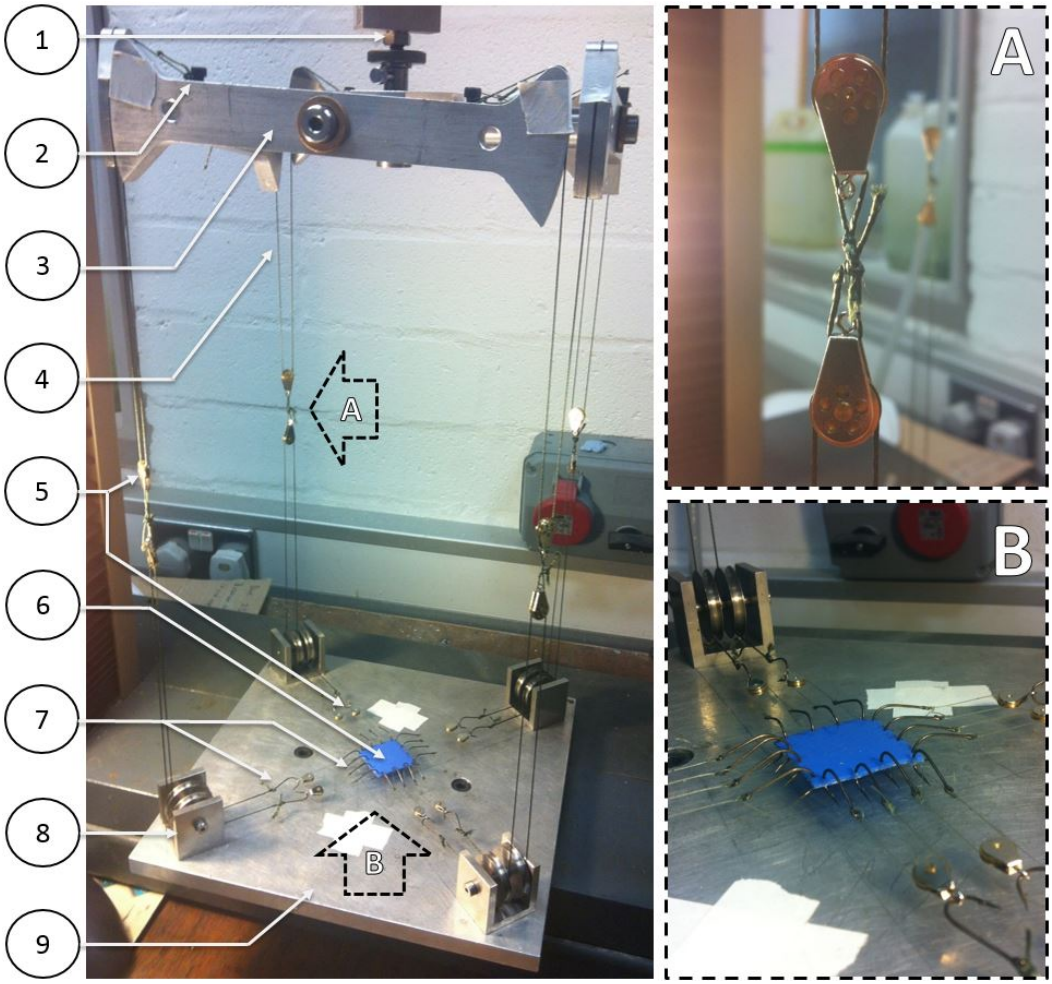

Figure 5.5: The equibiaxial testing device depicting the (1) load cell, (2) connection point of the tension line to the balance beam, (3) rotating beams, (4) high strength thread tension line, (5) equilibration pulley system, (6) test specimen, (7) high strength barbed hooks, (8) pulley bracket and (9) base plate.

The biaxial tests on porcine linea alba samples were carried out on a displacement-controlled Zwick Roell 2005 materials testing machine fitted with a 100 N load cell. The human biaxial tests, like the uniaxial tests, were performed with the same clamping setup secured in a mechanical testing system that was previously custom-made for the Musculoskeletal research group in Washington University [Fang et al. (2014)].

A preload corresponding to 0.15 MPa in each direction was applied, which lifted the sample from the surface of the base plate (see Figure 5.6A, B & C below). A speckle pattern of water resistant, oil-based, quick-drying ink was applied to the sample by rubbing an ink-laden toothbrush against a cooking sieve suspended immediately above it. This was to allow for adequate digital image correlation (DIC) based determination of the local deformations

of the tissues. DIC was used rather than discrete dots as the barbed hooks caused local deformation of the tissue and left corner regions unstressed. A test speed of 10 mm/min was used to ensure that the test remained quasi-static. The high resolution camera (Samsung HMXQF20), as seen in Figure 5.6D was used to record the deformation.

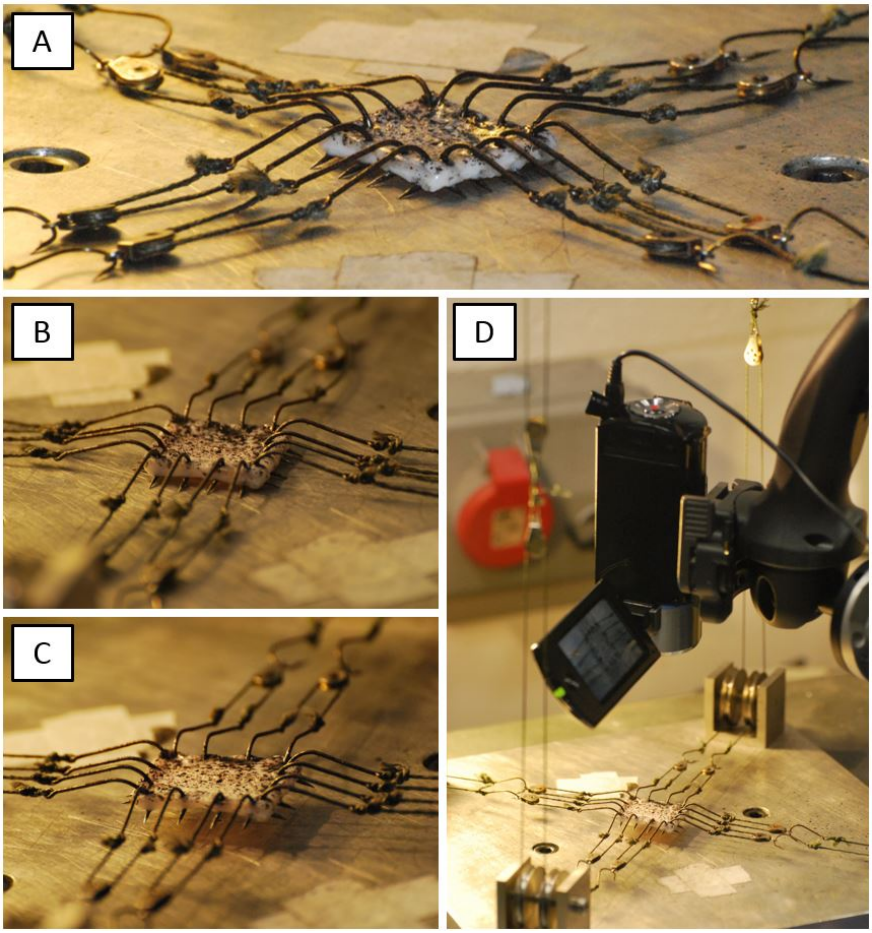

Figure 5.6: Equibiaxial testing of porcine linea alba showing a close-up of the specimen and attached hooks and minor pulleys (A), the sample before (B) and after (C) the application of a pre-load and the camera setup for recording the experiment (D).

The experiment was stopped when tearing began at the hooks (characterised by a 20% drop in force experienced by the load cell) or when the load cell force exceeded 90N (safety limit of the 100N load cell). The Cauchy stress was determined by dividing by the instantaneous cross-sectional area (thickness by the width inside the hooks) and then multiplying by the axial stretch (assuming incompressibility again). Pre-conditioning of samples was not employed in this study.

A custom MATLAB DIC and Tracking program [Eberl et al. (2006)] was used for biaxial

tensile strain analysis. For each test, a user-defined grid was layered over the initial image of the sample (Figure 5.7A below). The size of the grid applied to each sample was individually assessed to ensure that the spaces between hooks had no influence on the displacement of the gridded pattern. The relative change in distance between two grid-points was used to calculate the stretch.

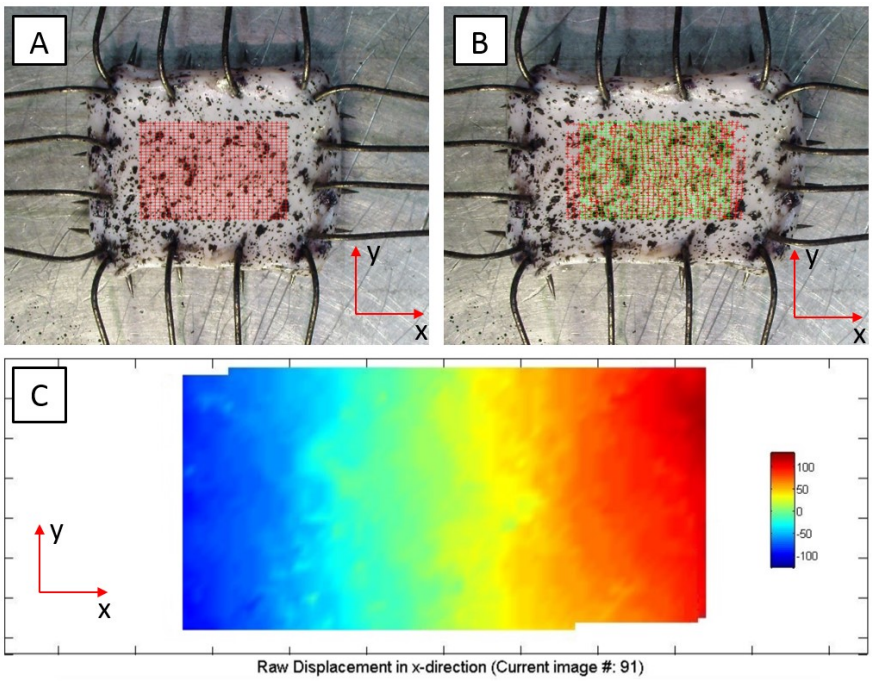

Figure 5.7: Equibiaxial analysis showing the application of a grid of user-defined size (A), the real-time deformation of said grid (B) and a longitudinal strain field plot (x-direction) of the displaced grid at the end of the experiment (C).

The path or track of the grid as it deforms (see Figure 5.7B; the green grid is the original and the red grid is the deformed result for that image/time-step) was recorded. A strain field plot derived from the grid displacement (Figure 5.7C) was used to assess alignment of experimental setup/hook placement (samples would ideally exhibit displacement symmetry). The accuracy of the DIC strain measurement method was assessed by comparison with manual marker tracking, see Table 11.1 in the Appendix, showing average differences of less than 1%.

5.2.4 Identifying Pre-Stress

The artificial 0.1MPa pre-stress applied to the uniaxial samples removes slack that the linea alba would not normally experience in-vivo (being subjected to a constant tension through the typical resting intra-abdominal pressure of 1kPa [Addington et al. (2008), Campbell & Green (1953), Cobb et al. (2005), Malbrain et al. (2004), Ravishankar & Hunter (2005)]). In order to quantify the amount of stretch the tissue experiences in-vivo, abdominal walls were artificially subjected to physiological resting conditions (using a surrogate rig previously designed in-house in Trinity College Dublin [Lyons et al. (2015)]) so the deformation/stretch could be measured. The bellies were therefore subjected to a ramp in pressure from 0-1kPa. A series of dots were applied to the linea alba aligned in both the transverse and longitudinal directions to measure the relative change in millimetres using vernier calipers (see below in Figure 5.8).

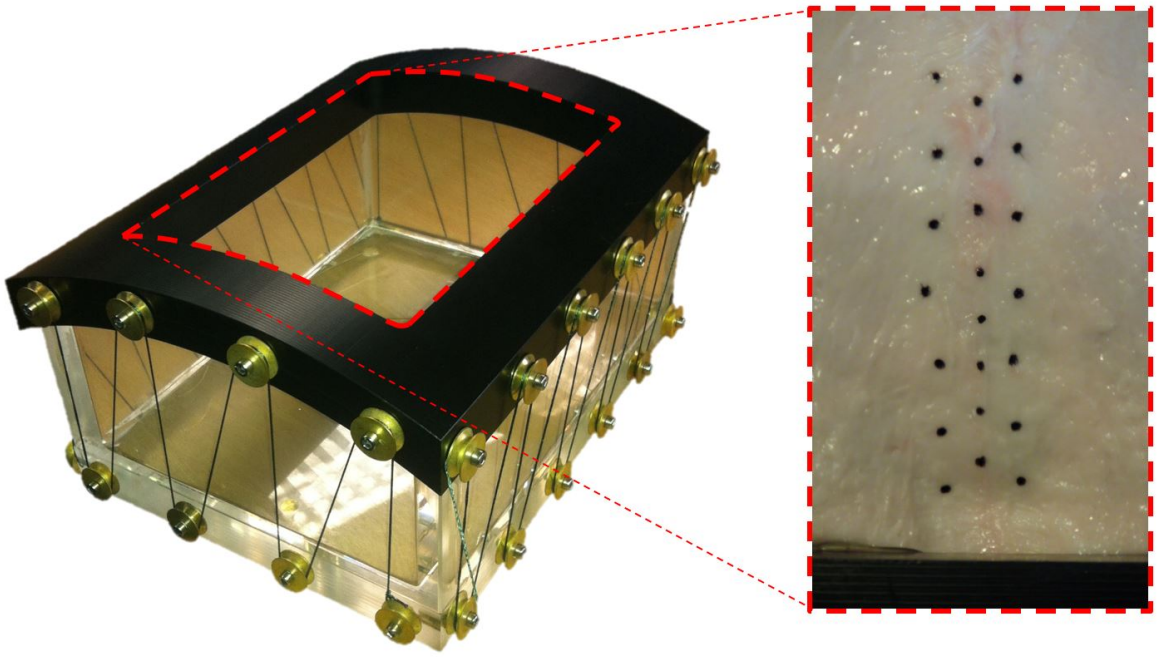

Figure 5.8: The surrogate rig used to aid measurement of pre-stretch showing an abdominal wall with dot placement along the linea alba.

The average of the recorded pre-stretch (λ; seen below in Table 5.5) was then applied to the raw data of some preliminary samples. Typically the corresponding stress observed for the given pre-stretch (applied to uniaxial and biaxial data profiles) was found to be approximately 0.1 MPa. Following this, an artificial pre-load of 0.1 MPa was applied to all

data during post-processing. This means that the data shifts back to the origin along both axes, eliminating any excessive toe-regions evident in any test that correspond to slack being taken up in the initial stages of each test. Its purpose is to essentially reduce variability in the experimental data.

Table 5.5: Pre-stretch calculation for both porcine and human abdominal walls.

Pre-Stretch		Sample 1			Sample 2		
		0 kPa	1 kPa	λ	0 kPa	1 kPa	λ
Human	Longitudinal	12	12.55	1.041	12.5	13.1	1.048
	Transverse	9.5	9.7	1.021	9.5	9.8	1.031
Porcine	Longitudinal	14.93	15.26	1.022	10	10.18	1.018
	Transverse	11.68	11.83	1.012	10	10.1	1.01

An example of this particular method of data-shifting can be seen below in Figure 5.9. The curve moves down both the x-axis and y-axis (stretch and stress respectively).

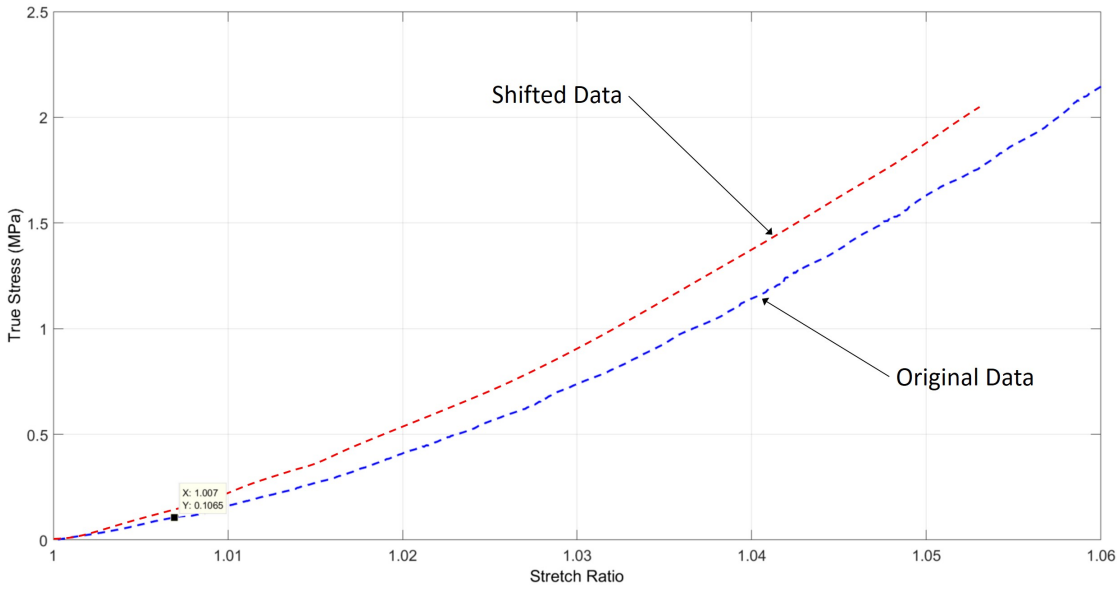

Figure 5.9: Shifting stress-stretch data by 0.1MPa.

5.2.5 Sample Vetting

Due to tissue preparation challenges, the results from some uniaxial tests could not be used. The presence or absence of regional bias in the stretch measurements (arising from skewed sample placement or tissue damage) was used to develop an accept/reject criterion. With this approach, a total of eight uniaxial porcine samples and three human samples were excluded.

The eligibility of each biaxial specimen was assessed by analysing the strain-field occurring within the sample. Samples exhibiting biased regional strain (most likely as a result of improper hook placement, skewed sample dimensions or damage to tissue structure), taking the form of irregular patterns or pockets of strain, were identified and subsequently rejected by analysing the homogeneity of the displacement of the grid as can be seen in Figure 5.7C. A total of three biaxial porcine samples and one human sample were rejected in this study.

5.2.6 Computational Modelling

The constitutive properties of porcine tissue were investigated using finite element analysis (FEA). In addition since the actual length to width ratio for the uniaxial test samples was approximately 2:1 (see Table 5.1) rather than the recommended 4:1 [ASTM (Standard E8/E8M)], the contribution of the effects of clamping on stress was also assessed using FEA. All FEA was performed using the open-source software FEBio (version 1.7, Musculoskeletal Research Laboratories, The University of Utah, USA [Maas et al. (2013)]). This section describes the constitutive model employed, the inverse optimisation methods for material parameter identification, and the FEA models used.

5.2.6.1 Constitutive Modelling

The porcine linea alba was modelled using the uncoupled hyperelastic strain energy density function (ψ) as seen in Eq. (5.3). This particular model was used as it was simple, available through FeBio, and has proven successful at modelling soft tissues in the past [Takaza, Moerman & Simms (2013)].

$$\psi = \frac{c}{m^2}\left(\tilde{\lambda}_1^{m_i} + \tilde{\lambda}_2^{m_i} + \tilde{\lambda}_3^{m_i} - 3\right) + \frac{\kappa}{2} ln\,(J) + \psi_f \tag{5.3}$$

The first term defines the deviatoric response of the ground matrix (a 1st order Ogden form) and contains the material parameters c and m and the deviatoric principal stretches $\tilde{\lambda}_1$, $\tilde{\lambda}_2$ and $\tilde{\lambda}_3$. The second term is a function of the Jacobian (or volume ratio) J and the bulk modulus κ and dictates the volumetric response. The last term ψ_f (see Eq. (5.4) describes fibrous reinforcement as a function of the fibre stretch $\tilde{\lambda}_f$ and the material parameters ξ and β (based on the FEBio implementation of the "fibre with exponential power law" with $\alpha = 0$

[Eberl et al. (2006)]):

$$\psi_f(\tilde{\lambda}_f) = \begin{cases} \psi = \frac{\xi}{\beta}\left(\tilde{\lambda}_f^2 - 1\right)^{\beta} & \tilde{\lambda}_f > 1 \\ 0 & \tilde{\lambda}_f \leq 1 \end{cases} \tag{5.4}$$

where ξ and β are material constants and $\tilde{\lambda}_f$ is the fibre stretch.

Soft tissues have a high water content and are often assumed nearly incompressible (implying $J \approx 1$), as they are in the current study. For uncoupled constitutive laws this is often achieved by choosing the bulk modulus κ to be several orders of magnitude higher than the deviatoric stiffness metrics. However, an excessively high bulk modulus leads to poor model convergence. Hence the bulk modulus was investigated separately here before the optimisation process, i.e. it was varied to enforce nearly incompressible behaviour and $J \approx 1$ while maintaining appropriate model convergence.

5.2.6.2 Inverse Optimisation

Inverse FEA was performed using MATLAB (R2013b, The Mathworks Inc., Natick, MA) to achieve material parameter optimisation (see also [Takaza, Moerman, Gindre, Lyons & Simms (2013), Takaza, Moerman & Simms (2013)] and the MATLAB toolbox presented in [Moerman et al. (2013)]) The inverse optimisation algorithm (Nelder-Mead implementation of the fminsearch function) minimises the sum of squared differences between the experimental and predicted Cauchy stress-stretch data (function tolerance of 0.0001). The Ogden ground matrix parameters (c and m) were first fitted using the uniaxial longitudinal loading data since in this case fibres are loaded in compression and do not contribute in the model. The fibre constitutive parameters (ξ and β) were then optimised separately using the uniaxial transverse loading data while the optimised ground matrix parameters were kept constant.

5.2.6.3 Finite Element Models

Three types of FEA models were constructed for this study (see Fig. 7). The first, shown in Figure 5.10A, is an idealised (nearly) uniaxial loading model (20 mm long, 10 x 10 mm in section). This model served to provide an initial fit of the material parameters. The model consists of tissue (N tri-linear solid hexahedral elements; Figures 5.10A-D) and a rigid

surface used to facilitate contact and applied deformation (N tri-linear quadrilateral shell elements; top surface of Figure 5.10A). While the bottom face is fully supported, the top surface is connected to the rigid surface which undergoes a prescribed motion upwards to apply near-uniaxial loading. Based on Eq. (6.2) a simulated uniaxial Cauchy stress can be derived for comparison to the experiment.

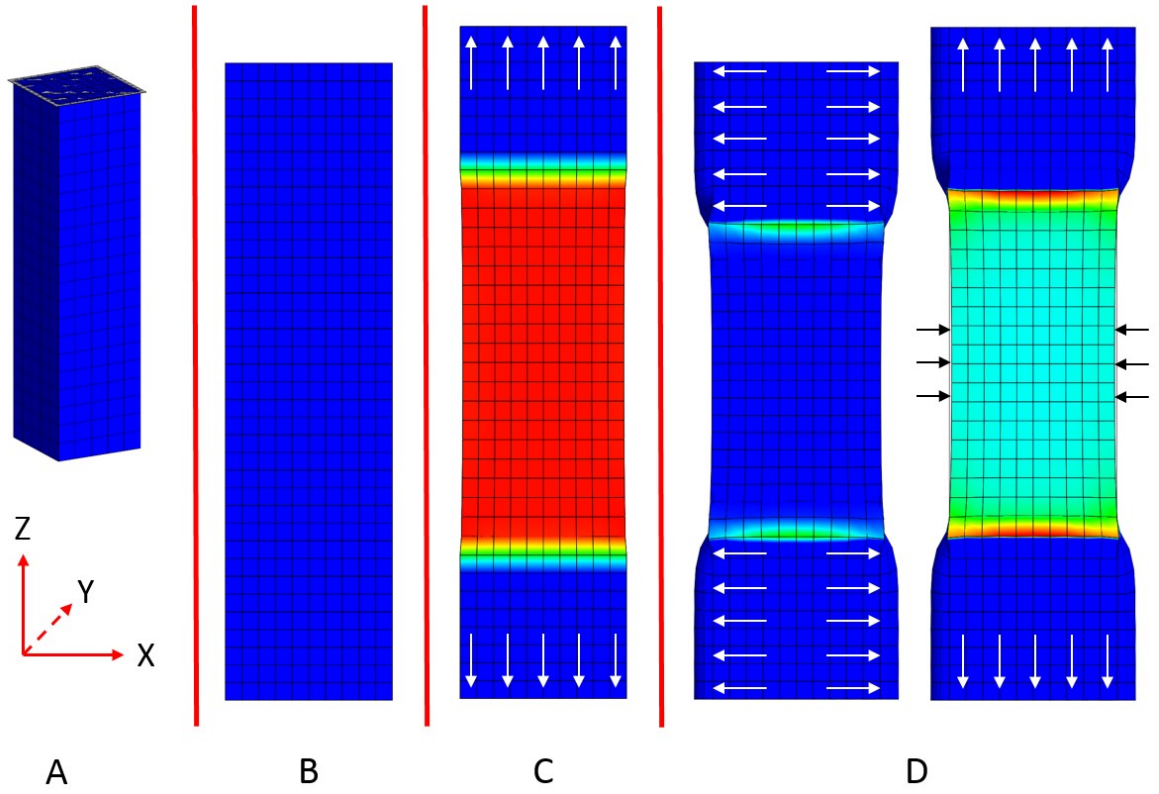

Figure 5.10: A depiction of the models used showing (A) the initial FEBio model for optimisation and (B) the final FEBio model before deformation, (C) for simple axial displacement and (D) 2-step deformation. The colour map indicates stress in the z-axis.

In addition two further 3-dimensional models were created to investigate the effect of clamping and sample dimensions (Figure 5.10B) (for along the fibre direction): 1) A case where a tensile stretch is applied without explicitly modelling tissue gripping and 2) a two-step case where tissue gripping is modelled explicitly (a grip induced thickness reduction step) followed by an applied tensile stretch.

For case 1, where no gripping induced compression is modelled, the nodes in the bottom grip region were fully fixed while at the top grip region nodes were constrained in the x- and y-direction and were subjected to a prescribed displacement in the positive z-axis direction,

see Figure 5.10C.

For case 2, where initial gripping is modelled, nodes at both the top and bottom end faces of the sample were constrained from displacing in the z-direction while nodes on both sides of the sample at the region of the grips were subjected to an equal displacement in the y-direction corresponding to 37.5% compression (derived experimentally) to simulate gripping, see Figure 5.10D. The surface nodes at the region of the grips were constrained from displacing in the x- and z-direction in order to simulate the high friction of the emery paper on the grips. In a second step, a subsequent uniaxial z-direction stretch was applied. In this step the nodes at one end of the sample, corresponding to those associated with the bottom grip, were once again fixed while the nodes at the opposite end were constrained in the x- and y-direction and subjected to the same prescribed displacement in the positive z-axis direction.

In both models the prescribed z-displacement led to 10% zdirection tensile strain under uniaxial conditions (corresponding to the typical maximum experimental strain). Figure 5.10D shows the relative expansion of the sample under the grips as compression is applied for model case 2 and also shows the sample as it begins to neck following z-direction tension, an effect common to both model types. The stress response of the most central element was exported for both models for comparison at equivalent levels of overall tissue stretch.

Preliminary material parameters for case 1 were determined by fitting to the average porcine uniaxial transverse experimental stress-stretch curve.

The effect of tissue sample aspect ratio on the stress state was investigated in both cases 1 and 2 by varying grip-to-grip lengths (gauge lengths) between 10 mm and 50 mm for a fixed sample width of 10 mm. The ratio of the difference of maximum stress between cases 1 and 2 at a stretch of 1.1 using the preliminary material parameters was then used to scale each uniaxial experimental stress-stretch curve to account for the effects of clamping present in the experiments. The average adjusted experimental curve was then used in a final optimisation process based on case 1 to obtain the material constants c, m, ξ and β. Mesh convergence tests were performed to identify optimum mesh size.

In addition, to assess the ability of the fibre reinforced composite model in predicting the porcine biaxial response of porcine linea alba, a simulation of the biaxial tests was generated with parameters derived from the uniaxial tests. This involved the same setup as the uniaxial

simulations but using typical biaxial dimensions (Table 5.3) and a prescribed traction force, rather than displacement, applied equally to all four sides of the sample (equivalent to the experiments).

5.3 Results

5.3.1 Uniaxial Loading

The Cauchy stress as a function of the applied stretch ratio for both transverse and longitudinal directions for all porcine samples is shown in Figure 5.11 below. The mean and 1 standard deviation relationships are also shown. The slope of the most linear region of the equivalent stress-strain relationship for each curve (a Young's modulus-like stiffness metric based on Cauchy stress/Engineering strain excluding the initial toe region) was approximately 61 MPa in the transverse direction and 7 MPa in the longitudinal direction. These slopes are characterised by the final 40% of each curve.

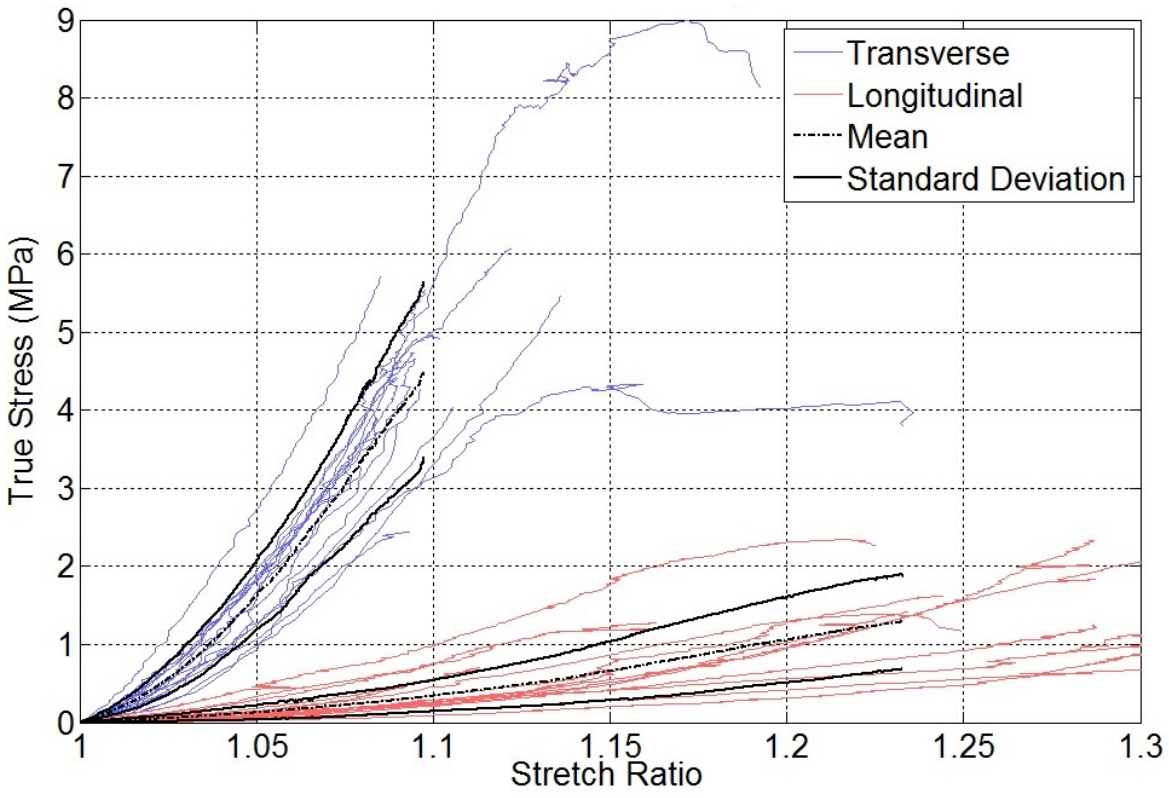

Figure 5.11: The combined porcine uniaxial data for both transverse (N=16) and longitudinal (N=16) directions.

Figure 5.12 below plots the uniaxial mean and standard deviation Cauchy stress versus stretch ratio of human tissue for both transverse and longitudinal directions. The slope of the averages was approximately 72 MPa in the transverse direction and 8 MPa in the longitudinal direction, as characterised again by the final 40% of each curve.

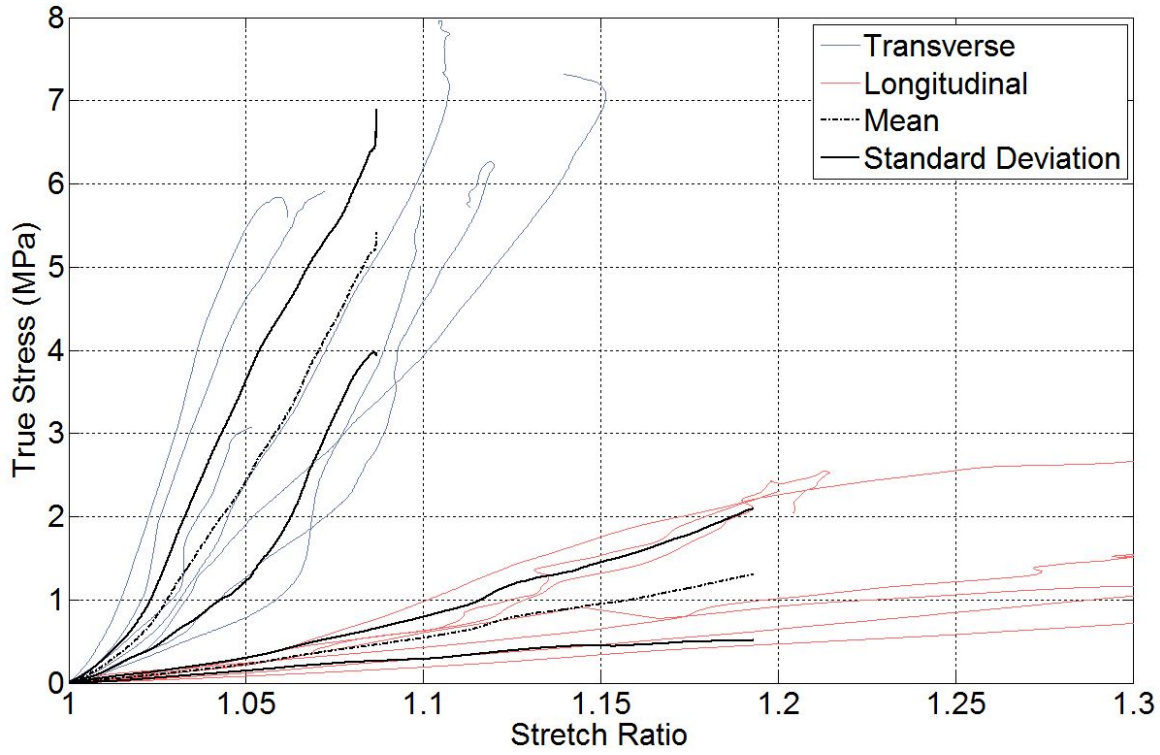

Figure 5.12: The combined human uniaxial data for both transverse (N=7) and longitudinal (N=7) directions.

5.3.1.1 Image Analysis Versus Machine Cross-Head Displacement

A measure of the effect that slippage from the grips and/or transducer deformation has on the overall measured mechanical properties of the porcine tissue specimens can be seen in Figure 5.13 below, which shows average Cauchy stress versus stretch ratio using either image based strain or machine cross-head displacement based strain. Samples processed using cross-head displacement yielded values of 35 MPa and 4 MPa (transverse and longitudinal directions respectively), approximately 42% different to those from image based analysis presented above (image analysis characterising a 75% increase in stiffness).

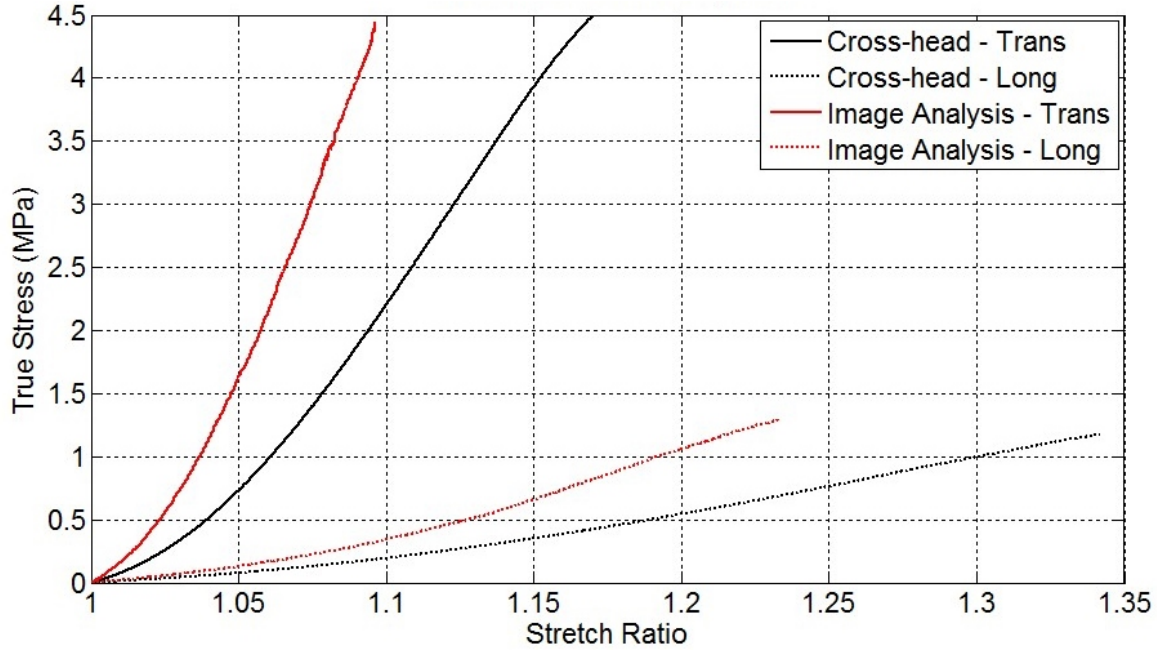

Figure 5.13: Comparison of the true stress versus stretch ratio estimations for stretches calculated from image analysis and from machine cross-head displacement of porcine specimens.

5.3.1.2 Freeze-Thaw Cycle Analysis

An investigation into the effects that freezing has on the mechanical properties of porcine tissue was investigated. A comparison of the mechanical stress-stretch characteristics of fresh versus frozen tissue can be seen below in Figure 5.14. Fresh samples yielded slope values of approximately 71 MPa and 11 MPa compared with the 61 MPa and 7 MPa seen in the frozen data. Using a two-tailed t-test to compare the average stress observed at 60% of the applied stretch (the point at which calculations of slope are made; see Section 5.3.1) for fresh and frozen tissue found no statistical significance in the difference between their means ($P = 0.4$ & $0.8 > 0.05$ for transverse and longitudinal directions respectively, see Figure 5.15).

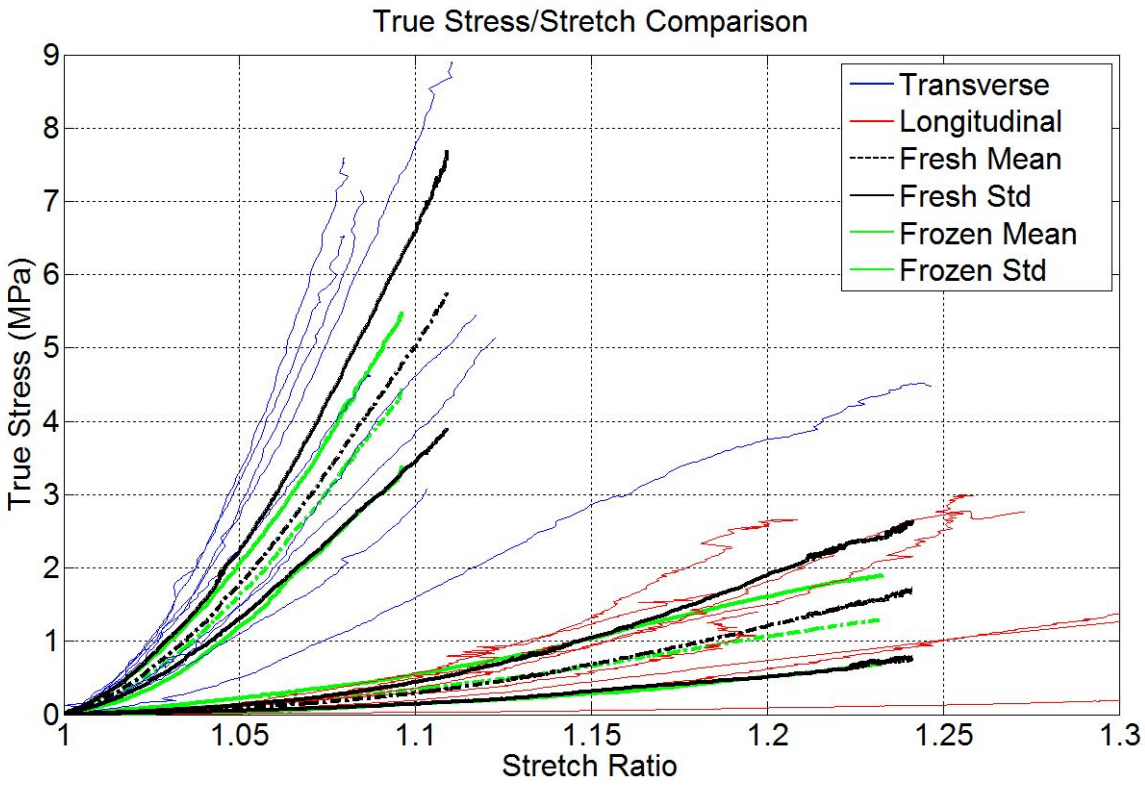

Figure 5.14: Comparison of the true stress versus stretch ratio profiles of fresh and frozen porcine tissue.

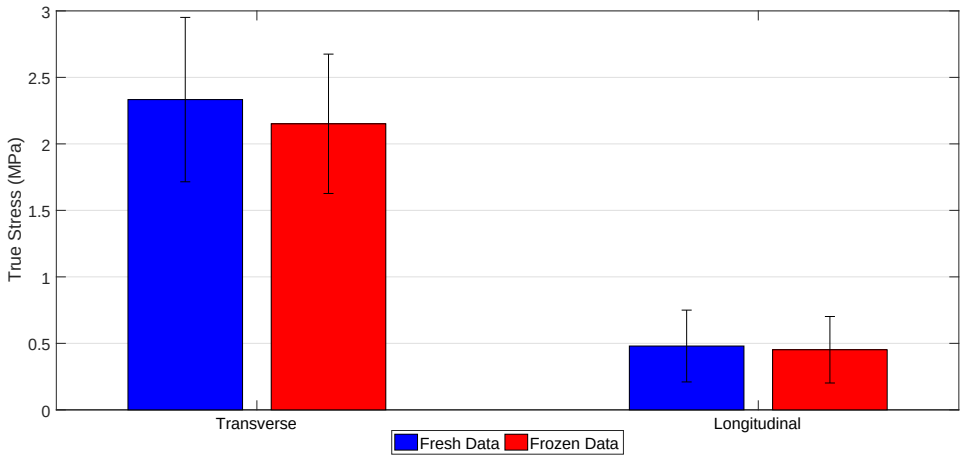

Figure 5.15: Comparison of the true stress versus stretch ratio profiles of fresh and frozen porcine tissue observed at 60% of the applied stretch; no significant difference observed.

5.3.2 Equibiaxial Loading

The mean and standard deviation of the Cauchy stress for biaxial porcine tests is presented against the stretch derived by DIC for both transverse (fibre) and longitudinal (cross-fibre) directions in Figure 5.16 below. The approximate linear stiffness for both orientations was found to be 240 MPa and 30 MPa respectively (again characterised by the last 40% of each curve). The results for individual samples (each having both a transverse and longitudinal profile) tested are also included for a more clear understanding of the variability. As this is a force-controlled experiment rather than a displacement controlled one, standard deviation of the stretch rather than the stress is used.

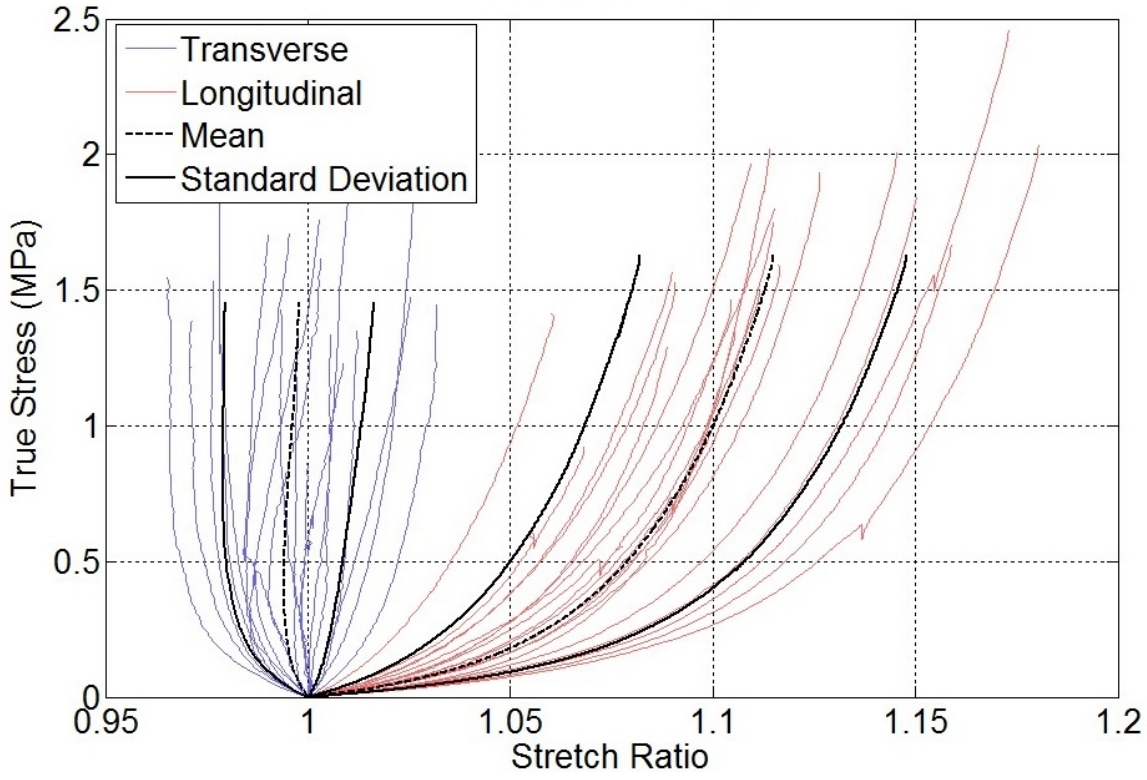

Figure 5.16: The combined porcine biaxial data for both transverse and longitudinal directions (N=20).

Figure 5.17 below plots the biaxial mean and standard deviation Cauchy stress versus stretch ratio of human tissue for both transverse and longitudinal directions. The slope of the averages was approximately 335 MPa in the transverse direction (slope is slightly negative) and 23 MPa in the longitudinal direction.

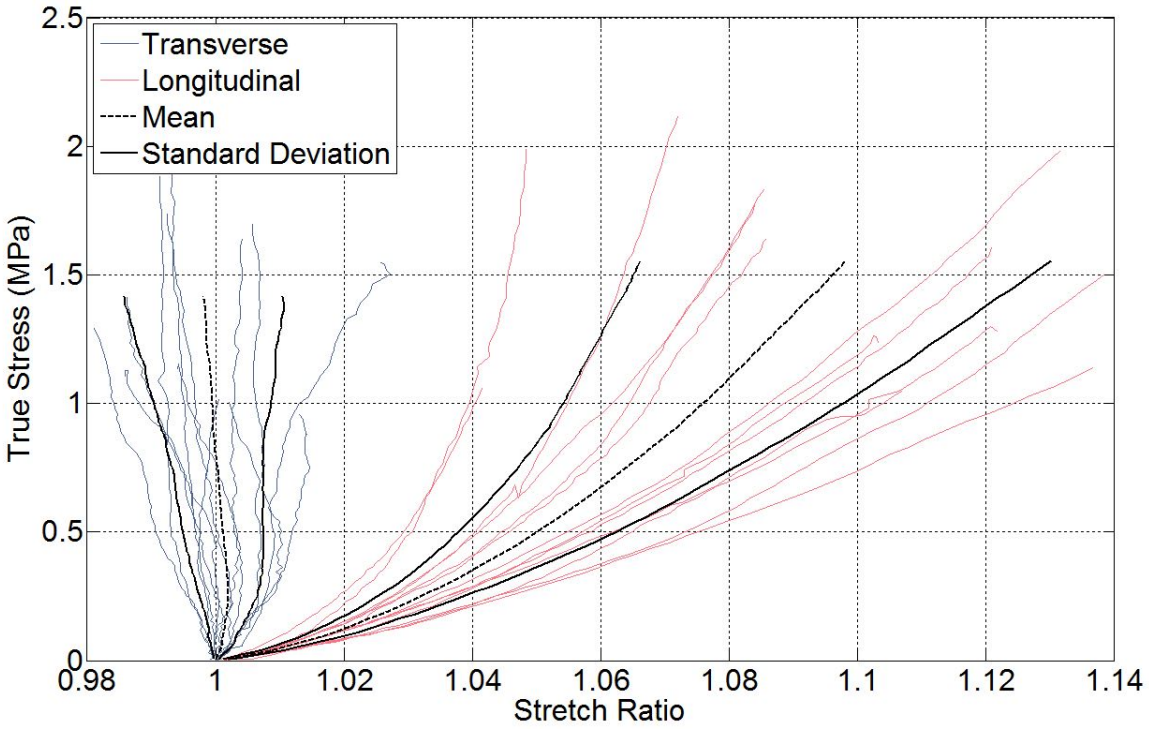

Figure 5.17: The combined human biaxial data for both transverse and longitudinal directions (N=13).

5.3.3 Computational Modelling

5.3.3.1 Bulk Modulus Optimisation for Near-Incompressibility

Figure 5.18 shows the effect of the bulk modulus (κ) on the peak stress. For a bulk modulus above 20 MPa the effect on the peak stress becomes relatively constant. It was observed that for κ = 20 MPa the volume ratio remained close to 1 with the effect on peak stress becoming constant (see Figure 5.18). Accordingly, κ was set to 20 MPa for all FEA.

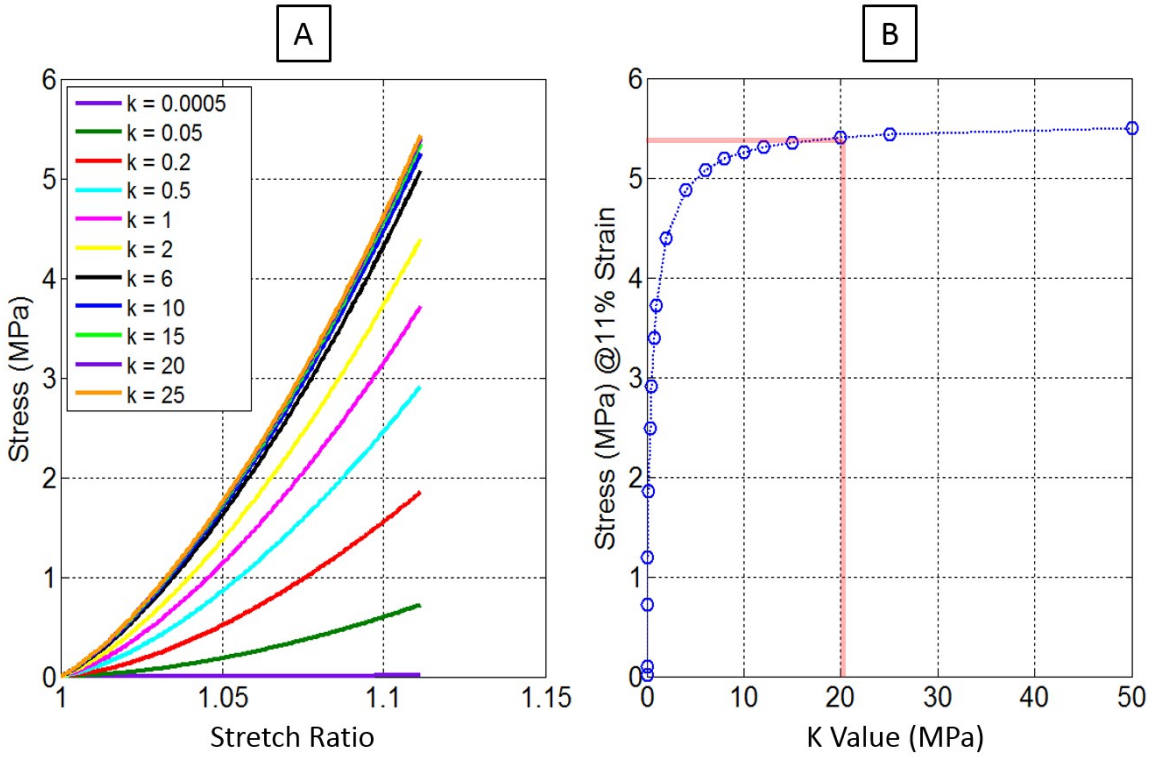

Figure 5.18: Influence of varying Bulk Modulus on stress/stretch response (A) and influence of varying Bulk Modulus on peak stress (B).

5.3.3.2 Inverse FEA Optimisation

Optimisation using the preliminary porcine uniaxial averages (Ogden model for the longitudinal average and fibre with exponential power law model for the transverse average) resulted in the preliminary porcine material parameters shown in Table 5.6:

Table 5.6: Porcine Model Parameters

	First Order Ogden Model		Exponential Power Law Model	
	c	m	e	b
Preliminary	1.399 ±1.023	9.64 ±(-1.112)	11.764 ±1.108	2.217 ±(-0.163)
Final	2.309 ±0.771	9.421 ±2.854	22.499 ±3.606	2.387 ±(-0.038)

Figure 5.19 shows the stress difference ratio observed at a stretch of 1.1 for case 1 (unclamped) compared to case 2 (clamped) based on the preliminary material parameters for a range of gauge lengths with sample width held constant at 10 mm.

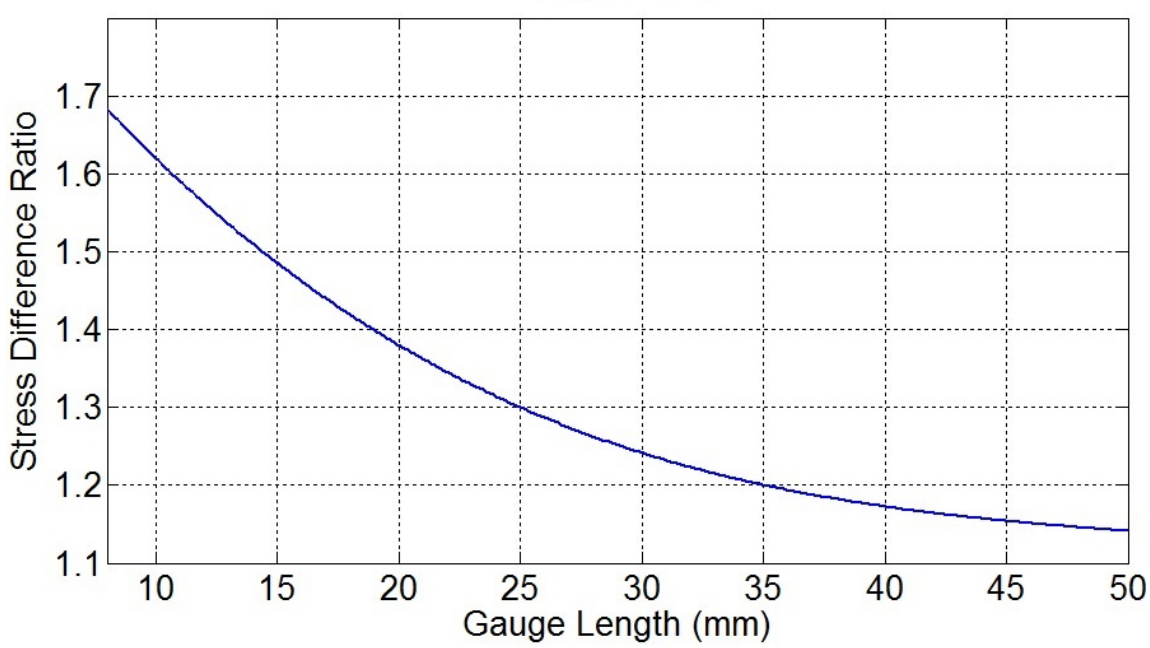

Figure 5.19: The porcine stress difference ratio between clamped and unclamped models of different gauge lengths at k=1.1.

Scaling the uniaxial data using the interpolated stress difference ratio for each experimental resulted in the adjusted Cauchy stress/stretch response seen in Figure 5.20 below. The data averages now yield a linear stiffness metric of 90 MPa and 10 MPa in the transverse and longitudinal directions respectively.

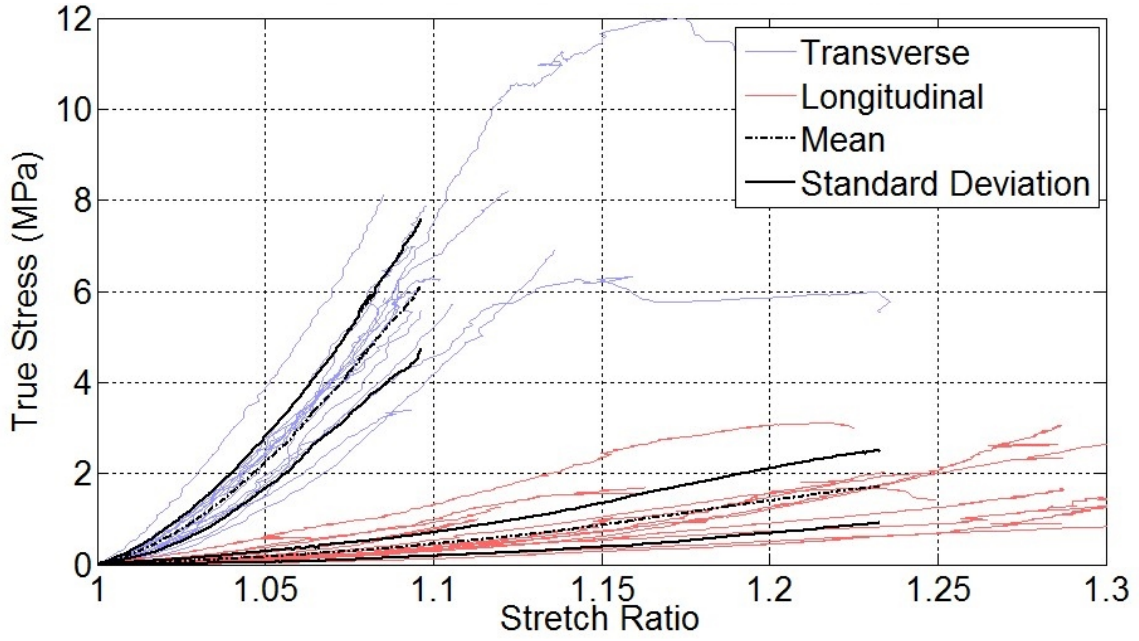

Figure 5.20: The adjusted porcine uniaxial data; accounting for effects of gripping by applying the stress difference ratio.

Optimisation using the adjusted uniaxial averages in Figure 5.20 resulted in the final material parameters shown in Table 5.6.

Figure 5.21 shows the average adjusted experimental longitudinal and transverse loading response for uniaxial tests and the inverse FEA derived model fits.

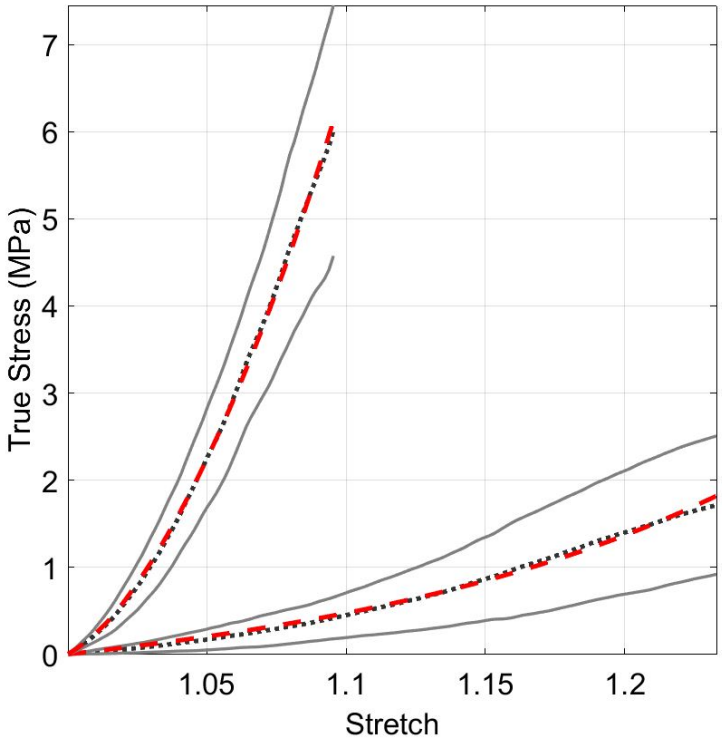

Figure 5.21: Fitting the adjusted porcine uniaxial experimental data using MATLAB-FEBio optimisation. The curve fits are in red while the adjusted experimental data is in black.

Figure 5.22 shows the average porcine experimental biaxial responses for the transverse and longitudinal directions and the corresponding finite element model predictions using the material parameters from Table 3. Biaxial simulations did not provide a good match to the experimental data; the simulations especially unable to replicate negative strain. This is possibly due to the fact that the fibre reinforced model describes a transversely isotropic material while the linea has a more complex, layered collagen architecture [Gräβel et al. (2005)] which may be causing it to behave differently under biaxial loading.

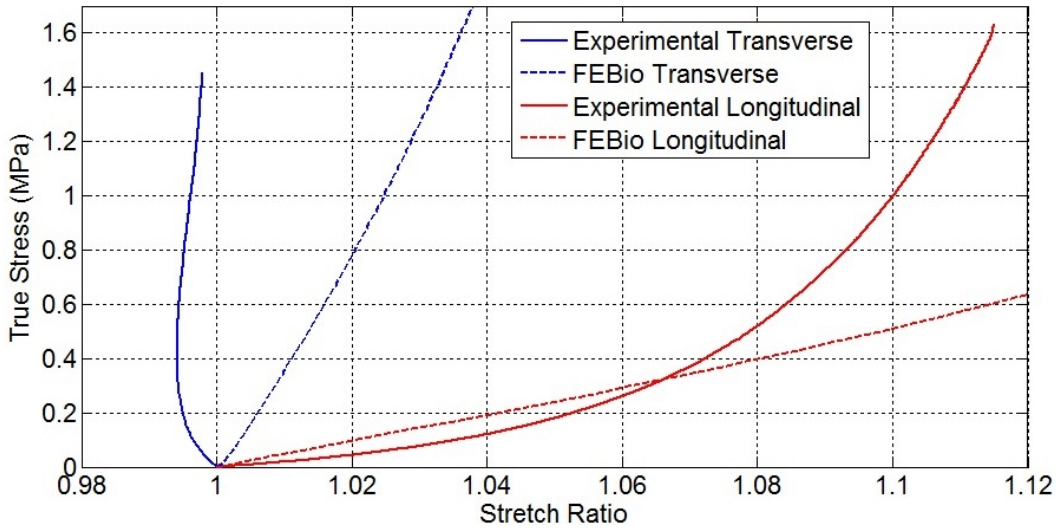

Figure 5.22: FEBio Biaxial tension simulations compared to the average experimental data.

5.4 Discussion

5.4.1 Physical Testing

5.4.1.1 Uniaxial Tests

The linea alba is one of the key structures involved in incisional hernia development, but its uniaxial and particularly biaxial properties are poorly understood. Existing publications present uncertain and sometimes contradictory results most likely due to both the difficulty in dissecting adequate samples and differing methodologies [Förstemann et al. (2011), Gräβel et al. (2005)]. Furthermore, there are no reports on the biaxial response of linea alba in the literature. Addressing these issues were the principal motivations for characterising the mechanical properties of porcine and human linea alba tissue which are reported in this paper.

Because of the necessity to obtain specimens in bulk, it was necessary to freshly freeze all tissue that was obtained in order to prevent decomposition. However, it has been hypothesized in the literature that the act of freezing causes ice crystals to form within the tissue that could subsequently change its mechanical behaviour, though most report differences that are not significant [Pelker et al. (1983), Reilly & Burstein (1974)]. No such study on linea alba tissue was ever found. Therefore, fresh and frozen porcine linea alba were tested (uniaxial) and compared. Very little difference was observed between each case. A 14% and 36% decrease

in stiffness noted with transverse and longitudinal directions respectively when freezing the tissue. However, no statistical significance was found in the difference between their means ($P = 0.4$ & $0.8 > 0.05$ for transverse and longitudinal directions respectively). It was therefore concluded that freezing does not significantly adversely affect the mechanical properties of the linea alba.

Porcine linea alba exhibits anisotropic behaviour, showing significantly greater stiffness (by a factor of around eight) in the transverse (fibre) direction compared the longitudinal (cross-fibre) direction (see Figure 5.11). An ex vivo inflation study performed by D. Tran et al. also shows the significant anisotropy of the linea alba as simulated IAP is increased [Tran et al. (2014)].

Human linea alba was found to exhibit very similar anisotropic behaviour (see Figure 5.12). Because of the age of the human specimens (predominantly elderly) before they died and the tissue harvested, the raw data appears more erratic than that of the porcine specimens which are the equivalent of young adult to middle age. Though showing a greater stiffness in the transverse and longitudinal direction (18% and 14% increase respectively), a two-tailed t-test to comparing the average stress observed at 60% the applied stretch (the point at which calculations of slope are made; see Section 5.3.1) for human and porcine tissue found no statistical significance in the difference between their means ($P = 0.23$ & $0.57 > 0.05$ for transverse and longitudinal directions respectively); see Figure 5.23 & 5.24). It therefore appears that both human and porcine tissue exhibit very similar behavior under uniaxial loading conditions.

An artificial pre-load of 0.1 MPa (like in the current study) was applied to the data presented by F*ö*rstemann and included in the figure below to provide a better comparison. This interpretation of the data provides a mechanical profile that is very similar to the human data obtained in the current study. The F*ö*rstemann data was found to be 15% and 37% stiffer in the transverse and longitudinal directions respectively. It would be expected that the image analysis derived data of the current study would be stiffer (see Figure 5.19). That it is not, however, may be down to differences in experimental protocol, how the tissue was harvested or the age or cause of death of the specimens.

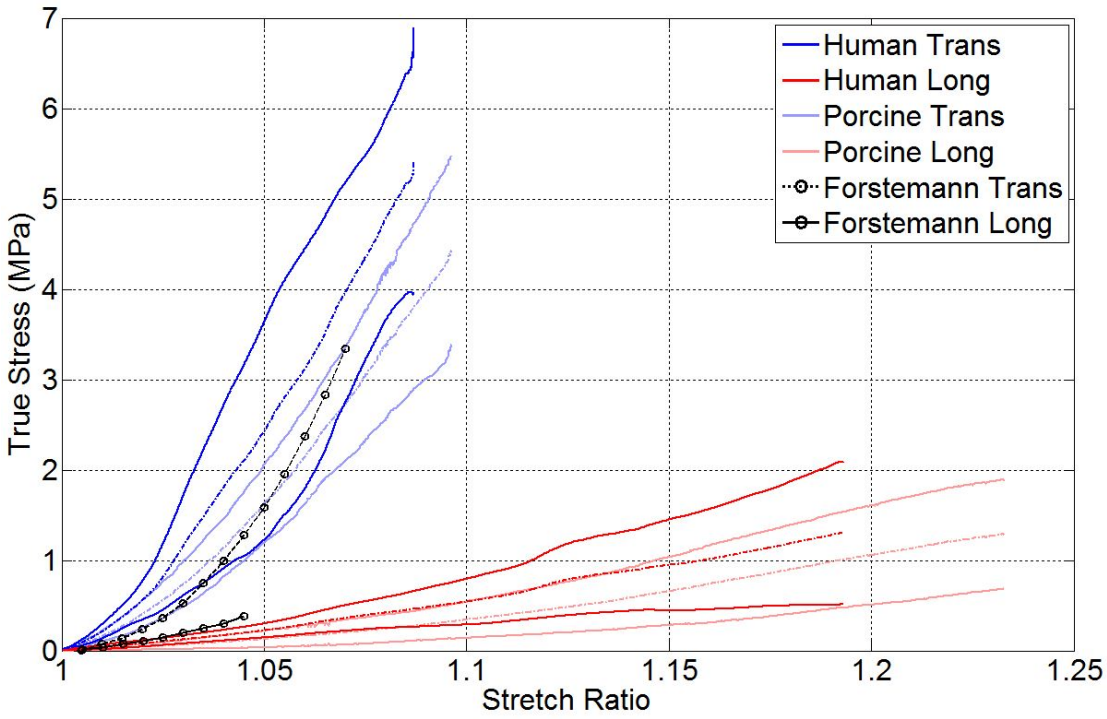

Figure 5.23: A comparison of the human versus porcine uniaxial mechanical characteristics obtained via image analysis. Data from F*ö*rstemann et al. (machine cross-head derived stretch) with artificial pre-load applied is included.

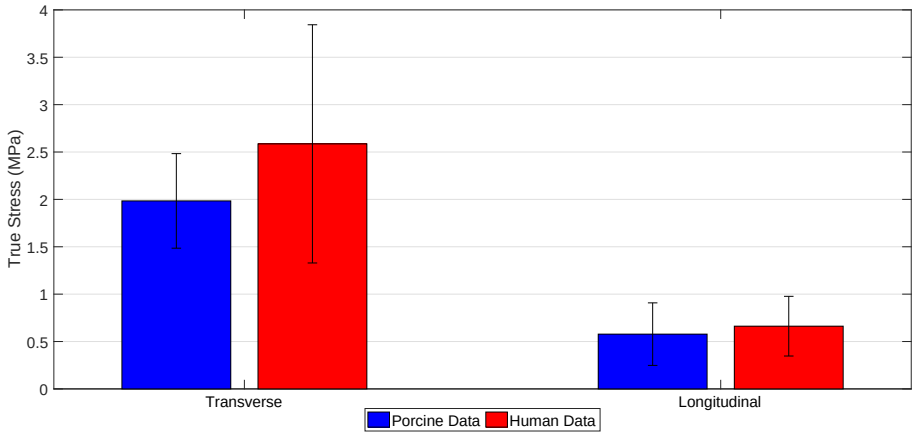

Figure 5.24: Comparison of the human versus porcine uniaxial data observed at 60% of the applied stretch; no significant difference observed.

Figure 5.25 below shows a comparison of the engineering stress versus stretch ratio results for the porcine samples from the current study compared to previously published human sample data [Förstemann et al. (2011), Gräβel et al. (2005)]. Several differences are

evident. The Gr*ä*ßel data show significant stresses at zero stretch, presumably due to the application of a pre-load, but this is not clarified. The F*ö*rstemann data shows a much more significant toe region at low stretches for the transverse case compared to the current data which may be due to differences in the application of a pre-load, but at high stretch ratios the stiffness is higher for the F*ö*rstemann data compared to the current study. For the longitudinal data, there is a good correspondence between the F*ö*rstemann data and the current data.

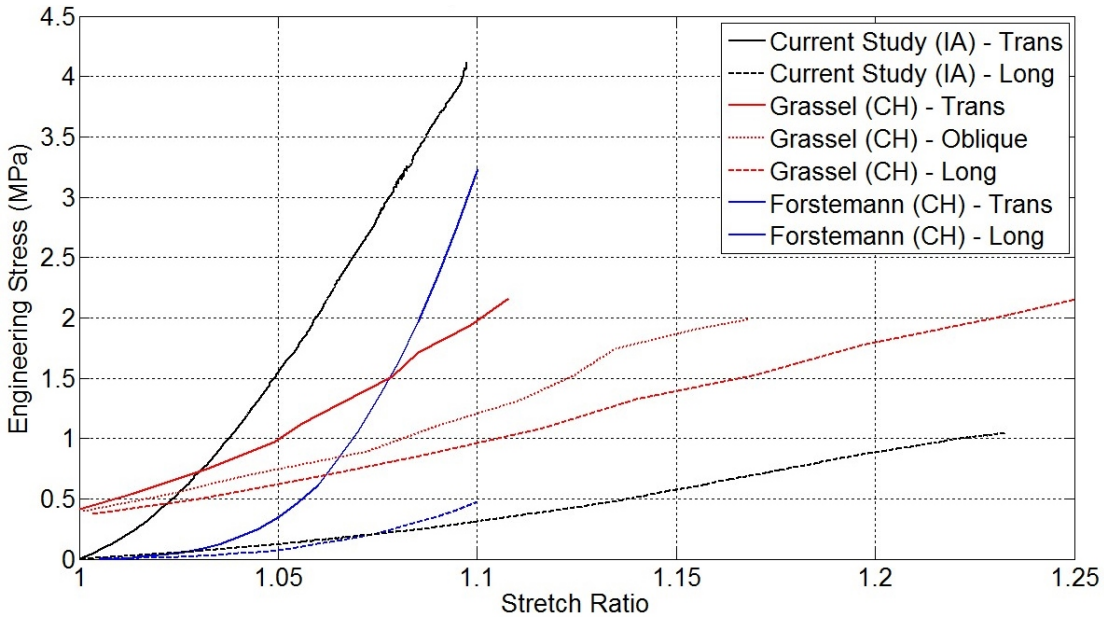

Figure 5.25: Image analysis (IA) derived averages versus that of the literature derived using machine cross-head displacement (CH).

However, there is a significant procedural difference between the current work and the F*ö*rstemann /Gr*ä*ßel approach, since the latter used machine cross-head displacement to estimate sample strain, whereas image based strain calculations were employed in the current work. A comparison of both methods from the current study (Figure 5.13) shows that both transverse and longitudinal cases exhibit an approximate 75% increase in perceived stiffness when using image based strain measurements compared to machine cross-head displacement, even though care was taken to minimise slippage. The F*ö*rstemann data may be susceptible to slippage of the sample in the grips, which would result in under-prediction of the stiffness of the tissue. If this is the case, then the stiffness of the F*ö*rstemann human samples should be higher than presented in Figure 5.25. Accordingly, it appears that human linea alba is therefore stiffer than porcine linea alba, at least in the transverse direction. Unfortunately, it

was not possible to verify or quantify whether slippage did occur in the F*ö*rstemann tests.

The more active lifestyle of humans might suggest a requirement for a stiffer linea alba. However, pigs have a greater proportion of the weight of the internal organs acting directly on the abdominal wall. Furthermore, pigs have a significantly greater BMI than humans (18.5-25 kg/m^2 for healthy humans and compared to up to 127 kg/m^2 in some breeds of pigs [Johnson & Nugent (2003)]) and obesity in humans is associated with increased IAP [Lambert et al. (2005)]. This means that the IAP for pigs should be considerably greater than the approximate 1 kPa average seen in humans [Addington et al. (2008), Campbell & Green (1953), Cobb et al. (2005), Lambert et al. (2005), Malbrain et al. (2004), Ravishankar & Hunter (2005)], though data is not available. These factors might result in a stiffer linea alba in pigs compared to humans. However, this is not evident from Fig. 16. It must be noted that humans have 12 pairs of ribs whereas pigs are known to have as many as 15. This means that muscle placement may differ which would result in aponeuroses that intersect with the linea alba at different angles and could be another explanation for the observed difference in the mechanical response between pigs and humans. Accordingly, the microstructure of the linea alba which defines its anisotropy may be slightly different in pigs than in humans.

5.4.1.2 Biaxial Tests

Linea alba is most likely subjected to biaxial loading in-vivo, though estimation of the magnitude of cranial to caudal loading is currently difficult and there is no literature on this mode of loading. It is acknowledged that equi-biaxial loading probably does not represent physiological loading as there are also diagonal loads present (mainly in the horizontal direction from the oblique muscles), but it may be more representative than uniaxial loading, and certainly provides useful additional information on the deformation behaviour of the tissue. Figure 5.16 shows the results of equi-biaxial loading of porcine linea alba. The equi-load biaxial porcine tests showed that stiffness of the transverse direction was found to be approximately eight times greater than the longitudinal direction, exhibiting an anisotropic response similar to that observed in the uniaxial tests, see Figure 5.11. Similarly, the equibiaxial human tests also show significant anisotropy (see Figure 5.17), the majority of the deformation occurring in the longitudinal direction of samples of both species.

On average, the transverse direction of both human and porcine samples experienced approximately zero strain under the equi-load biaxial tests. This corroborates the hypothesis for the uniaxial tests that in-vivo deformation of the linea alba occurs predominantly in the longitudinal/cranio-caudal direction (see Section 5.4.1.1). D. Tran et al. also reported examples of negative strain in the transverse direction [Tran et al. (2014)]. Similar findings were recently reported by Lyons et al. (2014) for porcine rectus sheath. Lyons et al. attempted to explain this behaviour by applying Hooke's law for transversely isotropic materials. It was found that due to the significantly higher transverse direction stiffness (≈6x stiffer than in the longitudinal direction), it was possible for the transverse direction to experience negative strain during tensile biaxial testing. As linea alba is similarly observed to have a large difference in approximate stiffness between transverse and longitudinal directions (≈7.5x and 14x stiffer in the transverse direction for both porcine and human tissue respectively; obtained from results in the current study) with samples from both species sometimes experiencing negative strain, the same explanation appears appropriate for the results of this study. This is the first biaxial data relating to porcine linea alba and may in future help with decisions relating to wound closure methods following laparoscopic surgery.

Figure 5.26 below depicts the comparison of the mechanical profiles of both human and porcine linea alba. Similarly to the porcine tissue, the human linea alba experienced approximately zero strain in the transverse direction under equi-biaxial loading. This can also be more acutely observed by the trend of individual tests seen in Figure 5.17. Though the initial toe region of the longitudinal profiles of both species appears to differ, a two-tailed t-test to comparing the average stretch observed at 60% of the applied stress (the onset of the linear region) for porcine and human tissue showed no statistical significance ($p = 0.32$) in the difference between their means in the transverse direction. However, a significant difference was observed in the longitudinal direction ($p = 0.011$, see Figure 5.27). This may be attributable to differences in physiology between the two species. Pigs have a greater number of ribs than humans which would result in differences in abdominal muscle attachment [Cooney et al. (2015)]. This may then correspond to aponeuroses that intersect at different angles at the linea alba. Further study of the respective tissue structures is needed to better understand this result.

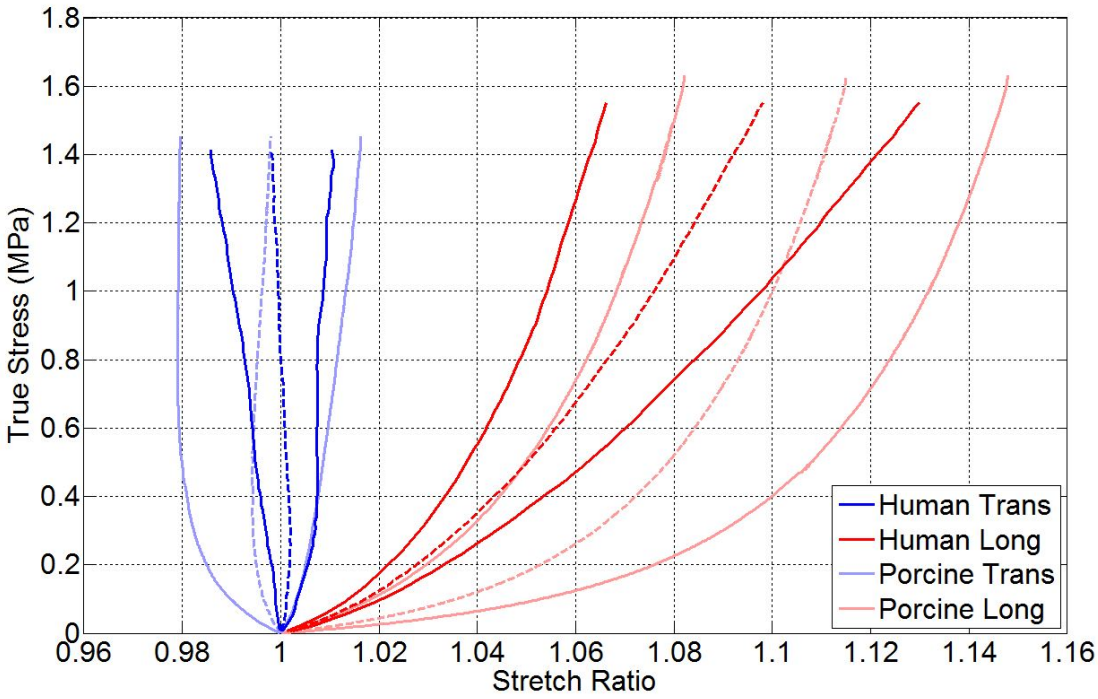

Figure 5.26: A comparison of the human versus porcine biaxial mechanical characteristics obtained via image analysis.

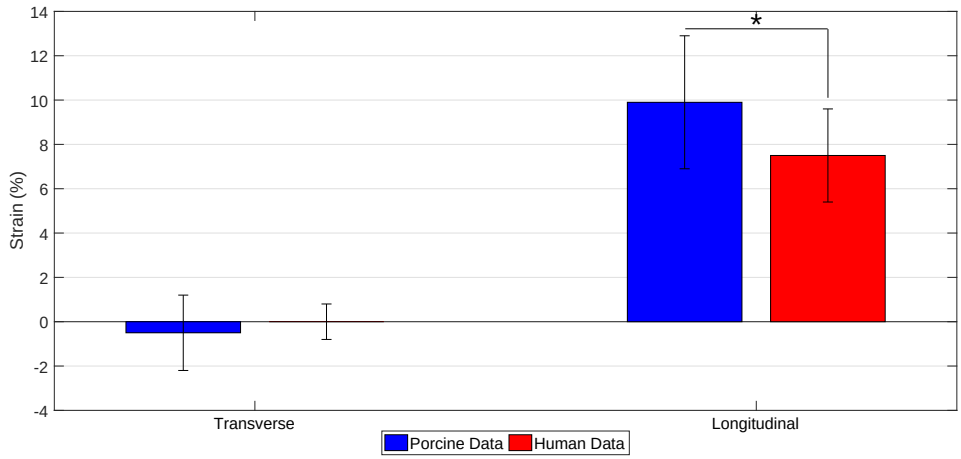

Figure 5.27: Comparison of the human versus porcine biaxial data observed at 60% of the applied stress; significant difference observed in the longitudinal direction ($p = 0.011$).

Modelling the stress occurring within the linea alba using Laplace's law for thin-walled cylinders, with human abdominal dimensions obtained from the literature [Duez et al. (2009)] and a typical extreme IAP of 20 kPa [Addington et al. (2008), Campbell & Green (1953), Cobb et al. (2005), Malbrain et al. (2004), Ravishankar & Hunter (2005)], the linea alba

would theoretically experience stresses as high as 1.3 MPa which could correspond to a strain of 4.7%. This is under the assumption that the cylinder in question is isotropic and, as such, these values are mid-range of the anisotropic experimental biaxial data. It also depends on there being similarities between human and porcine linea alba (when applying to porcine data); the differences of which appear to be very little judging from the data obtained in the current study. Only human dimensions were used for this analysis as no typical IAP ranges for pigs were found in the literature. However, pigs have been shown to be able to sustain artificially generated intra-abdominal pressure ranges similar to that of 1-20kPa in humans [Schachtrupp et al. (2003)].

The uniaxial and biaxial behaviour of porcine linea alba and rectus sheath are compared in Figure 5.28 below. For uniaxial loading, rectus sheath is stiffer than the linea alba; see Figure 5.28A. However, the rectus sheath exhibits a relative drop in stiffness for biaxial loading (Figure 5.28B) when compared with the linea alba. The rectus sheath also appears to be biased towards positive stretch (for equi-load biaxial tests) in the transverse direction rather than negative stretch. This may be as a result of the differences in stiffness observed between transverse and longitudinal directions. The transverse/longitudinal stiffness ratio for rectus sheath in uniaxial loading is approximately six compared to eight for linea alba, which might explain the observed differences for biaxial testing.

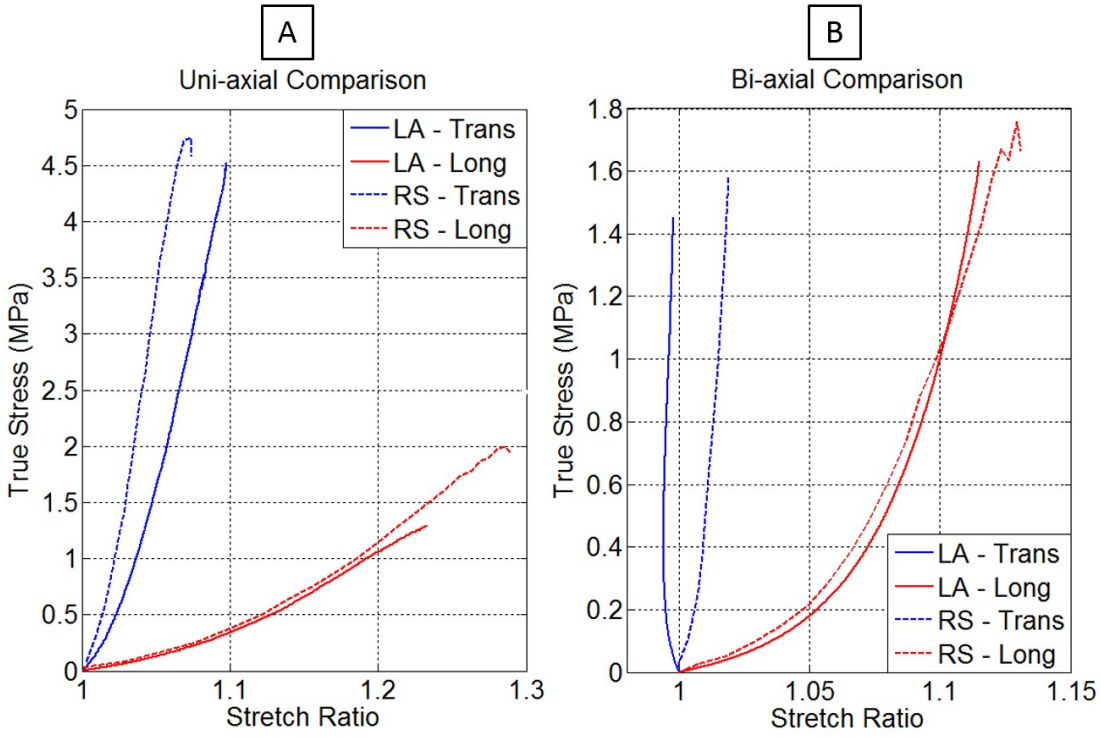

Figure 5.28: Comparison plots of the (A) uniaxial and (B) biaxial mechanical profiles of the linea alba (LA - as derived from the current study) and the rectus sheath (RS - as derived by Lyons et al.).

5.4.2 Comparative Accuracy of Tracking Methods

The percentage difference of the manual (Actual) and automated (Reported) calculations of four different regions for both tracking methods were recorded and their averages and standard deviations tabulated for comparison. The results can be seen in Table 11.1 in the Appendix. For brevity, this tabulated data describes only one sample from each analysis.

Cross-checking both tracking methods by manual interpretation found that both are comparatively effective at tracking and measuring deformation/stretch. Image analysis was found to yield slightly greater error (0.01% difference) and about double the deviation when compared with DIC. Image analysis is less comprehensive in that it tracks significantly less points than that of DIC. As such, inaccurate measurements due to bright spots caused by the reflection of light (evident in the fourth region of image analysis in Table 11.1 in the Appendix) will have a greater effect on the global average than is the case with DIC (the greater number of points acting to reduce the effect that error has on the average). However, both methods are only off by a fraction of a percent, making their comparative differences

irrelevant.

5.4.3 Computational Modelling

Due to the limitations of the physical size of the linea alba, it was not possible to meet ASTM guideline dimensions for individual samples (i.e. an ideal sample grip-to-grip to width ratio of 4:1) [ASTM (Standard E8/E8M)]. The FEBio modelling of a porcine case predicts that clamping actively pre-stresses each sample, with a significant influence on the predicted overall stress strain behaviour, see Figure 5.19. As clamping causes exudation of tissue along the z-axis, the overall longitudinal tissue strain for the clamped model (case 2) is less than for the unclamped model (case 1). Applying these results as a correction factor to each individual uniaxial experimental stress/stretch curve results in an adjusted approximation of the transverse and longitudinal stress/stretch presented in Figure 5.20.

While the fibre-reinforced material model was suitable for capturing the uniaxial behaviour of the tissue (see Figure 5.21), biaxial simulations did not provide a good match to the experimental data (see Figure 5.22). This is possibly due to the fact that the fibre reinforced model describes a transversely isotropic material while the linea has a more complex, layered collagen architecture [Gräβel et al. (2005)] which may be causing it to behave differently under biaxial loading.

Finite element modelling of the human data will be a focus of future study.

5.5 Conclusions

This study has characterised the anisotropic tensile mechanical behaviour of the linea alba for both transverse and longitudinal orientations under uniaxial and equi-load biaxial stretching. The transverse direction was found to be approximately eight times stiffer than the longitudinal direction under both uniaxial and biaxial loading respectively. There was negligible difference observed between the mechanical properties of fresh and frozen tissue. Optical surface marker tracking and digital image correlation methods were found to greatly improve the accuracy of stretch measurement. Equi-biaxial loading of the tissue resulted in deformation heavily biased towards deformation in the longitudinal direction. Finite element analysis

using a fibre-reinforced material model was used to assess the effects of tissue clamping and sample dimensions and hence adjust the uniaxial experimental data for subsequent inverse analysis to present optimised material parameters for the chosen fibre-reinforced composite constitutive model. Application of the constitutive model to the biaxial loading case shows significant differences compared to the experimental results. Finally, there were strong similarities observed between the mechanical properties of both human and porcine linea alba (though no suture/rupture analysis has been performed at this stage to validate this), leading to the conclusion that it may be possible to use porcine tissue as a surrogate for surgical device testing and development (a subject of future research).

Chapter 6

The Suture Pullout Characteristics of Human and Porcine Linea Alba

6.1 Introduction

This chapter details the experimental methods used in this thesis to determine the suture pullout characteristics of both human and porcine linea alba. Typically surgeons adhere to a guideline suture placement of a minimum of 1cm between each bite (bite separation), each bite being taken 1cm away from the cut margin of the linea alba (bite depth) [Bhat (2014), Mulholland & Doherty (2006)]. However, there is little in the literature that adequately justifies these parameters (see Section 3.4.2.2). Since there is a prevalence of post-operative incisional hernia associated with laparotomy and laparoscopic surgeries (see Section 2.6.2), this chapter attempts to identify the optimal parameters associated with suture-based wound closure (suture bite depth and separation, suture size (thickness) and the orientation of suture application) that could potentially reduce the incidence of hernia. To this end, uniaxial suture pullout experiments were performed on sections of linea alba (both human and porcine). Tissue structure and laparoscopic closure are also discussed in an effort to understand more clearly how the tissue behaves.

6.2 Materials and Methods

6.2.1 Sample Preparation

Fresh human tissue that has not been embalmed is difficult to obtain, and accordingly porcine tissue was used in this study. Pigs have a similarly sized heart and body length to humans but it is unknown if they share histological similarities. Nevertheless, pigs were chosen as a suitable substitute to humans. Thirty-six porcine abdominal walls were obtained from a swine abattoir (Rosderra Meats, Edenderry, Co.Offaly, Rep. of Ireland). Specimens were chosen at random from both male and female populations; all females being nulligravida. All were from adults, approximately 26-28 weeks in age and were frozen within 24 hours of death.

Despite the physiological similarities between swine and humans, it was necessary to evaluate the potential differences as the ultimate goal of this study is to help reduce the associated risk of surgical wound closure on humans. Therefore, in a collaborative effort with Washington University in St.Louis, 18 freshly frozen human cadaveric abdominal walls were obtained from the medical school located in the college. Specimens varied in age (>60 years) and sex and were of a caucasian background.

Prior to sample extraction porcine and human specimens were allowed to defrost for 36 hours at 4^oC. A transverse (fibre direction) rectangular section was then measured and cut from the abdominal wall following the midline and prepared for placement in a suture pullout apparatus (see Figure 6.1 (A) below with tissue and suture placement presented in (B) and (C)). Preparation involved placing the sample in grips with an emery paper surface before looping a suture (Ethicon polydioxanone sutures with a suture size of 1) twice through the sample a desired distance from the cut margin (bite depth) with each loop piercing the tissue a set distance apart (bite separation). The two free ends of the suture are tied to a fixed horizontal bar (see Figure 6.1 (C)) attached to the base part of the jig with the central loop arranged in a continuous fashion so as to let the lengths of suture equilibrate during testing (It is one piece; the suture loops around the bar before the second bite). The exact height and width of the cut sample was dependent on these variables with at least 5mm separating the bite from the edge of the grips and a minimum distance equal to that of the bite depth

or separation used (whichever is larger) separating each bite from the nearest vertical tissue edge to minimise edge effects.

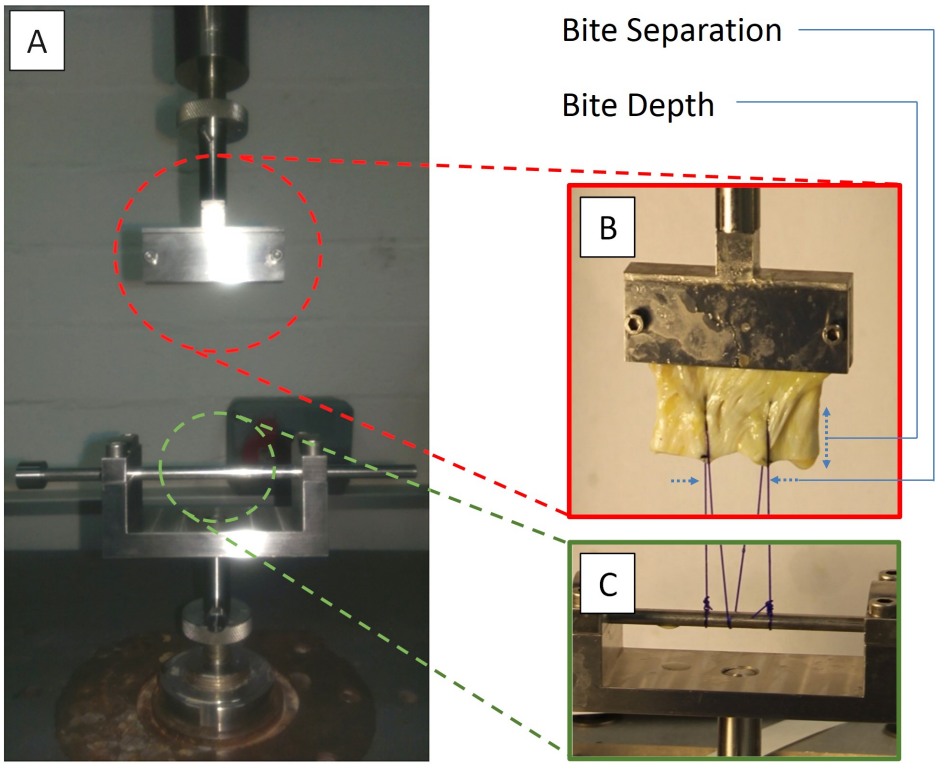

Figure 6.1: The suture pullout apparatus (A), showing an example of suture placement on the tissue (B) and the attachment of the suture to the base.

A typical plot of force versus standard travel of the machine cross-head can be seen below in Figure 6.2. Peak pullout force can be clearly identified by the abrupt drop in force at approximately 16mm travel (for this case only).

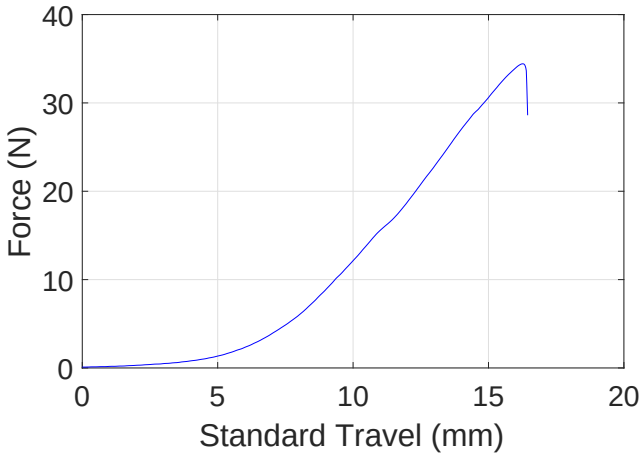

Figure 6.2: Force versus travel (mm) suture pullout plot.

6.2.2 Suture Bite Depth and Separation

For suture pullout tests comparing bite depth versus separation, a total of 60 rectangular linea alba samples were obtained from 36 different porcine specimens. Human tissue suture pullout tests performed in Washington University comprised of a total of 45 samples obtained from 18 human cadavers. A variety of different bite depth/bite separation combinations were used and a sample size of 3 was maintained throughout. Table 6.1 below shows the different combinations used with human experiments being limited to those highlighted in red.

Table 6.1: Sample size for each variable combination

Suture Pullout Tests		**Bite Depth Variable (mm)**				
		4	**7**	**10**	**13**	**16**
Bite Separation Variable (mm)	**2.5**	3	3	3	3	3
	5	3	3	3	3	3
	10	3	3	3	3	3
	15	3	3	3	3	3

In Figure 6.3, a schematic (not to scale) is shown which relates the bite depth and separation to a typical laparaotomy closure case but with two loops of suture being used experimentally, as in Figure 6.1, to vary both parameters on each sample.

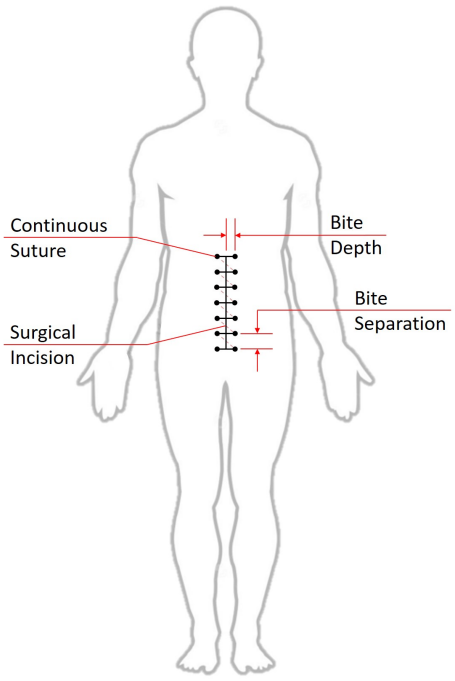

Figure 6.3: Schematic depicting the suture bite depth and separation of a typical laparotomy closure.

A custom suture pullout jig designed to conduct these tests was developed for integration with a Zwick Roell Z005 machine (Zwick/Roell GmbH Ulm, Germany) with a 2.5kN load cell attached from which a displacement-controlled tensile force could be applied; the same machine described in Chapter 5. The full assembly can be seen in Figure 6.1 (A) with an example of linea alba and suture placement seen in (B) and (C). A pre-load corresponding to 1N was applied to remove slack from the sutures. A test speed of 100mm/min was used to ensure repeatable analysis since lower test speeds introduced significant noise to the data and promoted gradual failure rather than sudden, making precise identification of the point at which the tissue fails difficult. Similar test speeds have been used in the literature [Campbell et al. (1989), Descoux et al. (1993)] making for a better comparison with the data produced from this current study. Each test was recorded using a high resolution camera (Samsung HMX-QF20) to aid in data analysis. The test was stopped when the suture pulled free of the tissue, characterised by a sudden significant reduction in force (>40% of the total). Analysis of each test was performed by scrutinising the corresponding force versus displacement graph produced using MATLAB. Human tests performed in Washington University were completed using a custom-built planar biaxial testing machine that was adapted for vertical uniaxial actuation for this study (see Figure 6.4 below)[Lake (n.d.)]. Both machines (America and Ireland), though different, are functionally identical in the application of deformation.

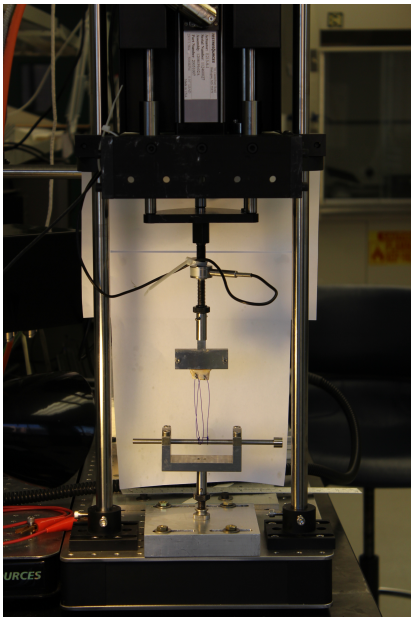

Figure 6.4: The suture pullout apparatus attached to the adapted tensile testing machine used courtesy of Washington University in St.Louis.

6.2.3 Number of Suture Bites

Laparotomy incisions most often exceed 7cm in length [Cuschieri & Hanna (2013)]. Therefore in order to evaluate the experiments of the current study that investigate solely the effect of two bites, it was necessary to perform subsequent suture pullout tests with the introduction of successive bites and make a detailed comparative analysis. Figure 6.5 shows the tissue placement and suture application for tests involving 2, 3 and 4 bites.

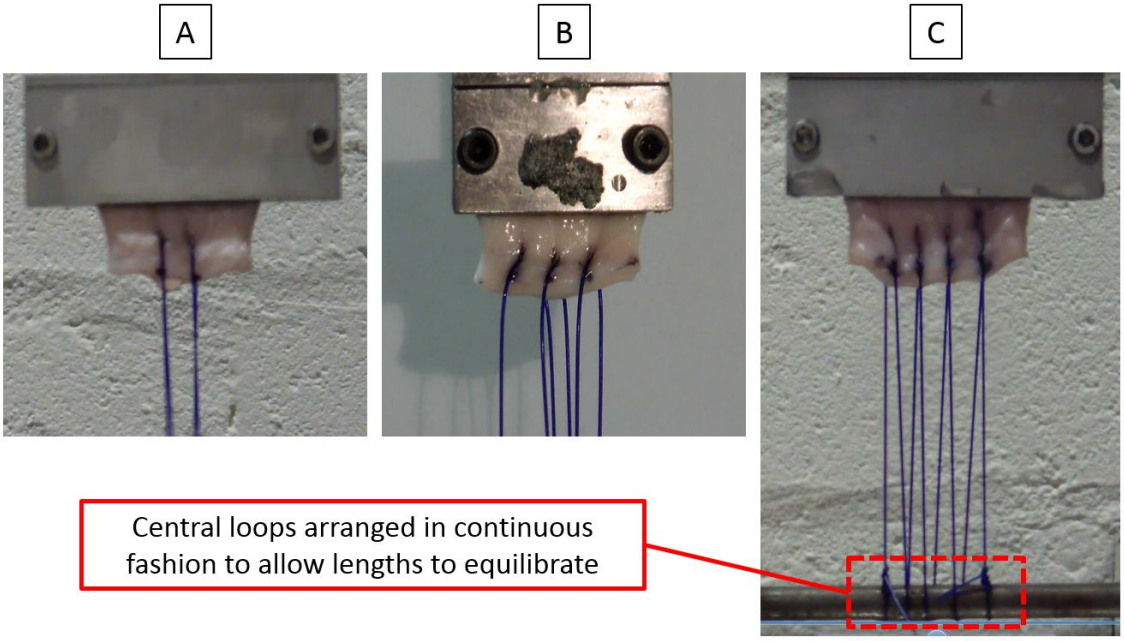

Figure 6.5: Examples of tests varying the number of bites on porcine tissue where (A) shows 2 bites, (B) 3 and (C) 4 for a bite separation of 5mm and depth of 4mm.

The total number of tests performed and variable assessed is expressed below in Table 6.2. Methodology remains the same as to that of the standard tests barring each successive loop of the suture.

Table 6.2: Sample size of the different variables investigated for successive number of suture bites.

Investigating Successive Bites		**[Bite Depth, Bite Separation]** [4, 5]	[7, 5]	[4, 10]
Number of Sutures	**2**	3	3	3
	3	3	3	1
	4	1	3	

The different parameters were compared by normalising the data to that of two sutures.

This necessitated the application of a normalisation factor to the recorded pullout force which is described below in Table 6.3.

Table 6.3: Factors normalising data to two sutures

# Suture loops	Bite Separation	Bite Depth	Factor Normalising to 2 Sutures
3	5	4	x(2/3)
	5	7	x(2/3)
	10	4	x(2/3)
4	5	4	x(2/4)
	5	7	x(2/4)

6.2.4 Orientation of Suture Application

Linea alba has been found to be anisotropic in nature [Cooney et al. (2015)]. It is therefore expected that a closed incision may behave differently depending on the orientation of the cut and the application of sutures. To this end, suture pullout tests and biaxial tests (emulating laparotomy and laparoscopic surgery cases) were performed in porcine linea alba to assess the effect that changing orientation of the incision may have.

6.2.4.1 Laparotomy Case

Emulating a laparotomy incision, suture pullout tests were performed on longitudinal (cross-fibre) sections of porcine linea alba for two variable types; bite separation of 5mm and 10 mm for a bite depth of 4mm. The results were then compared with that of standard suture pullout tests orientated in the transverse (cross-fibre) direction. The same experimental methods were maintained.

6.2.4.2 Laparoscopic Case

For a laparoscopic surgery case, biaxial tests were performed on square sections of porcine linea alba tissue with a 10mm incision closed with a single suture at the centre with a bite depth of 10mm [Bhat (2014), Mulholland & Doherty (2006)]. Figure 6.6 below describes the setup for both orientations.

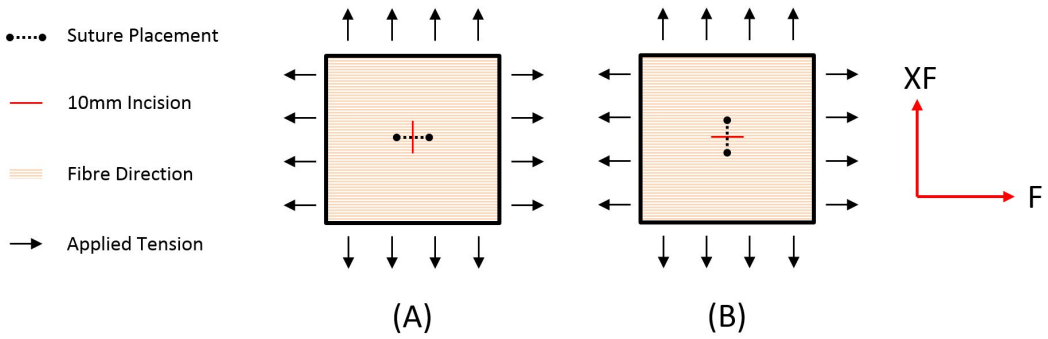

Figure 6.6: Incision and suture placement on a biaxial test specimen for the (A) transverse (fibre) direction and (B) Longitudinal (Cross-fibre) direction.

A biaxial apparatus was used to apply an equibiaxial load to all sides of the sample. The apparatus and experimental method used are identical to that seen in Chapter 5 [Cooney et al. (2015)].

6.2.5 Comparison of Suture Size

The effect of suture size (diameter of the suture) was also investigated. The greater the thickness of the suture, the more tension they can withstand due to their increased cross-sectional area. Ethicon absorbable sutures, commonly used in laparoscopic and laparotomy surgeries on internal fascia, were tested. Three suture sizes were investigated; polydioxanone suture (PDS) sizes of 2-0, 0 and 1 (diameters of 0.3mm, 0.35mm and 0.4mm respectively). Table 6.4 below outlines the different parameters tested along with the respective sample size.

Table 6.4: Types of variable tested and their associated sample size for suture size experiments

PDS	Bite Sep. (mm)	Bite Depth (mm)				
		4	**7**	**10**	**13**	**16**
2-0	**5**	3	3	3	3	3
	10			3		
	15			3		
0	**5**	3	3	3	3	3
	10			3		
	15			3		
1	**5**	3	3	3	3	3
	10			3		
	15			3		

The data depicting the size PDS 1 sutures were obtained from the standard suture pullout tests as described in Section 6.2.2.

6.3 Results

6.3.1 Number of Suture Bites

Figure 6.7 below shows a bar plot of suture pullout force normalised to two sutures (see Table 6.3) for double, triple and quadruple loops of suture for three different parameters. A one-way ANOVA test indicated that there was no statistical difference in the mean with the introduction of successive loops of suture ($P = 0.8388 > 0.05$). Two parameter combinations do not show any standard deviation. This is because only one sample was tested in each case.

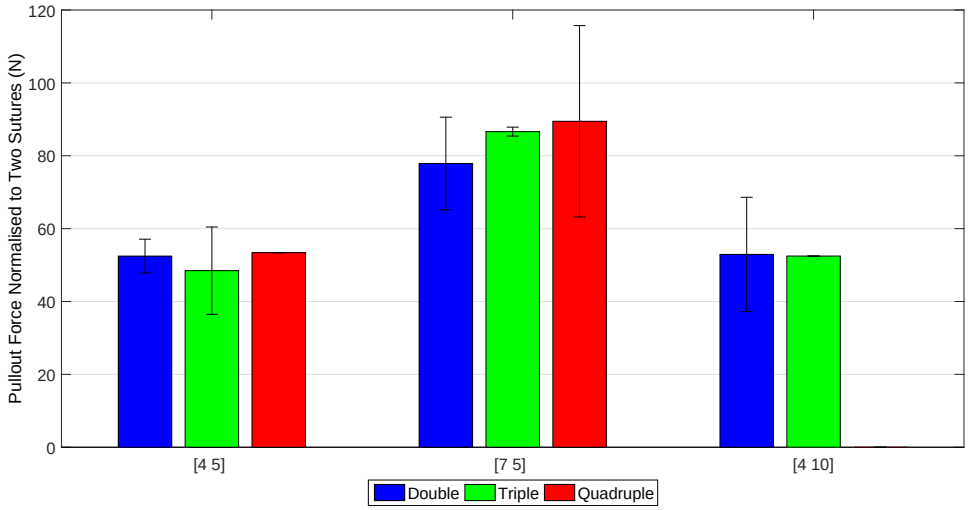

Figure 6.7: A comparison of the effect that increasing the number of bites has on the pullout force for various parameters (P = 0.8388 > 0.05).

6.3.2 Suture Orientation

6.3.2.1 Laparotomy Case

A comparison of the differences observed in pullout force with regards to sutures being applied in different orientations for a laparotomy case can be seen below in Figure 6.8 (porcine tissue only). A two-tailed t-test indicated that the means were significantly different when comparing opposing orientations of applied sutures for a [4,5] parameter combination (P = 0.046 < 0.05) with longitudinal (cross-fibre) sutures exhibiting a greater pullout force. However, no significant difference was observed between transverse and longitudinal directions for a [4,10] parameter combination (P = 0.424 > 0.05).

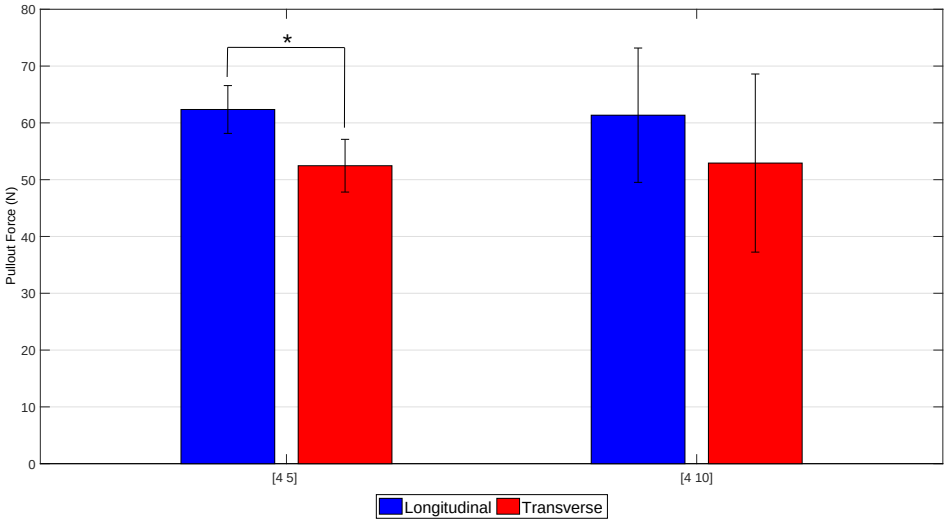

Figure 6.8: A comparison of the effect that changing the orientation of the suture has on the pullout force (Transverse versus Longitudinal; P = 0.424 > 0.05 for [4,5]).

6.3.2.2 Laparoscopy Case

A qualitative assessment of the effect of orientation in a laparoscopic case can be seen below in Figure 6.9. Part (A) shows a sample with a suture orientated in the transverse (fibre) direction and (B), the longitudinal (cross-fibre) direction as equibiaxial tension is applied (black dotted line signifies the suture). Images are taken at 0MPA, 0.8MPa and 1.6MPa and depict a step-by-step deformation of the tissue and incision. A light speckle pattern was applied to better visualise the deformation occurring throughout the tissue, allowing the measurement of the angle of distortion of the tissue. In part (A) the incision itself distorts, becoming longer and wider. However, judging from the speckle pattern, the tissue around the incision does not appear to distort. In part (B), from the speckle pattern it is possible to see the tissue around the incision severely distort; the suture preventing the fibres from displacing longitudinally in the centre while being free to do so at the edges of horizontal edges of the tissue. At 1.6MPa, the tissue distortion reaches a peak of $\approx 30^o$. The angle of distortion is a measurement of the angular change in a line between the suture bite and a random speckle in the pattern from 0MPa to 1.6MPa.

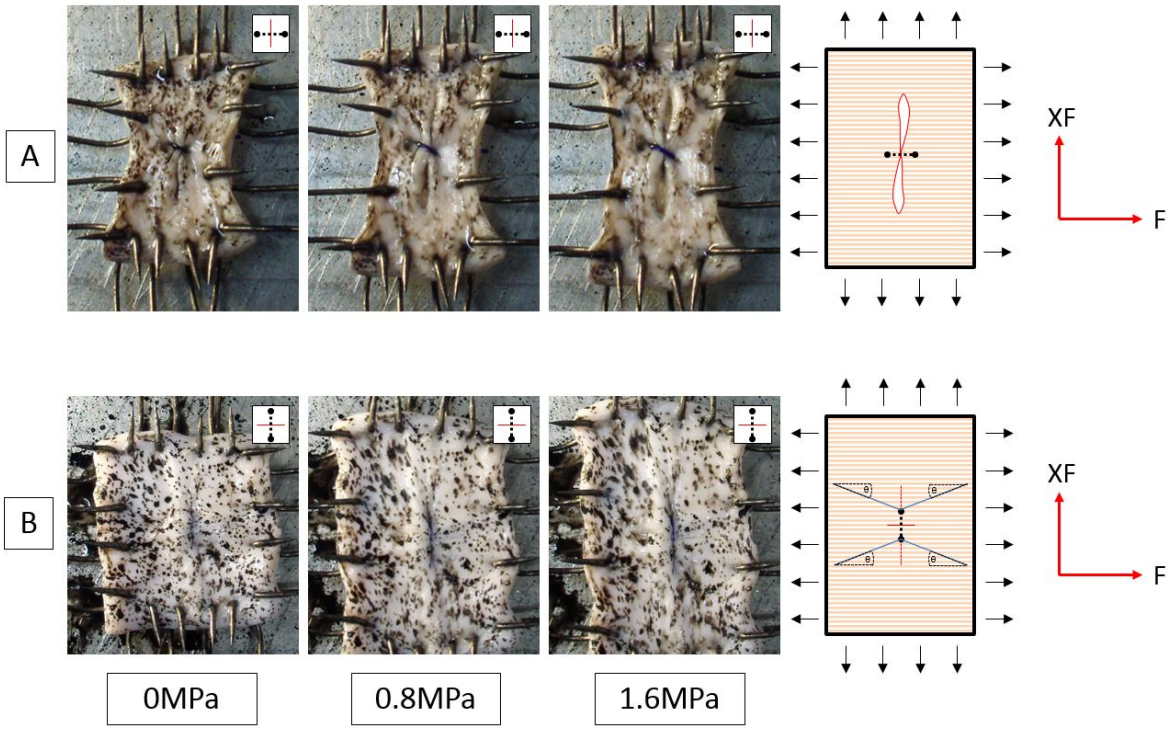

Figure 6.9: A comparison of the effect that changing the orientation of the suture has on a laparoscopic incision (Transverse (A) versus Longitudinal (B)).

Exact deformation was not measured using pattern analysis due to issues with pattern distortion which would have lead to a high source of error (a different ink was used due to the unavailability of the original ink used in the first study). However, biaxial deformation tests on linea alba with closed laparoscopic incisions will be a topic of future study using more suitable tissue ink.

6.3.3 Suture Bite Depth Versus Separation

Figure 6.10 shows a 3-dimensional plot of suture bite depth, bite separation and pullout force for porcine tissue. A quadratic surface was fit to this data, depicting an increase in pullout force as both the bite depth and/or bite separation are increased. The surface fit had a goodness of fit correlation coefficient of 0.99 and defines the point above which suture pullout/failure becomes increasingly probable.

The porcine data surface plane can be described by the following equation:

$$N_{Pullout} = 12.91 + (7.56)B + (2.95)S - (0.29)B^2 + (0.48)BS \\ -(0.44)S^2 + (0.009)B^3 - (0.02)B^2S + (0.03)BS^2 \quad (6.1)$$

where $N_{Pullout}$ is the pullout force in newtons (N), B is the bite depth in mm and S is the bite separation in mm.

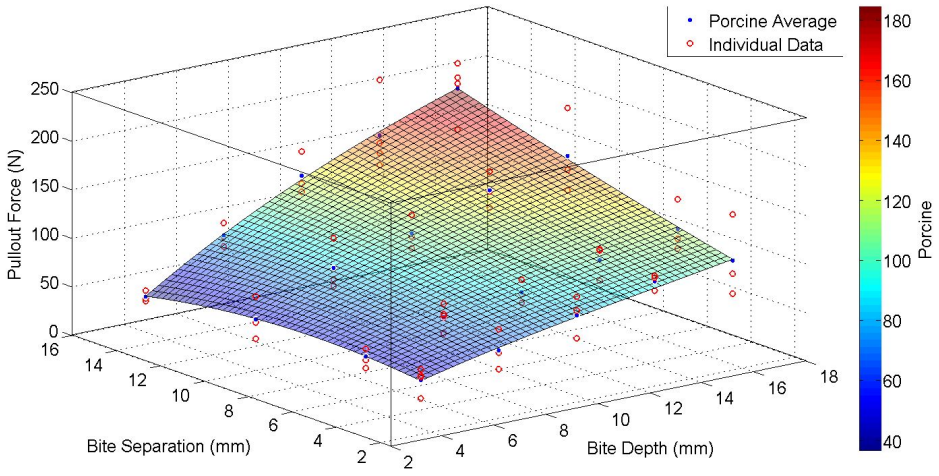

Figure 6.10: The raw pullout force data versus the respective bite depth and separation for porcine tissue.

Figures 6.11 & 6.12 below depict the linear regression fits of the data in Figure 6.10. Figure 6.11 assesses the relationship between bite separation for increasing bite depths while Figure 6.12 assesses the relationship between bite depth for increasing bite separations. In terms of the bite separation, low correlation coefficients (<0.2) are observed at low bite depths but become quite high (≈0.4) above a bite depth of 10mm. This suggests there is a increasing trend associated with bite separation, but only for larger bite depths. The bite depth at which this change occurs approximates to double the minimum bite separation.

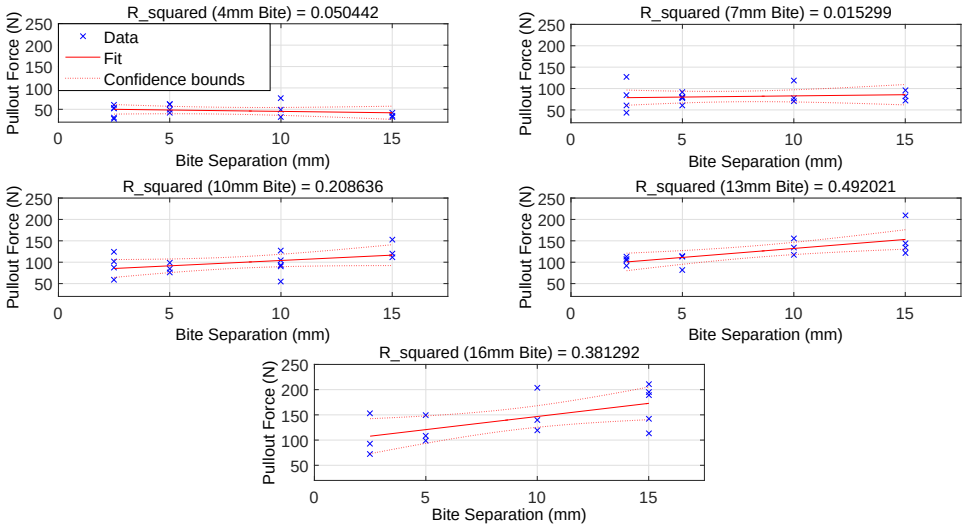

Figure 6.11: Fitted plots of the porcine data for the different bite depths of a given bite separation

Looking at the relationship between bite depths, very high correlation coefficients (as high as 0.7) are observed at all separations implying that small changes in bite depth will have a greater and more predictable impact on the pullout force than separation does; the variation of the data about the mean being less inn the case of bite depth (having a greater r^2 value).

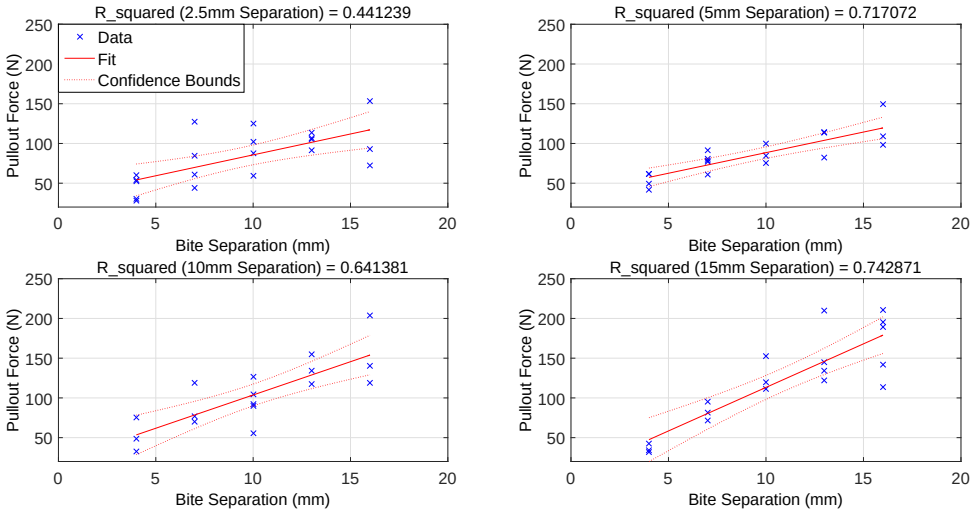

Figure 6.12: Fitted plots of the porcine data for the different bite separations of a given bite depth.

Figure 6.13 shows a 3-dimensional plot of suture bite depth, bite separation and pullout force per 10mm of porcine tissue which is more attributable to in-vivo situations as it relates a uniform incision length across all the data. A quadratic surface was again used to fit the

data, depicting an increase in force/mm as both the bite depth increased and a significant decrease in force/mm as bite separation is increased. The surface fit had a goodness of fit correlation coefficient of 0.96.

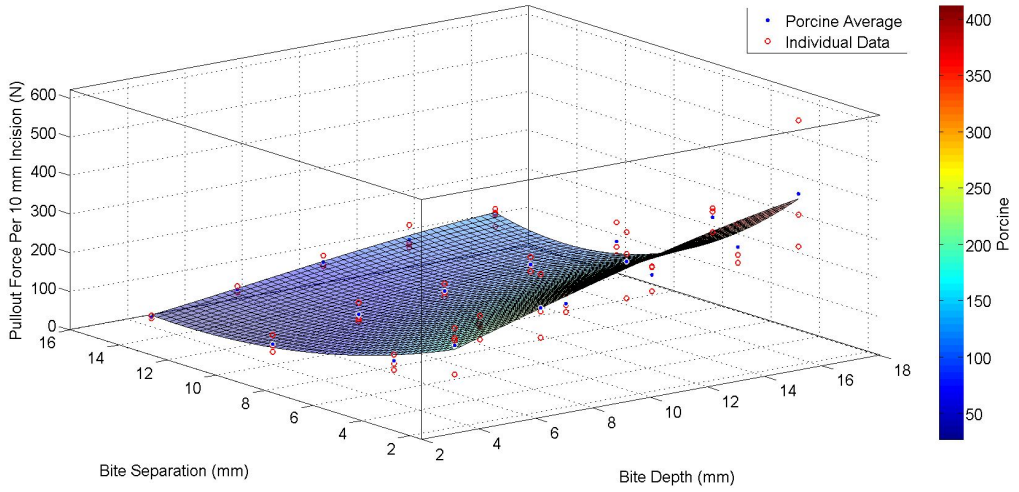

Figure 6.13: The porcine pullout force data normalised to account for the length of wound sutures would be applied across (profile akin to surgical situations).

Figure 6.14 shows a 3-dimensional plot of suture bite depth, bite separation and pullout ratio (data scaled to [10,10] parameter by dividing all the original data from Figure 6.13 by the [10,10] average) of porcine tissue which allows for a more appreciable comparison of the constituent parameters to the general standard used by surgeons [Bhat (2014), Mulholland & Doherty (2006)]. A quadratic surface was again used to fit the data, depicting an increase in pullout force as both the bite depth and/or bite separation are increased (similar to Figure 6.10). The surface fit had a goodness of fit correlation coefficient of 0.99.

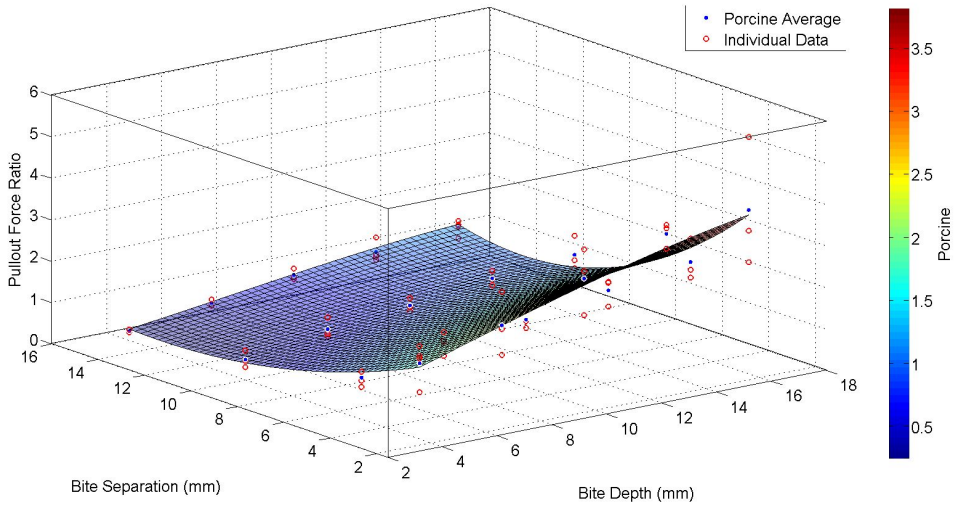

Figure 6.14: The plot of porcine pullout force ratio; pullout force per 10mm incision data scaled to a [10,10] parameter.

Figure 6.15 shows a 3-dimensional plot of suture bite depth, bite separation and pullout force of both human and porcine tissue. A quadratic surface was fit to both data, depicting an increase in pullout force as both the bite depth and/or bite separation are increased. The human surface fit had a goodness of fit correlation coefficient of 0.99 and defines the point above which suture pullout/failure becomes increasingly probable. A total of ≈4% difference observed between the average pullout force of both species.

The human data surface plane can be described by the following equation:

$$\begin{aligned} N_{Pullout} = 12.91 - (8.76)B - (15.56)S + (0.47)B^2 + (2.58)BS \\ +(0.51)S^2 - (0.009)B^3 - (0.042)B^2S - (0.06)BS^2 \end{aligned} \tag{6.2}$$

where $N_{Pullout}$ is the pullout force in newtons (N), B is the bite depth in mm and S is the bite separation in mm.

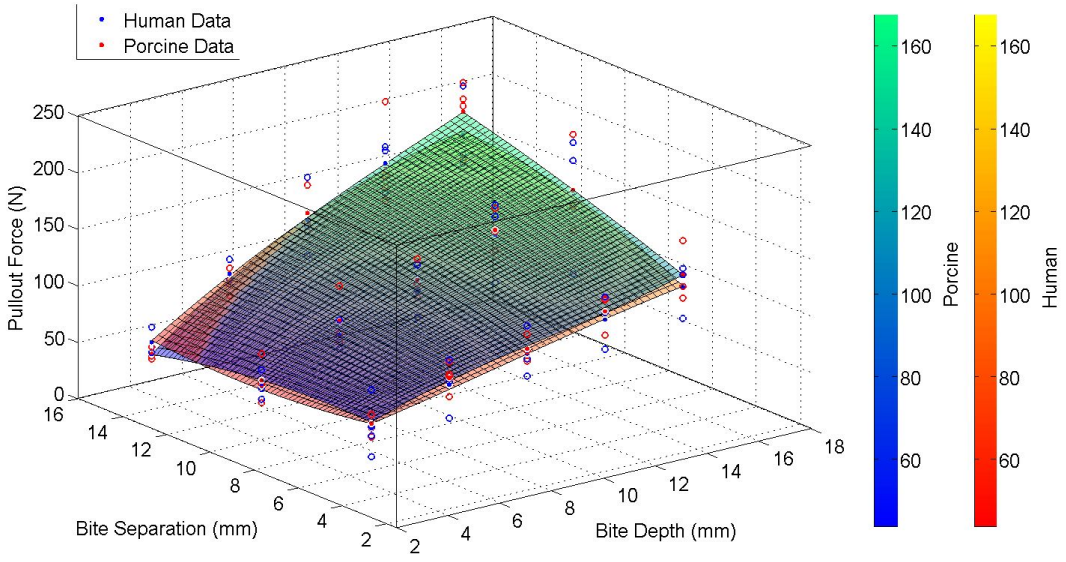

Figure 6.15: The raw pullout force data versus the respective bite depth and separation for both porcine and human tissue.

Figures 6.16 & 6.17 below depict the linear regression fits of the raw human and porcine data in Figure 6.15. The human data can be seen depicted in blue and the porcine data in red. Figure 6.16 assesses the relationship between bite separation for increasing bite depths while Figure 6.17 assesses the relationship between bite depth for increasing bite separations. In terms of the bite separation, low correlation coefficients (<0.3) are observed at low bite depths for both species but become quite high (≈0.5) above a bite depth of 10mm. This suggests there is a linearly increasing trend associated with bite separation, but only for larger bite depths. The bite depth at which this change occurs approximates to double the minimum bite separation.

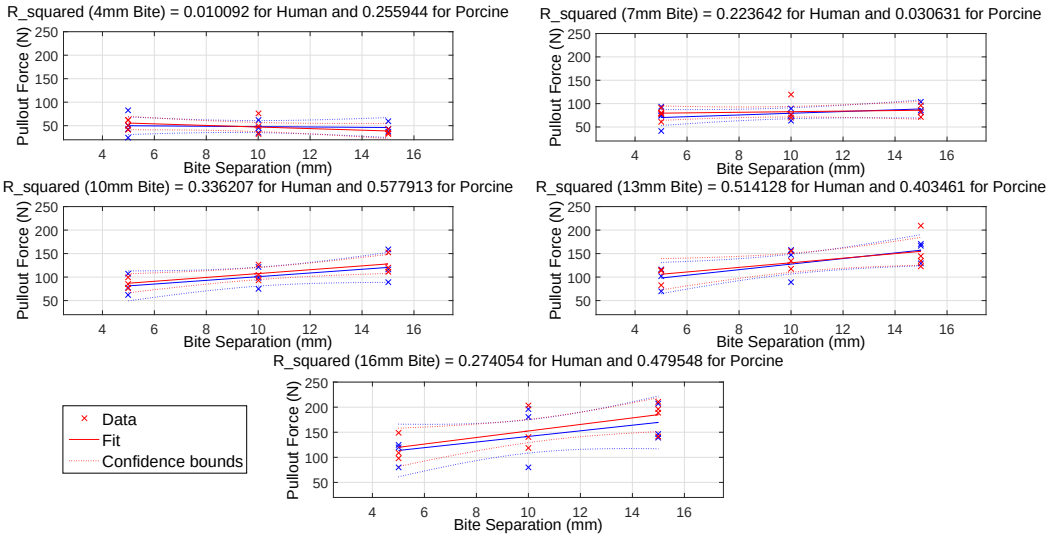

Figure 6.16: Fitted plots of the porcine and human data for the different bite depths of a given bite separation. The porcine and human data are coloured red and blue respectively.

Looking at the relationship between bite depths in the human data, very high correlation coefficients (as high as 0.7) are observed at all separations implying that small changes in bite depth will have a greater and more predictable impact on the pullout force.

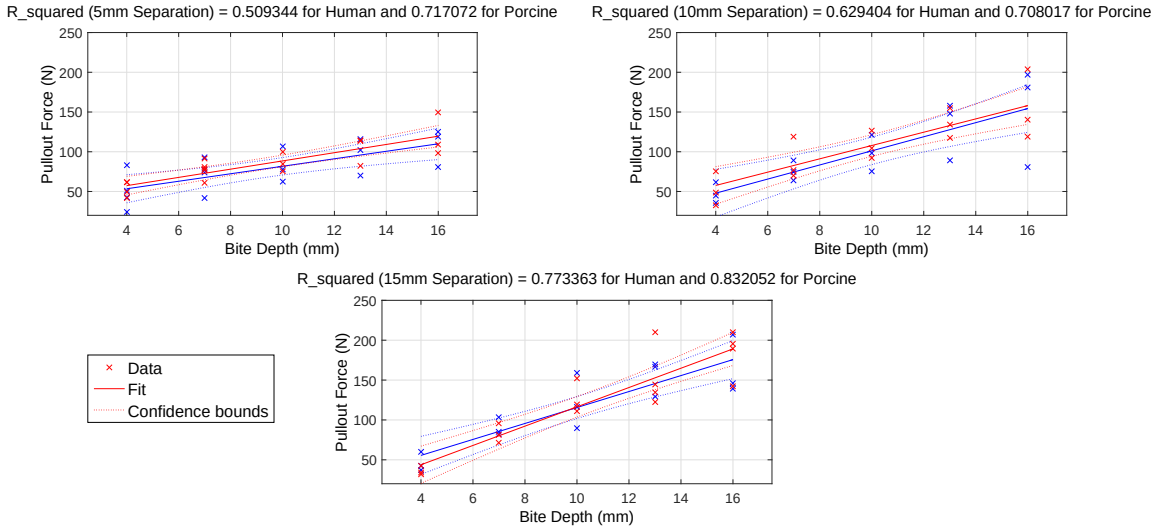

Figure 6.17: Fitted plots of the porcine and human data for the different bite separations of a given bite depth. The porcine and human data are coloured red and blue respectively.

Figure 6.18 shows a 3-dimensional plot of suture bite depth, bite separation and pullout force per 10mm incision for both human and porcine tissue which is more attributable to in-vivo situations as it relates a uniform incision length across all the data. A quadratic surface was again used to fit the human data, depicting an increase in force/mm as both the

bite depth increased and a significant decrease in force/mm as bite separation is increased. The surface fit had a goodness of fit correlation coefficient of 0.99. The average difference in pullout force observed between the human and porcine data was found to be ≈4%.

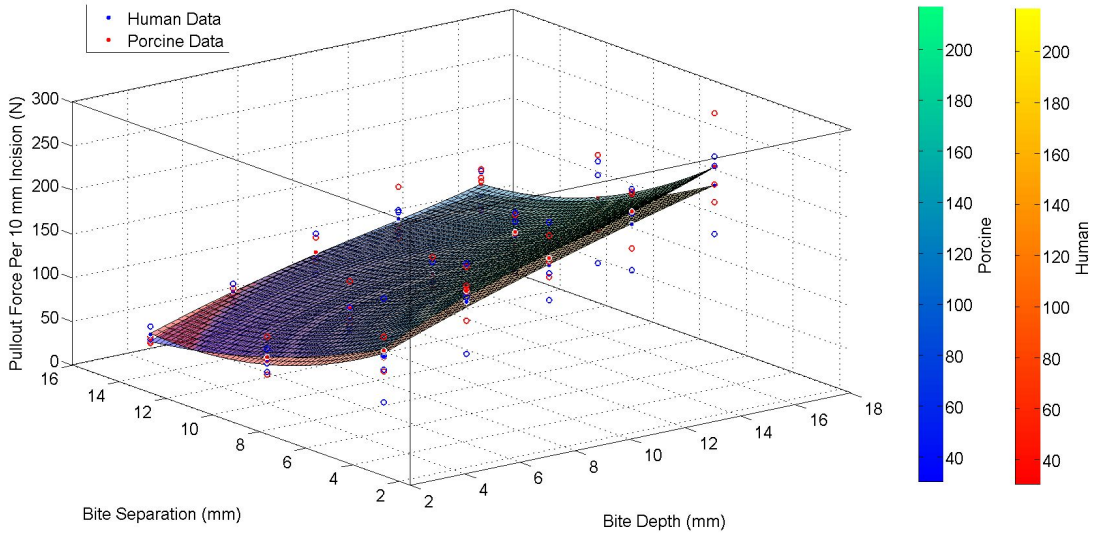

Figure 6.18: The porcine and human pullout force data normalised to account for the length of wound sutures would be applied across (profile akin to surgical situations).

Figure 6.19 shows a 3-dimensional plot of suture bite depth, bite separation and and pullout ratio (data scaled to [10,10] parameter by dividing all the original data from Figure 6.18 by the [10,10] average) for both human and porcine tissue which allows for a more appreciable comparison of the constituent parameters to the general standard used by surgeons [Bhat (2014), Mulholland & Doherty (2006)]. A quadratic surface was again used to fit the human data, depicting an increase in pullout force as both the bite depth and/or bite separation are increased (similar to Figure 6.15). The surface fit had a goodness of fit correlation coefficient of 0.99. On average, there was a ≈6% difference in pullout ratio observed between the porcine and human data.

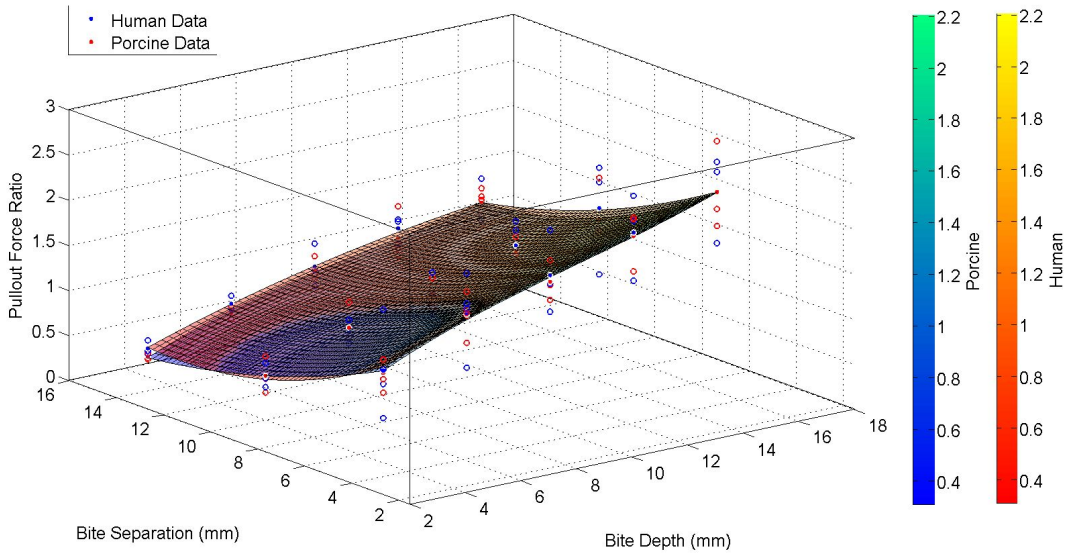

Figure 6.19: The porcine and human pullout force data scaled to a [10,10] parameter.

Both the human and porcine suture pullout data exhibit very significant similarities; near identical profiles depicting the same relationships. A total of ≈6% difference observed between the average pullout ratio of both species

6.3.4 Suture Size

The plotted results of the investigation into suture size on porcine tissue can be seen below in both Figure 6.20 which focuses on varying bite separation, and Figure 6.21 which describe the effects of changing bite depth for different suture sizes below. A one-way ANOVA test indicated that there was no statistical difference in the mean when different suture sizes are used with the same bite depth for different bite separations (P = 0.1263, 0.4483 & 0.4574 > 0.05 for bite separations of 5, 10 and 15mm respectively - see Figure 6.20).

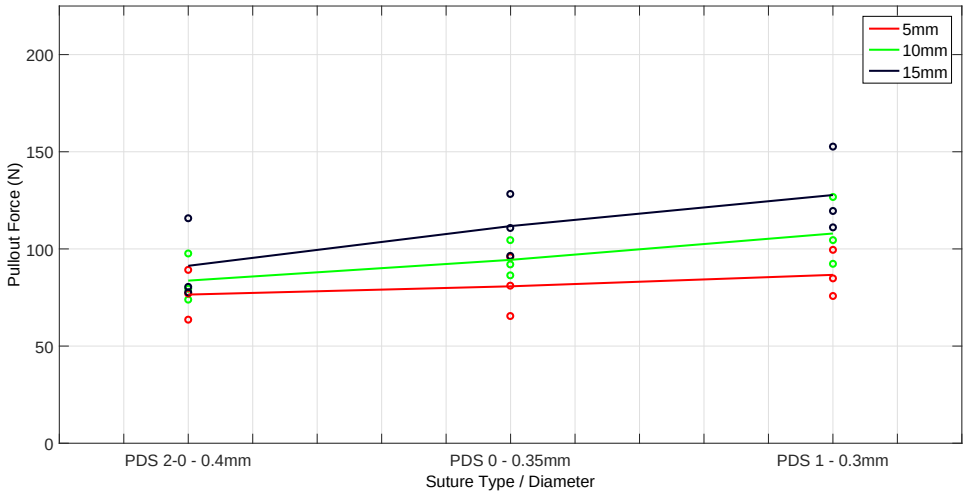

Figure 6.20: A plot of the different response in pullout force for three types of suture thickness for different bite separations.

A one-way ANOVA test indicated that there was no statistically significant difference between the means when different suture sizes are used with the same bite separation for different bite depths (P = 0.4237, 0.5878, 0.4484, 0.4103, 0.5483 > 0.05 for bite depths of 4, 7, 10, 13 and 16mm respectively - see Figure 6.21).

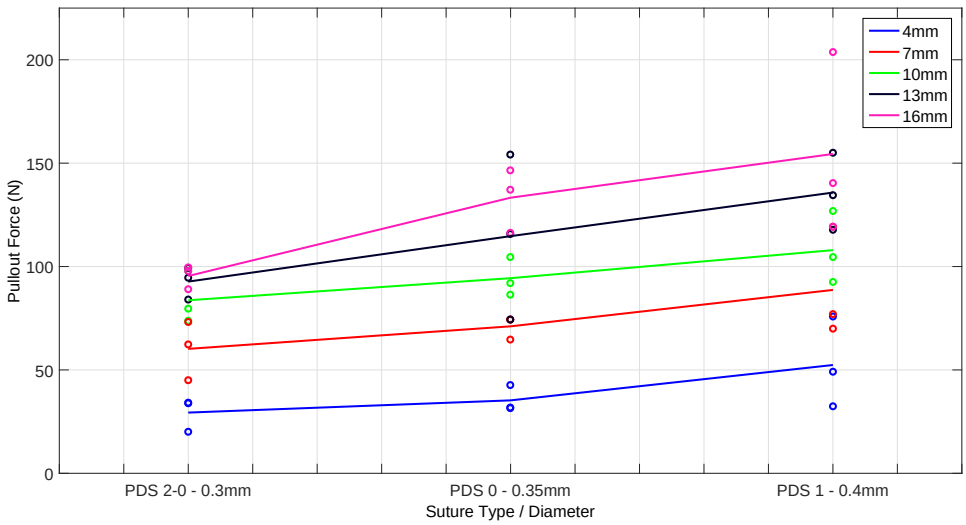

Figure 6.21: A plot of the different response in pullout force for three types of suture thickness for different bite depths.

6.4 Discussion

6.4.1 Edge Effects

As mentioned in Section 3.4.2.2, some research has been performed into identifying an ideal bite depth and width [Campbell et al. (1989), Descoux et al. (1993)]. It is reported that a bite depth of ≈9mm and a bite separation of between 10-15mm is ideal for secure wound closure (see Figure 6.22 below).

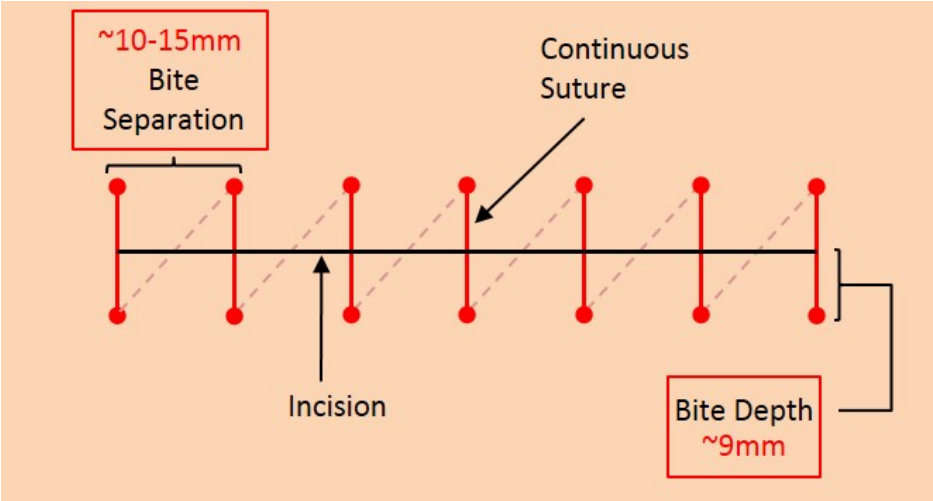

Figure 6.22: Graphic of the ideal bite depth and separation as reported by the literature.

While the data in the literature is informative, there are some particular points of concern that should be noted. In the case of bite depth, Campbell et. al performed similar experimental methods to the current study to measure pullout force at different bites in human tissue using only one suture bite. They observed an increasing trend as bite depth was increased. However, this trend ended suddenly in a plateau where pullout force remained the same despite the increase in bite depth. This corresponded approximately to the point at which the bite depth became greater than the distance from the suture bite to the edge of one side of the sample (see Figure 6.23 below); an edge effect impacting the results.

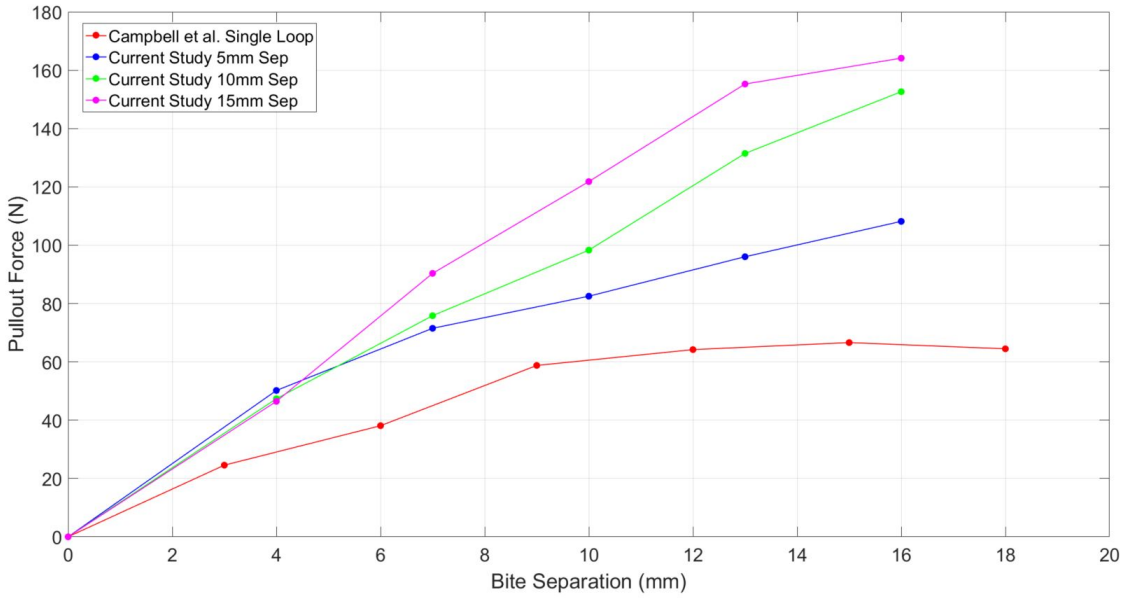

Figure 6.23: Comparison of current data versus Campbell et al.. Data from Campbell et al. showing the plateau in pullout force once bite size (bite depth) exceeds edge distance [Campbell et al. (1989)].

This phenomenon was also observed in the preliminary suture pullout experiments of this study. Initially, all samples were cut to accommodate a space equal to half the bite separation between each suture bite and the edge of the tissue. This was done to mimic an infinitely continuing pattern that was thought would reduce edge effects. However, it was noted that the anterior layer of the sample (oblique fibre orientation) tended to fail horizontally once the bite depth surpassed the edge distance. Two examples of such can be seen below in Figure 6.24.

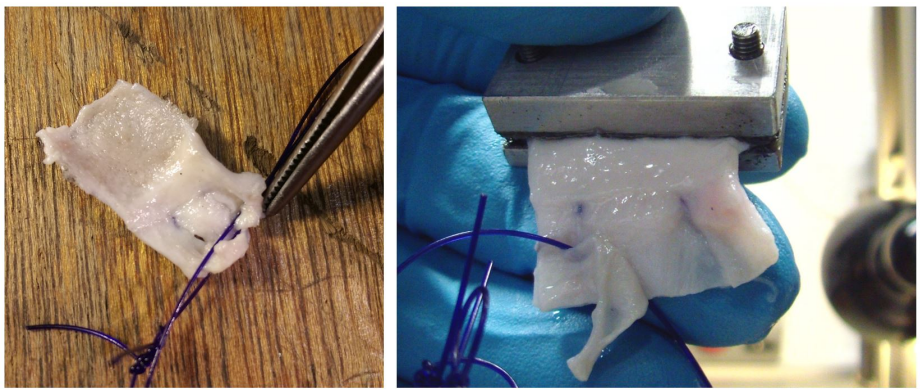

Figure 6.24: Anterior layer failing horizontally on specimens with a bite depth/separation of (A) [10, 10] and (B) [13, 10] using an edge distance of 5mm.

This artificially created weakness resulted in a lower pullout force; sometimes as much as half as what was observed in the final results. The thick oblique structure redirects some of the potential energy laterally. Reducing the horizontal length of the sample (cranio-caudal orientation) therefore diminishes the anterior layers structural contribution to resisting pullout.

While it could be argued that an edge distance of half the bite separation is more indicative of in-vivo scenarios, it must be noted that in order for that statement to be true in-vivo, the anterior layer would have to have a large defect midway between each bite (representing the cut edge of the sample in the pullout experiments). The propagation of failure of the anterior layer will always take the path of least resistance, and with a bite depth that is greater than the distance to the edge of the tissue, the anterior layer fails towards the horizontal tissue edge. This occurred in approximately 70% of cases where edge effects were not accounted for. In accordance with this, all suture pullout tests were required to have an edge distance that was greater than the bite depth or separation (whichever was bigger). As evidenced by the results in Figure 6.23, there was no plateau observed as was the case with the results from Campbel et al..

6.4.2 Number of Suture Bites

Using two bites instead of greater multiples is ideal as it maximises the amount of samples that can be obtained due to their smaller size and makes the experiment more repeatable and accurate by reducing experimental error associated with suture placement and being able to avoid natural defects such as blood vessels. However, all laparotomies incorporate large incisions and therefore utilise considerably more suture bites. Therefore it was necessary to test the assumption that using multiples of 2 bites can be directly related to greater multiples. To this end, multiples of 2, 3 and 4 were compared; data from samples with 3 and 4 bites adjusted to account for the extra bites (see Table 6.2 & Figure 6.7)

Statistical analysis was found to show no difference in the means even when either bite depth or separation is varied. As such, all suture pullout experiments in this study were performed using 2 suture bites. However it must be noted that due to time and material constraints, parameters [4, 5] for 4 bites and [4, 10] for 3 bites had a sample size of one. There was also no test performed on a sample with 4 bites for a [4, 10] parameter. However,

despite this, there is still a reliable comparison between the number of suture bites. The main goal of this study is to observe the suture pullout characteristics using different parameters and compare the results relative to one another to discover the strongest combination of bite depth and bite separation. The relative difference between parameters should not change depending on the number of suture bites used, otherwise suture pullout characteristics would be dependant on the length of the incision which could only be possible if the tissue properties of the linea alba were vastly different at any point along its length.

6.4.3 Suture Orientation

There is some contrary evidence in the literature that provides alternate views over whether there is a distinct advantage in using transverse incision over longitudinal incisions in surgery. Transverse incisions have been reported to reduce pain and pulmonary dysfunction following laparotomy procedures in some randomised trials [Grantcharov & Rosenberg (2001), Lindgren et al. (2001)], while other trials have found no advantage of transverse incisions [Brown et al. (2004), Greenall et al. (1980)]. It is therefore still a topic of some considerable debate and, as such, an attempt has been made in this study to provide a better understanding.

6.4.3.1 Laparotomy Case

Theoretically, it would stand to reason that sutures applied in a longitudinal orientation (transverse incision) would be more resistant to pullout as they are pulling across the transverse fibres of the central (and largest) layer of the linea alba as well as the rectus sheath (depending on the length of the incision. The results of the suture pullout tests comparing both orientations for two different bite separations seen in Figure 6.8, depict a statistically significant difference in the means of one parameter combination ([4,5]; $P = 0.046 < 0.05$); corroborating the theory that longitudinal samples as more resistant to pullout. However, using a [4,10] parameter combination resulted in no statistical significance being observed ($P = 0.424 > 0.05$); the variation in the data, and low sample size, making it difficult to determine significance. Therefore it is not clear which orientation performs better in terms of resistance to suture pullout.

There are several other issues with regards to transverse incisions that may be problematic. Firstly, the typical width of the linea alba is about 1-2cm [Beer et al. (2009)]. This means that to perform a laparotomy in this fashion would require the manipulation/cutting of the rectus muscle (as laparotomies are typically greater than 7cm [Cuschieri & Hanna (2013)]), which may irreparably damage the muscle as a result. Secondly is an issue that was observed during testing. Samples sometimes tended to fail to the sides (see Figure 6.25 (A) & (B)) despite the edge distance set, although with a continuous band of linea alba this might not happen. Overall this occurred three times in total; all instances were excluded from the analysis. There were also times when the tissue didn't fail at the bite of the suture at all, instead either failing at the grips (Figure 6.25 (D)) and other times quite often at the centre of the sample (Figure 6.25 (C)).Overall this occurred two times in total; all instances were excluded from the analysis. This could imply that sutures applied in the longitudinal orientation of the linea alba, being considerably less stiff than the transverse direction [Cooney et al. (2015)], may cause secondary defects to form at the bite of the suture. Fortunately, defects should not form elsewhere like in Figure 6.25 (C) & (D) as it would require non-physiological pressures to do so. Assuming Laplace's law for thin-walled cylinders applies, and using a fixed internal abdominal radius of curvature of 190.52mm (calculated using internal human dimensions from the literature [Duez et al. (2009)]), an internal pressure of 20kPa (typical physiological maximum [Addington et al. (2008), Campbell & Green (1953), Cobb et al. (2005), Malbrain et al. (2004), Ravishankar & Hunter (2005)]) would correspond to wall forces of 19.05N and 38.1N for a 5mm and 10mm defect (cylinder length); lower forces than what was observed to cause pullout in Figure 6.8 (tissue failure at the grips being of a similar order of magnitude of force as of that of normal suture pullout).

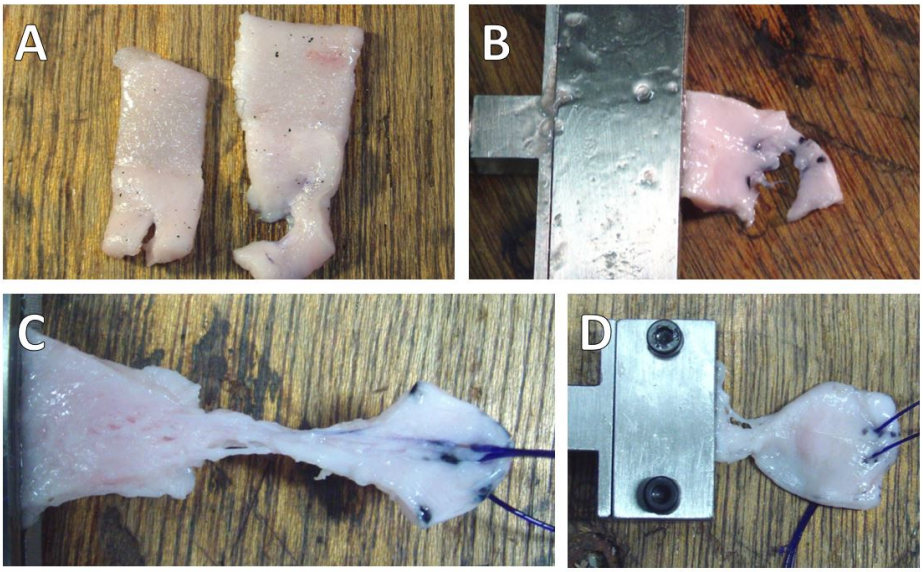

Figure 6.25: Four examples of improper failure of longitudinal suture pullout samples. Image (A) shows an example of transverse failure (left) for comparison.

Despite these experimental observations, there is not enough evidence to conclude that longitudinal applications of sutures may be detrimental to the tissue. It may therefore prove advantageous to close laparoscopic incisions in this way (typically being 1cm long; small enough to fit the linea alba width).

6.4.3.2 Laparoscopic Case

Biaxial tests on a laparoscopic defect showed that applying a suture in the transverse direction, the defect can extend by as much as ≈30% and widen as much as ≈2mm (see Figure 6.9 (A)). However, this is in terms of the maximum stress observed experimentally. If it is assumed that the typical extreme stress on the linea alba is around 1.3MPa (using Laplace's thin-walled theorem [Cooney et al. (2015)]) then, physiologically speaking, a 10mm laparoscopic defect could potentially extend as much as ≈24% and widen by as much as ≈1.6mm.

Contrary to this, applying a suture in the longitudinal direction does not appear to visually affect the defect in any extreme way. At worst, it warps the tissue slightly so there is a possible angular change to the transverse fibres at the defect site (at peak being $\approx 30^o$).

Overall it seems quite advantageous, at least for a laparoscopic case, to close a surgical defect by applying sutures in the longitudinal (cranio-caudal/cross-fibre) direction.

6.4.4 Suture Bite Depth Versus Separation

Observing the effect that bite depth and separation has on the pullout force in Figure 6.10 and Figure 6.15 for both human and porcine tissue, several notable trends can be seen:

1. As bite depth is increased, maximum pullout force linearly increases (r^2 = 0.50 - 0.77 for human and r^2 = 0.71 - 0.83 for porcine).

2. At large bite depths (>10mm), increasing separation also results in a linear increase in pullout force (r^2 = 0.27 - 0.51 for human and r^2 = 0.40 - 0.57 for porcine). Though at small bite depths (4-7mm) the relative increase in pullout force as bite separation is increased does not appear significant (r^2 = 0.01 - 0.22 for human and r^2 = 0.03 - 0.25).

3. From 5mm to 2.5mm separation there appears to be little difference in pullout force for all bite depths (see porcine data in Figure 6.10).

However, these results do not reflect a surgical situation whereby the incision length is fixed requiring more or less bites depending on the bite separation used. By normalising the data to a common length (10mm), quite different (some opposing) relationships were observed (see Figure 6.13 and Figure 6.18) which will have bearing on what effect each parameter would have in a realistic situation:

1. As bite depth is increased, maximum pullout force/mm linearly increases.

2. As bite separation is increased, pullout force/mm decreases almost asymptotically.

3. A significant increase in pullout force/mm was observed when going from 5mm to 2.5mm bite separation (see Figure 6.13).

The normalised plots (Figure 6.14 and Figure 6.19) that compare the [10, 10] parameter typically used in surgery with the rest of the data show that it's not as effective as it could potentially be, being closer on the scale to the weakest parameters (bite depth of 4mm) than the strongest (bite depth of 16mm). Resistance to suture pullout could be improved by as much as 120-290% (depending on a bite separation of between 5mm and 2.5mm) if the current standard of a bite depth and bite separation of 10mm was changed.

Overall, judging from the data, it is better to use bite depths as large as possible with bite separations as small as possible, being limited by the anatomy and the dexterity of the surgeon.

Typically surgeons go by suture length to wound length ratio (SL:WL) which is essentially length of one loop of suture over the bite separation (wound length in this case). Figure 6.27 below gives a simple explanation of how they are calculated. Typically, as outlined below, the preferred ratio is ≈4:1 [Bhat (2014), Israelsson & Jonsson (1993), Mulholland & Doherty (2006)].

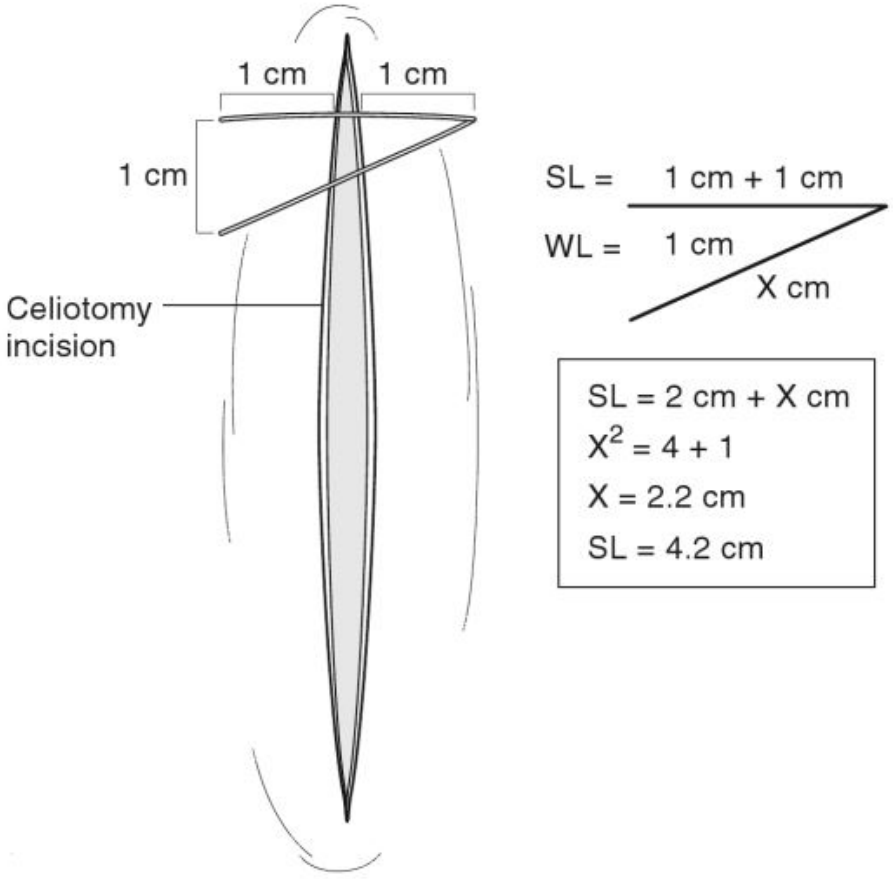

Figure 6.26: Typical bite depth and bite separation used by surgeons and the associated suture length to wound length ratio (SL:WL) [Mulholland & Doherty (2006)].

If a more optimised bite depth and separation such as a 16mm and 5mm were used, this ratio would instead change to ≈14:1, 3.5 times what is considered the current standard.

While the data indicated that a bite separation of 2.5mm would be optimal (see Figure 6.14), the way samples of this bite separation would sometimes fail (at bite depths ≥10mm)

is of some concern. Figure 6.27 below shows one such example. Before the tissue would fail outright, the space between the sutures would sometimes narrow until they contacted. This means that, not only does the stress increase due to the force being concentrated on a point location, but a defect 2.5mm wide forms. Also, accurate placement of the sutures at exactly that distance apart is difficult. Through human experimental error, suture bites could easily be placed closer together making a convergence of the suture bites during testing all the more likely. Cases such as this were not observed for any other parameter. As such, it is recommended to keep the bite separation to a minimum of 5 mm. It must be noted that this is not absolutely indicative of in-vivo scenarios and did not appear to affect the experiment pullout results (see the trends observed in Figure 6.12).

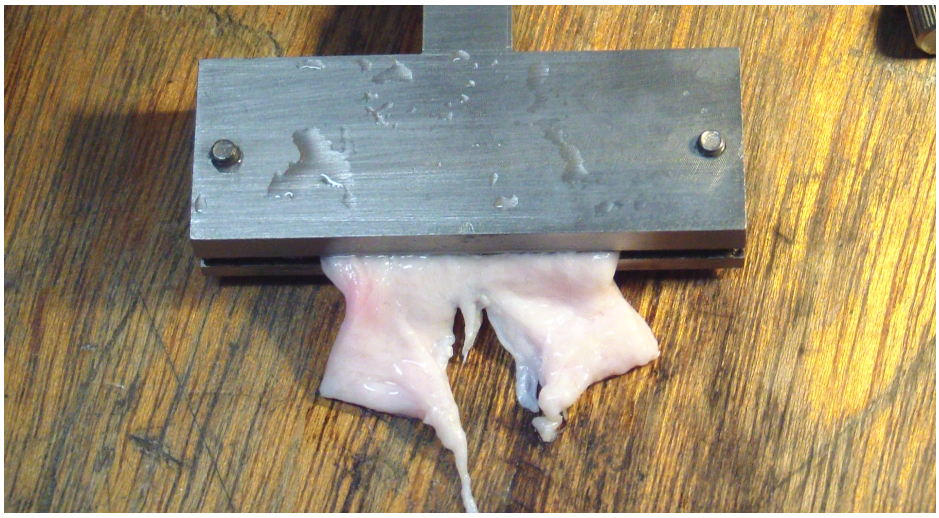

Figure 6.27: Convergence of sutures placed 2.5mm apart.

Of great interest is the fact that human tissue was found to exhibit almost identical suture pullout characteristics as that of porcine tissue (see Figure 6.15, Figure 6.18 and Figure 6.19). Though the physiology of both species is diverse, particularly in that the anchoring position of the lateral aponeurotic muscles slightly differs, the linea alba of both species retain the same function. The collagen architecture is therefore likely quite similar. This means that porcine tissue, or even live pigs, may be suitable to use as a surrogate to that of human, particularly in the area of device design and development. Without the need to perform human trials (if materials used are deemed bio-compatible), surgical devices could take significantly less time to develop.

6.4.5 Suture Size

Increasing suture size (diameter of the suture) would be expected increase pullout force correspondingly due to the increasing surface area of the suture acting on the tissue; though nothing of significance has been observed in the literature [Campbell et al. (1989)]. The data observed in both Figure 6.20 and Figure 6.21 looks to agree with the theory however, as both exhibit trends of increasing pullout force with greater suture size. Be that as it may, the change in the means is not significant due to the variation being quite large ($P = 0.1263$, 0.4483 & $0.4574 > 0.05$ for bite separations of 5, 10 and 15mm respectively and $P = 0.4237$, 0.5878, 0.4484, 0.4103, $0.5483 > 0.05$ for bite depths of 4, 7, 10, 13 and 16mm respectively - see Figure 6.20 & Figure 6.21). Therefore, choice of suture size, at least for a PDS of 2-0, 0, and 1, can be considered a matter of personal preference rather than medical necessity.

One personal point of note is the handling. The smallest size (PDS 2-0) proved to be the easiest to handle. Application of the suture and tying it of was quick and simple, though it took practice not to break the suture by applying too much pressure on the knot. The largest size (PDS 1) was naturally the most durable and could be handled more bluntly without fear of it breaking. However, its greater thickness meant that it was quite stiff and difficult to handle (like standard fishing line) making knot-tying more time-consuming and arduous task. Of the three sizes, PDS 0 was the most user-friendly, supple without being weak.

6.5 Conclusions

This study has characterised the uniaxial suture pullout characteristics of both human and porcine linea alba. Sutures applied in the longitudinal direction were found to be able to resist pullout more than sutures applied transversely. Applying a suture in the transverse direction on a laparoscopic defect can also result in significantly more deformation and widening of said defect than longitudinal sutures. Maximising the bite depth and minimising the bite separation (no lower than 5mm) as much as possible is recommended to significantly improve resistance to pullout; holding true for both humans and swine. There was no statistical evidence that suture size impacts resistance to pullout, though the average pullout force was seen to increase for bigger sutures. Judging from the data of this study, patients could benefit

from laparoscopic wounds closed with larger bite depths and smaller bite separations and may even benefit from making a lateral incision and applying sutures longitudinally, especially for laparoscopic surgery. Furthermore, with porcine tissue exhibiting similar suture pullout characteristics to that of human tissue, it may be possible to use porcine tissue as a surrogate to human tissue in the design and development of surgical devices.

Chapter 7

Optimising Suture-Based Wound Closure Using a Surrogate Abdominal Rig

7.1 Introduction

This chapter details the experimental methods used in this thesis to determine the optimum suturing characteristics with a laparotomy defect of the linea alba using a pressurised abdominal surrogate. Chapter 6 previously investigated the uniaxial suture pullout properties of both porcine and human linea alba which provided some conclusions on the ideal suture bite depth and bite separation for laparotomy wound closure. However, since the abdomen is itself a pressurised vessel, it is generally described as being subjected to multi-axial loading [Cooney et al. (2015), Förstemann et al. (2011)]; not solely in the direction of the abdominal muscles aponeurotic processes. To more adequately describe the effect that suture-based wound closure has on the apposition of the linea alba laparotomy defect, it is necessary to create an environment that adequately reflects an in-vivo standpoint. To this end, deformation tests on porcine linea alba (intact abdominal wall) with a suture-closed laparotomy incision were performed on a surrogate abdominal rig, designed in-house in Trinity College Dublin [Lyons et al. (2015)] in order to more accurately ascertain the ideal bite depth and bite separation of a continuous suture to be used for a laparotomy defect. This is achieved by measuring the

extent by which each bite depth/separation combination affects the apposition of the wound at increasing levels of pressure. Theoretical and experimental evaluation of suture pullout is also investigated in order to predict the pressure of suture pullout beyond what is capable of the surrogate rig.

7.2 Materials and Methods

7.2.1 Tissue Origin

Due to the difficulty in obtaining large quantities of intact human abdominal walls, pigs were chosen as a suitable tissue substitute to humans for this study due to their similarly sized heart and body length to humans. Thirty-six porcine abdominal walls were obtained from a swine abattoir (Rosderra Meats, Edenderry, Co.Offaly, Rep. of Ireland). Specimens were chosen at random from both male and female populations; all females being nulligravida. All were adults, approximately 26-28 weeks in age and were frozen within 24 hours of death.

Several whole human abdominal walls were also sourced for a minor part of this study in a collaborative effort with Washington University in St.Louis. The cadaveric specimens were freshly frozen and obtained through the medical school in the college. Specimens varied in age (>60 years) and sex and were of a caucasian background. Prior to sample extraction porcine and human specimens were allowed to defrost for 36 hours at 4^oC.

7.2.2 Deformation Tests

For the purpose of this study a surrogate rig, previously developed in-house in Trinity College Dublin, was used [Lyons et al. (2015)]. It consisted of a rectangular box (200mm x 150mm), designed to represent the abdominal cavity (see Figure 7.1 below), containing an oversize inflatable chimney balloon connected directly to a compressed air supply. Applying a known pressure via the compressed air supply fills the balloon situated inside the box base of the surrogate rig, thereby applying pressure to the abdominal wall immediately above it.

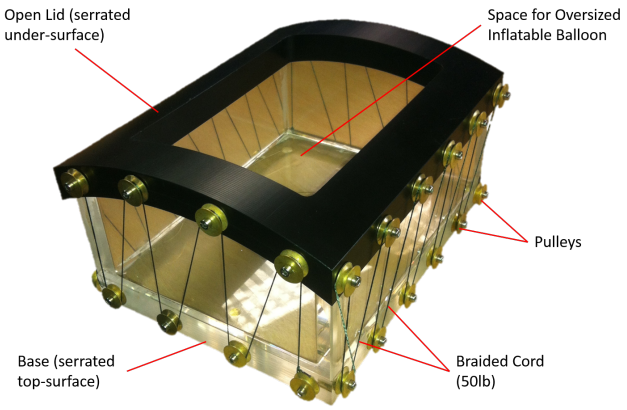

Figure 7.1: The surrogate rig containment box and lid with associated pulley system [Lyons et al. (2015)].

A lid is used to hold the abdominal wall in place. It contained a large rectangular hole (170mm x 120mm) in the middle to allow the abdominal wall to bulge out under applied pressure. The lid was compressed tightly against the abdominal wall and base rig using a system of pulleys and braided fishing line to prevent slippage (see Figure 7.1). The underside of the lid and topside of the walls of the box use serrated teeth (adapted from common household nutmeg-grater) to further prevent slippage of the abdominal wall upon application of pressure. To represent the curvature of the abdomen, both the top of the rig and lid were given a transverse radius of curvature of 200mm [Song et al. (2006*b*)]. No longitudinal radius of curvature was applied as it was assumed to be infinite.

A compressed air pipe network was used to facilitate accurate application and measurement of pressure (see Figure 7.2 below). Two pressure regulators were used; one for coarse pressure reduction of the high pressure compressed air supply followed by one for a more accurate and fine adjustment of the reduced supply. A series of valves allow passage of the air supply to the balloon with an exhaust valve (closed during normal operation) to return the system to atmospheric conditions at the conclusion of the experiment.

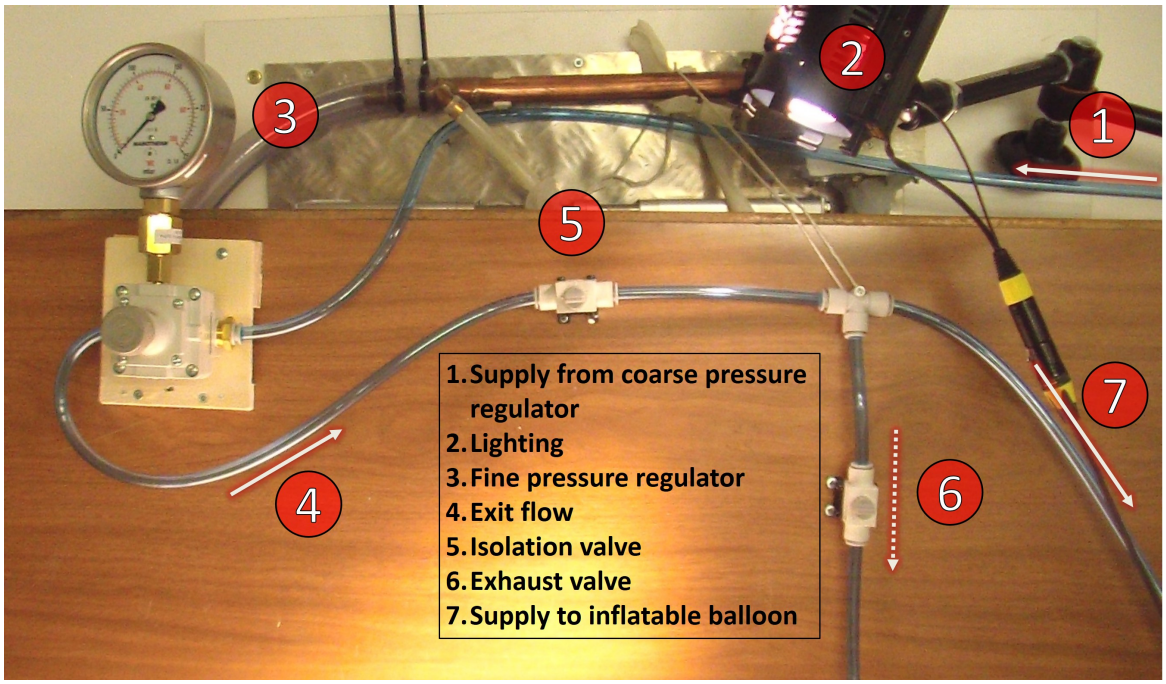

Figure 7.2: Compressed air pipe network setup.

Prior to setting up the experiment as seen in Figure 7.3A below, the abdominal walls (obtained from Rosderra Meats, Edenderry, Co.Offaly, Rep. of Ireland) were prepared such that the anterior fatty layer is removed. A 6cm laparotomy incision was then cut along the midline superior to the umbilicus; the maximum achievable incision length for use in the rig allowing for an even and comparable distribution of different suture application parameters. A continuous suture pattern was applied and the abdominal wall was then placed on the rig and centred before being cut to shape. The lid was placed on top and carefully tightened to the bottom half of the rig via the set of pullies. A series of dots were imprinted on the linea alba midway between each suture bite and in line with the sutures themselves (Figure 7.3B). Recording a closeup of the dot array, the experiment was initiated by first closing the exhaust valve and then ramping up the pressure at 0.33kPa/sec (1kPa every 3 seconds). The experiment ended when 25kPa was reached (just above the maximum physiological intra-abdominal pressure [Addington et al. (2008), Campbell & Green (1953), Cobb et al. (2005), Malbrain et al. (2004), Ravishankar & Hunter (2005)], or failure of the tissue occurs.

(A) (B)

Figure 7.3: The surrogate rig setup (A), showing an example of suture placement on the tissue (B).

For surrogate deformation tests comparing suture bite depth (distance from the cut margin of the linea alba) versus separation (distance from between each suture bite across the defect; stretch calculated from the dot array seen in Figure 7.4 below), a total of 45 abdominal walls were obtained from different porcine specimens. A variety of different bite depth/bite separation combinations were used and a sample size of 3 was maintained throughout. Table 7.1 below shows the different combinations used.

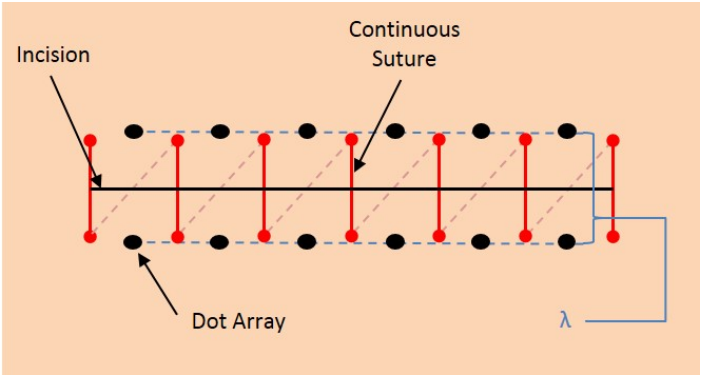

Figure 7.4: Application of the dot-array used to calculate stretch on the abdominal wall.

Table 7.1: Sample size for each variable combination

Surrogate Deformation Tests		Bite Depth Variable (mm) 4	7	10	13	16
Bite Separation Variable (mm)	5	3	3	3	3	3
	10	3	3	3	3	3
	15	3	3	3	3	3

Transverse stretch of the linea alba was measured where no defect is present in order to have a base reference to compare how effective each parameter combination is to providing a "normal" environment. Longitudinal stretch was also recorded for later use with the theoretical model. The transverse and longitudinal distance between a series of dots imprinted on the surface of the linea alba of the abdominal wall (see Figure 7.5 below) was recorded using image analysis (see Chapter 5) for increasing pressure. The longitudinal and transverse stretch was calculated by dividing each distance measurement by the original length at 0kPa pressure (see equation 7.1).

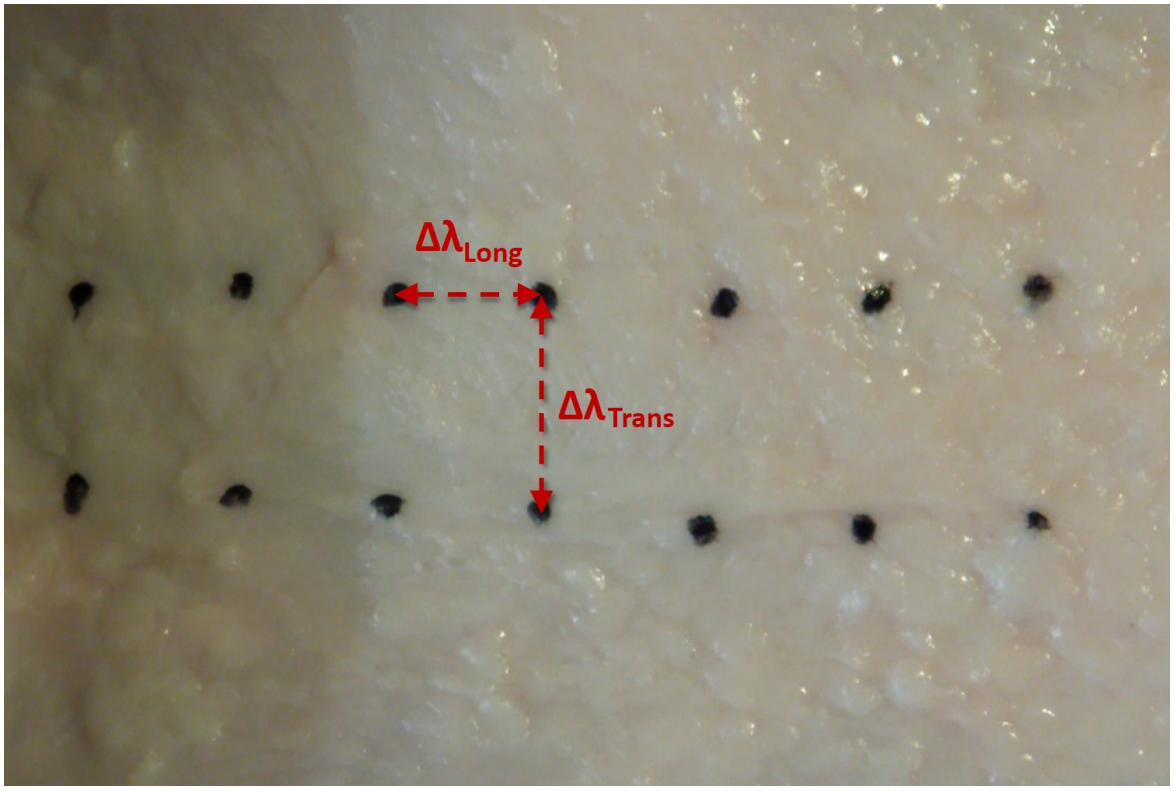

Figure 7.5: Stretch measurement of the linea alba as surrogate rig pressure increases (no defect).

$$\lambda = \frac{l_n}{l_0} \tag{7.1}$$

where λ is the stretch between two points, l_n is the length in pixels between two points for the nth iteration of incremental increase of pressure and l_0 is the original length at 0kPa.

Analysis of each test was performed by scrutinising the recorded surrogate rig pressure versus inter-bite stretch of the linea alba graph produced using MATLAB.

7.2.2.1 Physiology

For all experiments in the surrogate rig, the incision and suture patterns were applied to the supraumbilical side (the superior cranial side) of the linia alba. Figure 7.6 below shows an example of an experiment in the surrogate rig with a description of the shape of the linea alba. The infraumbilical and supraumbilical regions are shown above and below respectively rather than the other way around as it was the most conventional orientation to perform the experiment. Typically, the supraumbilical linea alba is between 20-30mm wide from umbilicus to xyphoid (bottom of sternum) while the infraumbilical linea alba (inferior caudal side) tends to be between 5-16mm up to two centimeters below the umbilicus [Beer et al. (2009)]. However, below this, the width of the linea alba can reduce to a tendinous junction between the rectus muscles. Therefore, to maintain experiment repeatability, all laparotomy incisions were made on the supraumbilical side where there was ample linea alba to work with. Furthermore, the size and shape of the umbilicus differed greatly between specimens making it very difficult to maintain repeatable testing. Accordingly, incisions were made $\approx$2cm above the umbilicus.

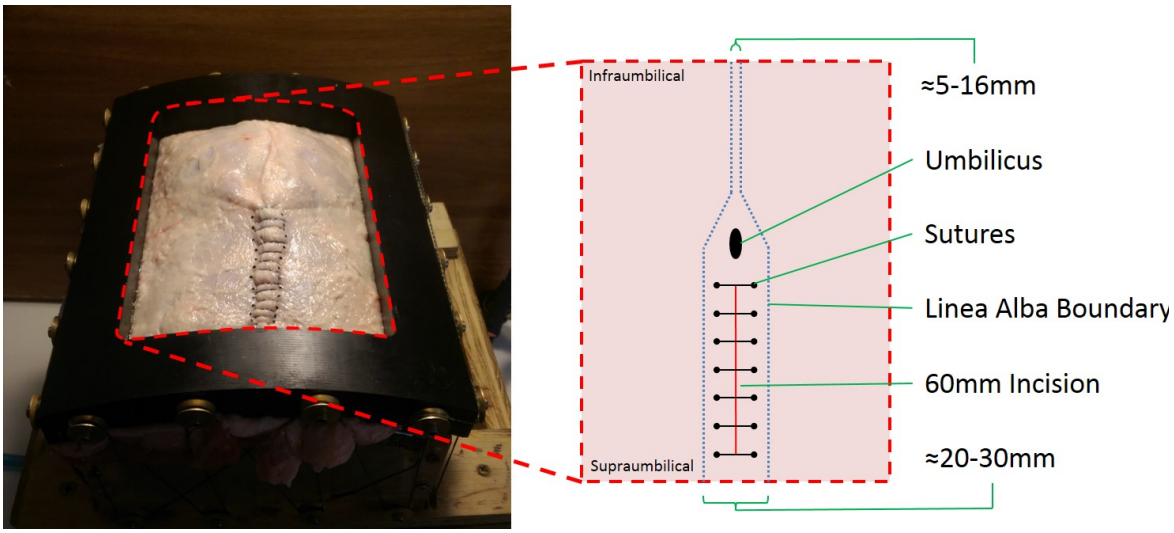

Figure 7.6: A depiction of the shape of the linea alba of the abdominal wall in the surrogate rig.

7.2.3 Theoretical Evaluation of Suture Pullout in the Surrogate Rig

Using the uniaxial suture pullout data obtained in Chapter 6, abdominal dimensions obtained from the literature [Duez et al. (2009), Förstemann et al. (2011)] and Laplace's law for thin-walled cylinders, it is possible to theoretically predict the failure pressure of a 60mm long incision of the linea alba for a variety of suture parameter configurations. This involved a three step process as follows:

1. Relating the pressure of the surrogate rig (IAP) to the force acting across the 60mm incision by rearranging the terms in Laplace's law.

    - changes in radius of curvature (Roc) of the belly as pressure is increased are accounted for through experimental measurement.
    - changes in defect length as pressure is increased is accounted by scaling using the longitudinal stretch.
    - changes in linea alba thickness as pressure is increased are negated through cancellation of terms.

2. Scale uniaxial pullout force data to account for a 60mm defect and ascertain corresponding pullout pressure by interpolating the theoretical data of the plot contrived in Step 1.

- results in a theoretical prediction of suture pullout pressure in the surrogate rig.

3. Use the experimental suture pullout pressure data, observed during the surrogate rig experiments, to ascertain corresponding pullout force over a 60mm defect by interpolating the theoretical data of the plot contrived in Step 1.

   - results in theoretical evaluation of suture pullout force over a 60mm defect.
   - used to validate model for the prediction of suture pullout pressure in the surrogate rig/abdomen.

A diagram of how each step relates can be seen below in Figure 7.7 below.

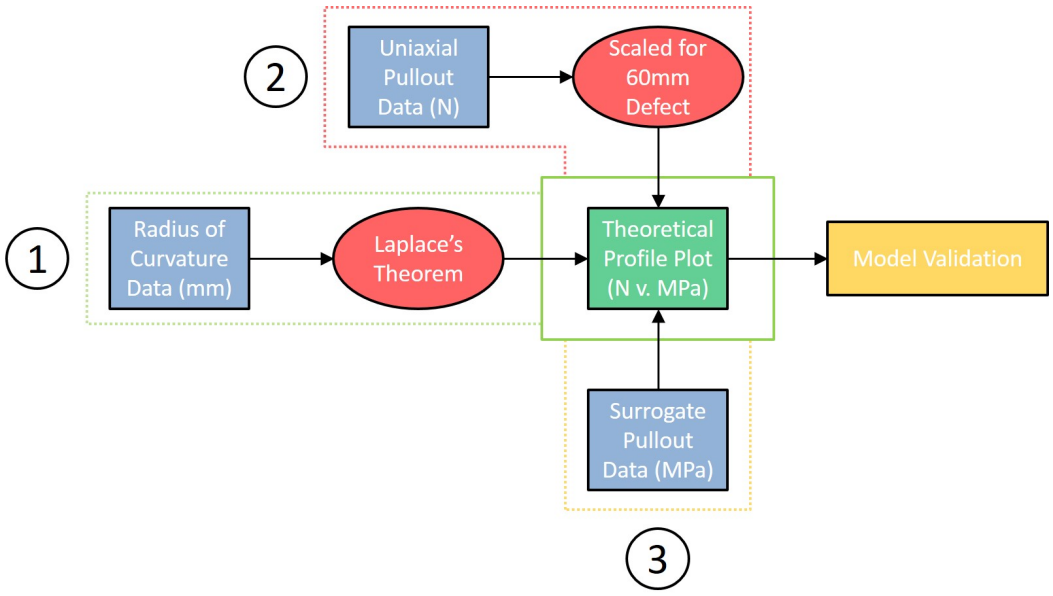

Figure 7.7: A process flow diagram showing the different steps for the creation and validation of the model.

7.2.3.1 Step 1

Laplace's law for thin-walled cylindrical pressure vessels (i.e. with a radius significantly larger than the thickness of the wall) was used to relate the pressure generated in the surrogate rig to the force acting transversely (fibre direction) across the linea alba for a 60mm defect. The law states that the hoop (tangental; σ_H) and longitudinal (σ_L) stresses can be simplified to internal pressure (P), radius (r) and thickness (t) as can be seen below in equations 7.2 & 7.3.

$$\sigma_H = \frac{P * D}{2t} = \frac{P * r}{t} \tag{7.2}$$

$$\sigma_L = \frac{P * D}{4t} = \frac{P * r}{2t} \tag{7.3}$$

Below in Figure 7.8 is an interpretation of the abdominal wall as a pressurised cylinder depicting the different terms of Laplace's law. The cylinder is orientated in the cranio-caudal direction (head-to-toe) with the sutured defect lying along its length.

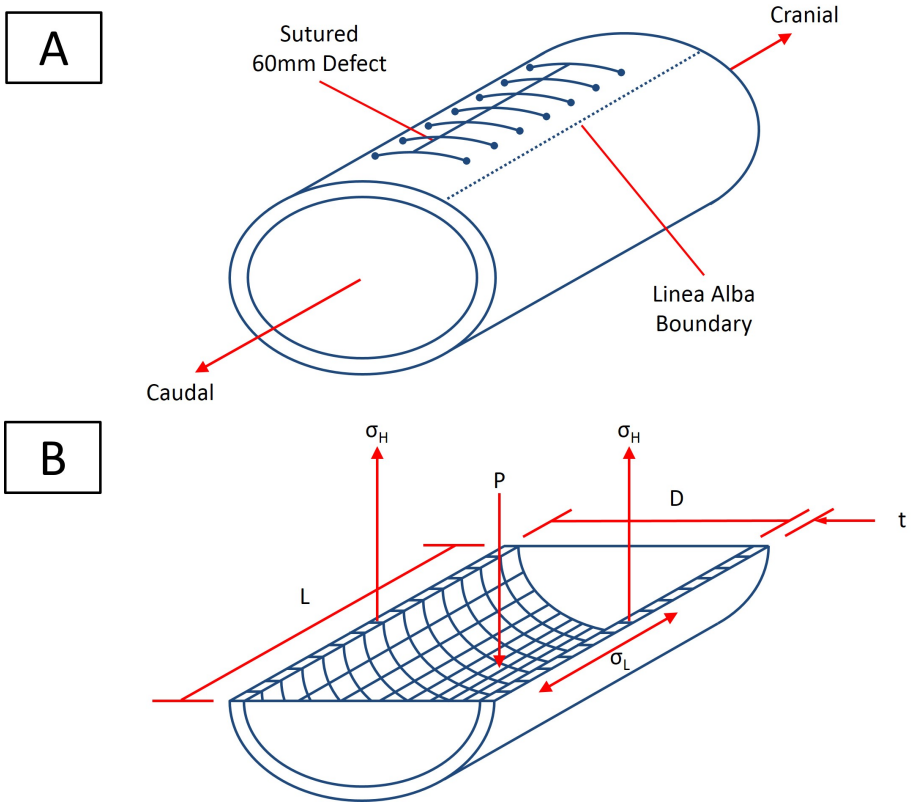

Figure 7.8: An example of the abdomen expressed as a cylinder extending cranio-caudally (A) with a cross-section labelling the different terms associated with Laplace's law (B).

The radius of curvature (Roc) of the abdominal wall in surrogate rig is continuously changing as pressure is increased. By letting the r-term in Laplace's theorems equal the radius of curvature of the belly, it is possible to account for this change per unit increase in pressure as outlined below in equation 7.4.

$$\sigma_H = \frac{P * Roc}{t}, \qquad \sigma_L = \frac{P * Roc}{2t} \tag{7.4}$$

However, the shape of the cross-section of the abdominal wall is not necessarily circular. The literature shows dimensions that would describe a more elliptical shape, having a major and minor axis [Duez et al. (2009), Förstemann et al. (2011)]. Therefore, using these dimensions obtained from the literature, it was possible to ascertain the radius of curvature of the minor axis (which describes the anterior most point along the linea alba very close to where surgeons typically make their incisions) using the equation for radius of curvature of an ellipse as seen below in equation 7.5.

$$Roc = \frac{a^2}{b} \tag{7.5}$$

where Roc is the radius of curvature of the minor axis, a = 141.1mm [Duez et al. (2009)] is the length of the major axis and b = 104.5mm [Duez et al. (2009)] is the length of the minor axis. The distension of belly measured experimentally is added to b as per increase in pressure to gauge the change in the Roc.

The change in the Roc was measured experimentally by recording the vertical displacement of the abdominal wall as pressure increased using MATLAB image viewer as can be seen in Figure 7.9. This displacement was then added to the length of the minor (b) axis for each corresponding unit increase in pressure.

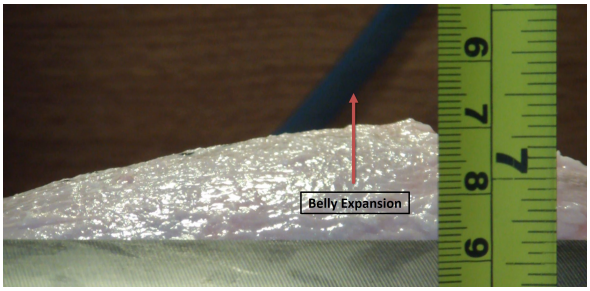

Figure 7.9: Pressure/expansion test showing belly expansion and the measurement tape used to gauge the exact vertical displacement of the belly.

Equating the hoop stress (σ_H) to the stress observed across the defect (σ_{Defect}), both acting in same direction (see Figure 7.8), results in equation 7.6 below where force across the defect is presented in terms of pressure, radius of curvature and length of the defect.

$$\sigma_H = \frac{P*r}{t}, \quad \sigma_{Defect} = \frac{F}{L*t}$$

$$\therefore \quad \frac{P*r}{t} = \frac{F}{L*t} \tag{7.6}$$

$$\therefore \quad P*r*L = F$$

where P is the pressure generated in the surrogate rig, L is the length of the incision, t is linea alba tissue thickness (average from all test specimens in Cooney et al. [Cooney et al. (2015)]) and F = The force across a 60mm incision.

The thickness term cancels meaning any change in thickness as pressure increases is disregarded. Change in defect length (L) was also accounted for by multiplying it by the corresponding stretch observed in the longitudinal direction as was mentioned in Section 7.2.2.

Using equation 7.6, a plot of surrogate rig pressure versus the force acting over the length of the defect was created.

7.2.3.2 Step 2

Each uniaxial parameter combination for suture pullout (a measure of force)) was scaled according to how many suture bites would be present in a 60mm defect. Therefore, the scaling factor is dependent on the bite separation. Each uniaxial test was performed with two suture bites; a bite separation of 5mm thereby requiring a scaling factor of 6.5 (see Table 7.2 below).

Table 7.2: Scaling factor for each bite separation.

Bite Separation (mm)	**Number of Suture Bites**	**Factor Scaling to 60mm**
5	13	x6.5
10	7	x3.5
15	5	x2.5

The scaled uniaxial results are then plot along the surrogate profile created in Step 1 by interpolating the data to find the corresponding rig pressure.

7.2.3.3 Step 3

Similar to Step 2, the range suture pullout data ascertained experimentally using the surrogate rig (a measure of pressure) was also plot along the surrogate profile created in Step 1 by interpolating the data to find the corresponding force acting across the defect. This allows for validation of the model, linking both the uniaxial suture pullout data and the multiaxial surrogate rig data in accordance with several assumptions used to simplify the model.

Over the course of the surrogate rig testing, some suture parameter combinations would pullout before the maximum applied pressure had been achieved. These were used to validate the theoretical model, helping to ascertain its accuracy. For cases of pressure or stretch where the value wasn't reached due to suture pullout, the data was extrapolated. This occurred five times in total out of 45 porcine abdominal walls tested.

7.2.3.4 Model Assumptions

In order for the model to work, certain assumptions need apply that may limit its effectiveness:

1. None of the pressure is generated by the application of force due to activation of the lateral muscles. The internal pressure (IAP) is the acting element.

2. Lack of longitudinal deformation occurring in unaxial tests is considered to have a negligible effect on the mechanical properties.

3. The anisotropic nature of the tissue (Chapter 5) is considered negligible.

4. The effective difference that the different test speeds of each study have on the mechanical properties of the tissue is considered negligible in comparison.

7.3 Results

7.3.1 Deformation Tests

Figure 7.10 below shows the 3-dimensional plots of stretch versus bite depth and bite separation of porcine tissue for increasing set levels of rig pressure (5kPa, 10kPa, 15kPa and 20kPa). In each case a 3rd order polynomial (poly(3,2)) surface was fit to the data which best

described it. There is an evident increase in stretch (at all pressures) as bite depth decreases and bite separation increases.

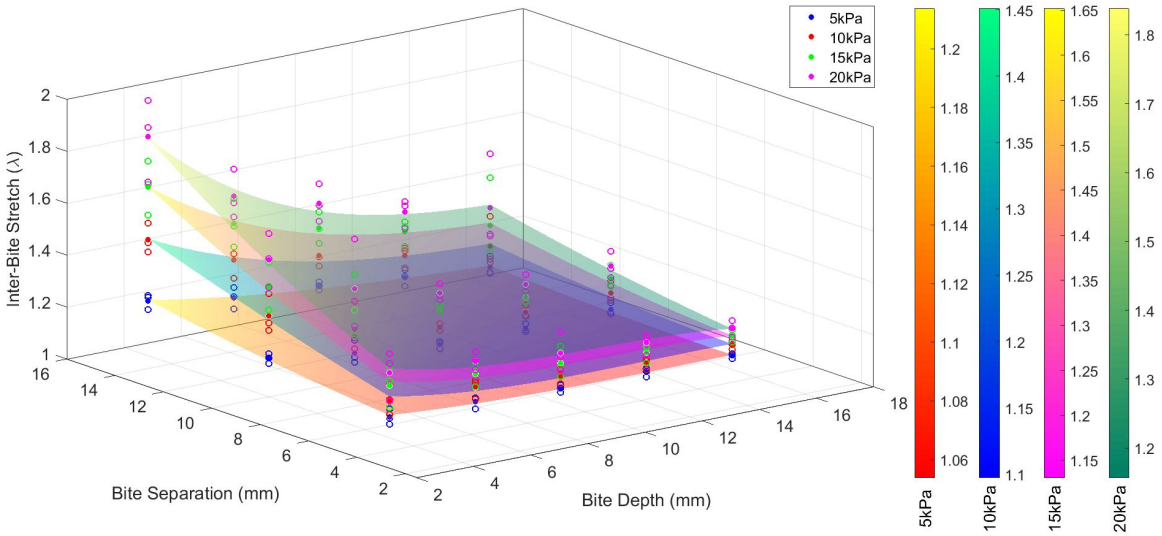

Figure 7.10: Stretch versus bite separation and bite depth for pressures of 5kPa, 10kPa, 15kPa and 20kPa.

The individual subplots of each surface plot in Figure 7.10 can be seen below in Figure 7.11. A reference plane (grey square horizontal plane) depicting the stretch for each particular value of rig pressure of a belly without defect can be seen in each graph. The mean stretch values of the reference plains are 1.029λ, 1.055λ, 1.072λ and 1.083λ for applied pressures of 5kPa, 10kPa, 15kPa and 20 kPa respectively. Alternatively, larger individual plots for each pressure case can be seen in Figures 11.2, 11.3, 11.4 & 11.5 in Chapter 11.

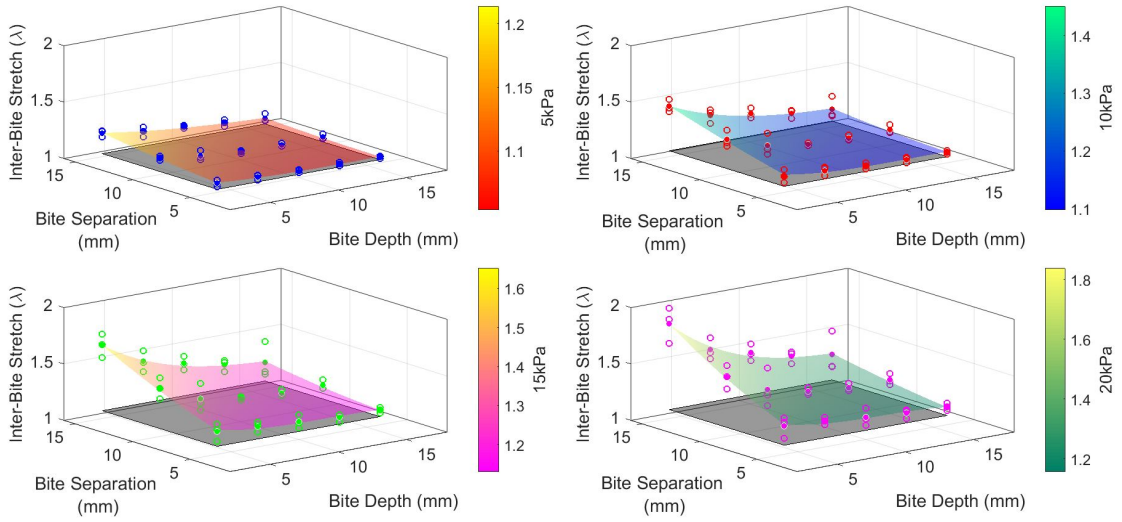

Figure 7.11: Individual plots of stretch versus bite separation and bite depth for pressures of 5kPa, 10kPa, 15kPa and 20kPa, showing the associated stretch of a standard belly without defect (grey horizontal plane).

Figure 7.12 below shows the 3-dimensional plots of applied rig pressure versus bite depth and bite separation of porcine tissue for increasing levels of recorded stretch (1.1λ, 1.15λ and 1.2λ; see Figure 11.1 in Chapter 11). In each case a 3rd order polynomial (poly(3,2)) surface was fit to the data which best described it. There is an evident increase in pressure as bite depth increases and bite separation decreases.

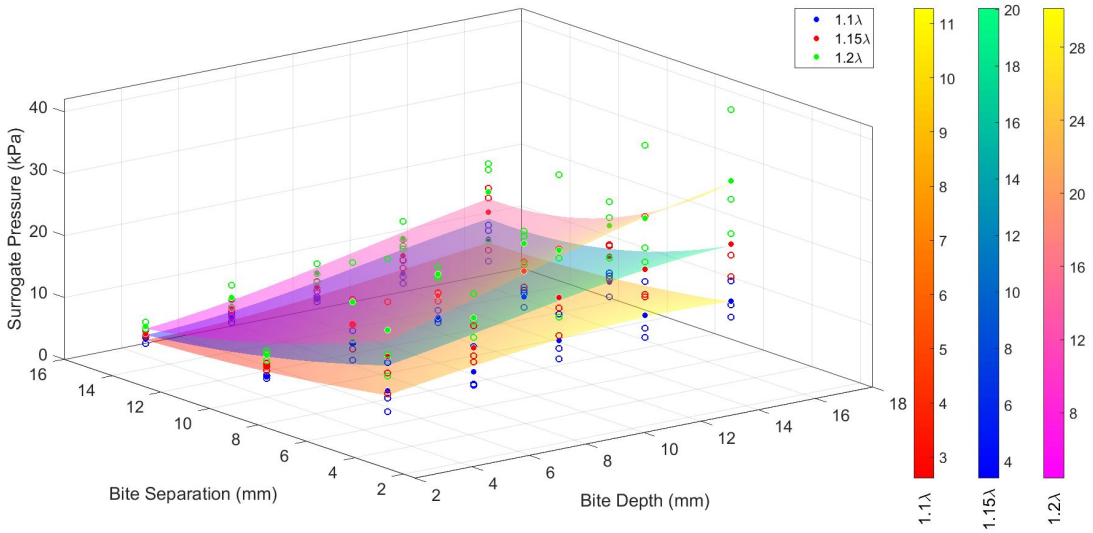

Figure 7.12: Pressure versus bite separation and bite depth for stretches of 1.1λ, 1.15λ and 1.2λ.

The individual subplots of each surface plot in Figure 7.12 can be seen below in Figure

7.13. Unfortunately, it is not possible to compare against a standard non-defect case as the stretch does not exceed 1.09λ (see Figure 11.1 in Chapter 11). Alternatively, larger individual plots for each stretch case can be seen in Figures 11.6, 11.7 & 11.8 in Chapter 11.

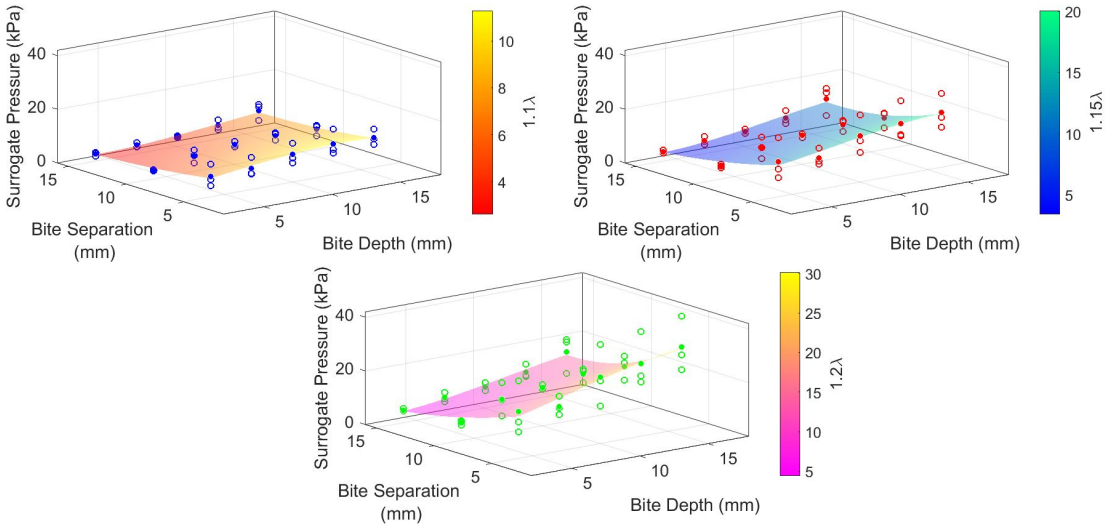

Figure 7.13: Individual plots of pressure versus bite separation and bite depth for stretches of 1.1λ, 1.15λ and 1.2λ.

Figures 7.14 & 7.15 below show 3-dimensional plots of suture bite depth, bite separation and [10,10] parameter ratio for varying pressure and varying stretch respectively. The [10,10] parameter ratio is obtained by dividing all data for a given pressure or stretch by the [10,10] parameter average, thereby relating all data relatively to the general standard as is used currently by surgeons [Bhat (2014), Mulholland & Doherty (2006)]. A 3rd order polynomial surface was again used to fit the data, depicting a very close approximation of all profiles to one another meaning that, for all values of applied pressure or recorded stretch, the relative value of each bite depth/bite separation parameter to the [10,10] parameter remains virtually the same.

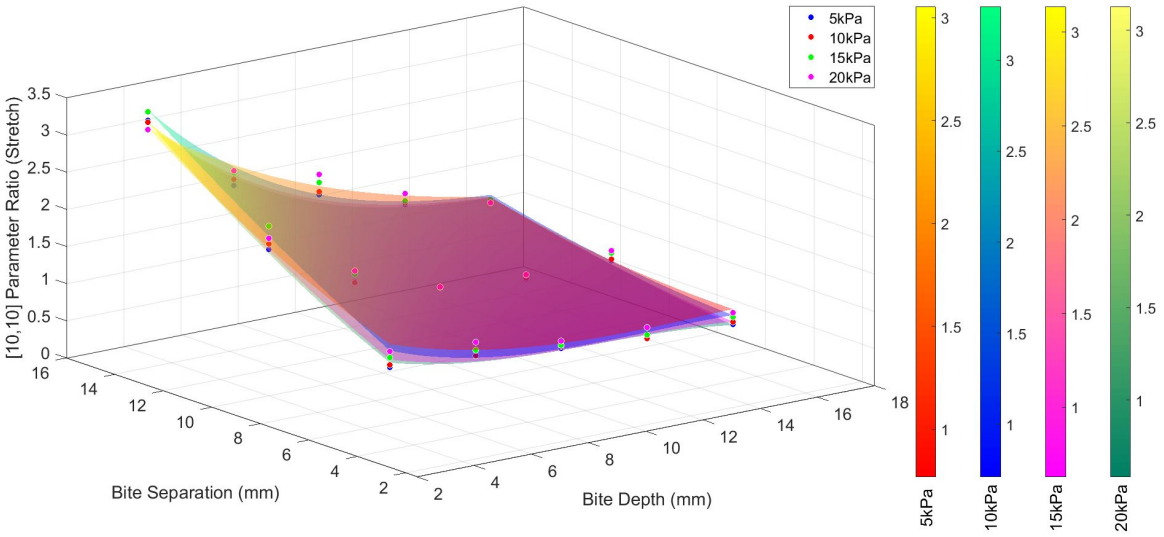

Figure 7.14: Stretch, scaled to a [10,10] parameter ratio, versus bite separation and bite depth for pressures of 5kPa, 10kPa, 15kPa and 20kPa.

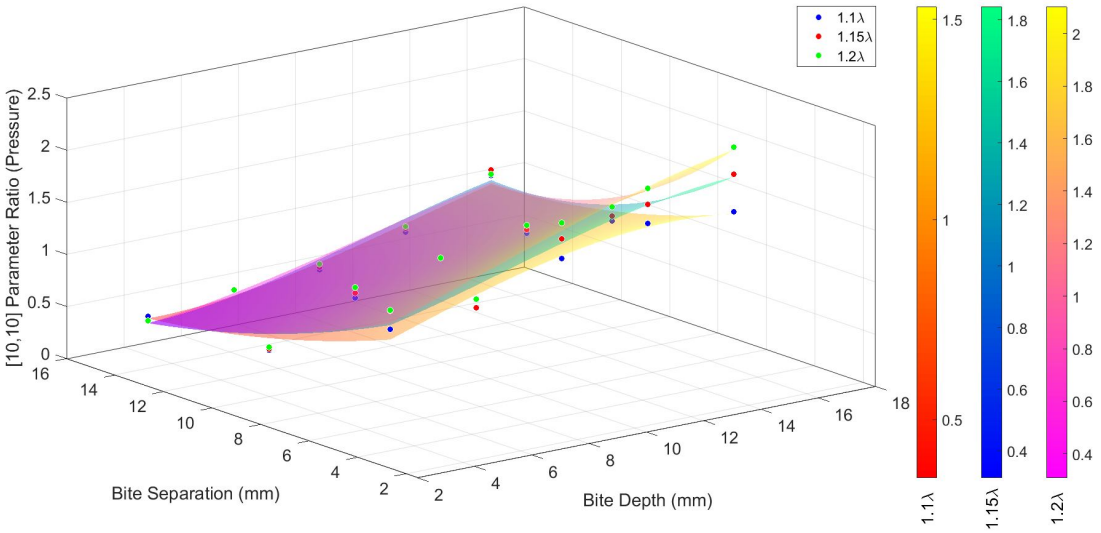

Figure 7.15: Pressure, scaled to a [10,10] parameter ratio, versus bite separation and bite depth for stretches of 1.1λ, 1.15λ and 1.2λ.

Figure 7.16 below shows the 3-dimensional plots of suture bite depth, bite separation and [10,10] parameter ratio for varying pressure and varying stretch respectively seen in Figure 7.15 with the equivalent plot of the porcine uniaxial suture pullout data scaled to the [10,10] parameter (see Figure 6.14 in Chapter 6). Interestingly, there is a very close approximation between the surrogate (transparent surfaces) and uniaxial (opaque surface mesh) data with both data sets exhibiting the same trend for increasing values of bite depth

and bite separation.

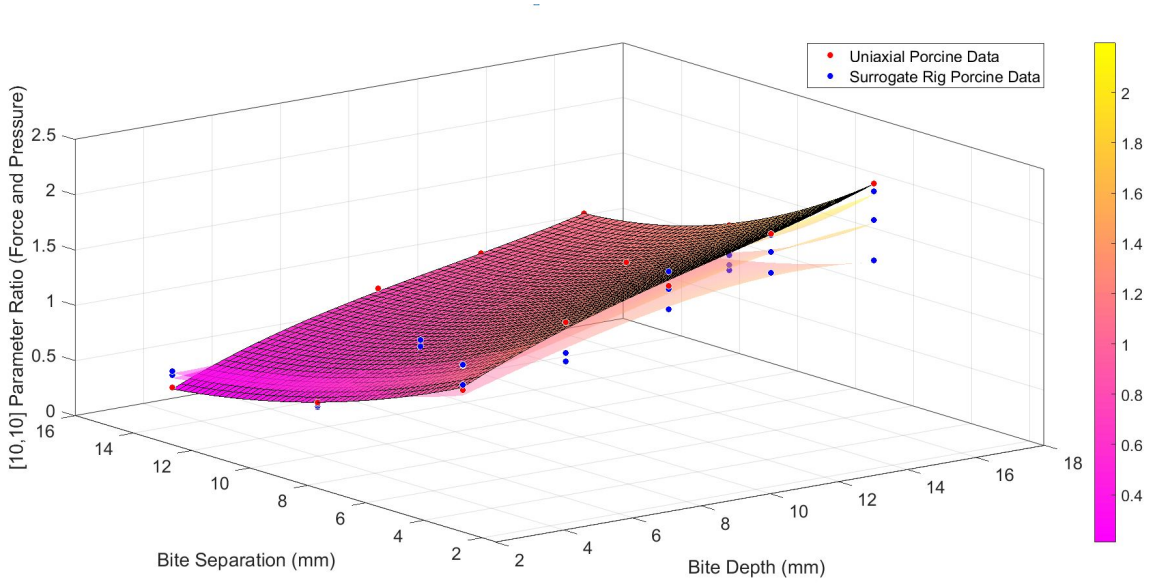

Figure 7.16: A plot of the uniaxial pullout data against the surrogate rig data, everything scaled to a [10,10] parameter for accurate comparison.

7.3.2 Theoretical Evaluation

The profile of the prediction of suture pullout in the rig can be seen below in Figure 7.17 for both human and porcine abdominal walls; depicting the theoretical hoop stress in response to a particular applied surrogate rig pressure. Using the uniaxial data from Chapter 6, the exact rig pressure/hoop stress required to make each suture parameter combination fail was plot along each profile. Only three parameter combinations ([15,4], [15,7] and [10,4]) lie within the physiological region; a region defined by the maximum typical physiological intra-abdominal pressure of 20kPa (≈240N force along the 60mm defect).

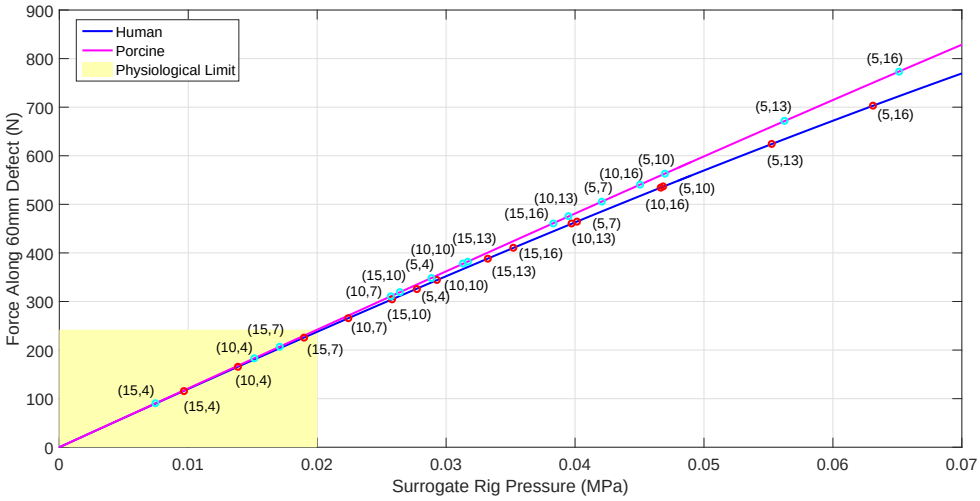

Figure 7.17: A plot of surrogate rig pressure versus theoretical hoop stress depicting the points at which suture pullout is expected.

Figure 7.18 below shows the suture pullout prediction for porcine tissue with the suture pullout pressure ranges observed experimentally in the surrogate rig. As the measurement of rig pressure was limited to an absolute maximum of 35kPa, it was impossible to observe failure for all parameter types. Therefore, only four ranges are listed ([15,4], [15,7], [10,4] and [10,7]). Parameter [15,4] is seen to fail in the range of 14.25-17.5kPa (fails twice), [10,4] in the range of 21.75-25kPa (fails 3 times) and [15,7] in the range of 27.5-34kPa (fails twice). Only the [15,4] parameter is observed to fail within the physiological region.

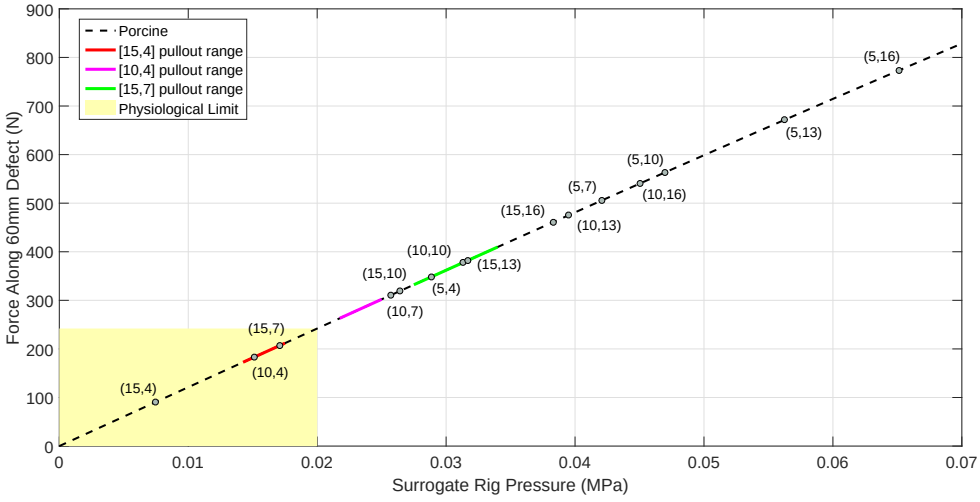

Figure 7.18: Experimental pullout range of porcine tissue ascertained during surrogate rig testing.

A numerical comparison of the average force and pressure of failure (suture pullout) for between uniaxial and surrogate rig experiments can be seen below in Table 7.3 and Figure 7.19. All predictions appear to underestimate surrogate rig pullout by varying but significant amounts, the largest offset (112%) represented by the [15,4] parameter. No obvious trend can be seen between the percentage differences of the different parameters.

Table 7.3: A comparison of the average force (N) and pressure (kPa) of suture pullout between uniaxial and surrogate rig experiments.

Bite Separation (mm)	**Bite Depth (mm)**	**Uniaxial Failure (N)**	**Surrogate Failure (N)**	**Uniaxial Failure (kPa)**	**Surrogate Failure (kPa)**	**% Diff.**
15	4	90.40	192.27	7.46	15.88	112
10	4	183.30	285.05	15.14	23.58	55
15	7	207.00	371.00	17.1	30.75	79

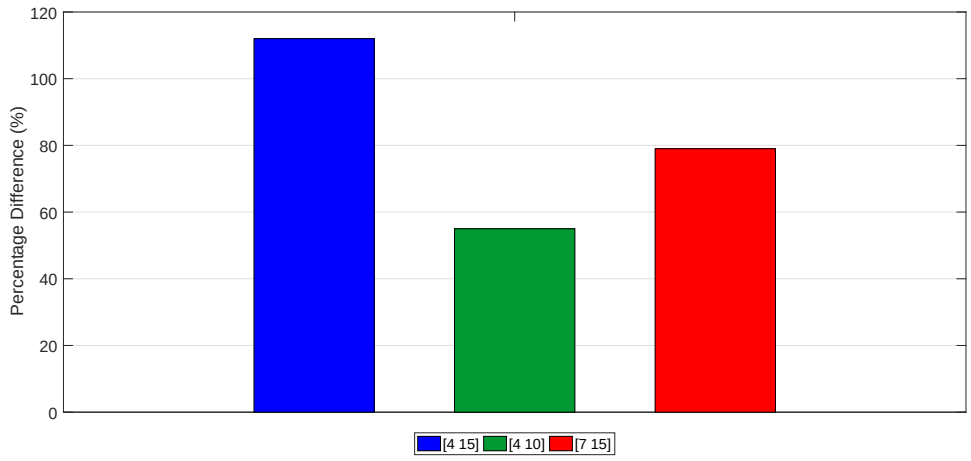

Figure 7.19: A percentage difference comparison between uniaxial and surrogate rig experiments.

Comparing the [4 10] uniaxial and surrogate results in terms of surrogate rig pressure (see Figure 7.20 below), no significant difference in mean pullout pressure was observed. It therefore remains unclear if the model is successful at accurately representing the mechanical characteristics of the surrogate abdominal rig. Only the [10 4] parameter was compared here as it was solely at this combination that failure occurred 3 times in the surrogate rig.

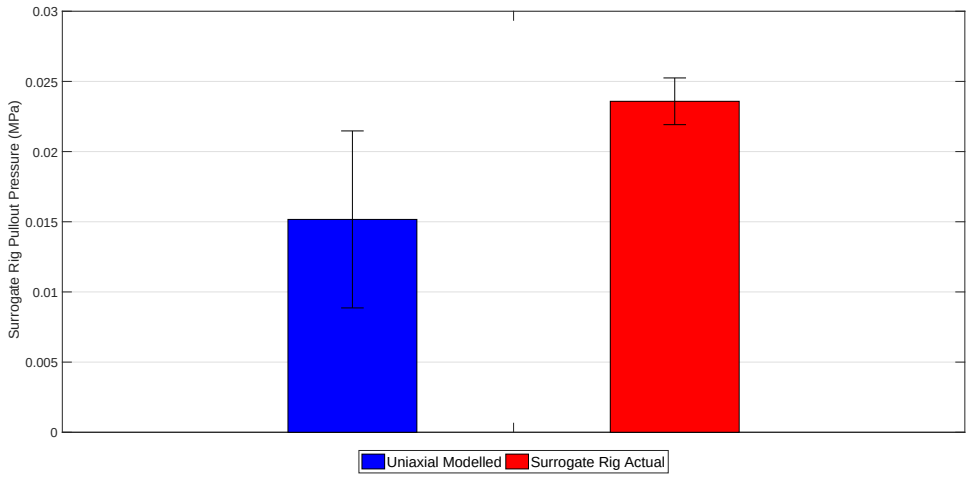

Figure 7.20: Difference in [4 10] modelled uniaxial and surrogate results.

7.4 Discussion

7.4.1 Deformation Tests

The most important aspect of wound closure is to retain apposition of the tissue (i.e. minimise the parting of cut edges of the tissue) so as to provide the best possible environment for tissue healing. As long as the cut edges are opposed, aggravation of the healing process is minimal ([Kingsnorth & LeBlanc (2013)]). This study focuses on inter-bite stretch as a measure of apposition. Observing the effect that bite depth and bite separation has on the inter-bite stretch for increasing levels of pressure in Figure 7.10 for porcine tissue, several notable trends can be seen:

1. As bite separation is increased, so too does inter-bite stretch.
2. At large bite separations (10-15mm), there is a significant decrease in inter-bite stretch as bite depth increases; becoming more significant with increasing pressure.
3. Both bite separation and bite depth appear to have a roughly equivalent effect for the same change in displacement.

Before making any conclusions on the optimal set suturing parameters, it is important to understand the difference with regards to the stretch observed in a belly without defect.

From Figure 7.11 it is apparent that no parameter combination results in the same amount of stretch as a non-defect case (the grey horizontal plane in each pressure case). However, some parameter combinations behave relatively worse than others. Table 7.4 and Figure 7.21 below show the percentage difference in stretch for the four most extreme parameter combinations at each pressure level. The parameter combination with the least difference is shown in green ([5,16]) with the one with the most shown in red ([15,4]) in the table. Both [5,4] and [15,16] appear to have a relatively similar effect though there appears to be very little variation about the mean percentage change in stretch at all pressures for bite separations of 5mm while separations of 15mm yield an obvious trend increase in stretch as pressure is increased; becoming more significant as bite depth is decreased. However, it is the [5,16] parameter combination that affects wound apposition the least.

Table 7.4: Percentage increase in stretch (no-defect versus defect).

% Increase in Stretch		**[Bite Separation, Bite Depth]**			
		[5,4]	**[5,16]**	**[15,4]**	**[15,16]**
Pressure (kPa)	**5**	179.31	79.31	631.03	168.97
	10	165.45	70.91	714.55	190.91
	15	180.56	79.17	802.78	230.56
	20	202.41	90.36	916.87	268.67

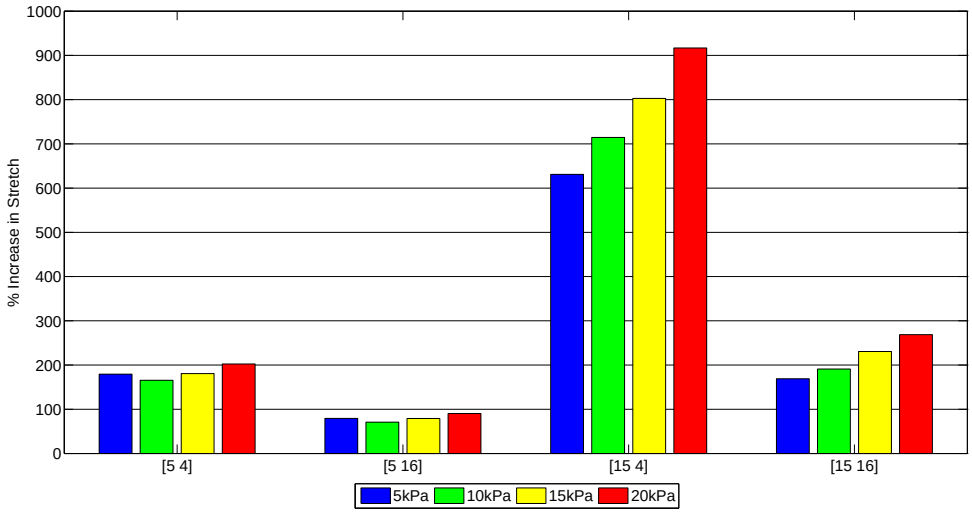

Figure 7.21: Percentage increase in stretch (no-defect versus defect).

From this it is evident that bite separation as low as possible and a bite depth as high as

possible works best to maintain wound apposition and consequently promote better healing, with a ten-fold difference being observed between the extreme suture parameter combinations ([5,16] and [15,4]).

Regarding the effect that bite depth and bite separation has on associated pressure for increasing levels of inter-bite stretch in Figure 7.12 & 7.13 for porcine tissue, several notable trends can be seen:

1. As bite depth is increased, pressure required to reach the specified stretch linearly increases; further increasing with cumulative stretch.

2. As bite separation is increased, pressure required to reach the specified stretch decreases almost asymptotically.

3. Both bite separation and bite depth appear to have a roughly equivalent effect for the same change in (mm).

The pressure profiles depict strikingly similar trends as seen in the normalised porcine data in Chapter 6; maximum apposition being achieved by using a bite depth as large as possible with a bite separation as low as possible due to the increased pressure required to further stretch the tissue between bites. Again parameter combinations [5,4] and [15,16] achieved a similar effect, both requiring almost the same amount of pressure to effect each level of stretch.

The relative plots (Figure 7.14 and Figure 7.15) that compare the [10, 10] parameter typically used in surgery with the rest of the data show that it's not as effective as it could potentially be. The results show that inter-bite stretch could be reduced by as much as ≈30-40% (depending on the applied pressure) with the pressure required to achieve an inter-bite stretch of 1.1-1.2λ increasing by as much as ≈50-110% by using a bite depth of 16mm and a bite separation of 5mm.

Figure 7.16 compares the normalised uniaxial data from Chapter 6 to the normalised surrogate data for varying levels of stretch. Interestingly, both depict data equivalently relative to each [10,10] parameter; the uniaxial data showing an improvement of ≈120% when switching to a [5,16] combination. This implies that, despite the tissue being subjected

to load in a singular direction and despite scaling the data to account larger wound length, the uniaxial results are applicable and relevant.

One point of note is the difference in variability when presenting the data in terms of the input pressure or output stretch. Greater variability is observed when presenting in terms of the output. Due to initial slack in the belly being taken up as pressure increases, the output curve is sloped in such a way that small changes in slope of the curve appear to effect greater change when presenting the data in terms of the output stretch than the input pressure. An example of this can be seen below in Figure 7.22 which simplifies what can be seen in Figure 11.1 in the Appendix.

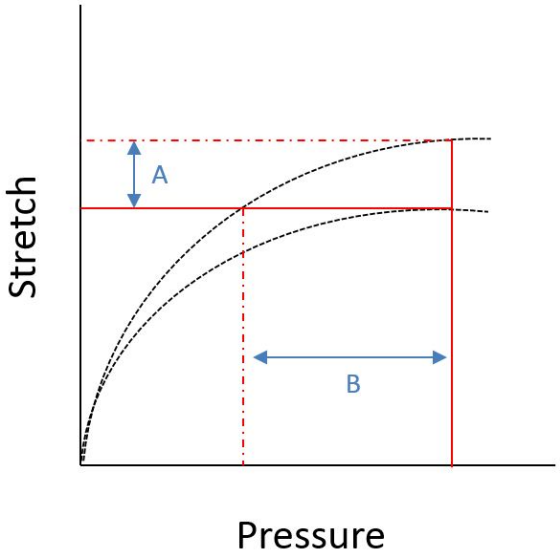

Figure 7.22: An example plot of stretch versus applied pressure depicting the difference in variability when presenting results in terms of the pressure input (A) or the stretch input (B).

7.4.2 Theoretical Evaluation

Using the Uniaxial data from Chapter 6 to predict suture pullout in the surrogate rig (and in-vivo should the model assumptions hold), only three parameter combinations ([15,4], [15,7] and [10,4]) failed within the typical physiological range of 20kPa. The [5,16] parameter describes a pullout pressure in the surrogate rig of approximately ≈65kPa, far beyond what is physically capable. Most parameters are predicted to pullout between 25-50kPa; still considerably high meaning, in terms of pullout, the majority of depth/separation combinations could be deemed acceptable. The human and porcine theoretical profile both appear quite

similar, characterised by a ≈7% difference in their slopes, but have a slightly different distribution of theoretical pullout (see Figure 7.17).

For porcine tissue pullout was observed in three parameter combinations ([15,4], [15,7], [10,4]). However, pullout was only observed twice for the [15,7] and [10,4] parameters and three times for the [15,4] parameter. Unfortunately, unlike the theoretical model, only one parameter was observed to have pullout within the physiological maximum of 20kPa ([15,4], see Figure 7.18). Theoretically, both the [15,4] and [10,4] average experimental values for pullout pressure offset the theoretical assumption by ≈8kPa, though it's not as exact in the case of [15,7] in which a ≈13kPa offset was observed (possibly due to the reduced sample size not adequately accounting for inter-specimen variation). However, the percentage differences observed between uniaxial and surrogate differ considerably for each parameter (see Table 7.4). One likely reason for this is that, although the model itself does account for change in length of the defect, the factor used to scale the uniaxial results (see Table 7.2) to the required defect length does not; after applying the factor the force is still representative of a 60mm defect length. The uniaxial tests experience only one axial deformation, not two as in the surrogate rig. Each uniaxial parameter force with a different bite separation would need to be scaled further by a different amount in each case in order to properly relate uniaxial and multiaxial experiments. Furthermore, Laplace's theorem relies on the assumption of a homogeneous material structure. However, it has been well documented that the linea alba is significantly anisotropic [Cooney et al. (2015)]. Therefore, a Laplace material should exhibit equi-biaxial deformation under simple biaxial loading testing conditions as is performed in Chapter 5, rather the axial bias deformation (biaxial) that can be seen with a material such as the linea alba.

Overall, it appears that the assumptions outlined in Section 7.2.3.4 significantly limit the model; the differences in deformation/load aplication between uniaxial and surrogate experiments being of particular concern. It may help if simple biaxial suture pullout tests were used rather than uniaxial tests. This may improve the relative percentage difference that is observed between uniaxial and surrogate tests currently.

Although only one parameter ([15,4]) was observed to pullout within the physiological limits, the ranges of both the [10,4] and [15,7] are within 10kPa. While it is not possible for the body to produce such extreme levels of IAP, an external force resulting from an impact

(such as a fall for example) could bring the IAP beyond what is natural. Even in healthy individuals, there have been reports of bowel perforation as a result of a significant increase in IAP from seat-belt restriction in car accidents [Agrawal et al. (2007), Biswas et al. (2014)]. The [10,10] parameter combination typically used by surgeons (presuming it to have a a pullout pressure of ≈40kPa in the rig if a similar offset from the uniaxial predictions is assumed, as seen in [15,4], [10,4] and [15,7], see Figure 7.18 and Table 7.4) appears to be sufficient for typical physiologically generated IAP, though it may not be enough reduce risk of pullout/hernia as a result of external forces. It would therefore be prudent to use a parameter combination for laparotomy closure that maximises resistance to suture pullout, such as the [5,16] parameter combination.

7.5 Conclusion

This study has characterised the ideal bite depth/bite separation parameters to be used with a suture-closed laparotomy surgery defect using a pressurised abdominal surrogate. Overall it was found that a bite separation as small as possible and a bite depth as large as possible works best to retain wound apposition to help promote better healing and less scarring of the tissue. Bite separations as low as 5mm were found to exhibit little difference in the percentage change of stretch at all levels of pressure when compared against a separation of 10mm which is typically used whereas separations of 15mm result in a trend increase. The uniaxial suture pullout study seen in Chapter 6 has shown favourably similar results as seen in the current study which utilises multiaxial loading; the normalised data showing equivalent relevance in both studies and showing that uniaxial studies on suture pullout of the linea alba can be relied upon despite the lack of longitudinal loading/deformation. A model was produced with the intention of it being able to predict suture pullout in the surrogate rig beyond what was capable in the rig itself (due to the limited maximum pressure of the rig). Unfortunately the prediction model of suture pullout in the rig didn't prove entirely efficient and was found to offset the experimental results by ≈8-13kPa possibly as a result of a combination of different material structure assumptions (anisotropic tissue with and isotropic model) and differences in load application/test-speed. However, future tests involving biaxial suture pullout experiments may provide a better basis for prediction.

Human tissue was found to have a similar theoretical rig pressure/hoop stress profile as that of porcine but a different distribution of theoretical pullout. To the author's knowledge, there is no evidence of examples of suture-based surrogate research in the literature.

Chapter 8

Discussion

Given the high incidence of incisional hernia after laparoscopic and laparotomy surgeries, there is an essential need for a more effective solution to aid defect closure that can reduce risk to the patient. Such a solution could also potentially reduce the financial impact on patients by eliminating the need for revision procedures. Typically, surgeons adhere to a guideline suture placement of a minimum of 1cm between each bite (bite separation), each bite being taken 1cm away from the cut margin of the linea alba (bite depth) during laparotomy closure [Bhat (2014), Israelsson & Jonsson (1993), Mulholland & Doherty (2006)]. However, there is little in the literature that adequately quantifies these parameters (see Section 3.4.2.2). Furthermore, patients who suffer from obesity are at considerably more risk of developing a hernia [Uslu et al. (2007)] post-operatively due to greater intra-abdominal pressure and a large fatty layer that inhibits the surgeons access, view and dexterity. Unfortunately the incidence of incisional hernia looks set to steadily rise due to increasing levels of obesity apparent in nearly all developed countries [Flegal et al. (2002)]. This outlines a clear need for a more robust solution to the current methodology of wound closure in laparoscopic/laparotomy surgery.

Initial development of a surrogate abdominal testing rig has previously been performed by Lyons et al. [Lyons et al. (2013)]. By creating a pressurised surrogate environment using conventional and easy-to-produce materials in combination with fresh biological tissues, it is possible to mimic abdominal loading as a result of IAP. This is, in particular, where the rig developed by Schwab et al. (as mentioned in Section 3.2) could be further developed

[Schwab et al. (2008)]. It allows for the possibility of testing and developing novel wound closure devices and methodologies accurately prior to further evaluation through human or animal trials.

An analysis of different laparotomy and laparoscopic surgeries performed on the abdomen in Section 2.2.1 & 2.2.2 shows that the linea alba, being the most common site of choice for larger surgical incisions, is the most important tissue implicated in incisional hernia development. In laparoscopic surgery, most port holes incised through the rectus sheath are usually 5mm or less and often involve passage through multiple layers of tissue and muscle, making incisional hernia less likely than would be the case through the linea alba.

Although the risk of incisional hernia of the linea alba is considerable (incidence as high as 20% for post-laparotomy surgery alone [Bucknall et al. (1982), Mudge & Hughes (1985), Park et al. (2006), Sanz-Lopez et al. (1999)]), there have been relatively few studies and fewer commercially available medical devices that attempt to address this concern. In Section 3.4.2.2 two studies were discussed that do attempt to define optimum placement of sutures in terms of an ideal suture bite depth and separation [Campbell et al. (1989), Descoux et al. (1993)]. However, problems with experimental procedure and differences in protocol mean it is difficult to obtain concrete conclusions. Campbell et al. assessed the effect of changing the bite depth on the recorded pullout force. However, edge effects were not taken into account in this study which could account for the eventual plateau of the observed trend in the results. Descoux et al. performed a similar study to ascertain ideal bite separation. It was reported that the pullout force dropped linearly as they were brought closer than 12mm apart. However, decreasing the bite separation would increase the number of bites if the wound length remained the same and it would therefore be expected that the pullout force would increase as the load would be divided across an increasing number of sutures. In their first experiment wound length was varied (the same number of sutures are used for each separation), which is not applicable to a specific surgical case while in the second experiment the separation is only varied by 9mm. Furthermore, the effect of changing separation as bite depth varies was not investigated in either study.

A device designed by SuturTec (see Figure 3.18 [Meade & Brecher (1995)]) may help reduce risk of incisional hernia by allowing the surgeon to more accurately define the bite depth during suture placement, though it doesn't allow for a controlled separation of suture

bites which would guarantee repeatability. However, since an optimum bite depth has not yet been adequately defined, it is not guaranteed to significantly reduce the risk of incisional hernia.

However, assessing the ideal method of suturing and application of sutures for surgical wound closure of the abdomen requires a clear understanding of the structural and mechanical properties of the linea alba as it would help define effectual significance of any solution. In Section 3.4.2.2 the evidence in the literature was found to be too disjointed and contradictory to rely on, emphasising the need for a more accurate assessment.

Following on from the objectives stated at the end of Section 1 & 3, Figure 8.1 below shows the experimental tasks and processes performed over the course of this project in order to address the knowledge deficit; the primary concerns being: 1) the mechanical properties of the linea alba, 2) the ideal bite depth/separation to minimise risk of incisional hernia and 3) the similarities between porcine and human tissue.

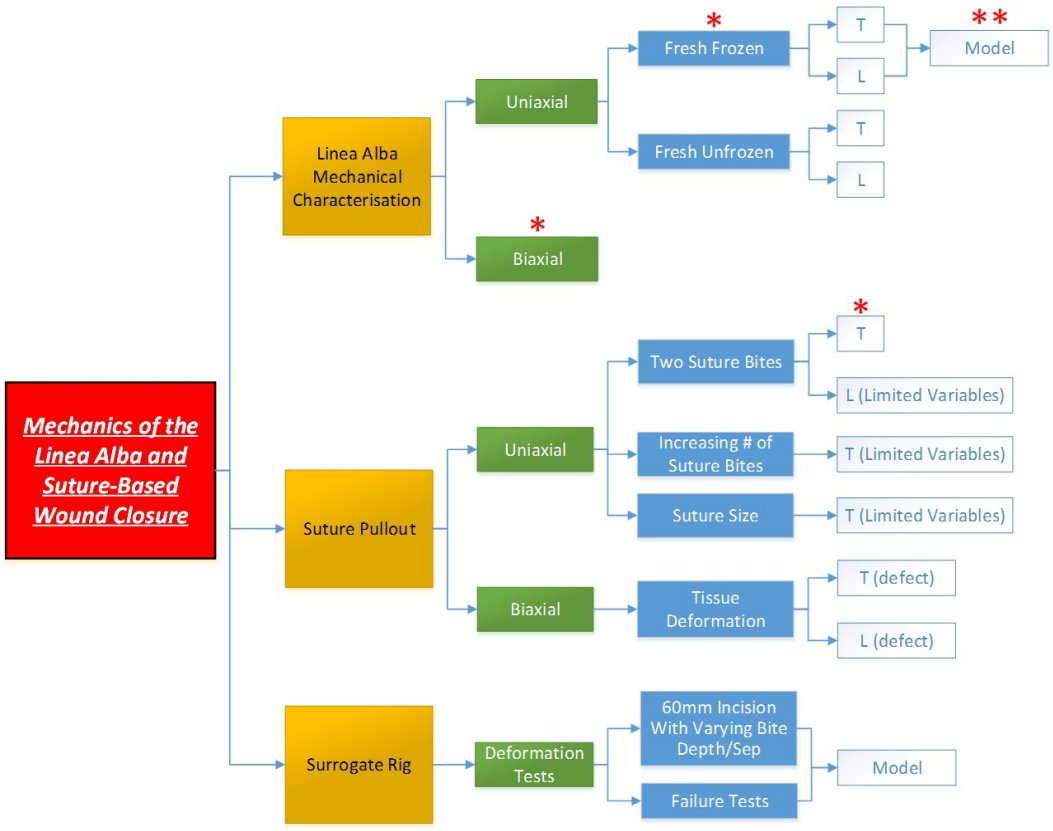

Figure 8.1: A process flow diagram of the experiments performed. [*] represents experiments performed on both human and porcine tissue and [**] represents a subset model utilising porcine mechanical data only; all other experiments involve just porcine tissue.

8.1 Linea Alba Mechanical Characterisation

An understanding of the structural properties of the linea alba was developed as a result of the contradictory results reported by existing publications [Förstemann et al. (2011), Gräβel et al. (2005)]. Uniaxial and biaxial tensile tests were performed on freshly frozen human ($\geq$60 years old) and porcine (26-28 weeks old) linea alba [Cooney et al. (2015)]. Custom Matlab codes were used to analyse the local displacement of selected specimen areas using image analysis and digital image correlation. The experimental results were presented in terms of Cauchy stress versus stretch ratio.

Porcine linea alba was shown to exhibit anisotropic behaviour, showing significantly greater stiffness (by a factor of $\approx$eight) in the transverse (fibre) direction compared the longitudinal (cross-fibre) direction (see Figure 5.11). Human linea alba was found to exhibit very similar anisotropic behaviour, showing the same relative difference between transverse and longitudinal directions (see Figure 5.12). While exhibiting a slightly greater stiffness in the transverse and longitudinal direction respectively, no statistical significance in the difference between the uniaxial porcine and human means (P = 0.23 & 0.57 > 0.05 for transverse and longitudinal directions respectively); see Figure 5.23). Similarly, there was no statistical significance (p = 0.32) found in the difference between their means in the transverse direction for biaxial tests. However, a significant difference was observed in the longitudinal direction (p = 0.011). This may be attributable to differences in physiology between the two species. Pigs have a greater number of ribs than humans which would result in differences in abdominal muscle attachment [Cooney et al. (2015)]. This may then correspond to aponeuroses that intersect at different angles at the linea alba. Further study of the respective tissue structures is needed to better understand this result. However, despite this, it appears that both human and porcine tissue exhibit similar mechanical behavior.

Although obtained using non image-based stretch measurement techniques, the human data presented by F*ö*rstemann et al. is close to that of the current study; lying within the standard deviation of the human and porcine data of the current study (see Figure 5.23 in Section 5.4.1.1) [Förstemann et al. (2011)]. However, a 75% increase in stiffness was observed in porcine tissue in Section 5.3.1.1 when switching to imaged-based stretch measurement. Since the Förstemann data was procured using non image-based stretch

measurement techniques, it would be expected that there would be a greater difference between it and the human data (image analysis derived stretch) of the current study. That there is little difference between averaged data of both studies may be down to the age/gender/health of the specimens before death.

Due to the limitations of the physical size of the linea alba, it was not possible to meet ASTM guideline dimensions for individual samples [ASTM (Standard E8/E8M)]. This resulted in a pre-stressing of the tissue through its initial bulging at the grips as it is clamped. As the grip-to-grip length was less than ideal it was possible that compression of the grips could have an effect on the stress at the centre of the sample. Computational modelling using FEBio was conducted to assess the effect that gripping had on the stress in the central element of the sample for a variety of grip-to-grip lengths. Figure 5.19 shows that, as grip-to-grip length increases stress at the central element of the model drastically decreases. Since the experimental grip-to-grip length varied between ≈10-30mm the actual stress at the centre of the sample should be between 1.62 and 1.25 times the observed experimental stress.

While the FEBio model was suitable for capturing the uniaxial behaviour of the tissue (see Figure 5.21), biaxial simulations did not provide a good match to the experimental data (see Figure 5.22). This is possibly due to the fact that the fibre reinforced model used describes a transversely isotropic material while the linea has a more complex, layered collagen architecture [Gräβel et al. (2005)] which may be causing it to behave differently under biaxial loading.

Since the publication of the uniaxial and biaxial data in Section 5, a recent study by Santamaria et al. on the biomechanics of porcine linea alba subjected to planar tension of transverse supraumbilical and infraumbilical samples has been performed that compares the uniaxial data of this study (see Figure 8.2) [Santamaría et al. (2015)]. Interestingly, the fitted stress/stretch curve of the supraumbilical samples of the current study was very close to that of the infraumbilical samples by Santamaria et al. Both experiments having a similar setup and test speed, it would be expected that the supraumbilical zone reported by Santamaria et al. would have a more similar stress/stretch response. That it is not is possibly as a result of differences in sample geometry. The maximum grip-to-grip to width ratio employed by Santamaria et al. was 1:1.6 and 1:4.9 for infraumbilical and supraumbilical samples respectively. However, a typical ratio of ≈2:1 was used for the supraumbilical uniaxial

samples of the current study (see Table 5.1 & 5.2 in Section 5.2.1). Since it was also reported that ratios of less than 4:1 may cause the sample to be pre-stressed to different degrees (see Figure 5.19 in Section 5.19), this difference in geometry between the two studies may be why disparate supraumbilical stress/stretch responses are observed [Cooney et al. (2015), Santamaría et al. (2015)].

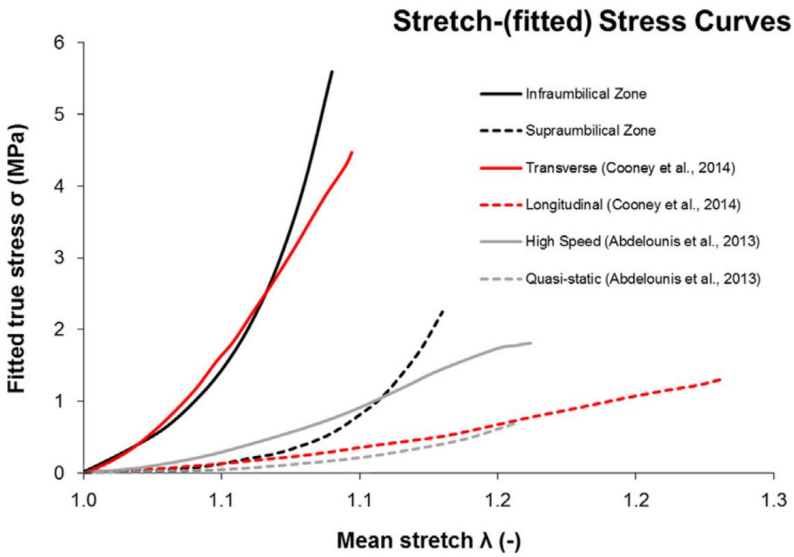

Figure 8.2: A comparison of the uniaxial data from Section 5 with data presented by Santamaria et al. [Santamaría et al. (2015)].

8.2 Suture Pullout

Due to some gaps in knowledge in the literature with reference to optimal suture bite depth and separation (see Section 3.4.2.2), a series of suture pullout experiments were performed to help develop a better suture-based wound closure methodology. A simple jig was designed to facilitate uniaxial suture pullout of the linea alba and identify the ideal bite separation/depth best able to resist pullout. Two loops of suture were passed through cut sections of porcine and human linea alba and a strain was applied to each sample until failure. The separation between bites and the depth to which they pierce the tissue was varied to allow for an assessment of a combination of the two variables rather than the single variable assessments that are typical in the literature [Campbell et al. (1989), Descoux et al. (1993)]. The normalised ratio plots (Figure 6.14 showing porcine data only and Figure 6.19 showing the porcine data and human data together) that compare the [10, 10] parameter typically used in surgery with all

other parameter combinations ([10,10] parameter combination being normalised to a value of 1 with all other combinations normalised relative to it) show that it's not as effective as it could potentially be, being closer in magnitude to the weakest parameters (with a bite depth of 4mm) than the strongest (with a bite depth of 16mm). Both the human and porcine data depict the same trends:

1. As bite depth is increased, pullout ratio linearly increases.

2. As bite separation is increased, pullout ratio decreases almost asymptotically.

3. A significant increase in pullout force/mm was observed when going from 5mm to 2.5mm bite separation (porcine data only; see Figure 6.13). Figure 6.10).

Both porcine and human data were found to be very similar with regards to suture pullout; a total of ≈5% average difference observed between the average pullout force and pullout ratio of both species (Figures 6.14 & 6.19). Though anatomical differences separate the two species (the extra ribs present in pigs culminating in a different location of oblique muscle attachment; see Section 5.4.1.1), the architecture of each tissue is not so diverse that the suture pullout characteristics deviate.

Resistance to suture pullout could be improved by as much as 120-290% (depending on a bite separation of between 5mm and 2.5mm) if the current standard of a bite depth and bite separation of 10mm was changed. Currently surgeons go by suture length to wound length ratio (SL:WL) which is essentially the length of one loop of suture over the bite separation (wound length in this case, see Figure 6.27). The most commonly suture length to wound length ratio is 4:1 [Bhat (2014), Israelsson & Jonsson (1993), Mulholland & Doherty (2006)] which translates to a bite depth and bite separation of 10mm each (see Figure 6.27). However, if the strongest combination of depth and separation as outlined in this study were used (16mm and 5mm respectively) then this would instead translate to a suture length to wound length ratio of 14:1, 3.5 times the current standard.

The pullout ratio plots (Figures 6.14 & 6.19) could potentially allow surgeons to tailor the wound closure technique to the patient. Linea alba geometry can differ considerably between patients. Therefore, should a maximum bite depth not be possible due to a linea alba of small

width, then the separation could be decreased to maintain an adequate level of resistance to pullout; the pullout ratio plots being used as a measure of suture pattern effectiveness.

An experiment on the the different orientation of suture application was also performed on porcine specimens to assess the effect on the pullout force from the tissue. Section 2.2.2 revealed that laparotomy incisions can be orientated differently depending on the purpose of the surgery. This experiment therefore explores the difference in the resistance to pullout that each orientation provides. Figure 6.8 depicts a statistically significant difference in the means of one parameter combination ([4,5]; $P = 0.046 < 0.05$); corroborating the theory that longitudinal samples as more resistant to pullout. However, using a [4,10] parameter combination resulted in no statistical significance being observed ($P = 0.424 > 0.05$); the variation in the data, and low sample size, making it difficult to determine significance. Therefore it is not clear which orientation performs better in terms of resistance to suture pullout. However, due to the limited thickness of the linea alba, transverse laparotomy incisions (with longitudinal suture application) would require the surgeon to manipulate/cut through both sheathes of the rectus muscle as well as the rectus muscle itself (as laparotomies are typically greater than 7cm [Cuschieri & Hanna (2013)]). As this can overcomplicate the surgery and increases risk to the patient, it may be advisable to avoid using transverse laparotomy incisions where possible. Nonetheless, it may prove advantageous to employ longitudinal suture placement in laparoscopic procedures as transverse incisions were found to result in an enlarged and warped defect in comparison to longitudinal incisions at the same level of stress under equibiaxial loading (see Figure 6.9).

Suture size was also investigated to assess if the increased surface area of a larger suture would correspond to an greater resistance to pullout. The data observed in both Figure 6.20 and Figure 6.21 show trends of increasing pullout force with greater suture size. However, the change in the means is not significant due to the variation being quite large ($P = 0.1263$, 0.4483 & $0.4574 > 0.05$ for bite separations of 5, 10 and 15mm respectively and $P = 0.4237$, 0.5878, 0.4484, 0.4103, $0.5483 > 0.05$ for bite depths of 4, 7, 10, 13 and 16mm respectively - see Figure 6.20 & Figure 6.21). Therefore, choice of suture size, at least for a PDS of 2-0, 0, and 1, can be considered a matter of personal preference rather than medical necessity; the limited diameter range engendering a lack of significance.

8.3 Surrogate Rig

While the uniaxial suture pullout data provides some novel conclusions, the lack of longitudinal loading/deformation makes the experiments differ from an in-vivo standpoint. In order evaluate the suture pullout experiment results deformation tests were performed on porcine linea alba (intact abdominal wall) with a suture-closed laparotomy incision using a surrogate abdominal rig, designed in-house in Trinity College Dublin [Lyons et al. (2015)] in order to compare the relative effect that changing the bite separation and bite depth of suture placement has on the apposition of the defect.

Predicting suture pullout in the surrogate rig using the pullout force data from Chapter 6 with Laplace's theorem for thin-walled cylinders did not adequately describe the observed pressure levels of pullout in the surrogate rig; underpredicting the surrogate pullout pressure for each case observed. One likely reason for this is that, although the model itself does account for change in length of the defect, the factor used to scale the uniaxial results (see Table 7.2) to the required defect length does not; after applying the factor the force is still representative of a 60mm defect length. The uniaxial tests experience only one axial deformation, not two as in the surrogate rig. Each uniaxial parameter force with a different bite separation would need to scaled further by a different amount in each case in order to properly relate uniaxial and multiaxial experiments. Furthermore, Laplace's theorem relies on the assumption of a homogeneous material structure. However, it has been well documented that the linea alba is significantly anisotropic [Cooney et al. (2015)]. Therefore, for Laplace's law to be more accurate, a material should exhibit equi-biaxial deformation under simple biaxial loading testing conditions as is performed in Chapter 5, rather the axial bias deformation (biaxial) that can be seen with a material such as the linea alba.

Although only one parameter ([15,4]) was observed to pullout within the physiological limits in the surrogate rig (see Figure 7.17), the ranges of pressure of pullout of both the [10,4] and [15,7] are within 10kPa. While it is not possible for the body to produce such extreme levels of IAP, an external force resulting from an impact (such as a fall for example) could bring the IAP beyond what is natural. Even in healthy individuals, there have been reports of bowel perforation as a result of a significant increase in IAP from seat-belt restriction in car accidents [Agrawal et al. (2007), Biswas et al. (2014)]. The [10,10] parameter combination

typically used by surgeons (presuming to have a pullout pressure of ≈40kPa in the rig if a similar offset from the uniaxial predictions is assumed, as seen in [15,4], [10,4] and [15,7], see Figure 7.18 and Table 7.4) appears to be sufficient for typical physiologically generated IAP, though it may not be enough to reduce risk of pullout/hernia as a result of external forces. It would therefore be prudent to use a parameter combination for laparotomy closure that maximises resistance to suture pullout, such as the [5,16] parameter combination.

Overall, it appears that the assumptions outlined in Section 7.2.3.4 significantly limit the model; the differences in deformation/load aplication between uniaxial and surrogate experiments being of particular concern. It may help if simple biaxial suture pullout tests were used rather than uniaxial tests. This may improve the relative percentage difference that is observed between uniaxial and surrogate tests currently. An accurate prediction of failure could prove very beneficial clinically as it could help a surgeon choose a bite depth and separation best suited to resist pullout for a specific lifestyle whereby it is known the patient is likely to experience elevated internal abdominal pressure due to external stimulus or their internal biology. Risk of damaging blood vessels (small bite separation) or muscle tissue (large bite depth) should be measured against the reward of improved resistance to pullout.

Observing the effect that bite depth and bite separation has on the inter-bite stretch for increasing levels of pressure in Figure 7.10 for porcine tissue, the combination with the least percentage difference in stretch from a "non-defect" case was found to be [5,16] with [15,4] showing the greatest (Table 7.4 and Figure 7.21). Both [5,4] and [15,16] appear to exhibit a relatively similar effect to percentage increase in stretch though there appears to be very little variation about the mean percentage change in stretch across different pressure levels for bite separations of 5mm while separations of 15mm yield an obvious trend increase in stretch as pressure is increased; becoming more significant as bite depth is decreased. However, it is the [5,16] parameter combination that effects wound apposition the least. However, though exhibiting the least percentage increase in stretch, [5,16] still results in almost a 100% increase compared with a no-defect case. Separation appears more important than depth with regards to wound apposition; resulting in a typically greater increase in stretch than changing bite depth would allow.

From this it is evident that bite separation as low as possible and a bite depth as high as

possible works best to maintain wound apposition and consequently promote better healing, with a ten-fold difference being observed between the extreme suture parameter combinations ([5,16] and [15,4]). This is in agreement with the suture pullout findings which also state that the [5,16] parameter combination is best suited towards maximum resistance against pullout.

Regarding the effect that bite depth and bite separation has on associated pressure for increasing levels of inter-bite stretch in Figure 7.12 & 7.13 for porcine tissue, several notable trends can be seen:

1. As bite depth is increased, pressure required to reach the specified stretch linearly increases.

2. As bite separation is increased, pressure required to reach the specified stretch decreases almost asymptotically.

3. Both bite separation and bite depth appear to have a roughly equivalent effect for the same change in (mm).

The pressure profiles provide similar conclusions as seen in the normalised porcine data in Chapter 6; maximum apposition, in this case, being achieved by using a bite depth as large as possible with a bite separation as low as possible. The parameter combinations [5,4] and [15,16] achieved a similar effect, both requiring almost the same amount of pressure to effect each level of stretch. In Figure 7.16, the ratio plots from both the suture pullout study (Chapter 6) and the surrogate deformation study (Chapter 7) depict a similar relationship between parameter combinations; the uniaxial data showing an improvement of $\approx$120% when switching to a [5,16] combination. This implies that, despite the tissue being subjected to load in a singular direction and despite scaling the data to account larger wound length, the uniaxial results are applicable and relevant.

The relative plots (Figure 7.14 and Figure 7.15) that compare the [10, 10] parameter typically used in surgery with the rest of the data show that it's not as effective as it could potentially be. The results show that inter-bite stretch could be reduced by as much as $\approx$30-40% (depending on the applied pressure) with the pressure required to achieve an inter-bite stretch of 1.1-1.2λ increasing by as much as $\approx$50-110% by using a bite depth of 16mm and a bite separation of 5mm.

It must be noted that fatigue of the suture and/or tissue was not assessed in this study nor in Chapter 6. Repeated loading of the suture may cause it to weaken. This would be further exacerbated by the suture degrading over time due to its exposure to bodily fluids. This could be a focus of future work; possibly utilising a bioreactor to determine a sutures effective strength over the course of its lifespan. However, reducing the bite separation and thereby increasing the number of bites would reduce load applied to each loop of suture which would in turn likely reduce fatigue of the suture.

8.4 Porcine Tissue as a Surrogate

Porcine tissue was observed to exhibit very close behaviour to that of human tissue in all three studies gathered in this thesis. From this it can be assured that device development and testing and the further development of wound closure methodologies on the linea alba using the surrogate rig (similar to that of which can be seen in [Lyons et al. (2015)]) can be performed using porcine tissue as a surrogate while maintaining accurate results.

However, it must be noted that all tissue obtained in these studies is freshly frozen. Though tests have shown that freezing the linea alba does not significantly effect its mechanical properties (see Figure 5.14), frozen muscle tissue has been shown to exhibit different mechanical properties to that of fresh muscle [Gottsauner-Wolf et al. (1995)]. Since the abdominal walls harvested for the surrogate abdominal rig tests were frozen and each contain an array of abdominal muscles, this may cause different behaviour to that of in-vivo abdominal tissue, despite that there is little direct physical connection between the abdominal muscles and the linea alba of the bellies used in this study (bellies having been cut to size). Therefore it may be necessary to perform fresh tissue testing in the surrogate rig, preferably no more than an hour after (since changes in the mechanical properties of muscles are time-dependent after death [Van Loocke (2007)]) death in order to further evaluate the rig. However, since preparation of the tissue before experimentation in the surrogate rig can take more than one hour, it may be prudent to use a more simplified experiment than that of the deformation tests performed in Chapter 7 to use for evaluation.

Chapter 9

Conclusions

The work of this thesis has provided new insights into the mechanics of the linea alba and suture-based wound closure. There existed a knowledge gap for the mechanical properties of the linea alba, particularly with relevance to the methods used to procure the stress-stretch data. Using image analysis and DIC techniques as well as modelling assumptions, new data on the structural properties of the linea alba was obtained for both human and porcine tissue, improving on the existing limited data in the literature by increasing the accuracy of measurement significantly. Significant anisotropy was observed in the tissue with deformation heavily biased towards deformation in the longitudinal direction under equal application of load. Equating the pressure induced on the abdominal wall to wall stress of the linea alba tissue showed that the linea alba is theoretically capable of withstanding the stress produced by raised IAP. Modelling showed that gripping affects the mechanical properties of the tissue. Accounting for this shortfall by scaling the results provided a theoretically true value for stress and strain within the tissue. Strong similarities were also observed between the mechanical properties of both human and porcine linea alba, leading to the conclusion that it may be possible to use porcine tissue as a surrogate for surgical device testing and development (a subject of future research).

Observing different layouts of suture placement, used in wound closure of the abdomen, in terms of varying the bite depth and separation of the suture and the effect of the orientation of placement was shown to affect the resistance to pullout for human and porcine tissue. Sutures applied in the longitudinal direction were found to be able to greater resist pullout than

sutures applied transversely. Applying a suture in the transverse direction on a laparoscopic defect can also result in significantly more deformation and widening of said defect than longitudinal sutures which may have an impact on the incidence of laparoscopic incisional hernia. Maximising the bite depth and minimising the bite separation (no lower than 5mm) as much as possible is recommended to significantly improve resistance to pullout; true for both humans and swine. There was no statistical evidence that suture size impacts resistance to pullout, though the average pullout force was seen to increase for bigger sutures. Judging from the data of this study, patients could benefit from laparoscopic wounds closed with larger bite depths and smaller bite separations and may even benefit from making a lateral incision with the longitudinal application sutures, especially for laparoscopic surgery.

A surrogate rig previously designed in Trinity College Dublin was used to ascertain the effect of depth/bite separation parameters have on wound apposition. Overall it was found that a bite separation as small as possible and a bite depth as large as possible works best to retain wound apposition and promote better healing and less scarring of the tissue. Bite separations as low as 5mm were found to exhibit little difference in the percentage change of stretch at all levels of pressure when compared against a separation of 10mm which is typically used in laparotomy surgery whereas separations of 15mm result in a trend increase. The results, comparing favorably with those obtained in Chapter 6, show that uniaxial studies on suture pullout of the linea alba can be relied upon despite the lack of longitudinal loading/deformation. A model produced with the intention of it being able to predict suture pullout in the surrogate rig beyond what was capable in the rig itself was unfortunately found to offset the experimental results by 8-13kPa possibly as a result of a combination of different material structure assumptions and differences in load application. However, future tests involving biaxial suture pullout experiments may provide a better basis for prediction. Human tissue was found to have a similar theoretical rig pressure/hoop stress profile as that of porcine but a different distribution of theoretical pullout. To the authors knowledge, there is no evidence of examples of suture-based surrogate research in the literature.

Providing a more detailed understanding of the behaviour of the linea alba under load as well as the effectual significance of different suturing methods in an in-vivo type environment, this project gives a basis upon which further research can be done to help reduce the likelihood

of the formation of incisional hernia. Furthermore, the use of porcine linea alba tissue in liu of human (which can be difficult to obtain) for biomechanical investigations can be a much more feasible option, making it possible to significantly increase sample size without losing relevance to humans while decreasing the monetary and temporal cost of the study.

9.1 Clinical Recommendations

From the work gathered in this thesis, two clinical recommendations were developed:

1. Maximise the bite depth and minimise the bite separation of the suture for laparotomy wound closure. A bite depth of 16mm and bite separation of 5mm is advised depending on the patients physiology.

2. Transverse incisions using a longitudinal application of sutures are recommended for laparoscopic surgery.

Consulting the clinical source for this project (surgeon and co-supervisor Des Winter) about the impact of these recommendations yielded some positive information. The cost in extra suture used for suture patterns with greater bite depth and smaller bite separations is not an issue as a sing suture is all that is required for any parameter combination. Since sutures are never reused and excess lengths of suture are dumped, the cost remains the same as would be for the commonly used [10,10] parameter combination. Furthermore, the time cost required to apply extra bites of suture remains a fraction of the amount of time the surgery as a whole takes and poses no added risk to the patient.

When asked if the recommended parameter combination of [5,16] is something that surgeons would be happy to implement immediately, the response was positive. Clinical trials would be impractical and very costly and changing the suturing parameter combinations was not considered to increase any further risk to the patient. The introduction of more bites of suture was said would not negatively effect wound healing as the damage theat the suture needle inflicts is negligible compared to a large laparotomy incision. Also, the linea alba having a sparse vasculature means that blood vessels can be easily avoided or manipulated out of the way of the suture.

Asked if warped defects had been observed during laparoscopic closure of longitudinal incisions (see Figure 6.9 A), such instances had not been noticed. However, as the abdominal space is not pressurised during wound closure, it would not be possible to view this effect during closure. ERAS[1] guidelines typically recommend a transverse incision over a longitudinal one, though research into the effectiveness of its use is still ongoing [Khan et al. (2009)]. Though it was mentioned that longitudinal midline incisions were typically preferred for laparotomies, it was agreed that the observed warping of longitudinal laparoscopic incisions help corroborate the benefit of choosing a transverse incision with longitudinally applied sutures for laparoscopic surgery. Again it was confirmed as change that surgeons would be happy to implement immediately.

[1] Enhanced Recovery After Surgery

Chapter 10

Further Work

Significant further research can follow the work of this project in a number of different ways. The surrogate abdominal rig is a valuable testing resource that has already shown promise in this project as well as others [Lyons et al. (2015)]. However, due to the use of frozen tissue in all studies performed with it so far, there is potential for further evaluation of the rig using fresh tissue; experiments taking place no more than two hours after specimen death. If it can be shown that the use of frozen tissue in the rig provides similar results to that of fresh, then it could be argued that the surrogate rig could negate the use of biomechanical human/animal trials, potentially saving the medical research community a vast amount of time and money.

There are two other methods that could be used to achieve this evaluation. One method may be to use MRI and sophisticated image analysis techniques. Physiological markers would have to be used to measure stretch (blood vessels rectus sheath/linea alba boundary) as the IAP is ramped up artificially. This would be very similar to the studies performed by Song et al. which use surface skin markers rather than internal markers (see Section 3.4.2.1). For a simplified alternative method, fresh and frozen abdominal wall tissue could be used in the rig with the skin and fat intact. Then, generating stretch data through image analysis of skin markers as pressure increases, this data could be compared to the data presented by Song et al. and evaluated accordingly [Song et al. (2006*a*,*b*)].

To further improve repeatable testing, it may also be prudent to develop a synthetic material that accurately mimics the behaviour of the porcine/human abdominal wall. This may require a composite of material types to represent the different muscles and acellular

tissues that are present. The material could be validated in the surrogate rig by ensuring that the relationship between pressure and inter-bite separation of the sutured defect is maintained.

The pullout prediction model outlined in Chapter 7 should also be improved by supplementing it with biaxial suture pullout data. The biaxial rig described in Chapter 5 may need to be modified to be able to contain a larger sample (including rectus muscle and rectus sheath with the linea alba) and be able to withstand the significantly greater pullout forces that are presented in Chapter 6, depending on if a 60mm defect or a scaled down version of it are used. A full 60mm defect sample should eventually be used to evaluate the assumption that a scaled down biaxial sample applies.

Size of the suture needle as well as the use of blunt or sharp needle tips may also have an impact on the pullout characteristics of the linea alba and would be an interesting topic of further study. However, it may be difficult to obtain different types of needle for the same suture type. To overcome this the different needles should be removed from there respective suture threads and used to pierce individual samples. since the suture thread is always thinner than the thickest part of the needle, it would be then possible to pass the thread through the needle defect in each case (though requiring some dexterity, it is possible to do so).

Fatigue of the suture and/or tissue was not assessed in Chapter 7 nor in Chapter 6. Repeated loading of the suture may cause it to weaken. This would be further exacerbated by the suture degrading over time due to its exposure to bodily fluids. This could be a focus of future work; possibly utilising a bioreactor to determine a sutures effective strength over the course of its lifespan.

Finally, it may be of interest to perform an SEM/histological study of the linea alba under different applications of stretch in different orientations and/or a case where there is a biaxial application of stretch. Takaza et al. performed such tests in assessing the microstructural response of muscle to applied deformation [Takaza et al. (2014)]. An investigation into the structural response of linea alba unde (how the collagen fibre bundles reorientate) would be an interesting topic of future research.

Chapter 11

Appendix

Table 11.1: Comparative analysis of DIC and Image Analysis methods.

Tracking Method	**Stretch Measurments From Separate Regions**						
Image Analysis	**Reported**	1.615	1.5718	1.4558	1.5274		
	Actual	1.6153	1.5625	1.4545	1.4893	**Average**	**Stdev**
	% Diff	-0.01857	0.5952	0.0893	2.5582	0.8060	1.1983
	Reported	1.2753	1.2298	1.2591	1.2778		
D.I.C	**Actual**	1.256	1.2307	1.2500	1.2705	**Average**	**Stdev**
	% Diff	1.5366	-0.0731	0.7280	0.5745	0.6915	0.6617

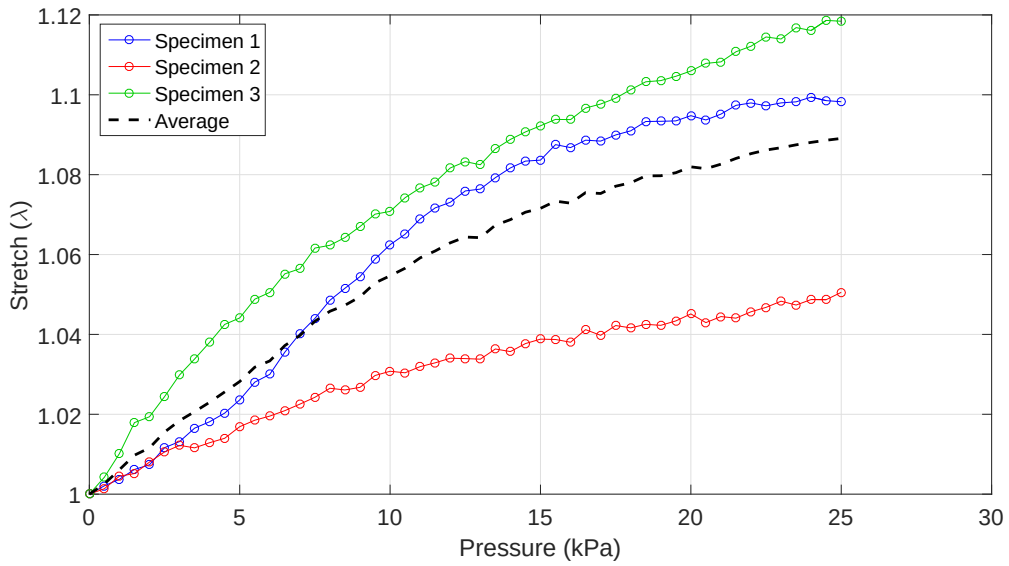

Figure 11.1: A plot of stretch versus applied pressure where no belly defect is present.

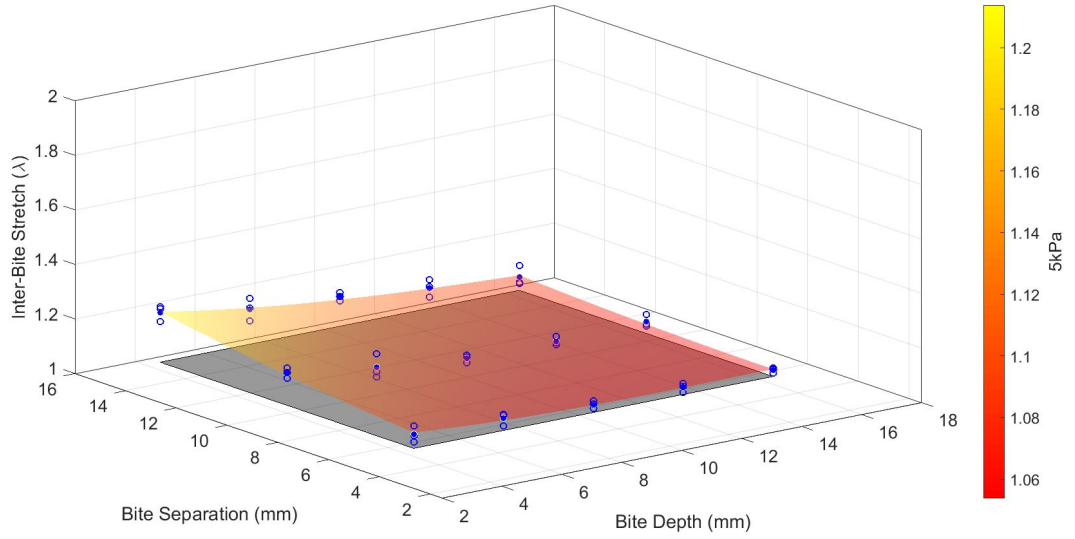

Figure 11.2: Stretch versus bite separation and bite depth for an applied pressure of 5kPa.

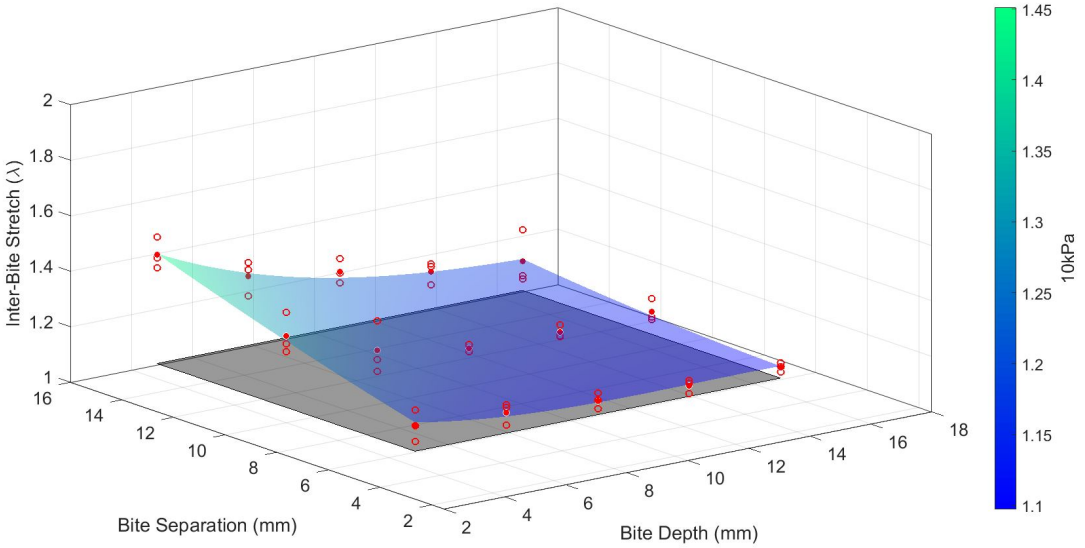

Figure 11.3: Stretch versus bite separation and bite depth for an applied pressure of 10kPa.

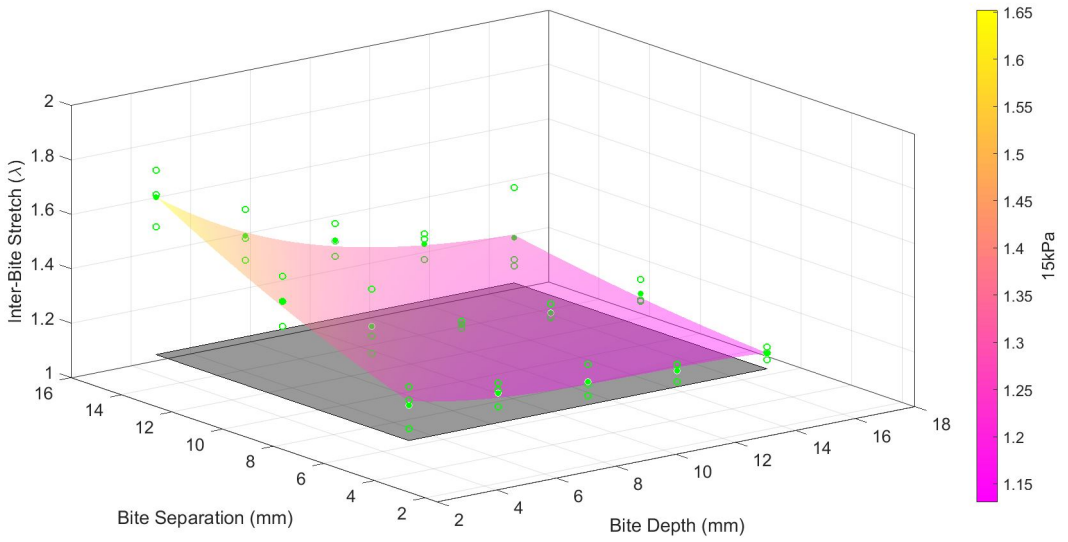

Figure 11.4: Stretch versus bite separation and bite depth for an applied pressure of 15kPa.

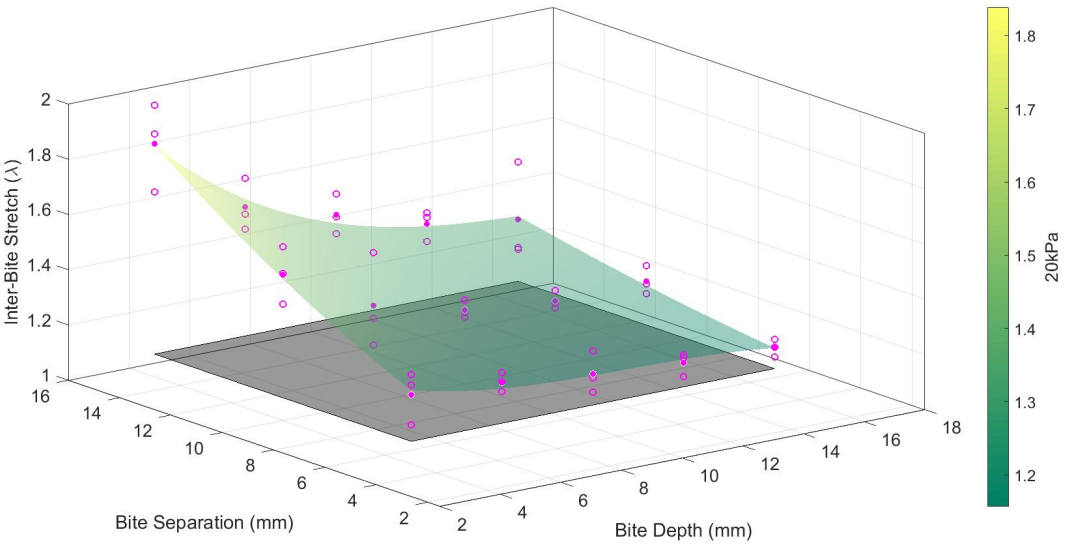

Figure 11.5: Stretch versus bite separation and bite depth for an applied pressure of 20kPa.

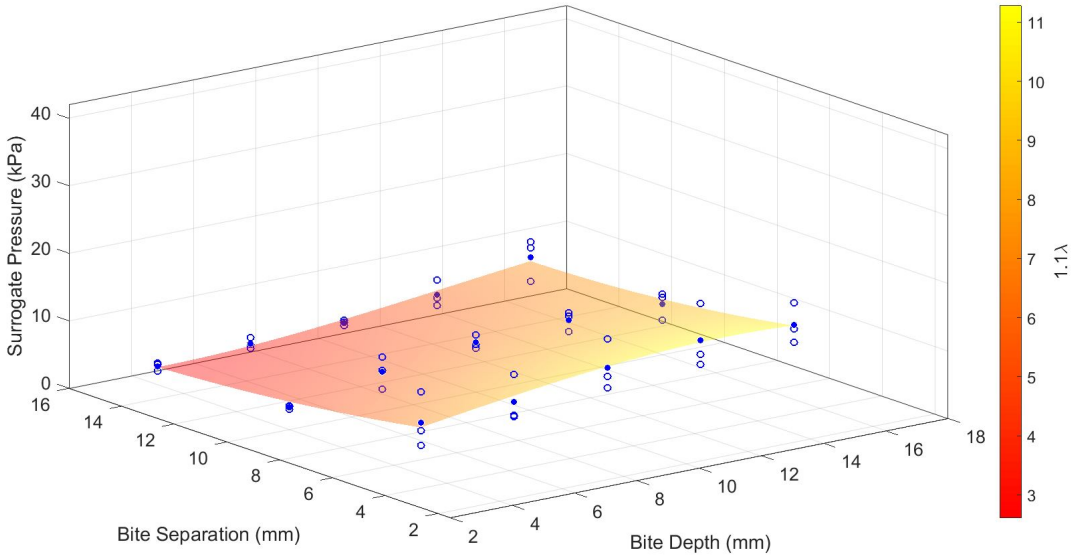

Figure 11.6: Applied pressure versus bite separation and bite depth for a stretch of 1.1λ.

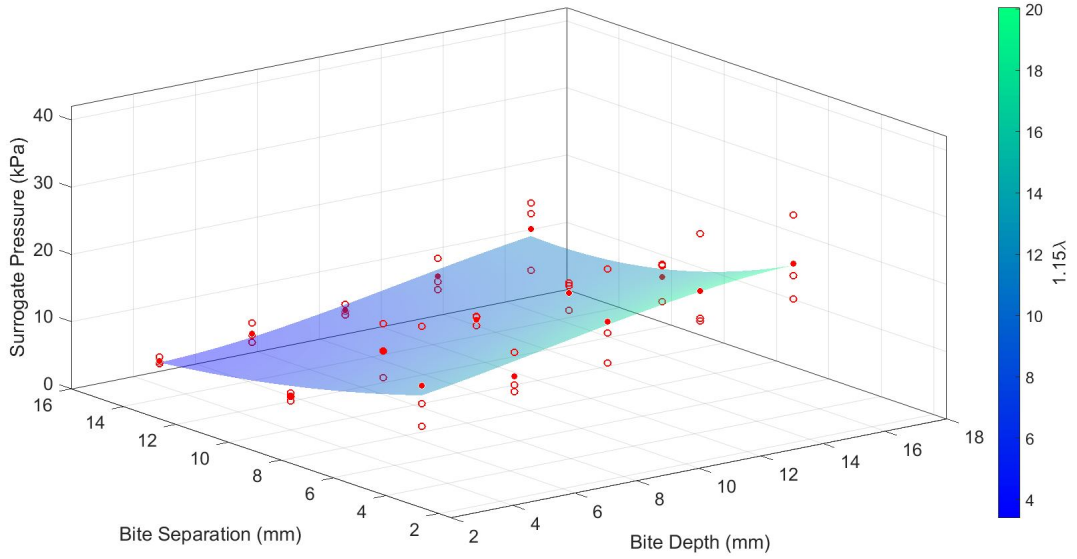

Figure 11.7: Applied pressure versus bite separation and bite depth for a stretch of 1.15λ.

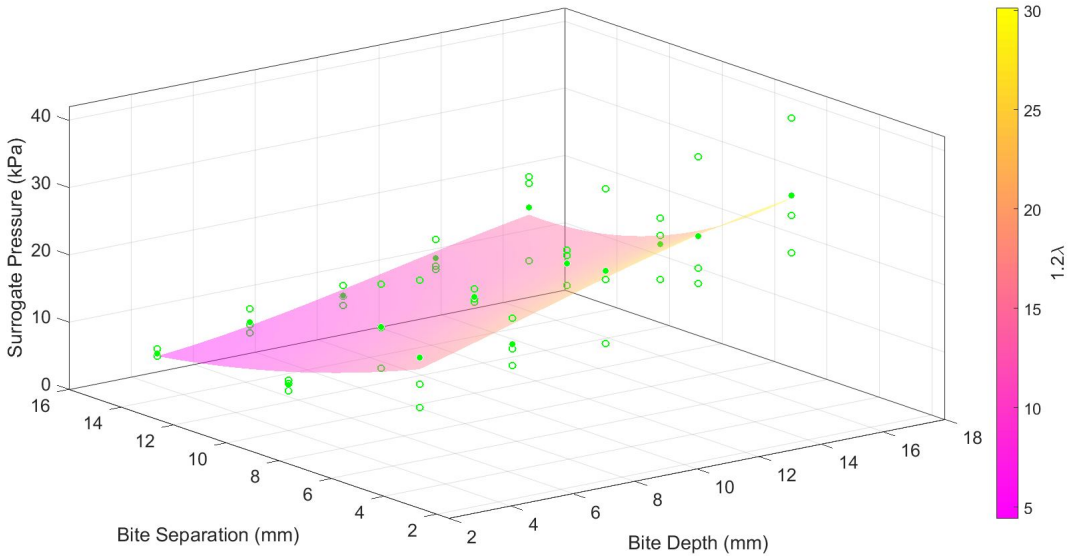

Figure 11.8: Applied pressure versus bite separation and bite depth for a stretch of 1.2λ.

Bibliography

ABRA - Abdominal | Dynamic Tissue Systems (n.d.).
URL: *http://dynamictissuesystems.com/products/abra-abdominal/*

Addington, W. R., Stephens, R. E., Phelipa, M. M., Widdicombe, J. G. & Ockey, R. R. (2008), 'Intra-abdominal pressures during voluntary and reflex cough', *Cough* **4**(2), 1–9.

Agrawal, V., Doelken, P. & Sahn, S. A. (2007), 'Seat belt-induced chylothorax: a cause of idiopathic chylothorax?', *CHEST Journal* **132**(2), 690–692.

Akin, M., Karakaya, M., Batkin, A. & Nogay, A. (1997), 'Prevalence of inguinal hernia in otherwise healthy males of 20 to 22 years of age', *Journal of the Royal Army Medical Corps* **143**(2), 101–102.

Antranik (2016), 'Graphical depiction of the abdominal anatomy in humans'.
URL: *http://antranik.org/muscles-of-the-abdominal-wall/*

ASTM (Standard E8/E8M) (2009), 'Standard test methods for tension testing of metallic materials', *Standard* (DOI: 10.1520/D5528-01R07E03. http://www.astm.org).

Axer, H., Keyserlingk, D. G. v. & Prescher, A. (2001*a*), 'Collagen fibers in linea alba and rectus sheaths: I. general scheme and morphological aspects', *Journal of Surgical Research* **96**(1), 127–134.

Axer, H., Keyserlingk, D. G. v. & Prescher, A. (2001*b*), 'Collagen fibers in linea alba and rectus sheaths: Ii. variability and biomechanical aspects', *Journal of Surgical Research* **96**(2), 239–245.

Beer, G. M., Schuster, A., Seifert, B., Manestar, M., Mihic-Probst, D. & Weber, S. A. (2009), 'The normal width of the linea alba in nulliparous women', *Clinical anatomy* **22**(6), 706–711.

Beldi, G., Wagner, M., Bruegger, L. E., Kurmann, A. & Candinas, D. (2011), 'Mesh shrinkage and pain in laparoscopic ventral hernia repair: a randomized clinical trial comparing suture versus tack mesh fixation', *Surgical endoscopy* **25**(3), 749–755.

Bell, R. M., Dayton, M. T. et al. (2012), *Essentials of general surgery*, Wolters Kluwer Health.

Ben Abdelounis, H., Nicolle, S., Otténio, M., Beillas, P. & Mitton, D. (2012), 'Effect of two loading rates on the elasticity of the human anterior rectus sheath', *Journal of the mechanical behavior of biomedical materials* .

Bendavid, R. (2001), *Abdominal wall hernias: principles and management*, Springer.

Bendavid, R. (2004), 'The unified theory of hernia formation', *Hernia* **8**(3), 171–176.

Berggren, J., Borwein, J. & Borwein, P. (2004), *Pi: A Source Book*, Springer.
URL: *http://books.google.ie/books?id=QlbzjN_5pDoC*

Bhat, S. M. (2014), *SRB's Surgical Operations: Text & Atlas*, Jaypee Brothers Medical Publishers (P) Ltd.

Biswas, S., Adileh, M., Almogy, G. & Bala, M. (2014), 'Abdominal injury patterns in patients with seatbelt signs requiring laparotomy', *Journal of emergencies, trauma, and shock* **7**(4), 295.

Bitterman, N. (2006), 'Technologies and solutions for data display in the operating room', *Journal of clinical monitoring and computing* **20**(3), 165–173.

Boess-Lott, R. & Stecik, S. (1999), *The Ophthalmic Surgical Assistant*, Basic bookshelf for eyecare professionals, SLACK.
URL: *https://books.google.ie/books?id=6e9bLlpph0QC*

Boldo, E., de Lucia, G. P., Aracil, J., Martin, F., Escrig, J., Martinez, D., Miralles, J. & Armelles, A. (2007), 'Trocar site hernia after laparoscopic ventral hernia repair', *Surgical endoscopy* **21**(5), 798–800.

Bourgeois, F. J., Gehrig, P. A. & Veljovich, D. S. (2005), *Obstetrics and gynecology recall*, Lippincott Williams & Wilkins.

Bowrey, D., Blom, D., Crookes, P., Bremner, C., Johansson, J., Lord, R., Hagen, J., DeMeester, S., DeMeester, T. & Peters, J. (2001), 'Risk factors and the prevalence of trocar site herniation after laparoscopic fundoplication', *Surgical endoscopy* **15**(7), 663–666.

Brandt, M. L. (2008), 'Pediatric hernias', *Surgical Clinics of North America* **88**(1), 27–43.

Brown, S., Goodfellow, P., Adam, I. & Shorthouse, A. (2004), 'A randomised controlled trial of transverse skin crease vs. vertical midline incision for right hemicolectomy', *Techniques in coloproctology* **8**(1), 15–18.

Bucknall, T., Cox, P. & Ellis, H. (1982), 'Burst abdomen and incisional hernia: a prospective study of 1129 major laparotomies.', *British medical journal (Clinical research ed.)* **284**(6320), 931.

Campbell, E. & Green, J. (1953), 'The variations in intra-abdominal pressure and the activity of the abdominal muscles during breathing; a study in man', *The Journal of Physiology* **122**(2), 282–290.

Campbell, J. A., Temple, W. J., Frank, C. B. & Huchcroft, S. A. (1989), 'A biomechanical study of suture pullout in linea alba', *Surgery* **106**(5), 888–92.

Cassar, K. & Munro, A. (2002), 'Surgical treatment of incisional hernia', *British journal of surgery* **89**(5), 534–545.

Chand, M., On, J., Bevan, K., Mostafid, H. & Venkatsubramaniam, A. (2012), 'Mesh erosion following laparoscopic incisional hernia repair', *Hernia* **16**(2), 223–226.

Chung, K. (2015), *Essentials of Hand Surgery*, JP Medical Limited.
URL: *https://books.google.ie/books?id=C5dHCgAAQBAJ*

Cinel, A., Piskin, B., Calik, A. & Kucuktulu, U. (1997), 'A method for the closing up of abdominal trocar wound', *Minimally Invasive Therapy & Allied Technologies* **6**(2), 139–141.

Cobb, W. S., Burns, J. M., Kercher, K. W., Matthews, B. D., James Norton, H. & Todd Heniford, B. (2005), 'Normal intraabdominal pressure in healthy adults', *Journal of Surgical Research* **129**(2), 231–235.

Cochran, P. (2010), *Laboratory Manual for Comparative Veterinary Anatomy & Physiology*, Nelson Education.

Cömert, A., Kökat, A. M., Akkocaoğlu, M., Tekdemir, İ., Akça, K. & Çehreli, M. C. (2009), 'Fresh-frozen vs. embalmed bone: is it possible to use formalin-fixed human bone for biomechanical experiments on implants?', *Clinical oral implants research* **20**(5), 521–525.

Cooney, G. M., Moerman, K. M., Takaza, M., Winter, D. C. & Simms, C. K. (2015), 'Uniaxial and biaxial mechanical properties of porcine linea alba', *Journal of the Mechanical Behavior of Biomedical Materials* **41**, 68–82.

Cooper, A. (1807), *The anatomy and surgical treatment of inguinal and congenital hernia [Part I]*, T. Cox... and sold.

Cuschieri, A. & Hanna, G. (2013), *Essential surgical practice: higher surgical training in general surgery*, CRC Press.

Damjanov, I. (2013), *Pathology for the health professions*, Elsevier Health Sciences.

Defense, U. (n.d.), *Surgical Methods*, Jeffrey Frank Jones.
URL: *https://books.google.ie/books?id=1TUjKrLCN3wC*

Demetriades, D., Inaba, K. & Velmahos, G. (2015), *Atlas of Surgical Techniques in Trauma*, Cambridge University Press.

Descoux, J. G., Temple, W. J., Huchcroft, S. A., Frank, C. B. & Shrive, N. G. (1993), 'Linea alba closure: determination of ideal distance between sutures', *Investigative Surgery* **6**(2), 201–209.

Di Zerega, G. S. & DeCherney, A. H. (2000), *Peritoneal surgery*, Springer.

Dorland, W. A. N. (1980), *Dorland's Medical dictionary*, Saunders Press.

Drake, R., Vogl, A. W. & Mitchell, A. W. (2009), *Gray's anatomy for students*, Elsevier Health Sciences.

Duez, A., Cotte, E., Glehen, O., Cotton, F. & Bakrin, N. (2009), 'Appraisal of peritoneal cavityŠs capacity in order to assess the pharmacology of liquid chemotherapy solution in hyperthermic intraperitoneal chemotherapy', *Surgical and radiologic anatomy* **31**(8), 573–578.

Eberl, C., Thompson, R., Gianola, D., Sharpe Jr, W. & Hemker, K. (2006), 'Digital image correlation and tracking', *MatLabCentral, Mathworks file exchange server, FileID* **12413**.

Fang, F., Sawhney, A. S. & Lake, S. P. (2014), 'Different regions of bovine deep digital flexor tendon exhibit distinct elastic, but not viscous, mechanical properties under both compression and shear loading', *Journal of biomechanics* **47**(12), 2869–2877.

Ferrone, R., Scarone, P. C. & Natalini, G. (2003), 'Late complication of open inguinal hernia repair: small bowel obstruction caused by intraperitoneal mesh migration', *Hernia* **7**(3), 161–162.

Fink, C., Baumann, P., Wente, M., Knebel, P., Bruckner, T., Ulrich, A., Werner, J., Büchler, M. & Diener, M. (2014), 'Incisional hernia rate 3 years after midline laparotomy', *British Journal of Surgery* **101**(2), 51–54.

Flegal, K. M., Carroll, M. D., Ogden, C. L. & Johnson, C. L. (2002), 'Prevalence and trends in obesity among us adults, 1999-2000', *Jama* **288**(14), 1723–1727.

Förstemann, T., Trzewik, J., Holste, J., Batke, B., Konerding, M., Wolloscheck, T. & Hartung, C. (2011), 'Forces and deformations of the abdominal wall - a mechanical and geometrical approach to the linea alba', *Journal of biomechanics* **44**(4), 600–606.

Frezza, E. E., Shebani, K. O., Robertson, J. & Wachtel, M. S. (2007), 'Morbid obesity causes chronic increase of intraabdominal pressure', *Digestive diseases and sciences* **52**(4), 1038–1041.

Fritsch, H. & Kühnel, W. (2008), *Color atlas of human anatomy: in 3 volumes. Internal organs. Vol. 2*, Vol. 2, Thieme.

Fuller, J., Scott, W., Ashar, B. & Corrado, J. (2003), 'Laparoscopic trocar injuries: a report from a us food and drug administration (fda) center for devices and radiological health (cdrh) systematic technology assessment of medical products (stamp) committee', *FADAUS Department of Health and Human Services, Editor* .

Ghavamian, R. (2010), *Complications of laparoscopic and robotic urologic surgery*, Springer.

Goswami, I. (2012), *Civil Engineering All-In-One PE Exam Guide: Breadth and Depth 2/E*, McGraw Hill Professional.

Gottsauner-Wolf, F., Grabowski, J. J., Chao, E. & An, K.-N. (1995), 'Effects of freeze/thaw conditioning on the tensile properties and failure mode of bone-muscle-bone units: A biomechanical and histological study in dogs', *Journal of orthopaedic research* **13**(1), 90–95.

Gould, J. C. & Philip, A. (2011), '22 principles and techniques of abdominal access and physiology of pneumoperitoneum', *Scientific American Surgery* .

Gräβel, D., Prescher, A., Fitzek, S., Keyserlingk, D. G. v. & Axer, H. (2005), 'Anisotropy of human linea alba: a biomechanical study', *Journal of Surgical Research* **124**(1), 118–125.

Grantcharov, T. P. & Rosenberg, J. (2001), 'Vertical compared with transverse incisions in abdominal surgery', *The European journal of surgery* **167**(4), 260–267.

Greenall, M., Evans, M. & Pollock, A. (1980), 'Midline or transverse laparotomy? a random controlled clinical trial. part i: Influence on healing', *British Journal of Surgery* **67**(3), 188–190.

Hegarty, N. (2007), 'Minimally invasive urologic surgery', *BJU International* **99**(6), 1546–1546.

Helgstrand, F., Rosenberg, J. & Bisgaard, T. (2011), 'Trocar site hernia after laparoscopic surgery: a qualitative systematic review', *Hernia* **15**(2), 113–121.

Hendrickson, D. (2004), *Wound Care Management for the Equine Practitioner*, Equine Made Easy Series, Teton NewMedia, Incorporated.
URL: *http://books.google.ie/books?id=FQnpUXB_7-kC*

Hendrickson, D. (2013), *Techniques in Large Animal Surgery*, Wiley.
URL: *http://books.google.ie/books?id=J4hp2713DJAC*

Heniford, B. T., Park, A., Ramshaw, B. J. & Voeller, G. (2000), 'Laparoscopic ventral and incisional hernia repair in 407 patients', *Journal of the American College of Surgeons* **190**(6), 645–650.

Hides, J., Wilson, S., Stanton, W., McMahon, S., Keto, H., McMahon, K., Bryant, M. & Richardson, C. (2006), 'An mri investigation into the function of the transversus abdominis muscle during Şdrawing-inŤ of the abdominal wall', *Spine* **31**(6), E175–E178.

Hollinsky, C. & Göbl, S. (1999), 'Bursting strength evaluation after different types of mesh fixation in laparoscopic herniorrhaphy', *Surgical endoscopy* **13**(10), 958–961.

Hollinsky, C. & Sandberg, S. (2007), 'Measurement of the tensile strength of the ventral abdominal wall in comparison with scar tissue', *Clinical Biomechanics* **22**(1), 88–92.

Imme, A. & Cardi, F. (2005), '[incisional hernia at the trocar site in laparoscopic surgery].', *Chirurgia italiana* **58**(5), 605–609.

Israelsson, L. & Jonsson, T. (1993), 'Suture length to wound length ratio and healing of midline laparotomy incisions', *British journal of surgery* **80**(10), 1284–1286.

Jenkins, E. D., Yom, V., Melman, L., Brunt, L. M., Eagon, J. C., Frisella, M. M. & Matthews, B. D. (2010), 'Prospective evaluation of adhesion characteristics to intraperitoneal mesh and adhesiolysis-related complications during laparoscopic re-exploration after prior ventral hernia repair', *Surgical endoscopy* **24**(12), 3002–3007.

Johnson, Z. & Nugent, R. (2003), 'Heritability of body length and measures of body density and their relationship to backfat thickness and loin muscle area in swine', *Journal of animal science* **81**(8), 1943–1949.

Kadar, N., Reich, H., Liu, C., Manko, G. F. & Gimpelson, R. (1993), 'Incisional hernias after major laparoscopic gynecologic procedures', *American journal of obstetrics and gynecology* **168**(5), 1493–1495.

Katkhouda, N. (2010), *Advanced laparoscopic surgery: techniques and tips*, Springer.

Kehoe, S. (2011), *Gynaecological Cancers: Biology and Therapeutics*, RCOG.

Khan, S., Gatt, M., Horgan, A., Anderson, I. & MacFie, J. (2009), 'Guidelines for Implementation of Enhanced Recovery Protocols'.
URL: *http://www.asgbi.org.uk/download.cfm?docid=BE0B52EE-AE0E-42C1-A10EDDE7BABDC57A*

Kingsnorth, A. & LeBlanc, K. A. (2013), *Management of abdominal hernias*, Springer Science & Business Media.

Kirilova, M., Stoytchev, S., Pashkouleva, D. & Kavardzhikov, V. (2011), 'Experimental study of the mechanical properties of human abdominal fascia', *Medical engineering & physics* **33**(1), 1–6.

Klinge, U., Müller, M., Brücker, C. & Schumpelick, V. (1998), 'Application of three-dimensional stereography to assess abdominal wall mobility', *Hernia* **2**(1), 11–14.

Knisley, M. (2013), 'Anterior abdominal wall and inguinal canal'.
URL: *http://www.studyblue.com/notes/note/n/lab-13-anterior-abdominal-wall-and-inguinal-canal/deck/7606159*

Kureshi, A., Vaiude, P., Nazhat, S. N., Petrie, A. & Brown, R. A. (2008), 'Matrix mechanical properties of transversalis fascia in inguinal herniation as a model for tissue expansion', *Journal of biomechanics* **41**(16), 3462–3468.

Lake, S. P. (n.d.), 'Musculoskeletal Group Resources'. Accessed: 2015-11-02.
URL: *http://lake.seas.wustl.edu/resources/*

Lally, C., Reid, A. & Prendergast, P. (2004), 'Elastic behavior of porcine coronary artery tissue under uniaxial and equibiaxial tension', *Annals of Biomedical Engineering* **32**(10), 1355–1364.

Lambert, D. M., Marceau, S. & Forse, R. A. (2005), 'Intra-abdominal pressure in the morbidly obese', *Obesity surgery* **15**(9), 1225–1232.

Lee, Y. & Hwang, K. (2002), 'Skin thickness of korean adults', *Surgical and Radiologic Anatomy* **24**(3-4), 183–189.

Leith, D. E., Butler, J. P., Sneddon, S. L. & Brain, J. D. (1986), 'Cough', *Comprehensive Physiology* .

Lindgren, P., Nordgren, S., Öresland, T. & Hulten, L. (2001), 'Midline or transverse abdominal incision for right-sided colon cancer - a randomized trial', *Colorectal Disease* **3**(1), 46–50.

Lissauer, T. & Clayden, G. (2007), *Illustrated Textbook of Paediatrics: With STUDENT CONSULT Online Access*, Elsevier Health Sciences.

Luijendijk, R. W., Hop, W. C., van den Tol, M. P., de Lange, D. C., Braaksma, M. M., IJzermans, J. N., Boelhouwer, R. U., de Vries, B. C., Salu, M. K., Wereldsma, J. C. et al. (2000), 'A comparison of suture repair with mesh repair for incisional hernia', *New England Journal of Medicine* **343**(6), 392–398.

Lyons, M., Mohan, H., Winter, D. & Simms, C. (2015), 'Biomechanical abdominal wall model applied to hernia repair', *British Journal of Surgery* **102**(2), e133–e139.

Lyons, M., Winter, D. C. & Simms, C. K. (2013), 'Extrusion properties of porcine intestines and surrogate materials for ventral hernia modelling', *Journal of the mechanical behavior of biomedical materials* **18**, 57–66.

Lyons, M., Winter, D. C. & Simms, C. K. (2014), 'Mechanical characterisation of porcine rectus sheath under uniaxial and biaxial tension', *Journal of Biomechanics* .

Maas, S., Rawlins, D., Weiss, J. & Ateshian, G. (2013), 'Febio theory manual', *Available from: http:/mrl.sci.utah.edu/software/febio* .

MacFadyen, B. (2004), *Laparoscopic surgery of the abdomen*, Springer.

Malbrain, M. L., Chiumello, D., Pelosi, P., Wilmer, A., Brienza, N., Malcangi, V., Bihari, D., Innes, R., Cohen, J., Singer, P. et al. (2004), 'Prevalence of intra-abdominal hypertension in critically ill patients: a multicentre epidemiological study', *Intensive care medicine* **30**(5), 822–829.

Martins, P., Peña, E., Jorge, R., Santos, A., Santos, L., Mascarenhas, T. & Calvo, B. (2012), 'Mechanical characterization and constitutive modelling of the damage process in rectus sheath', *Journal of the Mechanical Behavior of Biomedical Materials* **8**, 111–122.

McConnell, A. (2011), *Breathe strong, perform better*, Human Kinetics.

Meade, J. C. & Brecher, G. I. (1995), 'Suturing instrument with thread management'. US Patent 5,437,681.

Methe, K., Nayakwade, N., Bäckdahl, H., Johansson, B., Premaratne, G., Kumar, V. K., Patil, P., Dellgren, G. & Sumitran-Holgersson, S. (2013), 'Characterization of decellularized porcine hearts as scaffolds for tissue-engineering', *The Journal of Heart and Lung Transplantation* **32**(4), S70.

Middleton, E., Reed, C. E. & Ellis, E. F. (1978), *Allergy, principles and practice*, Mosby.

Minns, R. & Tinckler, L. (1976), 'Structural and mechanical aspects of prosthetic herniorrhaphy', *Journal of biomechanics* **9**(7), 435–438.

Moerman, K., Kerskens, C., Lally, C., Flamini, V. & Simms, C. (2009), 'Evaluation of a validation method for mr imaging-based motion tracking using image simulation', *EURASIP Journal on Advances in Signal Processing* **2010**(1), 942131.

Moerman, K. M., Holt, C. A., Evans, S. L. & Simms, C. K. (2009), 'Digital image correlation and finite element modelling as a method to determine mechanical properties of human soft tissue in vivo', *Journal of biomechanics* **42**(8), 1150–1153.

Moerman, K., Nederveen, A. & Simms, C. (2013), 'Image based model construction, boundary condition specification and inverse fea control: A basic matlab toolkit for febio computer methods in biomechanics and biomedical engineeering', *Utah, Salt Lake* .

Morales-Conde, S. (2002), *Laparoscopic ventral hernia repair*, Springer.

Moran, B. (2005), *Farquharson's Textbook of Operative General Surgery 9Ed*, Hodder Education.

Mudge, M. & Hughes, L. (1985), 'Incisional hernia: a 10 year prospective study of incidence and attitudes', *British journal of surgery* **72**(1), 70–71.

Mulholland, M. W. & Doherty, G. M. (2006), *Complications in surgery*, Lippincott Williams & Wilkins.

Mulier, J. P. J., Dillemans, B. R., Crombach, M., Missant, C. & Sels, A. (2009), 'On the abdominal pressure volume relationship.', *Internet Journal of Anesthesiology* **21**(1).

Nassar, A., Ashkar, K., Rashed, A. & Abdulmoneum, M. (1997), 'Laparoscopic cholecystectomy and the umbilicus', *British journal of surgery* **84**(5), 630–633.

Netter, F. H. (2010), *Atlas of human anatomy*, Elsevier Health Sciences.

Nezhat, C., Nezhat, F. & Nezhat, C. (2013), *Nezhat's Video-Assisted and Robotic-Assisted Laparoscopy and Hysteroscopy with DVD*, Cambridge University Press.

Nilsson, T. (1982), 'Biomechanical studies of rabbit abdominal wall. part i.âĂŤthe mechanical properties of specimens from different anatomical positions', *Journal of Biomechanics* **15**(2), 123–129.

Nolph, K. D. (1989), *Peritoneal dialysis*, Springer.

Nutton, V. (2004), *Ancient Medicine*, Sciences of Antiquity Series, Taylor & Francis.
URL: *http://books.google.ie/books?id=PREr9_rojrQC*

Park, A. E., Roth, J. S. & Kavic, S. M. (2006), 'Abdominal wall hernia', *Current problems in surgery* **43**(5), 326–375.

Patel, V. R. (2012), *Robotic urologic surgery*, Springer.

Pelker, R. R., Friedlaender, G. E. & Markham, T. C. (1983), 'Biomechanical properties of bone allografts.', *Clinical Orthopaedics and Related Research* **174**, 54–57.

PLAUS, W. J. (1993), 'Laparoscopic trocar site hernias', *Journal of laparoendoscopic surgery* **3**(6), 567–570.

Podwojewski, F., Otténio, M., Beillas, P., Guérin, G., Turquier, F. & Mitton, D. (2012), 'Mechanical response of animal abdominal walls< i> in vitro</i>: Evaluation of the influence of a hernia defect and a repair with a mesh implanted intraperitoneally', *Journal of biomechanics* .

Pond, W. G. (2003), *Pig production: biological principles and applications*, Cengage Learning.

Prendergast, P., Lee, T., Quinn, D., Dolan, F., Lally, C., Daly, S. & Reid, A. (2003), 'Analysis of prolapse in cardiovascular stents: a constitutive equation for vascular tissue and finite-element modelling', *Journal of biomechanical engineering* **125**(5), 692–699.

Rath, A., Attali, P., Dumas, J., Goldlust, D., Zhang, J. & Chevrel, J. (1996), 'The abdominal linea alba: an anatomo-radiologic and biomechanical study', *Surgical and Radiologic Anatomy* **18**(4), 281–288.

Rath, A., Zhang, J. & Chevrel, J. (1997), 'The sheath of the rectus abdominis muscle: an anatomical and biomechanical study', *Hernia* **1**(3), 139–142.

Ravishankar, N. & Hunter, J. (2005), 'Measurement of intra-abdominal pressure in intensive care units in the united kingdom: a national postal questionnaire study', *British journal of anaesthesia* **94**(6), 763–766.

Reilly, D. T. & Burstein, A. H. (1974), 'The mechanical properties of cortical bone', *The Journal of Bone & Joint Surgery* **56**(5), 1001–1022.

Rossi, A. & Rossi, G. (2001), *CT of the Peritoneum*, Springer.

Sanders, R. C. & Winter, T. C. (2007), *Clinical sonography: a practical guide*, Wolters Kluwer Health.

Santamaría, V. A., Siret, O., Badel, P., Guerin, G., Novacek, V., Turquier, F. & Avril, S. (2015), 'Material model calibration from planar tension tests on porcine linea alba', *Journal of the mechanical behavior of biomedical materials* **43**, 26–34.

Sanz-Lopez, R., Martinez-Ramos, C., Nunez-Pena, J., de Gopegui, M. R., Pastor-Sirera, L. & Tamames-Escobar, S. (1999), 'Incisional hernias after laparoscopic vs open cholecystectomy', *Surgical endoscopy* **13**(9), 922–924.

Schachtrupp, A., Tons, C., Fackeldey, V., Hoer, J., Reinges, M. & Schumpelick, V. (2003), 'Evaluation of two novel methods for the direct and continuous measurement of the intra-abdominal pressure in a porcine model', *Intensive care medicine* **29**(9), 1605–1608.

Schmidt, S. & Langrehr, J. (2006), 'Autologous fibrin sealant (vivostat®) for mesh fixation in laparoscopic transabdominal preperitoneal hernia repair', *Endoscopy* **38**(08), 841–844.

Schwab, R., Schumacher, O., Junge, K., Binnebösel, M., Klinge, U., Becker, H. & Schumpelick, V. (2008), 'Biomechanical analyses of mesh fixation in tapp and tep hernia repair', *Surgical endoscopy* **22**(3), 731–738.

Scott-Conner, C. E. (2009), *Operative anatomy*, Lippincott Williams & Wilkins.

Singh, V. (2011), *Anatomy of Abdomen and Lower Limb*, Elsevier India.

Skandalakis, L. J. & Skandalakis, J. E. (2013), *Surgical anatomy and technique: a pocket manual*, Springer Science & Business Media.

Slatter, D. (2003), *Textbook of Small Animal Surgery*, number v. 2 *in* 'Textbook of Small Animal Surgery', Saunders.
URL: *http://books.google.ie/books?id=B_nh6zSr4wUC*

Snell, R. S. (2011), *Clinical anatomy by regions*, Wolters Kluwer Health.

Song, C., Alijani, A., Frank, T., Hanna, G. & Cuschieri, A. (2006*a*), 'Elasticity of the living abdominal wall in laparoscopic surgery', *Journal of biomechanics* **39**(3), 587–591.

Song, C., Alijani, A., Frank, T., Hanna, G. & Cuschieri, A. (2006*b*), 'Mechanical properties of the human abdominal wall measured in vivo during insufflation for laparoscopic surgery', *Surgical Endoscopy And Other Interventional Techniques* **20**(6), 987–990.

Sørensen, L. T., Hemmingsen, U. B., Kirkeby, L. T., Kallehave, F. & Jørgensen, L. N. (2005), 'Smoking is a risk factor for incisional hernia', *Archives of Surgery* **140**(2), 119–123.

Strauch, B., Vasconez, L. O., Hall-Findlay, E. J., Lee, B. T. et al. (2009), *Grabb's encyclopedia of flaps*, Vol. 3, Wolters Kluwer Health.

Sugerman, H. J., Kellum Jr, J. M., Reines, H. D., DeMaria, E. J., Newsome, H. H. & Lowry, J. W. (1996), 'Greater risk of incisional hernia with morbidly obese than steroid-dependent patients and low recurrence with prefascial polypropylene mesh', *The American journal of surgery* **171**(1), 80–84.

Takaza, M., Cooney, G. M., McManus, G., Stafford, P. & Simms, C. K. (2014), 'Assessing the microstructural response to applied deformation in porcine passive skeletal muscle', *Journal of the mechanical behavior of biomedical materials* **40**, 115–126.

Takaza, M., Moerman, K. M., Gindre, J., Lyons, G. & Simms, C. K. (2013), 'The anisotropic mechanical behaviour of passive skeletal muscle tissue subjected to large tensile strain', *Journal of the mechanical behavior of biomedical materials* **17**, 209–220.

Takaza, M., Moerman, K. M. & Simms, C. K. (2013), 'Passive skeletal muscle response to impact loading: Experimental testing and inverse modelling', *Journal of the mechanical behavior of biomedical materials* **27**, 214–225.

Tank, P. W. & Grant, J. C. B. (2012), *Grant's dissector*, Lippincott Williams & Wilkins.

Tinelli, A. (2012), *Laparoscopic Entry: Traditional Methods, New Insights and Novel Approaches*, Springer.

TopClosure - 3S System (n.d.).
URL: *http://www.topclosure.com/*

Townsend, C. M. et al. (2004), *Sabiston textbook of surgery*, Elevier-Saunders.

Tran, D., Mitton, D., Voirin, D., Turquier, F. & Beillas, P. (2014), 'Contribution of the skin, rectus abdominis and their sheaths to the structural response of the abdominal wall ex vivo', *Journal of biomechanics* **47**(12), 3056–3063.

Ullah, S., Grant, R., Johnson, M. & McAlister, V. C. (2013), 'Scarpa's fascia and clinical signs: the role of the membranous superficial fascia in the eponymous clinical signs

of retroperitoneal catastrophe', *Annals of The Royal College of Surgeons of England* **95**(7), 519–522.

Uslu, H. Y., Erkek, A. B., Cakmak, A., Kepenekci, I., Sozener, U., Kocaay, F. A., Turkcapar, A. G. & Kuterdem, E. (2007), 'Trocar site hernia after laparoscopic cholecystectomy', *Journal of Laparoendoscopic & Advanced Surgical Techniques* **17**(5), 600–603.

Van Loocke, M. (2007), Passive mechanical properties of skeletal muscle in compression, PhD thesis, National University of Ireland, Galway.

Venkatasubramanian, R. T., Grassl, E. D., Barocas, V. H., Lafontaine, D. & Bischof, J. C. (2006), 'Effects of freezing and cryopreservation on the mechanical properties of arteries', *Annals of Biomedical engineering* **34**(5), 823–832.

Viidik, A. (1978), 'On the correlation between structure and mechanical function of soft connective tissues.', *Verhandlungen der Anatomischen Gesellschaft* (72), 75.

Ward, R. C. (2003), *Foundations for osteopathic medicine*, Lippincott Williams & Wilkins.

Weber, E. C., Vilensky, J. A., Carmichael, S. W. & Lee, K. S. (2011), *Netter's concise radiologic anatomy*, Elsevier Health Sciences.

Wexner, S. & Cohen, S. (1995), 'Port site metastases after laparoscopic colorectal surgery for cure of malignancy', *British journal of surgery* **82**(3), 295–298.

Wilkins, L. & King, J. (2002), *Anatomy and Physiology*, Lippincott professional guides, Lippincott Williams & Wilkins.
URL: *http://books.google.ie/books?id=H8_z-XaS_d0C*

Winter, D. C. (2013), private communication.

Wissing, J., van Vroonhoven, T. J., Schattenkerk, M. E., Veen, H., Ponsen, R. & Jeekel, J. (1987), 'Fascia closure after midline laparotomy: results of a randomized trial', *British journal of surgery* **74**(8), 738–741.

Wood, W. C., Staley, C. A. & Skandalakis, J. E. (2010), *Anatomic basis of tumor surgery*, Springer.

Zech, S., Goesling, T., Hankemeier, S., Knobloch, K., Geerling, J., Schultz-Brunn, K., Krettek, C. & Richter, M. (2006), 'Differences in the mechanical properties of calcaneal artificial specimens, fresh frozen specimens, and embalmed specimens in experimental testing', *Foot & ankle international* **27**(12), 1126–1136.

Zip 16 - Surgical Skin Closure (n.d.).
URL: *http://www.ziplinemedical.com/products/zip16/*

Zucker, K. (2001), *Surgical Laparoscopy*, Lippincott Williams & Wilkins.
URL: *http://books.google.ie/books?id=HzvvMGI5kLcC*